

# For Reference

NOT TO BE TAKEN FROM THIS ROOM



Ex LIBRIS  
UNIVERSITATIS  
ALBERTAEÆSIS















THE UNIVERSITY OF ALBERTA

RELEASE FORM

NAME OF AUTHOR           Tania H. Watts

TITLE OF THESIS           Structure and Assembly of Pili isolated  
                              from *Pseudomonas aeruginosa* strains PAK  
                              and PAO

DEGREE FOR WHICH THESIS WAS PRESENTED   Doctor of Philosophy

YEAR THIS DEGREE GRANTED   FALL 1983

Permission is hereby granted to THE UNIVERSITY OF ALBERTA LIBRARY to reproduce single copies of this thesis and to lend or sell such copies for private, scholarly or scientific research purposes only.

The author reserves other publication rights, and neither the thesis nor extensive extracts from it may be printed or otherwise reproduced without the author's written permission.





THE UNIVERSITY OF ALBERTA

Structure and Assembly of Pili isolated from  
*Pseudomonas aeruginosa* strains PAK and PAO

by



Tania H. Watts

A THESIS

SUBMITTED TO THE FACULTY OF GRADUATE STUDIES AND RESEARCH  
IN PARTIAL FULFILMENT OF THE REQUIREMENTS FOR THE DEGREE  
OF Doctor of Philosophy

DEPARTMENT OF BIOCHEMISTRY

EDMONTON, ALBERTA

FALL 1983





051 - 201

THE UNIVERSITY OF ALBERTA  
FACULTY OF GRADUATE STUDIES AND RESEARCH

The undersigned certify that they have read, and recommend to the Faculty of Graduate Studies and Research, for acceptance, a thesis entitled Structure and Assembly of Pili isolated from *Pseudomonas aeruginosa* strains PAK and PAO submitted by Tania H. Watts in partial fulfilment of the requirements for the degree of Doctor of Philosophy.





For my parents



## ABSTRACT

Pili were isolated from *Pseudomonas aeruginosa* strain PAO/DB2 and their properties compared with those of *P. aeruginosa* strain PAK and *Neisseria gonorrhoeae* pili. It was found that PAK and PAO pilin have similar molecular weights, share a common N-terminal amino acid sequence and are similar with respect to amino acid composition. The three types of pili were found to be indistinguishable by electron microscopy and to share a common antigenic determinant, which is most likely located in the homologous N-termini of the three proteins.

A variety of treatments were tested for their ability to dissociate PAK and PAO pili into subunits without denaturation of the protein. A detergent, octyl-glucoside, turned out to be the reagent of choice for this purpose. The pilin/octyl-glucoside complex was further characterized using the techniques of circular dichroism, viscometry, equilibrium dialysis, gel-exclusion chromatography, analytical ultracentrifugation and densitometry. At 1mg/ml pilin in 30mM octyl-glucoside, approximately 90% of the pilin subunits are in the dimer form. At infinite dilution, however, the sedimentation properties of the pilin/detergent complex reflect the pilin monomer and therefore, information could be derived about the shape of pilin in the pilin/detergent complex. PAK and PAO pilin were found to be fairly globular and were indistinguishable at the level of the





hydrodynamic studies. The pilin dimer appears to interact with one octyl-glucoside micelle (containing 26-27 detergent monomers).

X-ray fiber diffraction studies of PAK and PAO pili have shown that both pili are hollow cylinders of 52Å outer diameter and 12Å inner diameter with a girdle of low electron density at the center of the protein shell. The two strains of pili have similar diffraction patterns out to a resolution of 7Å in the equatorial direction and 4Å in the meridional direction. The pilin subunits are arranged in a helix with 5.06-5.08 units/turn of 40.8Å pitch for PAK pili and 41.3Å pitch for PAO pili. The  $\alpha$ -helices in the pilus are aligned roughly parallel to the fiber axis, giving rise to strong reflections at 10Å in the equatorial direction and at 5Å on the meridian of the diffraction patterns. The diffraction patterns of both gonococcal pili and bacterial flagella show a similar intensity distribution. A working model for pilus structure was derived based on the results of the X-ray fiber diffraction and hydrodynamic studies.

Removal of octyl-glucoside from the pilin/detergent complex resulted in the formation of flexible filaments of almost twice the diameter of native pili. These were called reassembled pilin filaments.

The proteins from the purified inner and outer membranes of *Pseudomonas aeruginosa* PAK and PAK/2Pfs were



subjected to SDS-polyacrylamide gel electrophoresis, transferred to nitrocellulose and treated with antiserum raised against purified pili. Bound anti-pilus antibodies were visualized by reaction with  $^{125}\text{I}$ -Protein A from *Staphylococcus aureus*. The results suggested that there is a pool of pilin subunits in both the inner and outer membrane of *P. aeruginosa* and that the pool size in the multipiliated strain is comparable with that of the wild-type strain. Since pilin appeared to be a membrane protein, it was of interest to attempt to reconstitute pilin into synthetic phospholipid vesicles. This was achieved by an octyl-glucoside dialysis procedure. Some preliminary characterization of the resulting pilin/vesicles was carried out. Circular dichroism studies suggested that pilin in the presence of phospholipids has the same conformation as pilin in the native pilus.

The spectral properties of three quaternary arrangements of PAK pili (native pili, pilin dimers in octyl-glucoside and reassembled pilin filaments) were compared using the techniques of alkaline pH titration monitored by absorption spectroscopy, solvent perturbation, circular dichroism and acrylamide quenching of intrinsic tryptophan fluorescence. It was found that tyrosine 24 and 27 are at a dimer/dimer interface in both native pili and in the reassembled pilin filaments and that dissociation of pili into dimers by octyl-glucoside results in the exposure of the two tyrosines



and in partial exposure of at least one of the two tryptophan residues in pilin.

To delineate the antigenic regions of pilin, the protein was cleaved at Arg<sup>30</sup>, Arg<sup>53</sup> and Arg<sup>120</sup>, to produce peptides TCI(1-30), TCII(31-53), TCIII(54-120) and TCIV(121-144). In addition, several smaller peptide fragments of TCIII and TCIV were tested for antigenicity. The purified peptides were coupled to BSA using a photo-sensitive cross-linking reagent, the N-hydroxy-succinimide ester of 4-azido benzoic acid, then subjected to immunological analysis using the 'ELISA' and 'Immunoblot' procedures with polyclonal antiserum. Four antigenic regions were identified: one in TCI was found to be common to both PAK and PAO pilin. The remaining three were found to be specific to PAK pilin. Modification of cysteine<sup>129</sup> and cysteine<sup>142</sup>, which are located in the C-terminal antigenic peptide did not result in a loss of antigenicity of this fragment or of intact pili.





## Acknowledgements

I am grateful to Dr. William Paranchych for providing me with the opportunity to carry out this research and for his continued guidance and encouragement in these endeavours. I would also like to thank Dr. L.S. Frost for her patience and advice as well as my fellow graduate students Dr. Glen Armstrong, Betty Worobec and Brett Finlay for contributing both scientifically and socially to my graduate career. Thanks are also due to Kathy Volpel for her excellent technical assistance and to Dr. P.A. Sastry for valuable discussions and for providing me with some of the purified peptides used in these studies.

The X-ray fiber diffraction studies were made possible by two visits to the European Molecular Biology Laboratory, Heidelberg, at the generous invitation of Dr. D.A. Marvin. I would like to thank Dr. Waltraud Folkhard, who collaborated directly in this work, as well as the other members of Dr. Marvins laboratory for their help and advice in these studies.

I would also like to extend my thanks to many other members of the Biochemistry department who contributed to this work. Kim Oikawa, for circular dichroism measurements, Vic Ledsham for ultracentrifugation, Dr. W. McCubbin for guiding me in the use of the fluorimeter, and Dr. C.M. Kay who made available these facilities and was always willing to discuss the results. I would also like to thank Dr. L.B. Smillie for the use of his facilities, Mike Natriss, for amino acid analysis and Mike Carpenter for N-terminal sequence analysis. The help of Dr. D. Scraba and Roger Bradley with electron microscopy was greatly appreciated. I am also grateful to Dr. R.N.A.H. Lewis for synthesis of octyl-glucoside, Dr. P.C.S. Chong, for synthesis of the reagent AB-OSu and to Ron Moore who carried out the immuno-electrophoresis experiments as a Biochemistry 501 project. Thanks are also due to Dr. M. James for providing a pinhole camera and for making available his facilities, as well as to Randy Read and Masao Fujinaga for valuable discussions on principles of symmetry.

Finally, I would like to thank my family for their continued support and encouragement throughout my studies and Dr. Jean Gariepy for his friendship and support. The friendly atmosphere of the Biochemistry Department has made these endeavours pleasant and rewarding and was greatly appreciated.

The financial support of the Medical Research Council of Canada and the Alberta Heritage Foundation for Medical Research in the form of studentships and operating funds is gratefully acknowledged.



## TABLE OF CONTENTS

	<u>Page</u>
Abstract. . . . .	v
Acknowledgements. . . . .	ix
Table of Contents . . . . .	x
List of Tables. . . . .	xvii
List of Figures . . . . .	xviii
List of Abbreviations . . . . .	xxii
 CHAPTER I. Introduction. . . . .	 1
A. The polar pili of <i>Pseudomonas aeruginosa</i> . .	2
B. Functions of <i>Pseudomonas</i> pili . . . . .	4
1. The role of pili in adherence of <i>Pseudomonas aeruginosa</i> . . . . .	4
2. Pilus-specific bacteriophage: evidence for retraction. . . . .	6
3. Twitching motility. . . . .	9
C. Studies on Other Types of pili . . . . .	10
1. Conjugative pili. . . . .	10
a. F pili. . . . .	11
b. EDP208 pili . . . . .	12
2. Type I pili of <i>Escherichia coli</i> . . . . .	13
3. The pili of Enterotoxigenic <i>E. coli</i> . .	14
a. K88 pili. . . . .	15
b. CFA/I pili. . . . .	17
4. Gonococcal pili . . . . .	18
D. Aims of the project. . . . .	21





CHAPTER II. Materials and Methods. . . . .	23
A. Materials. . . . .	23
1. Bacteria and bacteriophage. . . . .	23
2. Culture media and buffers . . . . .	23
3. Chemicals, enzymes and reagents . . . . .	24
B. Pili purification. . . . .	25
C. Phage growth . . . . .	28
D. Electron microscopy. . . . .	29
E. Pili dissociation and reassembly . . . . .	30
F. Competition plaque assay . . . . .	31
G. Polyacrylamide gel electrophoresis . . . . .	32
H. Separation of inner and outer membranes of <i>Pseudomonas</i> . . . . .	34
1. Membrane isolation. . . . .	34
2. Assays used in the characterization of membrane fractions. . . . .	36
a. Total membrane protein. . . . .	36
b. KDO by the thiobarbituric acid test	36
c. Succinate dehydrogenase activity. .	37
I. Reconstitution of pilin into a phospholipid bilayer. . . . .	38
1. Preparation of lipids for reconsti- tution. . . . .	38
2. Solubilization of lipids and reconsti- tution with pilin . . . . .	38
3. Characterization of lipid vesicles. . .	39
a. Determination of phospholipid to protein ratio . . . . .	39
b. Migration of vesicles on sucrose	



gradients . . . . .	40
c. Pronase digestion of pilin/vesicles	41
J. Protein/Peptide Chemistry. . . . .	41
1. Amino acid analysis . . . . .	41
2. N-terminal analysis . . . . .	42
a. N-terminal sequence determination .	42
b. Dansylation and thin-layer chromatography of the dansyl-amino acids .	42
3. Ninhydrin alkaline hydrolysis . . . . .	43
4. Two-dimensional peptide maps. . . . .	44
5. High voltage paper electrophoresis. . .	44
6. Citraconylation and enzymatic digestion	45
7. Peptide purification. . . . .	46
8. Coupling of peptides to bovine serum albumin . . . . .	47
K. Hydrodynamic methods . . . . .	48
1. Ultracentrifugation . . . . .	48
a. Sedimentation velocity. . . . .	48
b. Sedimentation equilibrium . . . . .	50
2. Viscometry. . . . .	51
3. Density measurements. . . . .	52
4. Equilibrium dialysis. . . . .	54
5. Gel exclusion chromatography. . . . .	55
L. Spectral methods . . . . .	56
1. Protein concentrations. . . . .	56
2. Circular dichroism. . . . .	57
3. Alkaline pH titration . . . . .	59
4. Solvent perturbation. . . . .	59



5.	Fluorescence measurements . . . . .	60
M.	Immunological methods. . . . .	61
1.	Preparation of antisera . . . . .	61
2.	Immuno-electrophoresis . . . . .	62
3.	Transfer of proteins from SDS-gels to nitrocellulose paper followed by immunological detection . . . . .	63
4.	Detection of antigenic species with ELISA . . . . .	66
N.	X-ray diffraction methods. . . . .	67
1.	Preparation of oriented fibers of pili. . . . .	67
2.	Diffraction methods . . . . .	68
3.	Measurements of positions and intensities of reflections. . . . .	71
4.	Radial electron density distribution. . . . .	73
5.	Generation of $\alpha$ -helical models and calculation of their transforms . . . . .	73
CHAPTER III. Purification and Preliminary Character ization of pili isolated from <i>Pseudomonas aeruginosa</i> strain PAO . . . . .		75
A.	Purification of pili . . . . .	76
B.	Molecular weight of pilin . . . . .	78
C.	Electron microscopy of purified pili . . . . .	81
D.	N-terminal analysis, tryptic peptide maps and amino acid compositional analysis. . . . .	81
E.	Immunological cross-reactivity between pili. . . . .	88
F.	Summary. . . . .	93
CHAPTER IV. Dissociation and Characterization of Pilin in Detergent . . . . .		96





A.	Some comments on the interaction of detergents with proteins . . . . .	97
B.	Dissociation of pili . . . . .	102
C.	Characterization of pilin in octyl-glucoside	109
1.	Measurement of detergent binding to pilin . . . . .	109
2.	Gel exclusion of pilin in detergent . .	111
3.	Partial specific volume of pilins . . .	115
4.	Sedimentation equilibrium . . . . .	117
5.	Sedimentation velocity. . . . .	120
6.	Determination of the Stokes' radius of pilin . . . . .	120
D.	Conclusions. . . . .	126
CHAPTER V.	X-ray diffraction studies of oriented pili fibers . . . . .	128
A.	Theory . . . . .	130
1.	Types of orientation observed in fibers	130
2.	Diffraction by a helix. . . . .	132
3.	The use of model building in solving the phase problem . . . . .	141
B.	Analysis of the diffraction patterns of PAK and PAO pili . . . . .	143
1.	Analysis of equatorial data . . . . .	145
a.	Crystalline reflections. . . . .	145
b.	The continuous equatorial transform. . . . .	147
2.	Determination of the helix parameters for PAK and PAO pili. . . . .	154
3.	Comparison of pili diffraction patterns	



with those of related structures. . . .	164
4. Orientation of the $\alpha$ -helices in pilin . . . . .	169
C. A model for the <i>Pseudomonas</i> pilus based upon X-ray diffraction and hydrodynamic studies .	173
D. Summary. . . . .	179
CHAPTER VI. Studies on the <i>in vitro</i> Assembly of pilin . . . . .	180
A. <i>In vitro</i> assembly of an alternate form of pilin filament . . . . .	180
B. A biological assay for pili. . . . .	186
C. Discussion . . . . .	190
CHAPTER VII. Pilin in the membrane of <i>Pseudomonas</i> <i>aeruginosa</i> . . . . .	192
A. Identification of pilin pools in the inner and outer membranes of <i>P. aeruginosa</i> . . . .	192
1. Separation of inner and outer membranes	192
2. Immunoblotting. . . . .	195
3. Evidence that extracellular pili do not contaminate the membrane preparations.	199
4. Discussion. . . . .	203
B. Reconstitution of pilin into synthetic phospholipid vesicles. . . . .	206
1. Reconstitution. . . . .	206
2. Evidence for tight association of pilin with the vesicles . . . . .	210
3. Circular dichroism of pilin/vesicles. .	214
4. Summary . . . . .	214
CHAPTER VIII. Spectral properties of three quaternary	



arrangements of PAK pilin. . . . .	217
A. Circular dichroism . . . . .	220
B. Alkaline pH titration of tyrosine residues. . . . .	222
C. Solvent perturbation . . . . .	230
D. Quenching of tryptophan fluorescence by acrylamide . . . . .	233
E. Conclusions. . . . .	236
CHAPTER IX. Mapping of the Antigenic Determinants of PAK pilin. . . . .	239
A. Immuno-electrophoresis of Pili. . . . .	240
B. Preparation of proteolytic fragments of PAK pilin. . . . .	244
C. Antigenicity of PAK pilin peptides . . . . .	246
D. Conclusions. . . . .	257
CHAPTER X. Perspectives. . . . .	260
A. Pilus structure. . . . .	260
B. Pilus assembly . . . . .	263
BIBLIOGRAPHY. . . . .	266
APPENDIX: Publications arising from this thesis . . . . .	279





# LIST OF TABLES

	<u>PAGE</u>
III-1. Amino acid composition of pilins.	87
IV-I. Effects of various agents on the aggregation state and secondary structure of pili.	105
IV-II. Determination of Stokes' radius of pilin in octyl-glucoside.	122
V-I. Indexing of crystalline reflections.	146
V-II. Helix parameters of PAK and PAO pilin.	163
VI-I. Inhibition of phage attachment to <i>Pseudomonas aeruginosa</i> .	189
VII-I. Characterization of isolated membranes.	194
VII-II. Fate of added [ $^{35}$ S]-pili during membrane isolation.	202



## LIST OF FIGURES

	<u>PAGE</u>
III.1. Electron microscopy of piliated cells.	77
III.2. SDS-polyacrylamide gel electrophoresis of pilins.	80
III.3. Electron microscopy of purified pili.	82
III.4. N-terminal amino acid sequences of pilins.	84
III.5. Two-dimensional chromatography-electrophoresis of pilin tryptic peptides.	86
III.6. Principles of ELISA.	90
III.7. ELISA showing cross-reactivity between PAK and PAO pili.	92
III.8. Cross-reactivity between pilins as demonstrated by 'Immunoblotting'.	94
IV.1. Circular dichroism spectra of PAK and PAO pili.	103
IV.2. Structure of some common detergents.	107
IV.3. Dissociation of pili in octyl-glucoside.	108
IV.4. Binding of octyl-glucoside to pilin.	110
IV.5. Gel exclusion chromatography of pilin in octyl-glucoside.	112
IV.6. Binding of octyl-glucoside to pilin as measured by gel chromatography.	114
IV.7. Sedimentation equilibrium analysis.	119
IV.8. Determination of the sedimentation coefficients of PAK and PAO pilin.	121
V.1. Types of orientation found in fibers.	131
V.2. Relationship between the Cartesian and polar-cylindrical coordinate systems.	133



V.3.	A simple helix and its diffraction pattern.	136
V.4.	Values of Bessel functions squared.	138
V.5.	X-ray fiber diffraction patterns of PAK and PAO pili at 75% relative humidity.	144
V.6.	Relation between unit lattice dimension and relative humidity.	148
V.7.	Continuous equatorial diffraction amplitudes.	151
V.8.	Radial electron density distribution.	153
V.9.	Diffraction pattern of PAO pili at a specimen to film distance of 10.4cm.	158
V.10.	" $n, l$ " plot for the helix selection rule, " $l$ " = $n - 5.08n$ .	159
V.11.	Measurements of reciprocal space coordinates on diffraction patterns.	160
V.12.	Determination of the helix parameters for PAK and PAO pili.	162
V.13.	Surface lattice representation of PAK and PAO pili.	165
V.14.	X-ray diffraction pattern of bacterial flagella.	166
V.15.	Diffraction patterns of gonococcal and PAK pili.	168
V.16.	Comparison of the observed transform with the transform calculated for $\alpha$ -helical models of 4 and 5 $u/t$ .	171
V.17.	Three models of subunit shape.	172
V.18.	Observed and calculated transforms of the three models shown in figure V.17.	174
V.19.	A model for pilus structure based on X-ray diffraction and hydrodynamic studies.	178
VI.1.	Dissociation and reassociation of pili.	181
VI.2.	Electron microscopy of native and reassembled	





pili.	183
VI.3. Electron micrograph of aged pili.	185
VI.4. A biological assay for native pili.	187
VII.1. Electrophoresis of <i>Pseudomonas</i> membranes.	197
VII.2. Autoradiography of membrane 'Immunoblots.'	198
VII.3. Electron micrographs of isolated membrane fractions.	201
VII.4. Chromatography of pilin/vesicles.	208
VII.5. Electron microscopy of pilin/vesicles.	209
VII.6. Sucrose density gradient centrifugation of pilin/vesicles.	212
VII.7. Circular dichroism of pilin/vesicles.	215
VIII.1. Primary structure of PAK pilin.	219
VIII.2. Far UV CD of three forms of pili.	221
VIII.3. Near UV CD of three forms of pili.	223
VIII.4. Effect of alkali on pilin secondary structure.	225
VIII.5. Denaturation of pili by guanidine-HCl and by heat.	226
VIII.6. UV absorption spectrum of pili.	227
VIII.7. Alkaline pH titration of pili.	229
VIII.8. Solvent perturbation with 20% DMSO.	232
VIII.9. Acrylamide quenching of tryptophan fluorescence.	235
VIII.10. Schematic representation of two possible packing arrangements of pilin dimers.	237
IX.1. Immuno-electrophoresis of pili.	242
IX.2. Chromatography of trypsin-digest of citra-conylated pili.	245
IX.3. Schematic representation of the locations of	



	antigenic peptides in PAK pilin.	248
IX.4.	ELISA of PAK pili and its peptide fragments.	250
IX.5.	Electrophoresis and 'Immunoblotting' of PAK pilin and its TC peptides.	253
IX.6.	ELISA of PAK pilin and its TC-peptides with anti-PAO pilus antiserum.	256



## ABBREVIATIONS

A	absorbance
AB-OSu	the N-hydroxysuccinimide ester of 4-azidobenzoic acid
adh	adhesion cistron
BSA	bovine serum albumin
c	concentration
CD	circular dichroism
CMC	critical micelle concentration
cpm	counts per minute
DCPIP	dichloroindophenylindolphenol
DMPC	dimyristoylphosphatidylcholine
DMSO	dimethylsulfoxide
DPPA	dipalmitoylphosphatidic acid
EDTA	disodium(ethylenedinitrilo)tetraacetate
ELISA	enzyme-linked immunosorbant assay
F <sup>+</sup>	<i>E. coli</i> carrying an F plasmid
F <sub>0</sub> lac	an F plasmid carrying the <i>E. coli</i> lac operon
IgG	immunoglobulin G
KDO	2-keto-3-deoxyoctonic acid
M	molecular weight
MOPS	morpholinopropane sulfonate
OG	n-octyl- $\beta$ -D-glucopyranoside
PBS	phosphate buffered saline
PEG	polyethylene glycol
pfu	plaque forming units





PMS	phenazinemetasulfate
PMSF	phenylmethane sulfonyl fluoride
POPOP	p-Bis[2-(5-phenyloxazolyl)]-benzene
PPO	2,5 diphenyloxazole
rh	relative humidity
$R_s$	Stokes' radius
SDH	succinate dehydrogenase
SDS	sodium dodecyl sulfate
SSC	standard saline citrate
TC	trypsin-citraconylated
TCA	trichloroacetic acid
TEMED	N,N,N',N'-tetramethylethylenediamine
TPCK	1-tosyl-2-phenylethyl-chloromethylketone
<i>tra</i>	transfer
tris	tris(hydroxymethyl)aminomethane
TSB	trypticase soy broth
$\mu\text{Ci}$	microCurie, $2.2 \times 10^6$ disintegrations per minute
UV	ultraviolet
$\bar{v}$	partial specific volume



## CHAPTER I

### Introduction

Houwink (1949) and Anderson (1949) first reported the existence of thin filaments, distinct from flagella, on the surfaces of bacteria. The terms fimbriae (Latin for thread or fiber; Duguid *et al.*, 1955) and pili (Latin for hair-like; Brinton, 1965) have been applied to these filaments. In this treatise, the terms pili (for several such filaments), pilus (for one such filament) and pilin (for the protein subunit making up the pilus) will be used exclusively. While bacterial flagella are uniformly 20nm in diameter and function exclusively in bacterial chemotaxis (reviewed by Silverman & Simon, 1977), bacterial pili exhibit a wide variety of morphologies and can also differ in their functions. Bacterial pili vary in length from 0.2-10  $\mu\text{m}$  and in diameter from 4-10nm and can be flexible or rigid (reviewed by Brinton, 1965 and by Ottow, 1975).

The conjugative pili (Novick *et al.*, 1976), typified by the F pilus of *Escherichia coli*, are primarily involved in the formation of mating pairs during bacterial conjugation (reviewed by Achtman & Skurray, 1977). These pili are always plasmid encoded and usually only one or two pili are expressed on the cell surface. A second class of pili, the somatic pili (Swaney *et al.*, 1977) are chromosomally encoded. Many of the somatic pili appear to be involved in the adherence mechanism of the organism (Beachey, 1980). In



some cases, somatic pili also confer on the bacterium a primitive form of motility, known as twitching motility (Henrichsen, 1975). Somatic pili are usually more numerous on the cell surface than are conjugative pili and can emerge either from the poles of the cell (polar pili) or they may be distributed at random over the cell surface (a peritrichous arrangement). Both conjugative and somatic pili are able to act as receptors for a variety of pilus-specific bacteriophage. A third class of pili can also be distinguished. These pili are plasmid encoded but function primarily in bacterial adherence. Pili of this type have been studied primarily in enterotoxigenic *E. coli* (discussed in section C, below).

The subject of this work is the polar pili of *Pseudomonas aeruginosa* strains PAK and PAO. These pili are chromosomally encoded (Bradley, 1980b) and, as will be seen below, are important in the adherence and hence in the pathogenesis of *Pseudomonas*.

#### A. The Polar Pili of *Pseudomonas aeruginosa*

The polar pili of *Pseudomonas aeruginosa* strains PAK and PAO (abbreviated PAK and PAO pili) are rigid filaments of 6nm diameter and 2.5 $\mu$ m average length (Bradley, 1972b; Weiss, 1971). By obtaining antiserum against pilated bacteria and adsorbing out the non-specific antibodies using *pil*<sup>-</sup> strains of bacteria, Bradley & Pitt (1975) determined that PAK and PAO pili were serologically unrelated. In





addition, the two strains were found to differ in their susceptibility to infection by various pilus-specific bacteriophage (Bradley, 1977; discussed in section B).

Bradley (1974) obtained a multipiliated mutant of PAK, PAK/2Pfs, which produced up to 200 polar pili per cell. The availability of such a highly pilated strain allowed Frost & Paranchych (1977) to purify sufficient pili to allow biochemical analysis of the PAK pilus. It was found that PAK/2Pfs pili consist of a single type of protein subunit, pilin, of molecular weight 17,800 according to amino acid compositional analysis and SDS-polyacrylamide gel electrophoresis. The purified pili were found to contain neither phosphate nor carbohydrate, in contrast to the findings of Brinton (1965) with Type I pili of *E. coli* (see section C, below). The wild-type and multipiliated strains were shown to be indistinguishable with respect to buoyant density in CsCl (1.295 g/ml), isoelectric point (pH 3.9) and amino acid composition. In addition, PAK and PAK/2Pfs pili were found to be immunologically indistinguishable by immunodiffusion analysis. The above studies (Frost & Paranchych, 1977; Frost, 1978) suggested that the mutation giving rise to the multipiliated phenotype was located outside the structural gene for pilin.

The sequence of the N-terminal 22 residues of PAK pilin was determined using automated Edman-degradation (Paranchych *et al.*, 1978). The N-terminal sequence of PAK pilin is



extremely hydrophobic, with only two hydrophilic residues (thr<sup>2</sup> and glu<sup>5</sup>). The N-terminal residue of PAK pilin is the unusual amino acid N-methylphenylalanine. The N-terminal sequence was found to be highly homologous with the N-termini of pilin isolated from *Neisseria gonorrhoeae* (Hermødsen *et al.*, 1978) and from *Moraxella nonliquefaciens* (Frøholm & Sletten, 1977), including N-methylphenylalanine at the N-terminus. Recently, the complete amino acid sequence has been elucidated for PAK/2Pfs pilin (Sastry *et al.*, 1983). It was found that PAK pilin consists of only 144 amino acids with a combined molecular weight of 15,000. Thus the PAK pilin subunit is about 15% smaller than originally anticipated. This discrepancy will be discussed further in Chapter III.

### B. Functions of Pseudomonas pili

*Pseudomonas* pili are not involved in bacterial conjugation. Their major function appears to be in the adherence of the bacterium to various surfaces and in surface translocation (twitching motility). In addition, *Pseudomonas* pili are utilized as receptors by a number of bacteriophage. It is the study of the interaction of bacteriophage with pili that has led to the concept of pilus retraction. Each of these attributes will be considered in more detail below.





## 1. The role of pili in adherence of *Pseudomonas*.

*Pseudomonas aeruginosa* is known as an "opportunistic pathogen." That is, it rarely causes problems in healthy individuals but can be highly invasive in compromised individuals (Young, 1977; Wood, 1976). Examples of compromised individuals are patients undergoing immuno-suppressive therapy, patients with extensive burns and patients with severe underlying disease, such as cystic fibrosis. In the case of cystic fibrosis, bronchopulmonary disease, to which *Pseudomonas* infection contributes, is one of the leading causes of death (Lenette *et al.*, 1974).

It has been established (Woods *et al.*, 1980b) that successful colonization by *Pseudomonas* is dependent on the adherence of the organism to host tissues. Woods *et al.* found that rough (piliated) strains of *Pseudomonas aeruginosa* were able to adhere to buccal cells isolated from cystic fibrosis patients, while smooth strains could not. Furthermore, the piliated strains were unable to adhere to the buccal epithelial cells of healthy individuals. It was suggested that this was due to the fact that cystic fibrotic individuals secrete abnormally high amounts of proteases which might damage the cell surface, thereby exposing attachment sites for *Pseudomonas*. This hypothesis was tested by treating healthy cells with trypsin, whereupon it was found that proteolysis of fibronectin, a cell surface glycoprotein, resulted in enhanced binding of *Pseudomonas* to the buccal cells. In another report (Woods *et al.*, 1980a),





it was shown that the presence of purified *Pseudomonas* pili in the attachment assay was able to inhibit binding of piliated *Pseudomonas* cells to the buccal epithelial cells. Furthermore, it was found that treatment of the bacteria with anti-pilus antisera blocked attachment of a homologous strain of *Pseudomonas*, but failed to block attachment of heterologous strains. The role of pili in adherence has also been established for a number of other gram negative bacteria (Beachey, 1980; section C, below).

## 2. Pilus-specific bacteriophage: evidence for pilus retraction.

Three distinct classes of bacteriophage depend on the presence of *Pseudomonas* pili for infection. PP7, a spherical RNA virus, adsorbs to the lateral surfaces of strain PAO1 of *Pseudomonas aeruginosa*, but is unable to infect strain PAK (Bradley, 1972a). This phage is analogous to the well-studied RNA phage, R17, which adsorbs to the sides of the F pilus (Crawford & Gesteland, 1964).

The filamentous phage Pf1 (Takeya & Amako, 1966) binds to the tip of the pili of strain PAK (Bradley, 1973a) but does not infect strain PAO (Bradley, 1972b). As viewed in the electron microscope, the phage and the pili are indistinguishable with respect to diameter but can be distinguished by antibody labelling (Lawn, 1967) which shows that the pili and phage interact end to end (Bradley, 1973a). Pf1 consists of a single stranded circular DNA



surrounded by a helical arrangement of coat protein molecules of molecular weight 6000 (Marvin & Hohn, 1969). In this regard it is analogous to the F-specific phage, M13' (or Fd).

A third class of virion, represented by phage PO4, appear to be less discriminate with respect to host specificity. PO4 adsorbs to the pili of strain PAK and PAO1 of *Pseudomonas*, although it infects PAO1 about 4-fold less efficiently than it does strain PAK (Bradley, 1974). PO4 is a double-stranded DNA phage, with a spherical head and a long non-contractile tail. The phage appears to bind to the pili by wrapping its tail fibers around the pilus (Bradley, 1974).

Originally, it was thought that the pilus receptors acted as tubes down which RNA (or DNA) from the infecting phage could pass (Brinton, 1965). However, it was difficult to conceive of a mechanism whereby the pilus could actively transfer three different kinds of nucleic acid. This led Marvin & Hohn (1969) to propose a mechanism involving retraction of pili into the bacterial cell. They suggested that adsorption of the filamentous phage to the tip of the pilus might trigger a conformational change which could be transmitted from one subunit to the next until it reached the base of the pilus causing a depolymerization of the pilin subunits into the membrane. This would have the result of bringing attached bacteriophage in contact with the cell





surface. Similarly, it was proposed that during bacterial conjugation, the interaction of the F pilus with its receptor on the recipient cell would stimulate retraction of the F pilus, thereby bringing the two cells into close proximity. Bradley (1972d) envisions a similar retraction mechanism for the interaction of spherical and tailed *Pseudomonas* bacteriophage with pili. There have been two schools of thought as to the stimulus for retraction. Marvin & Hohn (1969), as well as Bradley (1978) maintain that retraction must be stimulated. Previously, however, Bradley (1972a) had suggested that outgrowth and retraction occur continuously and spontaneously.

One prediction made by the retraction model of Marvin & Hohn (1969) is the existence of a pool of pilin subunits in the bacterial membrane. Recently, this has been demonstrated conclusively for K88 pili (Dougan *et al.*, 1983; discussed in section C).

Some experimental evidence for retraction of *Pseudomonas* pili has been obtained by Bradley (1972d, 1974). Bradley (1972d) showed that there is a 50% reduction in the length of pili upon incubation of *Pseudomonas aeruginosa* PAO1 with phage PP7. Theory predicts that if one phage particle is adsorbed per pilus and that the pilus can retract only as far as the phage, then pilus length should be reduced by an average of 50% upon adsorption of phage. Another line of evidence that Bradley has used to support





the retraction theory is the isolation of non-retractile multipiliated mutants, such as PAK/2Pfs. Phage PO4 and Pf1 can adsorb to PAK/2Pfs pili but are unable to infect this strain. Bradley interprets this result as due to the inability of the pili to retract, resulting in the resistance of multipiliated mutants to phage infection and in an increase in piliation, due to the occurrence of outgrowth without retraction (Bradley, 1974).

### 3. Twitching motility.

Twitching motility has been defined as flagella-independent surface translocation (Lautrop, 1961). It is generally studied under a microscope on thin agar surfaces and leads to the formation of a spreading zone which is lacking in bacteria unable to move on a solid surface. Henrichsen (1975) found this form of motility to be linked with the presence of pili on a number of gram negative bacteria, including *Pseudomonas*. Bradley (1980a) showed that *P. aeruginosa* strains PAK and PAO possessing retractile pili were able to exhibit this form of motility, while non-retractile mutants were not. In addition, treatment with pilus-specific antiserum or with phage PP7 (in the presence of RNase to prevent infection) inhibited twitching motility of PAK and PAO cells. Bradley suggested that the inhibition was due to the bound antibodies or the phage preventing full retraction. Although a detailed mechanism for twitching motility has not been proposed, Bradley suggests that pilus retraction and outgrowth are probably involved.



Thus it would appear that the retraction of pili plays a role in most of its functions: twitching motility, conjugation and bacteriophage adsorption. It is tempting to speculate that retraction of pili is also utilized in the adherence mechanism of piliated bacteria. Perhaps the pili initially attach to a receptor via their tips and then retraction takes place in order to bring the bacteria closer to the host cell surface, thereby allowing other attachment mechanisms to come into play.

### *C. Studies On Other Types of Pili*

Although this work is primarily concerned with the the polar pili of *Pseudomonas aeruginosa*, it is useful for comparative purposes, to consider some of the experimental data that has been acquired in the study of other types of pili. Although pili have been identified on the surfaces of most gram negative bacteria, only a few types of pili have been isolated and well-studied. Here we will consider only six specific examples, all of which are referred to in later discussions in the thesis.

#### **1. Conjugative pili: F and EDP208.**

As mentioned above, conjugative pili are encoded by self-transmissible plasmids and are necessary for the transfer of genetic material between donor cells and suitable recipient cells (Achtman *et al.*, 1971; Achtman & Skurray, 1977).





### a. F pili.

The F pilus is the most well-studied of the conjugative pili. According to electron microscopy, the F pilus has a diameter of 85 Å and can be up to 20 μm in length. The F pilin subunit has a molecular weight of 11,200, is highly hydrophobic and possesses 69% α-helix, according to circular dichroism studies (Date *et al.*, 1977). Brinton (1971) and Date *et al.* (1977) have reported that F pili are both phosphorylated and glycosylated, although the nature of the phosphate and sugar groups was not elucidated. However, Armstrong *et al.* (1981) was able to remove 65% of the carbohydrate and most of the phosphate by further purification of ColB2 pili (an F-like pilus). It was found that the pili preparations were contaminated with phospholipids which could only be removed by dissociation of the pilin into subunits in SDS, followed by column chromatography. After this treatment it was found that one mole of glucose remained per mole of pilin.

X-ray fiber diffraction studies of oriented fibers of F pili (Folkhard *et al.*, 1979a) have suggested that F pili are hollow cylinders of 80 Å outer diameter and 20 Å inner diameter. The F pilin subunits are arranged in four coaxial helices of pitch 128 Å. Each of the four helices is translated axially with respect to its neighbour to give a basic helix of 3.6 units per turn of 12.8 Å pitch.





The genetic organization of the transfer operon (tra operon), which encodes the functions necessary for the transfer of genetic material between cells has been studied by a number of groups (reviewed by Willets & Skurray, 1980). The operon consists of 19 cistrons, tra y - z, 12 of which have been implicated in the expression of pili on the cell surface (tra A,L,E,K,B,V,W,C,U,F,H,G). The traA gene encodes the F pilin structural gene (Minkley *et al.*, 1976).

b. EDP208 pili.

Another well-studied conjugative pilus is the EDP208 pilus, encoded by the F.lac plasmid EDP208 which was originally isolated from *Salmonella typhi* (Falkow & Baron, 1962). In contrast to wild-type conjugative pili, which only produce 1-2 pili per cell, derepressed mutants can be obtained of EDP208 which produce up to 20 pili per cell. EDP208 differs from F<sup>+</sup> strains in being insensitive to the F-specific RNA phage R17, while both types of pili can serve as receptors for M13 phage (Armstrong *et al.*, 1980). The two types of conjugative pili are also similar according to electron microscopy and X-ray fiber diffraction studies (Folkhard *et al.*, 1979b). The EDP208 pilin subunit has a molecular weight of 11,500 (Armstrong *et al.*, 1980) and is isolated together with tightly associated carbohydrate and phosphate, as was the case with F pilin. However, Armstrong *et al.* (1981) were able to remove all the carbohydrate and phosphate from EDP208 pilin by further purification, as discussed above. Both the amino acid composition of EDP208



pilin and the circular dichroism spectra of the pili in deoxycholate are similar to those obtained with F pili (Armstrong et al., 1980).

The sequence of the N-terminal 12 residues of EDP208 pili has been determined (Frost et al., 1983). The N-terminal amino acid is N-acetylthreonine. The N-terminal 12 residue fragment, obtained by tryptic cleavage of intact EDP208 pili, contains the major antigenic determinant of the protein (Worobec et al., 1983).

## 2. Type I pili of *E. coli*.

Type I (or common) pili are 70Å diameter filaments found on most strains of *E. coli* (both pathogenic and non-pathogenic strains). They consist of a pilin subunit of molecular weight 16,600 (Brinton, 1965) to 19,000 (McMichael & Ou, 1979). These groups both reported the presence of a reducing sugar on the pilin subunit, although it has not been well characterized. Isoelectric precipitation of Type I pili at pH 3.92 results in the formation of crystalline aggregates which have been studied by X-ray fiber diffraction (Brinton, 1965; Mitsui et al., 1973). Mitsui et al. determined from the diffraction pattern of an oriented wet gel of Type I pili, that the subunits were arranged in a simple helix with 3.15 units per turn and an axial rise per subunit of 8.09Å. Type I pili can be dissociated into smaller aggregates by boiling at pH 2 (Brinton, 1965). Eshdat et al. (1981) have reported the reversible dissociation of Type I



pili by the addition and removal of saturated guanidine-HCl. However, no evidence as to the degree of secondary structure remaining in pilin or the final aggregation state was provided in this study.

The primary function of Type I pili appears to be in bacterial adherence. The pili bind to erythrocytes of several animal species (Salit & Gotschlich, 1977), to epithelial cells (Ofek & Beachey, 1978) and to leukocytes (Blumenstock & Jann, 1982). The binding in all cases can be inhibited by the addition of D-mannose, hence the terminology mannose-sensitive pili.

### 3. Pili encoded by plasmids carried by enterotoxigenic *E. coli*.

Enterotoxigenic *E. coli* cause diarrheal illnesses. The bacterial strains involved are characterized by their ability to proliferate in the small intestine and by the production of one or more types of enterotoxin. All the strains studied thus far carry plasmids which encode a pilus operon, responsible for the adherence of the organism to the intestinal epithelium, as well as carrying the genes for the production of the enterotoxins (reviewed by Gaastra & de Graaf, 1982).





a. K88 pili.

K88 pili are encoded by plasmids carried by enterotoxigenic *E. coli* responsible for neonatal diarrhoea in pigs. The pili have been shown to mediate the adherence of the *E. coli* to the porcine small intestinal epithelium (Jones & Rutter, 1972). Subsequently, Nagy *et al.* (1978) found that injection of pregnant swine with purified K88 pili resulted in the protection of the piglets from neonatal diarrhoea caused by enterotoxigenic *E. coli*. The receptor for K88 pili on the porcine intestinal epithelium is believed to contain a terminal  $\beta$ -D-galactosyl moiety (Gibbons *et al.*, 1975).

K88 pili are 7nm in diameter and 0.2-1 $\mu$ m in length (Stirm *et al.*, 1967). The K88 pilin subunit exists in several antigenic variants (K88ab, K88ac, K88ad and K88ad(e)) of molecular weights varying from 23,500-26,000 according to SDS-polyacrylamide gel electrophoresis (Mooi & de Graaf, 1979). The amino acid compositions of all four variants were found to be similar and all lacked cysteine. The primary sequence of the K88ab pilin subunit has been determined by amino acid sequencing (Klemm, 1981) and by the determination of the base sequence of the cloned gene (Gaastra *et al.*, 1981). It was found that the K88ab pilin subunit was synthesized with a 21 residue cleavable signal sequence at its N-terminus. The mature K88ab pilin subunit consists of 264 amino acids. The C-terminus is more hydrophobic than the N-terminus, with the longest stretch of



non-hydrophilic residues being 8 residues long. Partial sequencing studies of other K88 variants (Gaastra *et al.*, 1979), has shown that the N-terminal 22 residues and the C-terminal 24 residues are fairly conserved, suggesting that the antigenic variability occurs at the center of the pilin primary sequence.

The genetic organization of the K88ac pilin operon has been elucidated by Dougan and collaborators (Dougan *et al.*, 1983; Kehoe *et al.*, 1981; Shipley *et al.*, 1981). By isolating and mapping the K88ac determinant and various K88ac-defective mutants, it was found that five cistrons, arranged in two or more operons, were required for normal expression of K88ac pili on the bacterial cell surface. These were called the *adhA* through E (for adhesion cistron). The *adhD* cistron encodes the K88ac pilin subunit (M=23,500), and is in a separate operon from the *adhA*, B and C cistrons, although all 4 cistrons are clustered on a 6.5 kilobase HindIII-EcoRI fragment. The *adhA* encodes a 70,000 dalton polypeptide which is found in the outer membrane of *E. coli* minicells harbouring the cloned pilus operon. The *adhB* and C cistrons encode two proteins of 29,000 and 17,000 daltons, respectively, which are found primarily in the periplasm of the minicells. The product of the *adhE* cistron has yet to be identified. The K88ac pilin subunit was found in both the inner and outer membrane fractions of the *E. coli* mini-cells. A similar series of studies have been initiated on the K88ab determinant (Mooi *et al.*, 1979, 1982). This





group suggested that an 89,000-dalton polypeptide (analogous to the 70,000-dalton polypeptide of the K88ac operon), serves to anchor the pilus to the outer membrane, while the periplasmic proteins, the products of the *adhB* and C, are thought to be involved in post-translational modification.

b. CFA/I pili.

CFA/I (for colonization factor antigen I) pili were first identified as a new antigen on the surface of *E. coli* H-10407, isolated from a patient in Bangladesh with a severe cholera-like diarrhoea (Evans *et al.*, 1975). These pili are encoded by a plasmid harboured by this strain of *E. coli* and confer on the bacteria the ability to adhere to the upper intestinal tract of humans. In addition, the plasmid encodes two bacterial toxins, LT and ST (for heat-labile and heat-stable toxins) which are responsible for the clinical manifestations of the disease (Sack, 1975). The adherence of CFA/I pili to various model tissue systems is mannose resistant. However, hemagglutination of erythrocytes by CFA/I positive *E. coli* strains can be inhibited by the addition of mono- and digangliosides (Faris *et al.*, 1980).

CFA/I pili are 7nm in diameter, about 1 $\mu$ m in length and are peritriciously arranged on the bacterial cell surface (Evans *et al.*, 1978). The molecular weight of the CFA/I pilin subunit was determined to be 14,500 by SDS-polyacrylamide gel electrophoresis and by amino acid analysis (Klemm, 1979). The amino acid sequence of CFA/I pilin (Klemm, 1982)





indicates no homology with K88 pilin, PAK pilin or with the N-terminal sequences of Type I pilin (Hermodsen, 1978) or EDP208 pilin (Frost *et al.*, 1983).

#### 4. Gonococcal pili.

*Neisseria gonorrhoeae* (or gonococcal) pili are chromosomally encoded (Meyer *et al.*, 1982) and have been implicated in the adherence of gonococci to host mucosal surfaces (Swanson, 1973). Gonococcal pili are approximately 6nm in diameter and 1-4 $\mu$ m in length (Swanson *et al.*, 1971). The pili from various clinical isolates of gonococcal pili vary in subunit molecular weight, amino acid composition and in immunological cross-reactivity (Buchanan, 1975; Robertson *et al.*, 1977). The molecular weight of gonococcal pilin from various strains has been reported to be between 17,500 and 21,000, according to SDS-polyacrylamide gel electrophoresis. In addition, isogenic variants from a single strain of *Neisseria gonorrhoeae* can produce at least two distinct pili types (Lambden *et al.*, 1980). As mentioned above (section A), the N-terminal 22 amino acid residues of gonococcal pilin are highly homologous with the N-termini of PAK and *Moraxella nonliquefaciens* pilins (Hermodsen *et al.*, 1978; Paranchych *et al.*, 1978; Frøholm & Sletten, 1977). Recent protein sequencing results (K.C.S. Chen, unpublished; cited in Meyer *et al.*, 1982) indicate that the N-terminal 49 residues of pili from three different gonococcal isolates are conserved, while the C-terminal sequence is variable. Schoolnik *et al.* (1982b) have isolated the two largest



cyanogen bromide fragments of gonococcal pilin from four strains of *Neisseria gonorrhoeae* (CNBr2, residue 7-ca. 96; CNBr 3, residue ca. 97-160) and shown that a type-specific, immunodominant antigenic determinant of gonococcal pilin resides in the C-terminal fragment, CNBr3, while an immunorecessive, common antigenic determinant was located in CNBr2. Schoolnik *et al.* (1982a) were able to block hemagglutination of erythrocytes by *Neisseria gonorrhoeae* cells upon addition of CNBr2, suggesting that this fragment of gonococcal pilin harbours the receptor binding domain of the protein. Similarly, Gubish *et al.* (1982) have demonstrated that CNBr2 blocks the binding of gonococci to Chinese Hamster Ovary (CHO) cells. By separating the cell surface proteins of the CHO cells by polyacrylamide gel electrophoresis and transferring them to nitrocellulose, Gubish *et al.* were able to show that CNBr2 was binding to a protein(s) of molecular weight 14-16,000 on the CHO cells. Furthermore, treatment of the CHO cells with trypsin or exoglycosidases abolished this binding, suggesting that the receptor for gonococcal pilin is a glycoprotein. Earlier studies by this group (Buchanan *et al.*, 1978), involving the inhibition of binding of gonococci to host cells, have suggested that the host receptor for gonococcal pili may resemble the terminal oligosaccharide of gangliosides. In addition, galactosidase treatment of pili or CNBr2 was found to cause a reduction of binding of pili or the proteolytic fragment to CHO cells. It should be mentioned that





previously, Robertson *et al.* (1977) had reported the presence of 1-2 hexose residues per mole of purified gonococcal pilin.

Recently, Meyer *et al.* (1982) have suggested that the antigenic variability at the C-terminus of gonococcal pilin, arises by a gene switching mechanism. Using the cloned pilin gene as a probe to test other gonococcal strains, they determined that the turn-on and turn-off of pilus expression involved a chromosomal rearrangement. This led them to suggest that a similar type of rearrangement could be used to produce antigenic variants of gonococcal pilin with a conserved N-terminus and a variable C-terminus, analogous to the mechanism of antigenic variability in trypanosomes (Williams *et al.*, 1979; Bernards *et al.*, 1981). Meyer *et al.* also found that, although the gonococcal pilin gene was expressed in *E. coli*, no pili appeared on the cell surface, implying that other factors are necessary for gonococcal pilin assembly.

To summarize, the pili studied to date all consist of a single type of protein subunit, pilin, of molecular weight varying from 11,000 to 26,000. X-ray fiber diffraction studies of F and Type I pili suggest that, in general, the pilin subunits are helically arranged in the pilus. Some pili (Type I, F, gonococcal) are thought to be glycosylated. However, the existence of a covalent linkage between the pilin polypeptide chain and a sugar has yet to be





demonstrated. Therefore, the carbohydrate associated with these pili may turn out to be a tightly bound contaminant, as was the case with EDP208 pili (Armstrong *et al.*, 1981). Several types of pili do, however, appear to interact with carbohydrate (in the form of glycolipid or glycoprotein) on host cell surfaces. The findings of Brinton (1965), Frost (1978) and Armstrong (1981), among others, suggest that pili are hydrophobic assemblies which are fairly resistant to enzymatic digestion and the action of denaturants. Finally, genetic analysis of the F, K88 and (in part) the gonococcal pilus operons suggests that pilus assembly is a complex process involving several gene products.

#### *D. Aims of the Project*

At the time this work was initiated, the work of Frost (1978) represented as thorough an analysis as any that had been carried out on purified pili. In addition, the elucidation of the complete amino acid sequence of PAK pilin was under way (Sastry *et al.*, 1983). Therefore, a series of biophysical approaches were used in order to gain as much structural information as possible about the PAK pilus, which, together with the sequence information would allow us to begin to address such questions as:

- 1). What are the nature of the interactions which maintain pilus structure and specify its assembly?
- 2). To what extent does the structure of the pilus explain its functional properties: adhesion, twitching motility and



retraction?

Although these studies were primarily focussed on PAK pili, which had already been purified (Frost & Paranchych, 1977), it was of interest to extend some of the structural analyses to PAO pili which had not yet been purified. In addition, the availability of pili purified from other bacteria was taken advantage of to provide experimental controls in many of the experiments.



## CHAPTER II

### Materials and Methods

#### A. Materials

##### 1. Bacteria and bacteriophage

*P. aeruginosa* strain PAK (ATCC 25102) is the host for phage Pf and PO4. *P. aeruginosa* PAK/2Pfs is a multipiliated mutant of wild-type PAK that is resistant to phage Pf and PO4. Frost & Paranchych (1977) have shown that 2Pfs pili are indistinguishable from wild type PAK pili. The multipiliated mutant of *P. aeruginosa* PAO, PAO/DB2, originated from a cross involving PAO1264 (FP39) X PAO-2001/PP7 in which PAO-2001/PP7 colonies with non-retractile pili were selected. Both multipiliated *Pseudomonas* strains were kindly provided by D.E. Bradley, Memorial University, St. John's, Newfoundland.

The bacteriophage PO4, which infects PAK and to a lesser extent, PAO strains (Bradley, 1973) was also obtained from D.E. Bradley. The filamentous phage Pf1 which is specific for strain PAK of *Pseudomonas* was obtained from the American Type Culture Collection (ATCC 25102-B2).

##### 2. Culture Media and Buffers

L-Broth consists of 1% tryptone, 0.5% yeast extract (DIFCO) 1% NaCl, pH 7.2. Low sulfate MOPS media (Paranchych & Graham, 1962) is 0.1M potassium morpholinopropane





sulfonate (MOPS), 0.1M N-Tris(hydroxymethyl)-methylglycine (Tricine),  $10^{-4}$ M  $\text{FeSO}_4$ , 0.19M ammonium chloride, 0.003M potassium sulfate,  $5 \times 10^{-5}$ M  $\text{CaCl}_2$ , 0.05M  $\text{MgCl}_2$ , 0.5M NaCl plus 1ml per litre of a micronutrient solution containing  $3 \times 10^{-6}$ M  $(\text{NH}_4)_6\text{Mo}_7\text{O}_{24}$ ,  $4 \times 10^{-4}$ M  $\text{H}_3\text{BO}_3$ ,  $3 \times 10^{-5}$ M  $\text{CoCl}_2$ ,  $10^{-5}$ M  $\text{CuSO}_4$ ,  $8 \times 10^{-3}$ M  $\text{MnCl}_2$  and  $10^{-5}$ M  $\text{ZnSO}_4$ . For each litre of MOPS media, 10ml of 50% glucose and 10ml of 0.132M  $\text{K}_2\text{HPO}_4$  were added as sources of carbon and phosphate, respectively.

TSB agar consists of 30g/litre tryptic soy broth (DIFCO) and 15g/litre DIFCO bactoagar. TSB agar was used for growth of cells on large trays for purification of pili and for phage assays. Nutrient agar is 0.8% (w/v) DIFCO nutrient broth and 1.5 or 2% DIFCO agar. Water agar consists of either 0.3% or 0.7% (w/v) DIFCO bacto agar in water. All bacterial media were autoclaved for 20 minutes at 20 lb/in<sup>2</sup> at 126°C except MOPS media which was filter sterilized.

Standard saline citrate (SSC) is 0.15M NaCl, 0.015M sodium citrate, pH 7.0. Phosphate buffered saline (PBS) contained 8.0g NaCl, 0.2g  $\text{KH}_2\text{PO}_4$ , 1.15g of  $\text{Na}_2\text{HPO}_4 \cdot 12\text{H}_2\text{O}$ , 0.2g KCl in 1 litre of double distilled water, pH 7.4.

### 3. Chemicals, enzymes and reagents

All solutions were prepared from analytical grade reagents in double distilled water unless otherwise stated.

Octyl-glucoside (n-octyl- $\beta$ -D-glucopyranoside) was obtained from Sigma Chemical co. and was found to be >99%



pure by thin layer chromatography on silica-G using  $\text{CHCl}_3$ - $\text{CH}_3\text{OH}$  (15:1) as a solvent. Some octyl-glucoside was kindly provided by Dr. Ruthven Lewis, University of Alberta. n-octyl-[' $^{14}\text{C}(\text{U})$ ]- $\beta$ -D-glucopyranoside was obtained from New England Nuclear at a specific activity of 314mCi/mmol and a concentration of 0.093 mg/ml in ethanol:water (9:1). octyl-glucoside was stored in a dessicator at  $-20^\circ\text{C}$ .

Acrylamide (electrophoresis pure) was obtained from BDH Chemicals Ltd., Poole, England. Dichloroindolphenylindol-phenol (DCPIP) and phenazinemetosulfate (PMS) were obtained from SIGMA. All phospholipids and detergents were also purchased from SIGMA. Trypsin(TPCK) was purchased from Worthington Biochemical Corp.

Toluene scintillation fluid consisted of 0.5g POPOP (p-Bis[2-(5-phenyloxazolyl)]-benzene) and 6.0g of PPO (2,5 diphenyloxazole) in 1 liter of toluene. Both chemicals were scintillation grade and were obtained from Eastman chemicals.

### *B. Pili Purification*

PAK/2Pfs and PAO/DB2 cells were grown on solid TSB medium in large pans as described by Frost & Paranchych (1977) and harvested by scraping the surface of the agar. The cells from 24 trays (approximately 100g, wet weight) were resuspended in 1l of standard saline citrate (SSC) and then stirred with a magnetic stirrer for 1hr at  $4^\circ\text{C}$ , after





which the cells were passed through a sieve to remove bits of agar. Removal of pili from the surface of the cells was accomplished by blending 200ml portions for 2 minutes at 2000 rpm at 0° C in a Sorvall Omnimixer. The cells were removed by centrifugation at 10,000xg for 15 minutes. To recover pili which were trapped in the cell pellets, the cells were twice resuspended in a total of 600ml of SSC and the supernatants were pooled. Finally, the supernatants from all three centrifugations were recentrifuged to remove any remaining cells. To the cell supernatant, sodium chloride was added to a concentration of 1M, sodium azide to 0.1% (w/v) and polyethylene glycol 6000 (PEG 6K) to a concentration of 1% (w/v). The preparation was allowed to stand at 4°C for 16hr during which time a phase separation occurs and the pili and flagella become insoluble. The pili/flagella precipitate was collected by centrifugation at 8000xg for 20 minutes. To remove flagella, the pH of the solution was adjusted to 4 (using HCl) and ammonium sulfate was added to a concentration of 10% (w/v). The solution was allowed to stand at 4°C for 2hr. Pili precipitated under these conditions, while the flagella remained in the supernatant. The ammonium sulfate precipitation step was repeated 2-3x until no flagella could be seen in the samples, as monitored by electron microscopy. After dialysis to remove ammonium sulfate, the pili, dissolved in water, was applied to a preformed CsCl step gradient. The gradient consisted of 5ml of CsCl of density 1.50 g/ml, a 4ml step containing CsCl of





density 1.40 g/ml, followed by three 2.5ml steps of density 1.30, 1.20 and 1.10. 20ml of pili (containing 20-30 mg of protein) was added to each 16 ml gradient and the samples were centrifuged at 20,000 rpm in a Beckman SW27 rotor using a Beckman L2-65B ultracentrifuge. As was reported by Frost & Paranchych (1977), the pili banded at a density of 1.3 g/ml. CsCl was removed by dialysis against 0.1% sodium azide. Finally, the pili were pelleted at 100,000xg in a Beckman 60Ti rotor. The pili were judged pure when SDS-polyacrylamide gel electrophoresis showed a single protein band from heavily loaded samples (100 $\mu$ g loaded onto 2mm thick gels). One usually obtains 100-200 mg of PAK/2Pfs and PAO/DB2 pili per 100g of cells, using this purification scheme.

The purified pili were assayed for possible contamination by organic phosphate by hydrolyzing 1-2mg of pili in acid and assaying the hydrolysate for total phosphate using the method of Ames (1966; described in section I.2.a). No detectable phosphate was released under conditions in which 1 mole of phosphate per mole of pilin would have been readily detected. Similarly, 1mg samples of pili, hydrolyzed in acid and lyophilized, were assayed for contaminating carbohydrate. This analysis was performed by Dr. L.S. Frost, using the methods described for carbohydrate analysis of PAK pili (Frost & Paranchych, 1977). No contaminating carbohydrate was detected by these procedures. In addition, no amino sugars were detected in acid hydrolysates of PAO pilin using a Beckman 121 amino acid analyser programmed to detect



amino sugars.

For the preparation of [ $^{35}\text{S}$ ]-labelled pili, 1 ml of a standing overnight culture of PAK/2Pfs was diluted into 500 ml of low sulfate MOPS media with 0.5% (w/v) glucose added as a carbon source. The cells were grown for 6 hr (to a cell density of  $2 \times 10^8$  cells/ml) at which time 5 mCi of  $\text{Na}_2^{35}\text{SO}_4$  (specific activity 933 mCi/mmol; New England Nuclear) was added. The cells were grown for a further 13 hours to a cell density of  $2 \times 10^9$  cells/ml. Pili were removed by blending for 2 minutes at 2,000 rpm in an omni-mixer and the cells were then removed by centrifugation at 8,000xg. The remainder of the purification was as described above, for unlabelled pili. The specific activity of the resulting pili was  $1.4 \times 10^7$  cpm/mg. A total of 4 mg of pure pili were obtained.

Radioactivity was measured by spotting aliquots on 2.3cm filter disks (Whatman #3), drying at  $110^\circ\text{C}$  and adding 5ml of toluene scintillation fluid, prior to counting in a Beckman LS-230 liquid scintillation counter.

### *C. Phage Growth*

The bacteriophage PO4 was grown on double-layer agar plates as described by Bradley (1973). Briefly, 6 inch diameter 2% nutrient agar plates were covered with a layer containing 3.0ml of 0.3% water agar, 0.2ml of various dilutions of bacteriophage stock solution in SSC and 1ml of





a standing overnight culture of PAK cells. Following incubation at 37°C overnight, PO4 phage was harvested from plates which showed confluent lysis. The phage were harvested by adding 7ml of L-Broth to each plate and shaking gently for 3hr. The plates were decanted and the cells removed by centrifugation. The resulting phage preparations were assayed using 1.5% TSB agar plates overlayed with 2.5ml of 0.7% water agar containing 1ml of phage (at varying dilutions) and 100 $\mu$ l of bacteria (from a standing overnight culture). 1 in 100 and 1 in 10 serial dilutions were made into 1ml of SSC and the 10<sup>-8</sup>, 10<sup>-9</sup> and 10<sup>-10</sup> dilutions were plated. The PO4 phage obtained by this method was found to contain  $8.8 \pm 0.9 \times 10^{10}$  pfu/ml, (pfu=plaque forming units).

Pf1 phage was also grown and assayed using the double-layer agar method. Pf1, like other filamentous phage, is extruded into the medium without lysing its host. However, small plaques are observed due to the inhibitory effect of phage infection on bacterial growth. The Pf1 stock solution prepared using the double layer agar method gave  $1.8 \times 10^{10}$  pfu/ml when assayed as described above. Growth of the phage in liquid culture was also attempted, but this resulted in approximately 10-fold less pfu/ml.

#### *D. Electron Microscopy*

Samples for electron microscopy were applied to copper grids which had been coated with parlodion and carbon. Samples were negatively stained with sodium





phosphotungstenate (NaPT), pH 7-7.2. The bacterial cells were stained with 1% (w/v) NaPT, while the purified pili were stained with 1.5-2% NaPT. Samples were photographed in a Philips EM 300 transmission electron microscope which had been calibrated with paracrystalline tropomyosin (obtained from L.B. Smillie). Pili were photographed at a magnification of 62,000, while bacterial cells were photographed at a magnification of 27,300. The diameters of pili and the reassembled pilin filaments was measured on 3X enlarged prints using a calibrated 10X magnifying glass. 30 measurements were carried out on each structural type.

#### *E. Pili Dissociation and Reassembly*

For the testing of various treatments for their ability to dissociate pili into subunits, the pili were routinely dissolved at a concentration of 1mg/ml in a solution containing 50mM sodium phosphate (pH 7) plus the reagent in question. Samples were dialyzed at 4°C, for 24 hours against each buffer, prior to ultracentrifugation or circular dichroism measurements.

For the preparation of pilin dimers in octyl-glucoside pili were suspended at a concentration of 1 mg/ml in 30 mM octyl-glucoside (n-octyl- $\beta$ -D-glucopyranoside; Sigma) and 50 mM sodium phosphate, pH 7.2. Solubilization was allowed to take place at room temperature for 30 minutes, followed by centrifugation for 5 minutes at 15,600 x g in an Eppendorf microcentrifuge, in order to remove any large



insoluble material.

Reassembly of pilin into 9nm filaments was accomplished by dialysis of the pilin dimers in octyl-glucoside against 3 changes of distilled water for 48 hours. Similar results were obtained if the dialysis was carried out against 50 mM sodium phosphate buffered at pH 7.2 or against 5mM Tris buffer, pH 8.0 containing either 5mM MgCl<sub>2</sub> or 10mM EDTA. The assembly process was monitored by viscometry as described below (section K.2).

#### *F. Competition Plaque Assay*

The competition plaque assay tests the ability of various forms of pili to bind to bacteriophage, thereby preventing the attachment of the phage to the piliated bacterial cells with the result that a decrease in the number of plaque forming units is observed. The plaque assay uses the double-layer agar method described above (section C). Varying amounts of intact pili, pilin dimers or reassembled pilin filaments were added to 1ml of 10<sup>-9</sup> and 10<sup>-10</sup> dilutions of PO4 phage (8.8x10<sup>10</sup> pfu/ml ) and incubated for 2hr at room temperature. After 2hr, 100  $\mu$ l of a standing overnight culture of *P. aeruginosa* PAK cells was added and the entire contents of the tube was mixed with 2.5ml of 0.7% water agar and poured onto TSB plates. The number of plaques was counted after incubation for 12-16hr at 37°C. The same procedure was used in the competition assay with Pf1 phage.





### G. Polyacrylamide gel electrophoresis

SDS-polyacrylamide gel electrophoresis was carried out by the method of Lugtenberg *et al.* (1975) as follows: For most experiments a slab gel apparatus with 0.8mm teflon spacers and a 20-well sample comb (purchased from Bethesda Research Laboratories) was used. For electrophoresis of *Pseudomonas* membranes, however, a home-made slab gel apparatus with 1.2mm thick spacers was used. The thinner gels with teflon spacers gave superior resolution. The running gels in both cases were 10-12cm long and the stacking gels were 1-2cm long. For electrophoresis experiments involving pure pili or *Pseudomonas* membranes, the running gel contained 15% acrylamide-0.27% methylene bisacrylamide and the stacking gel contained 7% acrylamide-0.18% bisacrylamide. For experiments with the peptides TCI and TCIII a 20% acrylamide-0.36% bisacrylamide gel was used together with the 7% stacking gel. The peptide-BSA conjugates were electrophoresed on a gel containing 10% acrylamide-0.18% bis in the running gel and 4% acrylamide-0.1% bisacrylamide in the stacking gels.

The gels were prepared using stock solution I which contained 44% (w/v) acrylamide, 0.8% (w/v) methylene bisacrylamide in water and stock solution II, which contained 30% (w/v) and 0.8% (w/v) of the two components respectively. A 0.8mm thick running gel consisted of 7.65ml of solution I, 0.55ml of a freshly made solution of 10mg/ml





ammonium persulfate, 0.45ml of 10% SDS, 8.45ml of 1M Tris-HCl, pH 8.8 and 5.35 ml of water. After filtering and degassing, 10 $\mu$ l of N,N,N',N'-tetramethylethylenediamine (TEMED) was added and the solution was poured into the gel apparatus and covered with a thin layer of polymerizing buffer (0.1% (w/v) SDS, 0.15% (w/v) ammonium persulfate and 0.05% (v/v) TEMED). After the running gel had polymerized (about 30 minutes), the polymerizing buffer was poured off and a stacking gel containing 2.25ml of solution II, 0.21ml of ammonium persulfate (10mg/ml), 0.09 ml of 10% SDS, 1.25ml of 0.25M Tris-HCl pH 6.8, 5.74 ml of water and 10 $\mu$ l of TEMED. For gels of higher or lower percent acrylamide, the amounts of solution I and II were altered and the total volume was maintained by adjusting the amount of water added.

For 0.8mm thick gels, 1-5 $\mu$ g of lyophyllized protein was dissolved in 10-20  $\mu$ l of sample buffer which contained 1.25ml of Tris-HCl (0.25M, pH 6.8), 1ml of 10% SDS, 1ml of 50% glycerol, 0.2ml of  $\beta$ -mercaptoethanol, 0.2ml of 0.04% bromophenol blue and 0.35ml of H<sub>2</sub>O. Samples were boiled for 10-20 seconds in sample buffer. Prolonged heating is to be avoided since it causes heat-dependent aggregation of pilin resulting in accumulation of material at the top of the gel. For smaller peptides (of  $M < 7000$ ) it was often necessary to load as much as 20 $\mu$ g of peptide. For gel electrophoresis of total membrane proteins, up to 100  $\mu$ g of protein was added to the 1.2mm thick gels.



The electrophoresis running buffer contained 0.25M Tris-HCl (pH 8.3), 0.192M glycine, 0.1% SDS. The gels were run at 18mA constant current until the samples had entered the running gel and then were run to completion at 25 mA constant current (approximately 6hr). After electrophoresis, the gels were stained overnight in a solution containing 0.35% (w/v) Coomassie blue, 25% (v/v) isopropanol and 10% (v/v) glacial acetic acid. Destaining was accomplished in 10% (v/v) acetic acid, 10% (v/v) methanol in water. Destaining was complete in 2-3 hr if the gel was shaken gently at 37°C against 2 or 3 changes of destain solution.

#### *H. Separation of Inner and Outer Membranes*

##### **1. Membrane Isolation**

Inner and outer membranes were separated by the method of Hancock and Nikaido (1978) with the modification that the starting material was 4 litres of PAK (or PAK/2Pfs) grown in L-Broth shaking for 12 hr. Briefly, the cells were harvested by centrifugation at 8,000xg and washed by resuspending in 800 ml 30 mM Tris-HCl pH 8.0 followed by recentrifugation. The washed cells were then resuspended in 20 ml 20% (w/v) sucrose in Tris to which 1 mg of pancreatic DNase and 1 mg of pancreatic RNase had been added. The cell suspension was then passed 2-3 times through a pressure cell at 15,000 psi. Subsequently, 2 mg of hen egg white lysozyme was added, followed 10 minutes later by 3.5 mg of the protease inhibitor phenylmethane sulfonyl fluoride (PMSF). Unbroken cells were removed by centrifugation at 10,000xg and the





supernatants were applied to sucrose gradients consisting of 1 ml of 70% sucrose in Tris, 6 ml of 15% sucrose in Tris and 6 ml of sample. After centrifugation at 187,000xg for 1 hr in a Beckman ultracentrifuge using an SW41 rotor, the bottom 2 ml was collected and applied to a second sucrose gradient which consisted of 1ml of 70% sucrose and 3ml each of 64%, 58% and 52% sucrose in Tris-HCl (30mM, pH 8.0). 2ml of crude membranes were applied to each gradient and the samples were centrifuged at 183,000xg in a Beckman SW41 rotor for 14hours at 4°C. Four bands were obtained, one at each step. The bottom band, OM1, was translucent white and consisted of highly purified outer membrane. The topmost band, IM, was red and consisted of highly purified inner membrane. The intermediate bands, OM2 and M, were orangish in colour and contained a mixture of the two types of membrane. The four bands were separated by puncturing the bottom of the nitrocellulose centrifuge tubes and collecting the four membrane fractions dropwise. The membrane samples were diluted with distilled water and centrifuged at 177,700xg for 2hr in a Beckman 60Ti rotor to remove sucrose. The pellets were resuspended in a small amount of distilled water and stored at -20°C.

For experiments in which [<sup>35</sup>S]-pili were added to monitor the efficiency of removal of extracellular pili from the membrane preparations, the labelled pili were added to the cells in 50 ml Tris buffer prior to the second centrifugation. The amount of starting culture was 250 ml





for these experiments.

## 2. Assays used in characterization of membrane fractions

### a. Total membrane protein.

Total membrane protein was assayed by the method of Lowry *et al.* (1951) with the modification that SDS was added to the samples to a concentration of 0.1% (w/v) prior to addition of the reagents for the protein determination.

### b. 2-keto-3-deoxyoctonic acid by the thiobarbituric acid test.

The lipopolysaccharide sugar, 2-keto-3-deoxyoctonic acid (KDO) was assayed using the method of Osborn *et al.* (1972) as follows: Aliquots of each membrane fraction, containing 0.1-0.5mg of protein, were precipitated with 5ml of 10% cold trichloroacetic acid (TCA) and the precipitates were collected by centrifugation at 4°C for 10 minutes at 20,000xg. The pellets were washed twice in 5ml of distilled water and resuspended in 0.7ml of 0.018N sulfuric acid and hydrolyzed at 100°C for 20 minutes to release KDO. KDO was assayed directly in the hydrolysate by the thiobarbituric acid test:

To 0.2ml of hydrolysate, 0.25ml of 0.025N  $\text{HIO}_4$  in 0.125N sulfuric acid was added and the mixture was incubated for 20 minutes at room temperature. Then, 0.5ml of 2% sodium arsenite in 0.5N HCl was added with shaking. The mixture was allowed to stand for 2 minutes to allow the iodine colour to discharge and then 2ml of 0.3% thiobarbituric acid was added



with stirring and the tubes were heated at 100°C for 20 minutes. The absorbance was measured at 548nm. A standard curve was constructed using pure KDO obtained from SIGMA chemical co. 1  $\mu$ mol of KDO gives rise to an absorbance of 19.3 at 548nm in this assay.

c. Succinate dehydrogenase activity.

The activity of succinate dehydrogenase in each membrane fraction was assayed by the method of Kasahara & Auraku (1974). Briefly, 0.3ml of Tris-HCl (50mM, pH 8.0), 0.1ml of 4mM KCN, 0.1ml of 20mM disodium succinate and 2.4ml of water were mixed and allowed to reach thermal equilibrium at 25°C. Following this, 0.1ml of the membrane preparation and 20 $\mu$ l of Triton X-100 were added and the preparation was allowed to stand at 25°C for 15 minutes. The reaction was initiated by adding dichloroindophenylindolphenol (DCPIP) and phenazinemetasulfate (PMS) as the terminal and intermediate electron acceptors, respectively. 10 $\mu$ l of 0.012M DCPIP was added at zero time followed immediately by the addition of 10  $\mu$ l of 18mg/ml PMS (stored in the dark). The contents of the tube were rapidly mixed by inversion, transferred to a cuvette, and the decrease in adsorbance as a function of time was recorded. The initial reaction velocity was determined from the slope of the linear portion of the plot of  $A_{548}$  vs. time. 1 unit of activity was defined as the amount of enzyme catalyzing the reduction of 1  $\mu$ mol of DCPIP in one minute. The molar extinction coefficient of DCPIP is  $2.2 \times 10^4 \text{ cm}^{-1} \text{ mol}^{-1}$ . The final result was expressed as





units per mg of membrane protein.

## *I. Reconstitution of pilin into a bilayer*

### **1. Preparation of lipids for reconstitution**

40mg of dimyristoylphosphatidylcholine (DMPC) and 5mg of dipalmitoylphosphatidic acid (DPPA) were weighed into a test tube. To this was added 5mg of cardiolipin, as an ethanolic solution. The mixture was partially dried in a speed vac concentrator (Savant Instruments, Hicksville, N.Y.) attached to a Sargent-Welch vacuum pump until only 0.5ml of solution remained. At this point, 1ml of chloroform to which one drop of water had been added was added to the lipids in ethanol and the mixture was left standing at room temperature until the lipids went into solution (about 2-3hr). The mixture was then redried in the speed vac concentrator and washed two times by adding 1ml of diethyl ether and redrying.

### **2. Solubilization of lipids and reconstitution with pilin in octyl-glucoside.**

1.5ml of a solution consisting of 1.25% octyl-glucoside, 5mM Tris-HCl (pH 8.0), 0.1mM EDTA and 20mM ammonium sulfate was added to the dried lipids and the mixture was heated at 50° for one hour to remove residual solvents. The mixture was then sonicated until clear (about 10 minutes) in a 12ml polyallomer tube using the microprobe of a Bronwill Biosonic III sonicator at maximum power. The sample was immersed in ice during sonication. Immediately after





sonication, 3mg of pilin in a 3ml solution containing 30mM octyl-glucoside, 5mM Tris-HCl, pH 8.0, 0.1mM EDTA, and 20mM ammonium sulfate was added and the solution was mixed by swirling. The solution was then shaken at 37°C for 10 minutes to ensure homogeneity and then the detergent/lipid/pilin mixture was dialyzed against 4 changes of 1 litre of 10mM Tris-HCl, pH 8.0, 0.2mM EDTA, 10% methanol at 4°C over a 24 hour period. The dialyzed material was concentrated by centrifugation at 50,000 rpm in a Beckman SW60Ti rotor for 3 hours. The resulting gelatinous pellet was resuspended in 1ml of 10mM Tris-HCl (pH 8), 0.15M NaCl and applied to a 1x70cm Sepharose 4B column which had been equilibrated in the same buffer. 0.4ml fractions were collected at a flow rate of 6ml/hr. For the preparation of lipid vesicles without pilin, the entire procedure was repeated without the addition of protein. For preparation of [<sup>35</sup>S]-pilin/vesicles, 1.0mg of labelled pilin ( $1.4 \times 10^7$  cpm/mg) was used.

### 3. Characterization of lipid vesicles.

#### a. Determination of protein:phospholipid ratio.

The protein content of the pilin-containing vesicles was assayed by the method of Lowry *et al.* (1951) in the presence of 0.1% SDS. The lipid content of the vesicles was determined by assaying for total phosphate by the method of Ames (1966). In this assay, the phosphate is first released by ashing the phospholipids in magnesium nitrate. 30 $\mu$ l of 10% magnesium nitrate in 95% ethanol was added to 10-100 $\mu$ l



of sample in a pyrex tube and the tubes were shaken to dryness over a flame until the brown fumes disappeared. After cooling, 0.3ml of 0.5N HCl was added and the tubes were capped with marbles and heated in a boiling water bath for 15 minutes. After cooling, 0.7ml of solution C (see below) was added and the tubes were incubated at 37°C for 1 hour. The absorbance was read at 820nm. A standard curve was constructed using 0-100 $\mu$ g of DMPC as the standard. Solution C (made fresh daily) consists of 1 part solution A and 6 parts solution B. Solution A is 10% (w/v) ascorbic acid (kept at 4°C, stable up to 4 weeks). Solution B consists of 0.42% ammonium molybdate.4H<sub>2</sub>O in 1N H<sub>2</sub>SO<sub>4</sub> (kept at room temperature).

b. Migration of vesicles in sucrose gradients.

Linear sucrose gradients (4.2ml, 0-64%), containing 30mM Tris-HCl, pH 8.0, were prepared in 4.5ml polyallomer tubes. 0.25ml of sample (vesicles, pili, or pilin/vesicles) was layered on the top of the gradient and the samples were centrifuged at 35,000 rpm in a Beckman SW50.1 rotor for 3hr. For the high salt experiments, the samples were incubated in 0.5M NaCl for 30 minutes prior to loading them onto the gradients. For the high pH experiments, the pilin/vesicles were incubated in 0.1M ammonium carbonate, pH 10.5, prior to applying the sample to the sucrose gradient. The gradients were fractionated by puncturing the bottom of the tubes and collecting 0.25-0.5 ml fractions dropwise. The absorbance of the samples were read and then aliquots were removed for





radioactive counting (on filters in toluene scintillation fluid) or for determination of the protein concentration.

c. Pronase digestion of [ $^{35}\text{S}$ ]-pilin vesicles.

Pronase digestion was carried out in 0.1M ammonium bicarbonate, pH 8.1, for 16h at 37°C. Pronase (from *Streptomyces griseus*, CALBIOCHEM.) was added to 1% (w/v) to a 0.5ml solution of pilin/vesicles in ammonium bicarbonate consisting of 0.1mg of [ $^{35}\text{S}$ ]-pilin and 2mg of phospholipids. After digestion, the vesicles were centrifuged at 35,000 rpm for 3hr in an SW50.1 Beckman rotor and the amount of radioactivity associated with the pellet and supernatant material was determined.

## *J. Protein/peptide chemistry*

### 1. Amino acid analysis

Amino acid analyses were carried out on a Durram D-500 amino acid analyser. Samples were hydrolyzed for 24, 48 and 72 hour in 6N (constant boiling) HCl containing 0.1% phenol in evacuated sealed tubes at 110°C. For most residues, the average value from the three time periods of hydrolysis was used. For serine and threonine, values were estimated by extrapolating to zero hydrolysis time and for isoleucine, leucine and valine, the 72 hour value was used. Cysteine and methionine were determined as cysteic acid and methionine sulfone by oxidizing with performic acid (Moore, 1963). The value for tryptophan was determined by hydrolyzing the protein in 3N p-toluene sulfonic acid as described by Liu





and Chang (1971). N-methylphenylalanine analysis was by the method of Coggins and Benoit (1970) in which a halved buffer ninhydrin flow through the reaction coil of a Beckman 121 amino acid analyzer allowed the detection of N-methyl-phenylalanine. For routine analysis of protein concentration, the hydrolysis period was 48hr, for peptides hydrolysis was for 24 hr.

## 2. N-terminal analysis

### a. N-terminal sequence analysis.

The N-terminal sequence of PAO pilin was determined by two automated EDMAN degradations on 150 and 80 nmol of PAO pili, with a Beckman 890B sequencer using either the 1M quadrol buffer system of Edman & Begg (1967) or the 0.1M quadrol system of Brauer *et al.* (1975). The reagents used in the identification of the phenylthiohydantoin derivatives were exactly as described by Paranchych *et al.* (1978).

### b. Dansylation and thin layer chromatography of the dansyl amino acids.

Dansylation of the amino-terminal residues of various peptides was carried out as follows (Hartley, 1970): 5nmol of peptide in 0.1M sodium bicarbonate was lyophilized in a 5mm pyrex tube and then dissolved in 10 $\mu$ l of double distilled water and 10 $\mu$ l of dansyl chloride (1-2mg/ml in acetone). The tubes were covered with parafilm and incubated for 1 hour at 37°C, after which the samples were lyophilized in a speed vac concentrator. The lyophilized,



dansylated samples were then hydrolyzed in 50 $\mu$ l of constant boiling HCl at 110°C in sealed tubes for 16 hours. The hydrolyzed material was dried and resuspended in 8 $\mu$ l of acetone:acetic acid 3:2 (v/v) for identification of the dansyl amino acids by thin layer chromatography. Thin layer chromatography was carried out in 3 solvent systems on 2 inch square microcrystalline cellulose sheets exactly as described in Needleman (1975). The presence of a single N-terminal dansyl-amino acid was used as one criterion of peptide purity.

### 3. Ninhydrin alkaline hydrolysis

Peptide concentrations were estimated by hydrolyzing lyophilized samples in 125 $\mu$ l of 5N NaOH (by taking the samples to dryness at 250°C). The samples were then neutralized by the addition of 0.25ml of 30% acetic acid. The number of amino groups in the hydrolyzed samples was determined by the addition of 250 $\mu$ l of ninhydrin solution (10ml of ninhydrin solution contains 0.2g of ninhydrin, 0.03g of hydrindantoin, 7.5ml of methylcellulose and 2.5 ml of 4N sodium acetate, pH 5.5, added in that order). The solutions were heated for exactly 15 minutes in a boiling water bath and 1.5ml of 1.5% ethanol was added to the cooled solutions. The absorbance was read at 570nm. A standard curve was constructed using 0-150 nmol of L-leucine.





#### 4. Two-dimensional peptide maps

Two-dimensional chromatography-electrophoresis was performed on 10x20cm plastic sheets which had been coated with a 0.1mm layer of microcrystalline cellulose (DEL 400, Brinkman). The samples were spotted 6cm from the anode and 2cm from the edge of the sheet. The first dimension was ascending chromatography in n-butanol-pyridine-water-acetic acid 5:4:4:1 (v/v) and was carried out until the solvent front was 1cm from the top of the sheet. Electrophoresis in the second dimension was carried out at 500V for 45 minutes using 8% formic acid-2% acetic acid (pH 1.8). Under these conditions, all the peptides migrated toward the cathode. The peptides were stained with ninhydrin:cadmium (Heathcoat & Haworth, 1969). The reagent consists of mixing a solution of 1% ninhydrin in acetone with a solution of 5g of acetic acid in acetone with a solution of 5g of Cadmium acetate in 250ml of acetic acid, 500 ml of water in a ratio of 7:1.

#### 5. High voltage paper electrophoresis

High voltage paper electrophoresis was carried out at pH 6.5 in pyridine-acetic acid-water 100:4:900 (v/v) and at pH 1.8 in acetic acid-formic acid-water 87:25:888 (v/v). Approximately 50-200 nmol of peptide was spotted as a 2-6cm wide streak at the center of the pH 6.5 paper or 11.5 cm from the anode end of the pH 1.8 paper. Electrophoresis was carried out on Whatman no. 1 filter paper at 3000V for 45 minutes (50 minutes for the separation of TCII and TCIV). The peptides were visualized by cutting away a strip from





the electropherogram and staining with ninhydrin:Cadmium. The peptide bands were cut out and eluted with water.

## 6. Citraconylation and enzymatic digestion

Citraconylation was carried out by the method of Gibbons & Perham (1970) with minor modifications as cited in Sastry *et al.* (1983). Briefly, pili dissolved in 0.05M sodium phosphate (pH 8.1) at a concentration of 3-4mg pilin/ml was treated with a 40-fold molar excess of citraconic anhydride over the number of lysines/monomer. The citraconic anhydride was added in small aliquots over a period of 4hr at 25°C with constant stirring. The pH of the reaction was maintained by the addition of 1N NaOH. After completion of the reaction, the protein was dialyzed against 4 changes of 2l of 0.1M ammonium bicarbonate, pH 8.1. Trypsin digestion was carried out on the dialyzed material directly. The digestion was carried out at 37°C for 16 hours. The enzyme was initially added at a 1 in 50 molar ratio, with a further addition after 3 hours to a final concentration of 0.04 moles of trypsin per mole of pilin. Following trypsin digestion, the soluble and insoluble fractions (abbreviated TC-soluble and TC-insoluble, for trypsin-citraconylated) were separated by centrifugation. Deblocking of the lysine residues was carried out after the initial fractionation of the TC-soluble material on Sephadex G50 (see below). This was important in preventing aggregation. Decitraconylation was accomplished by incubation in 10% formic acid at 25°C for 6hr. The tryptic subfragments of



TCIII, prepared by digestion of decitraconylated TCIII, were obtained from Dr. P.A. Sastry, as was the subfragment of TCIV (residue 128-144) (obtained by chymotryptic digestion of carboxymethylated whole pilin).

## 7. Peptide purification

TCI was purified from the TC-insoluble material by chromatography in the presence of 30mM octyl-glucoside. Approximately 2mg of TC-insoluble material was solubilized in 1ml of 30mM octyl-glucoside/ 0.05M  $\text{Na}_2\text{PO}_4$ , pH 7.0 and centrifuged to remove residual insoluble material. The supernatant was applied to a 1x40cm Sephadex G75 column equilibrated in the same detergent/buffer system. The major peak, TCI, was desalted on a 1x10cm Sephadex G10 column, which also removes most of the detergent. TCI was judged pure by the appearance of a single sharp band on SDS-polyacrylamide gels, by N-terminal analysis (by dansylation, Hartley, 1970) and by amino acid analysis.

The TC soluble material was initially fractionated on a Sephadex G50 column equilibrated with 0.1M  $\text{NH}_4\text{HCO}_3$ , pH 8.1 and eluted at a flow rate of 8ml/min. 5ml fractions were collected. TCIII obtained from this separation was judged pure by the criteria listed above.

TCII and TCIV, which coelute on G50 were further purified by high voltage paper electrophoresis at pH 6.5 followed by electrophoresis at pH 1.8 at 3000 volts for 50 minutes (section J5, above). Details of the purification of





the smaller fragments which were obtained in pure form from P.A. Sastry will appear elsewhere (Sastry, Pearlstone, Smillie & Paranchych, manuscript in preparation).

#### 8. Coupling of peptides to bovine serum albumin

The photosensitive cross-linking reagent, the N-hydroxysuccinimide ester of 4-azidobenzoic acid (AB-OSu) was obtained from P.C.S. Chong. Its synthesis was as described by Chong & Hodges (1981). The starting material for the  $^{14}\text{C}$  reagent was 4-amino-[1- $^{14}\text{C}$ ]-benzoic acid. The specific activity of the  $^{14}\text{C}$ -labelled AB-OSu was 6100 cpm/nmol. Cross-linking of the peptide to BSA was carried out as described by Worobec *et al.* (1983) but on a much smaller scale. Briefly, 50-75 nmol of each peptide was dissolved in 30  $\mu\text{l}$  of 0.16%  $\text{NaHCO}_3$ . 1  $\mu\text{mol}$  (0.3mg) of AB-OSu dissolved in 30  $\mu\text{l}$  of dioxane was added to the peptide with gentle shaking. The reaction was allowed to proceed at  $0^\circ\text{C}$  for one hour and then at room temperature overnight. The mixture was applied to a 1x25cm Sephadex G25 column equilibrated with 0.1M ammonium bicarbonate (pH 8.1) and eluted at a flow rate of 3ml/hr. 0.25 ml fractions were collected. The column effluent was monitored at 280nm and by spotting 2  $\mu\text{l}$  samples of each fraction onto filters and counting. The elution profile of the peptides was very similar to that obtained by Worobec *et al.* (1983). The void volume peak, containing azido-[ $^{14}\text{C}(1)$ ]-benzoyl-peptide, was pooled and an aliquot was hydrolyzed for amino acid analysis prior to the addition of BSA. From this analysis we could determine the





degree of incorporation of radiolabel in the peptide. From the specific activity of the  $^{14}\text{C}$ -labelled AB-OSU, the peptide concentration in the peptide-BSA conjugate after photolysis could be determined by radioactivity measurements.

The BSA-azido-benzoyl-peptide mixture was lyophyllized and resuspended in 50-100  $\mu\text{l}$  of 0.05M sodium phosphate, pH 7.0. All steps up to this point were carried out in the dark. Photolysis was carried out for 1-1.5 hr at  $4^{\circ}\text{C}$  using an RPR 208 preparative reactor (Rayonet; The Southern New England Ultra-violet co., Middletown, Conn.) equipped with 350nm lamps. The reaction mixture was then applied to a Sephadex G50 column (1x25cm) equilibrated with 1mM HCl, 0.05% NaN<sub>3</sub>, and eluted at a flow rate of 4ml/hr. The first peak, containing the covalent peptide-BSA complex, was pooled and lyophyllized.

### *K. Hydrodynamic methods*

#### **1. Ultracentrifugation**

Ultracentrifugation was carried out in a Beckman Model E ultracentrifuge with RITC temperature control equipped with either Schlieren optics or with a UV optical system with multiplex and scanner. All runs were carried out at  $20^{\circ}\text{C}$ . Sample preparation was as described above (Section E).

##### **a. Sedimentation velocity.**

The sedimentation coefficient,  $s$ , is determined from



the position,  $r$ , of the protein boundary in the ultracentrifuge cell as a function of time,  $t$ , using the relation,

$$s = 1/\omega \, d \ln r / dt$$

where  $\omega$  is the angular velocity in radians per second.  $s$  is determined from the slope of a plot of  $r$  vs.  $t$  and is expressed in Svedberg units,  $S$ , where  $1S = 10^{-13}$  seconds. The sedimentation coefficients were corrected for solvent effects using the relation (Svedberg and Pederson, 1940):

$$s_{20,w} = s_{obs} \left( \eta_T / \eta_{20} \right) \left( \eta / \eta_w \right) \frac{(1 - \bar{v} \rho_{20,w})}{(1 - \bar{v} \rho_{T,sol})}$$

where  $s_{20,w}$  is the sedimentation coefficient in water at  $20^\circ\text{C}$ ,  $s$  is the measured sedimentation coefficient,  $(\eta_T / \eta_{20})$  is the viscosity of water at temperature  $T$ , relative to water at  $20^\circ\text{C}$ ,  $(\eta / \eta_w)$  is the viscosity of the solvent relative to water,  $\bar{v}$  is the protein partial specific volume,  $\rho_{20,w}$  is the density of water at  $20^\circ\text{C}$  and  $\rho_{T,sol}$  is the density of the solvent at temperature,  $T$ .

For the determination of the sedimentation coefficients of PAK and PAO pilin, Schlieren optics were used. The distance,  $r$ , of the maximum ordinate of the Schlieren gradient from the center of the cell was measured on films at a magnification of 10. To obtain  $s_{20,w}$ , the sedimentation coefficients were determined as a function of pilin concentration in 30mM octyl-glucoside. The concentration of





pilin in octyl-glucoside was determined by amino acid analysis or by the Lowry protein determination using a correction factor of 0.7 (to relate the BSA standard curve to the concentration determined from amino acid analysis).

For the determination of the sedimentation coefficient of pili in the presence of denaturants and detergents, UV absorption optics were used. These sedimentation coefficients were corrected for the viscosity of the solvent, but not for the solvent density in most cases. Where literature values were unavailable, solvent viscosity was determined with an Oswald viscometer (see below). The velocity used in these runs was between 28,000 and 60,000 rpm, depending on the aggregation state of the pili.

#### b. Sedimentation equilibrium measurements.

The weight average molecular weight of PAK and PAO pilin in octyl-glucoside was determined as a function of loading concentration ( $C_0$ ) in a conventional sedimentation equilibrium experiment as described by Chervenka (1970). The runs were carried out at 17,000 rpm and utilized UV optics with multiplex and scanner. The concentration of protein ( $c$ ) as a function of its position ( $r$ ) in the cell at equilibrium was measured from the UV scans. The weight average molecular weight is determined from a plot of  $\ln c(r)$  vs  $r^2$  using the relation:

$$M_w(r) = \frac{2RT}{(1-\bar{v}\rho)\omega^2} \frac{d\ln c(r)}{dr^2}$$





where  $R$  is the universal gas constant and the other terms have been defined. A program written by Wolodko (1974) was used to obtain point average molecular weights. The program fits  $\ln(c)$  vs  $r^2$  to a second degree polynomial using a least squares procedure and calculates the point average molecular weights from the slope. The input to the program was the measured values of  $r$ ,  $c$  (as an absorbance measurement), the protein partial specific volume, the solvent density, the angular velocity, the temperature and a cell constant. For plots of  $M$  vs concentration, the absorbance measurements were converted to protein concentrations using an extinction coefficient of 1.3, for a 1mg/ml solution of pili in a 1cm cell at 280nm (see section L1, below). Samples were dialyzed against octyl-glucoside for 48hr prior to the sedimentation equilibrium measurements. In order to determine the concentration dependence of  $M$ , runs were carried out at loading concentrations between 1 and 0.4 mg/ml.

## 2. Viscometry

Viscosity measurements were carried out in a 0.5 ml capacity Oswald Viscometer (Cannon 25A294) held at 20°C in a constant temperature water bath. The flow time for water was about 8.6 minutes in this viscometer. The results were expressed as:

$$\eta_{sp}/c = \left( \frac{t_2 \rho_2}{t_1 \rho_1} - 1 \right) \div c$$

where  $t_2, t_1$  are the flow times from protein/detergent and



detergent alone, respectively. The approximation that  $\eta_{rel} = t_2/t_1$  was used throughout.

For pilus dissociation experiments, 1 mg/ml samples of pilin at various concentrations of detergent were dialyzed overnight against the same concentration of detergent to provide suitable blanks for viscometry. For assembly experiments it was necessary to know the rate of detergent removal. Therefore, a calibration curve of octyl-glucoside concentration versus time of dialysis at 4°C was carried out using n-octyl-[<sup>14</sup>C(U)]-β-D-glucopyranoside to follow detergent removal. At 4°C, a 1 mg/ml solution of pili in octyl-glucoside (1 ml) dialyzed against 1 litre of distilled water resulted in equilibration in 12 hours. Because protein concentrations changed slightly during dialysis, the protein concentration was determined on each sample subsequent to the viscosity measurement.

### 3. Density Measurements

Density measurements were carried out using an Anton Paar precision densimeter Model DMA 60 at 20 ± .005°C. This densimeter is of the mechanical oscillator type (Kratky *et al.*, 1973) and consists of a U-shaped tube which can be filled to a highly reproducible volume. The temperature of the tube is maintained using a circulating water bath (Lauda K2 thermoregulator). Density measurements are measured by recording the period of oscillation, T, of the tube when it is filled with various solutions. The difference in density





between two solutions,  $\rho_2 - \rho_1$ , is given by,

$$\rho_2 - \rho_1 = A (T_2^2 - T_1^2)$$

where A is a machine constant, determined by measuring T for solutions of known density. For this purpose, T was measured when the tube was filled with dry air and with water. The measurements were made for a total of 15 minutes each. Individual measurements of T are displayed on the digital readout every 20,000 oscillations (about every minute). The average value of T over the 15 minute period was used. In between samples, the tube was washed first with water, then with 3N HCl/50% ethanol, again with water, then with methanol and finally the tube was dried with a stream of air (dessicated). Samples were allowed to come to thermal equilibrium before making measurements. The densities of phosphate buffer, of various concentrations of detergent in phosphate buffer and of various concentrations of pili in phosphate buffer and octyl-glucoside were determined in order that the partial specific volume of octyl-glucoside and of the pilin/octyl-glucoside complex could be determined. Seven measurements of density were made for each type of pilin at protein concentrations between 1.5 and 5 mg/ml. The  $\bar{v}$  for detergent was determined at 10 concentrations both above and below the critical micelle concentration (CMC). The partial specific volume,  $\bar{v}$  is given by the relation,





$$\bar{v} = 1/\rho_0 \left(1 - \frac{\rho - \rho_0}{c}\right)$$

where  $\rho$  and  $\rho_0$  are the density of the sample and the solvent, respectively and  $c$  is the concentration of the solute in g/ml.

#### 4. Equilibrium Dialysis

Equilibrium dialysis measurements were carried out at room temperature in 1 ml cells attached to a wheel which tumbled the cells at 10-15 rpm. 1 mg/ml pili solutions in a given concentration of detergent were dialyzed against the same concentration of detergent containing the radioactive label. Dialysis was carried out for 24 to 96 hours, after which time samples were removed for counting on filters in toluene scintillation fluid. For concentrations of detergent below 30mM, equilibrium was generally reached within 24 hrs. At higher detergent concentrations, however, longer periods of dialysis were required. Sufficient [ $^{14}$ C]-octyl-glucoside was added so that a difference in CPM (protein side of membrane) vs CPM (detergent-only-side) of at least 5% was obtained under the conditions used. For example, the specific activity of octyl-glucoside was 40 cpm/nmol for the experiment carried out at a total concentration of 30mM octyl-glucoside. By increasing the amount of radioactivity in the experiments carried out at lower octyl-glucoside concentration, we could detect the binding of as little as



2 moles of detergent/mol of protein. Octyl-glucoside binding to the standard proteins used in the calibration of the gel exclusion column was carried out at 30mM octyl-glucoside using the same procedure. The standard protein samples contained 80-90nmol of protein per ml.

## 5. Gel exclusion chromatography

The pilin molecular weight in octyl-glucoside was determined by gel exclusion chromatography on a Sephadex G200 (Pharmacia Fine Chemicals) of dimensions 1 x 25cm which had been equilibrated with 2 column volumes of octyl-glucoside, 0.05M Na<sub>2</sub>PO<sub>4</sub>, pH 7.0. A calibration run was carried out under the same conditions using 0.5 mg each of Bovine serum albumin (M=65,000), ovalbumin (M=43,000), Myoglobin (M=17,000), cytochrome c (M=13,000) and bacitracin (M=1411). 2 separate calibration runs were carried out (one with BSA, myoglobin and bacitracin; the other with ovalbumin, cytochrome C and bacitracin) so that species close together in molecular weight could be resolved.

Gel exclusion chromatography in the presence of [<sup>14</sup>C]-octyl-glucoside was carried out using the same column described above. The column was equilibrated with 2 column volumes of 30mM [<sup>14</sup>C]-octyl-glucoside at a specific activity of 6830 cpm/ $\mu$ mol. Pilin dissolved in the labelled octyl-glucoside was applied to the column and 0.5ml fractions were collected. The amount of protein in each fraction was determined by measuring the absorbance at 280nm and using an



extinction coefficient for pilin of 26.5/ $\mu$ mol (at 280nm in a 1cm cell). 100 $\mu$ l aliquots of each fraction were counted to determine the amount of octyl-glucoside associated with each fraction. The specific activity used in these calculations was taken from the baseline of radioactivity drawn through the radioactivity profile of the column.

### *L. Spectral methods*

#### **1. Protein concentration**

Most protein concentrations used in the spectral measurements were calculated from the extinction coefficient at 280nm of 1.3, for a 1mg/ml solution of pili in a 1cm cell. This value was determined by measuring the absorbance of samples whose concentrations had been determined by quantitative amino acid analysis (as described in section J1). It should be noted that, to alleviate scattering problems, longitudinal aggregates were removed by centrifugation of the samples for 5 minutes at 15,600xg in an eppendorf microcentrifuge. The supernatant was then removed, its absorbance measured as described below, and aliquots were removed for amino acid analysis.

Unless otherwise stated, all spectral measurements were carried out in 0.05M  $\text{Na}_2\text{PO}_4$ , pH 7.





## 2. Circular Dichroism

The circular dichroism studies of Chapter IV were performed on a Cary model 60 recording spectropolarimeter equipped with a Cary 6001 CD attachment, in accordance with the methodology of Oikawa *et al.* (1968). Concentrations were determined by amino acid analysis and molar ellipticities were calculated using a mean residue weight of 107 (determined from the amino acid composition of PAK pilin).

In the absence of any buffer, significant light scattering was observed for intact pili due to the formation of longitudinal aggregates which have been observed in the electron microscope (Chapter VI). However, in the presence of 50 mM phosphate buffer, the apparent sedimentation coefficient decreases slightly, the ellipticity at 220 nm decreases by 10%, and less noise was observed in the spectra. A further increase in buffer concentration had no effect on the CD spectrum or the apparent sedimentation coefficient. During the run the dynode voltage did not exceed 0.6 KV at 200 nm.

The percent  $\alpha$ -helix and  $\beta$ -sheet were calculated using the experimental ellipticities at 215, 220 and 225 nm and the theoretical values for 100%  $\alpha$ -helix, 100%  $\beta$ -sheet and 100% random coil, provided by Chen *et al.* (1972), using the equations:



$$[\theta]_{215} = -25.7 f_{\alpha} - 9.43 f_{\beta} + 0.669 f_c$$

$$[\theta]_{220} = -29.5 f_{\alpha} - 6.06 f_{\beta} + 1.80 f_c$$

$$[\theta]_{225} = -28.7 f_{\alpha} + 1.54 f_{\beta} + 0.264 f_c$$

where  $f_{\alpha}$ ,  $f_{\beta}$  and  $f_c$  are fraction  $\alpha$ -helix,  $\beta$ -sheet and random coil respectively and  $[\theta]_{\lambda}$  is the molar ellipticity at the wavelength specified by the subscript.

The circular dichroism measurements described in Chapter VII and Chapter VIII were carried out on a Jasco J500C spectropolarimeter according to the methodology of Oikawa *et al.* (1968) with pantoyl-lactone as an additional standard. Molar ellipticities were calculated as stated above. Longitudinal aggregates of pili were removed by centrifugation, to reduce the light scattering problems prior to the measurement of the absorbance of the samples (for the determination protein concentration). The fraction  $\alpha$ -helix and  $\beta$ -sheet were determined using a program developed by Provencher and Glöckner (1981) which analyzes CD spectra as a sum of spectra of 16 proteins whose structures had been determined by X-ray crystallography. The input to the program was the molar ellipticities in 1nm intervals from 190 to 240nm. As a check on the calibration, of the instrument a CD spectrum was obtained for hen egg-white lysozyme (one of the proteins in the reference set) and run through the program. We obtained 41%  $\alpha$ -helix and 22%  $\beta$ -structure in agreement with the results of Provencher and Glöckner.





For the determination of the circular dichroism spectra of pilin reconstituted into phospholipid vesicles, a preparation of vesicles which did not contain pilin, but were of the same size as the pilin/vesicles, were used as a blank. The protein concentration used in this experiment was about 0.3 mg/ml.

### 3. Alkaline pH titration

Samples were prepared for measurement of absorbance and ellipticity as a function of pH as follows. 0.2M buffers were prepared at each pH using sodium phosphate or sodium bicarbonate buffers. 2mg/ml solutions of each of the three forms of pilin aggregate were diluted 2-fold into each buffer solution and the sample was used both for determination of the ellipticity at 222nm and for a UV absorbance scan from 350 to 260 nm. In the case of pilin/octyl-glucoside, the buffers were made up in octyl-glucoside so as to maintain the detergent concentration. Absorption measurements were made on a Cary model 219 spectrophotometer using 1cm matched cells. Examination of the UV absorption spectra between 350 and 320nm showed that light scattering was minimal provided that the samples had been centrifuged to remove large aggregates as described above.

### 4. Solvent perturbation measurements

Solvent perturbation experiments were carried out on a Cary 118c spectrophotometer operated in the autoslit mode. Difference spectra were recorded at a full scale absorbance





range of 0.05 at a scan rate of 0.1 nm/sec. The reference and sample cells were thermostated with a circulating water bath (Lauda K 2R thermoregulator). The experiments used split compartment tandem cells with a path length of 0.874 cm. The baseline was generated with 2mg/ml protein in both the reference and sample cell in one compartment and with 40% DMSO in the other compartment of both cells (the DMSO was made up in octyl-glucoside for the experiments with pilin/octyl-glucoside). The contents of the sample cell were then mixed and the spectrum recorded. Then the contents of the reference cell were mixed and a second baseline recorded. If the second baseline differed substantially from the first, the results were discarded. The perturbation spectra of N-acetyl-tryptophan and N-acetyl-tyrosine ethyl ester were determined separately and as a 1:1 molar ratio so that the contribution of tryptophan and tyrosine at each wavelength could be recorded. The effect of octyl-glucoside on these spectra was also tested.

## 5. Fluorescence measurements

Fluorescence measurements were carried out on a Perkin-elmer MPF-44B spectrofluorometer operating in the ratio mode with 5nm bandwidths for excitation and emission slits. A constant temperature of 20°C was maintained in the cells by a circulating water bath. The excitation wavelength used was 295nm to ensure that light absorption was primarily due to tryptophan. The initial  $A_{295}$  of the protein was  $\leq 0.05$  to avoid the inner filter effect. The fluorescence



quenching was measured at the emission maximum of the sample and was initiated by the addition of 10  $\mu$ l aliquots of 8M acrylamide solutions to both the sample and a blank (to correct for acrylamide adsorption). Cells of 1 cm pathlength were used and stirring was by a magnetic 'flea.' The protein solutions were 2.0 ml. The results were plotted as  $F_0/F$ , where  $F_0$  is the initial fluorescence and  $F$  is the fluorescence after addition of quencher, corrected for dilution of the protein.

### *M: Immunological methods*

#### 1. Preparation of Antisera

The anti-pilus antisera used in the immunoelectrophoresis experiments and in the identification of pilin pools in the membranes of *Pseudomonas* (Chapter VII) was prepared as follows: New Zealand white rabbits were injected intravenously with 500  $\mu$ g of pure PAK or PAO pili in sterile saline. A total of 3 injections, 3 days apart were administered, and antisera was collected 4 weeks after the first injection.

For the ELISA and Immunoblot experiments, antisera against PAO and PAK pili was obtained from New Zealand white rabbits by an alternate procedure, which gave higher titers: 100 $\mu$ g of pure pili dissolved in an equal volume of Freund's complete adjuvant was injected subscapularly and intramuscularly in the gluteal area. The pili were thoroughly mixed with the adjuvant by squirting the solution





back and forth using a double hubbed syringe. Booster injections were administered at two one month intervals with 100  $\mu$ g of pili dissolved in an equal volume of saline and Freund's incomplete adjuvant. The rabbits were bled 2 weeks following the second booster injection. The antiserum from one rabbit (for each type of pili injected) was used for the mapping of the antigenic determinants (Chapter IX), so that variations between animals did not complicate the results.

## 2. Immuno-electrophoresis

Counter- and rocket-immuno-electrophoresis were carried out as described by Tsang & Marusyk, (1980). Briefly, counter-immuno-electrophoresis was carried out on 8x8cm gel-bond film, covered by a 20ml layer containing 1% agarose, 3% Triton X-100 and 3% polyethylene glycol 6000. Wells were placed in two rows, 3cm apart. 10 $\mu$ g of pili in 10 $\mu$ l of Tris buffer was placed in each of the row of wells closest to the cathode. In the opposite wells, 50 $\mu$ l of 1 in 2 serial dilutions of anti-pilus antisera were placed. Electrophoresis was carried out for 16h at 3V/cm in Tris-glycine electrophoresis buffer, pH 8.3 (described in section G). The precipitin lines were visualized as follows: The gel was dried by overlaying it with paper towels and a heavy object. The gel was then washed with PBS (5x5minutes) and redried. The gel was then stained and destained with Coomassie blue by the method of Fairbanks *et al.* (1971). Rocket immuno-electrophoresis was carried out in a similar manner except that the gel was prepared in two parts. The





upper gel consisted of 15ml of 1% agarose/Triton/PEG as above plus 5% v/v antiserum. The lower gel in which wells were cut for the pili samples consisted of 5ml of the same gel, minus the antiserum. Electrophoresis was carried out for 20h at 3V/cm.

### 3. Transfer of proteins from SDS-polyacrylamide gels to nitrocellulose paper followed by immunological detection.

Proteins were transferred from SDS-polyacrylamide gels to nitrocellulose paper, reacted with anti-pilus antibodies and the bound antibodies detected using the methodology of Towbin *et al.* (1979) with the modification that  $^{125}\text{I}$ -Protein A from *Staphylococcus aureus* was used in place of  $^{125}\text{I}$ -labelled sheep immunoglobulin G.

Transfer to nitrocellulose was carried out using an Electro-blot apparatus (E-C apparatus). The gel was placed on a piece of filter paper which had been soaked in electrophoresis buffer and placed on the cathode side of the electrophoretic grid. The gel was overlayed with a piece of nitrocellulose paper (.45  $\mu\text{m}$ , Schleicher and Schuell) that had been pre-hydrated in distilled water. Care must be taken at this point to eliminate air bubbles between the gel and the nitrocellulose paper. The nitrocellulose paper was then covered with a second piece of moistened filter paper (Whatman 3M), followed by a sponge (also soaked in buffer), to hold the gel in place. The electrophoresis buffer consisted of 0.025M Tris-HCl, pH 8.3, 0.192M glycine and 20%



(v/v) methanol. The buffer was stored at 4°C prior to use, so that when the transfer was carried out at room temperature, the buffer acted as a coolant. The buffer was circulated by means of a pump during electrophoresis and could be reused several times. Electrophoresis was carried out for 2-6 hour at 4mA/cm<sup>2</sup>. For thin gels (0.8mm thick), it was found that proteins up to 68,000 daltons were completely transferred within 3 hour. This was determined by staining the gel with Coomassie blue after transfer of the proteins. However, with the thicker gels (1.2mm), used in the electrophoresis of *Pseudomonas* membranes, proteins of molecular weight 25,000 and greater were still visible in the gel after 4 hours of transfer, although pilin was quantitatively transferred within this time period. Usually, samples were run in duplicate so that one half of the gel could be stained and the proteins from the other half of the gel transferred to nitrocellulose.

Pilin or peptide fragments of pilin bound to the nitrocellulose paper were detected by reacting the transfer first with anti-pilus antibodies and then with <sup>125</sup>I-Protein A to detect the bound IgG. The assay involves the use of two buffer systems. Buffer I consists of 150mM NaCl, 5mM EDTA, 50mM Tris-HCl pH 7.4, 0.25% gelatin and 0.05% (v/v) Nonidet P40 (nonionic detergent P40, an octyl-phenol-ethyleneoxide condensate containing an average of 9 ethylene oxide per molecule, obtained from SIGMA Chemical co). Buffer II consists of 1M NaCl, 5mM EDTA, 50mM Tris-HCl pH7.4, 0.25%





gelatin and 0.4% (w/v) sarcosyl (97% n-lauryl-sarcosine, SIGMA).

After transfer of the proteins to nitrocellulose, the paper was immersed in 25-50ml of Buffer I containing an appropriate dilution of antisera (1:50 to 1:500 in these studies). The nitrocellulose paper could be stored in a moist filter paper in a sealed plastic bag for up to one week prior to initiation of the reaction. The transfer was incubated with antisera for 2-12 hour (routinely left overnight) at 37°C with shaking. This was followed by a 2 hour washing step in 50ml of buffer I (this step may be extended for up to 12hr) also at 37°C with shaking, and then  $^{125}\text{I}$ -Protein A diluted in buffer I was added and the transfer was incubated for a further 2-12 hour. 1  $\mu\text{Ci}$  of  $^{125}\text{I}$ -Protein A (obtained from New England Nuclear at a specific activity of 87-97  $\mu\text{Ci}/\mu\text{g}$ ) was added per 8x12 cm nitrocellulose transfer. After incubation with  $^{125}\text{I}$ -Protein A, the nitrocellulose transfer was washed for 1 hour in Buffer II (50ml) at 37°C with shaking. Prolonged incubation in Buffer II is to be avoided, since the high salt and high detergent appears to cause loss of the bound proteins from the nitrocellulose paper with time. Finally, the transfers were washed thoroughly with distilled water and dried between paper towels. The dried nitrocellulose transfers were used directly for autoradiography using KODAK X-OMAT AR film. The film was exposed at -70°C for 2 to 7 days and then developed in a KODAK X-OMAT developer. It should be noted





that streaking of the bands on the final autorad was often observed with strong antigens. It was found that the streaking problem could be alleviated by loading less material onto the gel to be transferred. For example, 2-5  $\mu\text{g}$  of PAK pilin was normally loaded onto 0.8mm gels for staining purposes. However, for transfer to nitrocellulose and immunological detection, it was necessary to reduce this amount to 0.1-0.5  $\mu\text{g}$  to avoid streaking.

#### 4. Detection of antigenic species with ELISA

The principles of the enzyme-linked immunosorbant assay (ELISA) have been described by Voller *et al.* (1974) and are explained in Chapter III. PAK and PAO pili were dissolved in coating buffer (0.5M sodium bicarbonate, 0.1% sodium azide, pH 9.6) at concentrations between 1 and 10  $\mu\text{g}/\text{ml}$ . It was found that saturation of the wells of the microtiter plates occurred at concentrations of PAK and PAO pili between 4 and 5  $\mu\text{g}$  per ml, therefore all subsequent experiments were carried out using pili at 5  $\mu\text{g}/\text{ml}$ . The peptides used in these studies were coated at concentrations of 1-1.5 nmol/ml. Doubling this amount did not result in higher readings in the assay and therefore, these concentrations were assumed to be saturating. 0.2ml of antigen in coating buffer was placed in the wells of microtiter plates (Immulon I, Dynatech Laboratories Inc., Alexandria, Va.). After incubation for 16hr at 4°C in a moist atmosphere, the antigen saturated wells were washed 3 times for 3 minutes each in phosphate buffered saline containing 0.05% (v/v) Tween 20



(PBS-Tween). Following the washing step, the wells were filled with various dilutions of rabbit anti-pilus antiserum diluted in PBS-Tween containing 1% (w/v) BSA. Incubation with antiserum was for 2 hr at room temperature. The resulting antigen/antibody complexes were then incubated with alkaline phosphatase-conjugated goat-anti-rabbit antiserum (obtained from Boehringer-Mannheim and used at a 1:2000 dilution in PBS-Tween). Incubation in the conjugate was for 2-2.5 hr at room temperature. Following a further three washes in PBS-Tween, the alkaline phosphatase substrate, p-nitrophenylphosphate (obtained from Sigma as 5mg tablets) was added as a 1mg/ml solution in 10% diethanolamine. After an appropriate time interval (about 15 minutes) the absorbance at 405 nm was determined with a Titertek multiscan ELISA plate reader. In general, 1 in 2 serial dilutions of antiserum were made starting at a 1:500 dilution.

## *N. X-ray Diffraction Methods*

### **1. Preparation of oriented fibers of pili**

Pili were centrifuged in 0.8ml nitrocellulose tubes (used with appropriate adaptors) in an SW50.1 rotor at 35,000 rpm for 2.5 hour at room temperature. The pellet was resuspended to a concentration of 10-50mg/ml in distilled water. Storage of concentrated pili solutions for 1-2 weeks at 4°C promoted the formation of a birefringent phase (Lapointe & Marvin, 1973). Fibers were prepared from these





solutions by placing a 5-10 $\mu$ l drop of concentrated pili between the ends of two glass rods which had been placed 0.8-1.5mm apart on a glass slide using plasticine supports. The glass rods were prepared from 10 $\mu$ l capillary tubes (Drummond microcaps) by sealing the ends in a flame and coating them with silicone (SIGMACOTE). The fibers were immediately transferred to a 98% relative humidity (r.h.) environment to allow slow drying. After 48 hr at 98% r.h., the fibers were transferred to a 92% r.h. atmosphere chamber for 24 hour and then to a 75% r.h. chamber for a further 24hr. The relative humidity was controlled using saturated NaCl (75% r.h.), saturated K<sub>2</sub>HPO<sub>4</sub> (92%) and saturated CuSO<sub>4</sub>.5H<sub>2</sub>O (98%; Spencer, 1962). The resulting fibers were cemented to the glass rod at one end (using 5 minute epoxy cement) and cut free at the other end. Fibers could be stored indefinitely at 75% r.h., 25°C. Preparation of the fibers was usually carried out at room temperature since no improvement was observed by preparing fibers at 4°C or at 37°C. For preparation of non-crystalline specimens, a fiber which had been shown to diffract well was placed in a quartz capillary and swelled by adding a drop of water. The capillary was then sealed.

## 2. Diffraction methods

The diffraction methods used have been described by Marvin *et al.* (1974). Pinhole cameras (Langridge *et al.*, 1960) were used for routine measurements at a specimen to film distance of 7.5cm. Diffraction patterns were also





recorded at a specimen to film distance of about 10.5cm in order to enlarge the low angle region. The latter diffraction patterns were recorded using a double focussing camera similar to that described by Franks (1958). Exposures were for 48-72 hour with the Frank's camera and for 8-24 hour with the pinhole camera's. Measurements in Edmonton were made with a 4.5cm specimen to film distance pinhole camera purchased from Struther Arnott (Purdue University).

The precise specimen to film distance was determined by dusting the fiber with finely powdered calcite, to give a diffraction ring at  $3.029\text{\AA}$ . The specimen to film distance is given by the relation,

$$SF = D/\tan 2\theta$$

where  $D$  is the measured distance of the calcite ring from the origin of the diffraction pattern and  $\theta$  is determined from Bragg's law,

$$n\lambda = 2d\sin\theta$$

where  $d$  is the distance in real space of the calcite ring ( $3.029\text{\AA}$ ),  $\lambda$  is the wavelength of copper  $K_{\alpha}$  radiation ( $1.5418\text{\AA}$ ) and  $n=1$ .

The fibers were aligned in the camera using an optical bench which also allowed the tilt of the fiber to be specified. The tilt angle,  $\gamma$ , required for a given



layer-line to intersect the sphere of reflection is given by the relation,

$$\gamma = \sin^{-1} (1.5418 Z/2)$$

where  $Z$  is the reciprocal space coordinate of the layer-line of interest.

Cameras were filled with helium to reduce air scatter. Humidity control (and therefore control of the water content of the fiber) was achieved by bubbling helium through saturated salt solutions (listed by Marvin, 1966). All X-ray diffraction measurements were carried out at room temperature.

X-rays were generated on a Jarrel-Ash microfocus unit or on an Elliot GX18 rotating anode generator with a Cu target and nickel filtering of X-rays. The generators were run at 40kV, 40-45mA (ac current). Scattered X-rays were recorded on Ilford Industrial G film and later on KODAK NO-SCREEN film, since Ilford industrial G was removed from the market. Film was developed for 5 minutes in Ilford phenisol, development was stopped in 2% (v/v) acetic acid and films were fixed for 4 minutes in Ilford Hypam. A film pack of several films was used in each camera for each exposure so that a film of suitable exposure could be selected for integration of the intensities.



### 3. Measurement of positions and intensities of reflections

Positions of intensity on diffraction patterns were measured using a computer program called GUCKMAL, written by J.E. Ladner, which is an extension of the system described by Marvin *et al.* (1974). Films were digitized using an Optronics scanner on-line to a Nord-10 computer, on a 50 $\mu$ m x 50 $\mu$ m raster. The digitized plots were then displayed on the screen of a Tektronix TK 4014 computer terminal using threshold plots. Parts of the image could be magnified and the threshold for plotting could be varied. The positions of intensity were either measured by setting the cursors of the Tektronix at the center of the spot or by using the cursors to draw a box around the spot and from this box, calculating the center of gravity. The tilt of the fiber could be calculated by GUCKMAL using the coordinates of the reflections in all 4 quadrants of the film, using the equations of Franklin & Gosling (1953). The (x,y) coordinates measured by GUCKMAL were converted to polar-cylindrical coordinates in reciprocal space, as described by Marvin *et al.* (1974), using the calcite diffraction ring for calibration. The integrated intensities of the crystalline reflections were determined using this program and local background was subtracted (as described in Wachtel *et al.*, 1974). Films were scaled together by fitting the strongest crystalline amplitude of every set (the 1,1 reflection) to the continuous equatorial diffraction amplitudes.





The continuous intensity distribution along the layer-lines was determined using an approach initiated by Wachtel *et al.* (1974), using a set of programs similar to those described by Makowski (1978). The program RADSG is a fortran program for the analysis of intensity data where the contributions of adjacent layer-lines overlap. Using this program, the layer lines were deconvoluted for the Gaussian angular intensity distribution due to the disorientation of particles in the fiber. The input to the program was the intensity data from one film quadrant as measured on the Optronics scanner, after conversion to cylindrical-polar coordinates. The polar raster had radial intervals of 100  $\mu\text{m}$  which corresponds to distances of less than  $10^{-3}\text{\AA}$ . A set of disorientation functions and background were fit to the intensity distribution in each radial shell using a least squares procedure. The disorientation functions were centered on the theoretical positions of layer lines, calculated from the tilt of the fiber relative to the X-ray beam and from the layer-line spacing. Several trials were carried out to refine the tilt angle and the standard deviation of disorientation which produces the best fit to the data. Since background was calculated for each radial shell independently, the calculated background had high frequency fluctuations especially at radii that include strong intensity, therefore the background was smoothed manually, by inspection.



#### 4. Radial electron density distribution

The radial electron density distribution was calculated from the continuous equatorial diffraction amplitudes using the constrained regularization method of Provencher (1979). This method minimizes the danger of artifacts caused by the instability of the least-squares solution to noise in the data, by constraining the solution to the smoothest non-negative one that is consistent with the data. Since the radial density is centrosymmetric about the origin, only real amplitudes need be considered. The radial electron density is cylindrically averaged, as the particles can have all possible rotations about their long axes. The expression for the radial electron density in a two-dimensional projection can be given by: (Klug *et al.*, 1958),

$$\rho(r) = \pm 2\pi \sum_R ( \langle |F(R)|^2 \rangle_\psi )^{\frac{1}{2}} J_0(2\pi Rr) R \Delta R$$

where  $\langle \rangle_\psi$  indicates the cylindrical averaging.

#### 5. Generation of $\alpha$ -helical models and calculation of their transforms

$\alpha$ -helical models were generated using a program called OPTKNOB which generates line segments (specifying the direction of a helix, for example), places structural units on each line segment (in this case alanine in a conformation predicted for a coiled coil) and generates coordinates for molecules related to the source structure by helical symmetry. The packing of  $\alpha$ -helical segments, representing



part of the pilin subunit, was modified using OPTKNOB until no unfavourable close contacts ( $<4\text{\AA}$ ) were reported by OPTKNOB. A second program HELTRAN (for helical transform) was used to calculate the transforms of various models. This data was then converted to layer-line plots for comparison with the observed transform using a program called DIFF. These programs are part of a package, FIBER, developed by D.A. Marvin and colleagues at the European Molecular Biology Laboratory, Heidelberg, Germany. The methods used in the model building approach to solving structures have been discussed in detail by Marvin & Wachtel (1975, 1976).





### CHAPTER III

#### Purification and Preliminary Characterization of Pili Isolated from *Pseudomonas aeruginosa* strain PAO

Previous studies of *Pseudomonas* pili have focussed on strain PAK and the multipiliated mutant, PAK/2Pfs (Frost & Paranchych, 1977; Frost *et al.*, 1978; Paranchych *et al.*, 1978). The extension of these studies to the pili of strain PAO of *Pseudomonas* (PAO pili) was of interest for several reasons. Firstly, the study of a homologous series of proteins is often useful in identifying structurally and functionally important features. Secondly, strain PAO of *Pseudomonas* has been the subject of extensive genetic analysis (Holloway, 1975) and Bradley (1980b) has recently demonstrated the mobilization of the chromosomal determinants of PAO pili by FP plasmids. Therefore, it is likely that genetic analysis of the pilus operon will be forthcoming for strain PAO rather than strain PAK. A third reason for comparing PAK and PAO pili is the increasing interest that has been shown in recent years in the use of pili as vaccines against bacterial infection (Nagy *et al.*, 1978; Schoolnik *et al.*, 1982). A prerequisite to preparing a pilus vaccine is a knowledge of the variation in antigenic structure of the protein between different strains of bacteria.

In this chapter, the purification and initial characterization of PAO pili is described and the results obtained



are compared with those obtained for PAK/2Pfs pili by Frost and collaborators. Some of these comparisons have been extended to include pili isolated from *Neisseria gonorrhoeae* (gonococcal pili) since (as will be seen below and in Chapter V) these pili show some structural similarity to *Pseudomonas* pili.

#### *A. Purification of PAO pili*

Several multipiliated, non-retractile mutants of *P. aeruginosa* PAO were obtained from D.E. Bradley, Memorial University, St. John's Newfoundland. The most highly pilated of these, PAO/DB2, was selected for further study. Figure III.1 shows an electron micrograph of PAK/2Pfs cells and of PAO/DB2 cells. It can be seen that both bacterial strains produce numerous pili which emerge from one or both poles of the bacterial cell. In addition, a single flagellum is often observed emerging from the same or an opposite pole of most cells.

The purification procedure adopted for PAO pili (and for subsequent purifications of PAK/2Pfs pili) was a modification of the procedure originally developed by Frost & Paranchych (1977). The cells were grown on solid media, harvested and the pili mechanically removed as described by Frost & Paranchych (1977) and in Materials and Methods. After the removal of cells, the pili and flagella were selectively precipitated out of the cell supernatant by the addition of polyethylene glycol 6000 to a concentration of



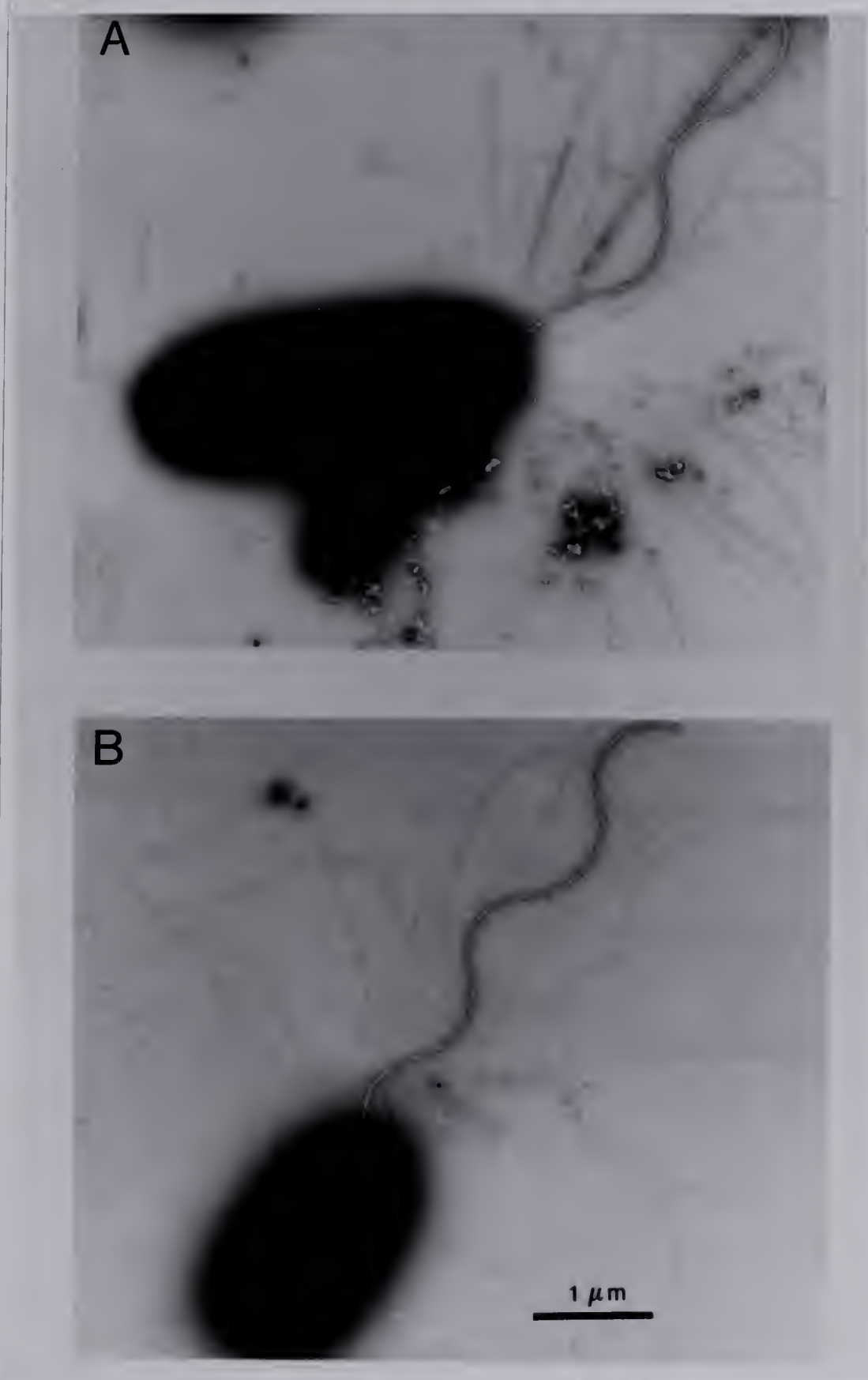


Figure III.1. Electron micrographs of A. PAK/2Pfs and B. PAO/DB2 cells which have been negatively stained with sodium phosphotungstenate.





1% (w/v). Separation of pili from flagella was accomplished by treatment of the preparation at pH 4 (to dissociate flagella into flagellin subunits) and by repeated cycles of precipitation with ammonium sulfate at a concentration of 10% (w/v). Finally, the pili were banded on a CsCl step gradient which served to remove any contaminating membrane vesicles or cell debris. Using this procedure, 100-200mg of pure pili were obtained per 100g of cells.

The pili were judged pure by the appearance of a single band on SDS-polyacrylamide gels and by the absence of flagella or membrane fragments as monitored by electron microscopy. In addition, a single N-terminal residue was detected by the dansyl-Edman procedure (see below). The pili were also found to be free of contaminating carbohydrate and phosphate using the procedures described in Materials and Methods.

### *B. Molecular Weight of Pilin*

Previously, Frost & Paranchych (1977) reported a molecular weight for PAK pilin of  $17,800 \pm 300$  based upon its migration in SDS-polyacrylamide gels and upon amino acid compositional analysis. However, the determination of the complete amino acid sequence of PAK pilin (Sastry *et al.*, 1983) revealed that the pilin subunit consists of 144 amino acid residues with a combined molecular weight of 15,000. Examination of the amino acid composition reported by Frost & Paranchych (1977; tabulated in Table III-I) suggests that



the intact pili used in the determination of the amino acid composition of PAK and PAO pilins were contaminated with amino acid or peptide material. Furthermore, in the gel system used (that of Weber and Osborn, 1969), pilin appeared to migrate at an apparent molecular weight greater than that of myoglobin ( $M=17,000$ ), implying that pilin migrates anomalously in that gel system.

Figure III.2A shows a 15% SDS-polyacrylamide gel prepared by the method of Lugtenberg (1975), as described in Materials and Methods. The migration positions of 5 types of pilin and several standards are shown. It can be seen that PAK and PAO pilin (lanes 1 and 2) have very similar mobilities in this gel system, implying a similar molecular weight. From the calibration curve shown in figure III.2B one can determine that PAK and PAO pilin have an apparent molecular weight of  $15,000 \pm 500$  (the error limits were derived by comparing the mobilities of the pilins on three gels). From the central lane which contains a mixture of 4 types of pilin, one can determine that gonococcal pilin migrates at an apparent molecular weight of 18,000 and is clearly resolvable from PAK pilin. Similarly, CFA/I pilin, which is reported to have a molecular weight of 14,500 (Klemm, 1979), migrates at a molecular weight of 14,500 in this gel system and is clearly resolved from PAK pilin.



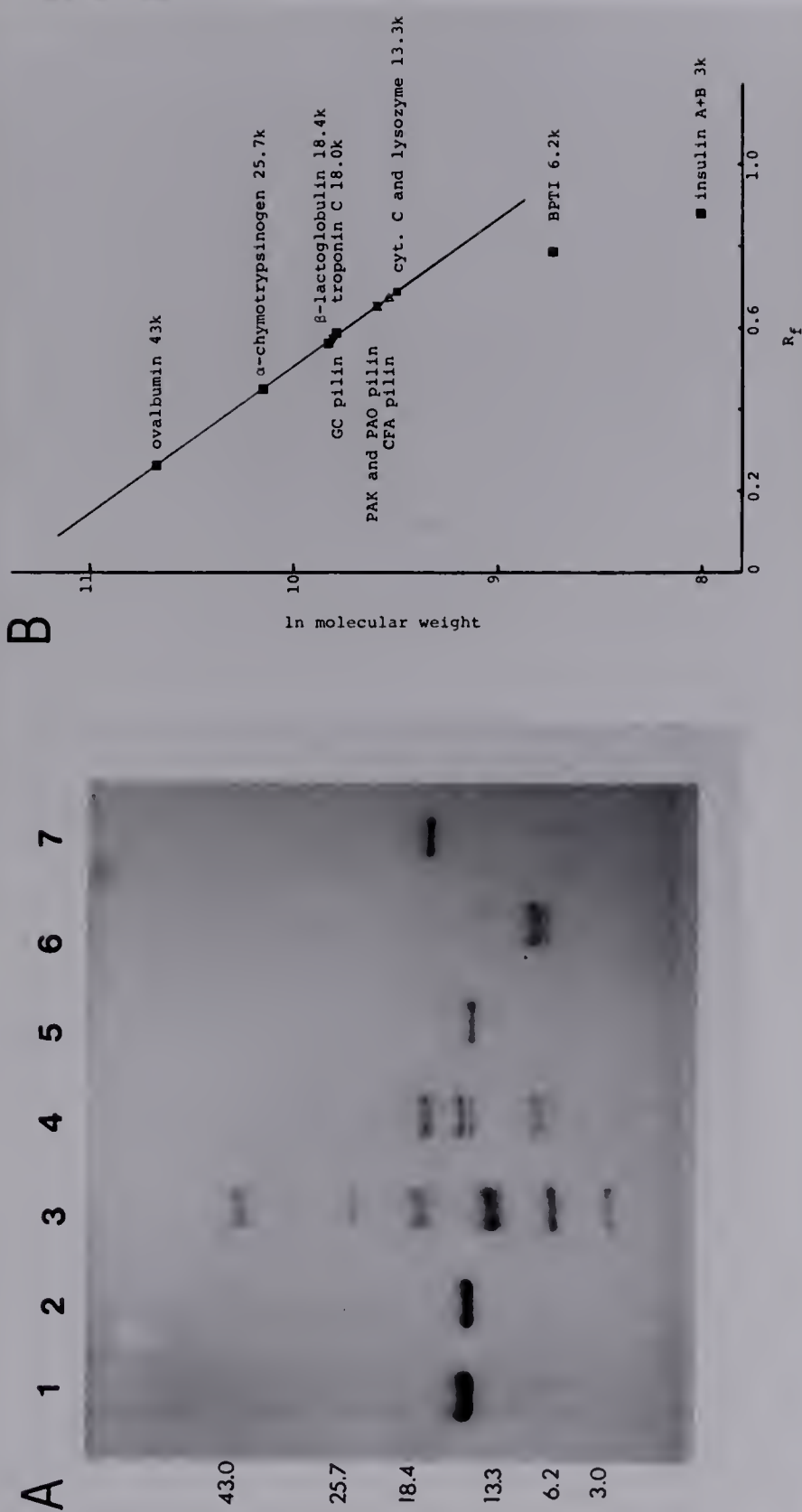


Figure III.2 SDS-polyacrylamide gel electrophoresis of pilins. A. Coomassie blue stained gel. 1=PAK pilin; 2=PAO pilin; 3=from top to bottom, ovalbumin, α-chymotrypsinogen, β-lactoglobulin, lysozyme+cytochrome C (doublet), bovine pancreatic trypsin inhibitor (BPTI) and the A and B chains of insulin. The molecular weights of the standards are indicated in thousands to the left of the gel. 4=from top to bottom, gonococcal, PAK, CFA/I and EDP208 pilins; 5=CFA/I pilin; 6=EDP208 pilin; 7=rabbit skeletal troponin C (obtained from R.S. Hodges).

B. A calibration plot of the gel shown in A; ■, standards; Δ, pilins.





### *C. Electron Microscopy of Purified Pili*

Electron micrographs of purified PAK, PAO and gonococcal pili, negatively stained with sodium phosphotungstate, are shown in figure III.3. It can be seen that all 3 types of pili are rigid filaments of uniform diameter and varying lengths. The diameters of the three types of pili were measured at a further magnification of 10-fold on 185,000x prints and were found to be indistinguishable within experimental error. The diameter obtained was  $52 \pm 4 \text{ \AA}$  which is fairly similar to the diameter of 6nm reported for PAK pili by Bradley (1972b). The arrows indicate unusual structures which are often observed at the ends of pili, particularly in old preparations. These will be discussed further in Chapter VI.

### *D. N-terminal Analysis, Tryptic Peptide Maps and Amino Acid Compositional Analysis of PAO Pilin*

#### **1. N-terminal analysis**

Purified PAO pili were subjected to N-terminal analysis using the automated Edman-degradation procedure as described in Materials and Methods. It was found that the N-terminal 20 residues of PAO pilin were identical to those of PAK pilin including the unusual amino acid N-methylphenylalanine at the N-terminus. Since this work was carried out, P.A. Sastry has initiated amino acid sequencing studies of PAO pilin and has found that this homology extends to residue 53, while the C-termini of the two pilins are quite



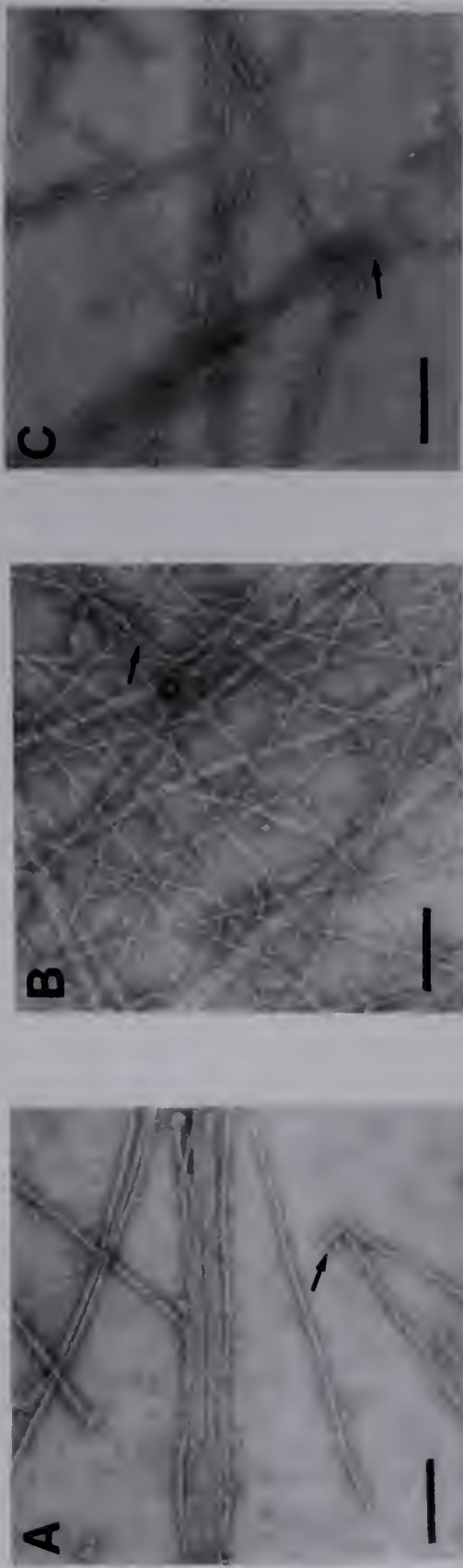


Figure III.3. Electron microscopy of purified pili. A. PAK/2Pfs pili; B. PAO/DB2 pili; C. gonococcal pili. The bar indicates 100nm. The arrows indicate unusual structures which will be discussed further in Chapter VI.



different (Sastry, Pearlstone, Smillie & Paranchych, unpublished results).

Figure III.4 shows a comparison of the sequence of the N-terminal 50-60 residues of PAK, PAO and gonococcal pilin. Paranchych *et al.* (1978) first noted the striking homology in the N-terminal 20-25 residues of PAK and *Neisseria gonorrhoeae* pilins. As mentioned in Chapter I, this region of homology was also common to *Moraxella nonliquefaciens* pilin (Frøholm & Sletten, 1977). It can be seen in figure III.4 that there is little homology between the *Pseudomonas* and gonococcal pilins after residue 30, while PAK and PAO pili are highly homologous up to residue 53, with only 3 conservative substitutions at positions 39, 40 and 50. The sequence of the C-terminal cyanogen bromide fragment (residue ca. 97-160; not shown) of gonococcal pilin (G. Schoolnik, personal communication) also bears no homology to the C-terminus of PAK pilin (Sastry *et al.*, 1983). The complete amino acid sequence of PAK pilin (reproduced from Sastry *et al.*, 1983) is shown in Chapter VIII, figure VIII.1.

## 2. Tryptic peptide maps of PAK and PAO pili

To further compare the primary structures of PAK and PAO pilins, tryptic digestion of the two types of pili was carried out, followed by two-dimensional chromatography-electrophoresis as described in Materials and Methods. The resulting two-dimensional peptide maps are reproduced in





PAK:	MePhe-Thr-Leu-Ile-Glu-Leu-Met-Ile-Val-Val-Ala-Ile-Ile-Gly-Ile-	15
PAO:	MePhe-Thr-Leu-Ile-Glu-Leu-Met-Ile-Val-Val-Ala-Ile-Ile-Gly-Ile-	10
GC :	MePhe-Thr-Leu-Ile-Glu-Leu-Met-Ile-Val-Ile-Ala-Ile-Val-Gly-Ile-	5
PAK:	Leu-Ala-Ala-Ile-Ala-Ile-Pro-Gln-Tyr-Gln-Asn-Tyr-Val-Ala-Arg-	20
PAO:	Leu-Ala-Ala-Ile-Ala-Ile-Pro-Gln-Tyr-Gln-Asn-Tyr-Val-Ala-Arg-	25
GC :	Leu-Ala-Ala-Val-Ala-Leu-Pro-Ala-Tyr-Gln-Asp-Tyr-Thr-Ala-Arg-	30
PAK:	Ser-Glu-Gly-Ala-Ser-Ala-Leu-Ala-Ser-Val-Asn-Pro-Leu-Lys-Thr-	35
PAO:	Ser-Glu-Gly-Ala-Ser-Ala-Leu-Ala-Thr-Ile-Asn-Pro-Leu-Lys-Thr-	40
GC :	Ala-Gln-Val-Ser-Glu-Ala-Ile-Leu-Leu-Ala-Glu-Gly-Gln-Lys-Ser-	45
PAK:	Thr-Val-Glu-Glu-Ala-Leu-Ser-Arg-Gly-Trp-Ser-Val-Lys-Ser-Gly-	50
PAO:	Thr-Val-Glu-Glu-Ser-Leu-Ser-Arg-	55
GC :	Ala-Val-Thr-Glu-Tyr-Leu-Asn-His-Gly-Lys-Trp-Pro-Gln-	60

Figure III.4. N-terminal amino acid sequences of PAK pilin (Frost et al., 1977; Sastry et al., 1983); PAO pilin (this work and Sastry et al., unpublished) and gonococcal pilin (Hermodson et al., 1978; G. Schoolnik, personal communication). Residues which differ from those in PAK pilin have been outlined.



figure III.5. It can be seen that 13 PAK peptides and 13 PAO peptides were observed. Of these, 6 showed similar mobilities on the two dimensional peptide maps, suggesting possible sequence homology. In fact, examination of the sequence of PAK pilin (Sastry *et al.*, 1983), suggests that one should observe 16 PAK tryptic peptides, therefore it would appear that these are not completely resolved by this procedure. On the other hand, for PAO pilin, 13 tryptic peptides were expected on the basis of the amino acid composition (see below).

### 3. Amino acid composition of PAO pilin

The amino acid composition of PAO pilin was calculated from the results of amino acid analyses on samples which had been hydrolyzed for 24, 48 and 72 hr, as described in Materials and Methods. Table III-I shows the results obtained for intact PAO pili compared with those calculated by P.A. Sastry (Sastry, Pearlstone, Smillie & Paranchych, unpublished) from the amino acid compositions of 4 purified peptide fragments of PAO pilin obtained by tryptic digestion of citraconylated pili. It can be seen that the amino acid composition of intact PAO pili leads to a high estimate of molecular weight as compared to the molecular weight obtained in SDS-polyacrylamide gels. On the other hand, analysis of the amino acid composition of the purified peptide fragments gave a result that is in agreement with the results obtained by SDS-polyacrylamide gel electrophoresis. As can be seen in Table III-I, a similar overestimate of the



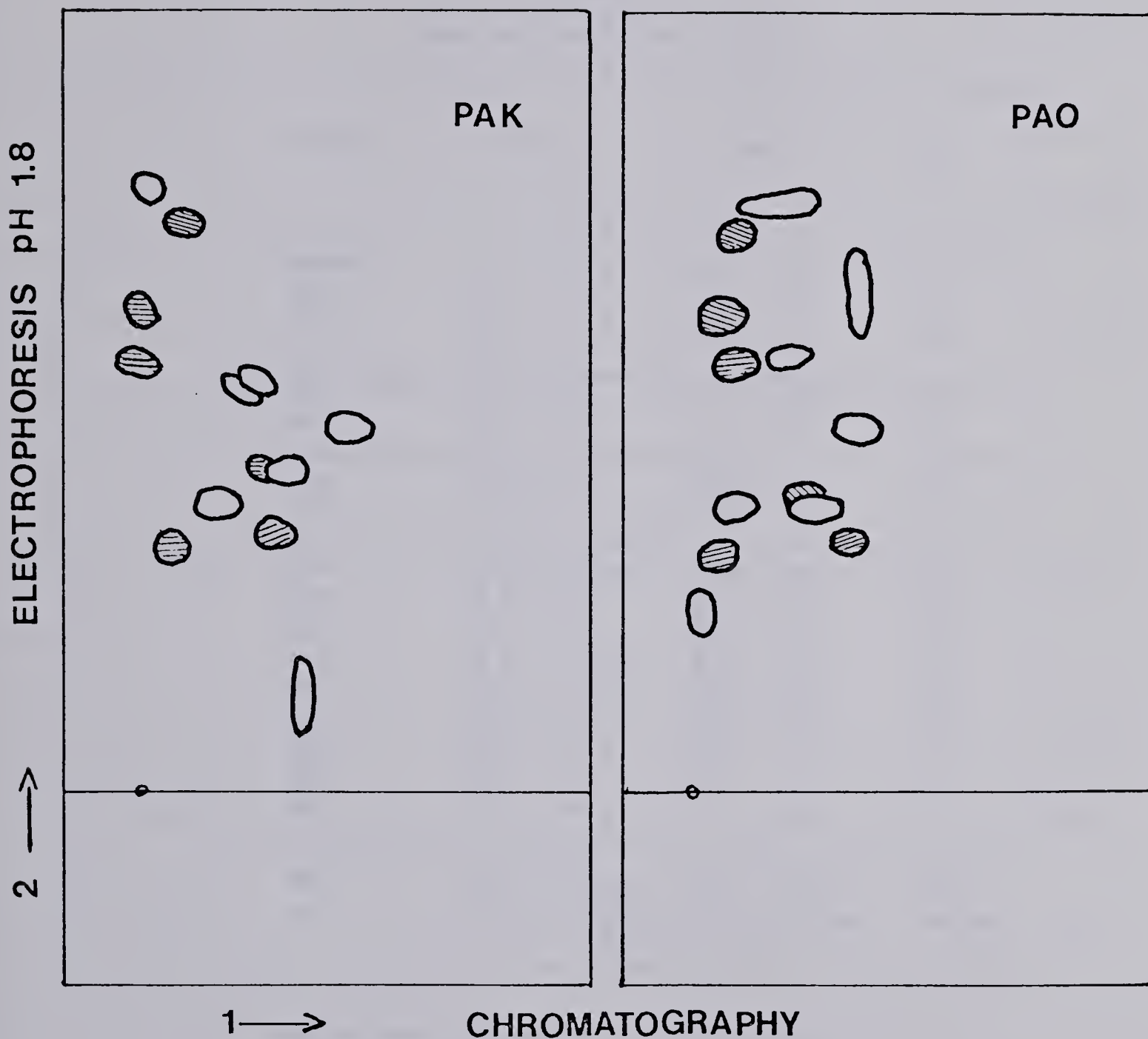


Figure III.5. Two-dimensional chromatography-electrophoresis of PAK and PAO tryptic peptides, carried out as described in Materials and Methods. The soluble material from 5nmol of digested pili was applied at the origin of 10x20 cm microcrystalline cellulose-coated plastic sheets. The peptides were visualized by staining with ninhydrin:Cadmium. The hatched spots indicate peptides from the two strains of pili which have similar mobilities.





TABLE III-I  
Amino Acid Composition of Pilins

RESIDUE	PAO		PAK		GC
	a	b	c	d	e
MePhe	1	1	1	1	1
Phe	2.8	3	2.3	2	1
Tyr	3.0	3	2.2	2	5
Trp	0.9	1	2.0	2	3
Lys	9.2	8	14.8	12	17
Arg	3.8	3	4	3	6
Asx	16.0	13	14.9	12	16
Glx	13.8	12	14.9	11	17
Ile	14.2	13-14	11.7	12	9
Leu	8.9	9	14.0	12	12
Val	11.0	9	9.0	8	14
Thr	19.5	19	15.0	15	10
Ser	9.9	11-12	9.9	8	9
Ala	22.2	18-20	23.8	19	16
Gly	15.0	12	17.7	14	12
Cys	3.0	2	3.9	2	2
Met	3.0	3	2.1	2	2
Pro	7.8	6	9.7	7	5
His	0	0	0	0	3
SUM	165	146-150	173	144	160
M	17,000	15,300- 15,600	17,800	15,000	16,680

- Based on amino acid analysis of purified intact pili as described in Methods.
- Based upon the amino acid composition of the 4 tryptic peptides obtained from citraconylated pilin (P.A. Sastry, personal communication).
- Based on the amino acid composition reported by Frost & Paranchych (1977).
- From the amino acid sequence (updated from Sastry et al., 1983).
- From the amino acid composition of 3 CNBr fragments, (G. Schoolnik, personal communication).



molecular weight of PAK pilin was obtained by Frost & Paranchych (1977) using the amino acid composition obtained from whole pili.

It can be seen from Table III-I that the overall amino acid composition of PAK and PAO pilin are quite similar. Both proteins lack histidine, contain a comparable number of proline residues and similar proportions of acidic and basic residues. PAK and PAO pili both possess 51% hydrophobic residues, where hydrophobic residues are defined as all the non-polar residues excluding proline, since proline is usually found on the surface of proteins. Also shown in Table III-I is the amino acid composition of gonococcal pilin (based upon partial sequence data on cyanogen bromide peptides, G. Schoolnik, personal communication). Although gonococcal pilin differs from the *Pseudomonas* pilins in containing 3 histidine residues, the overall composition shows some similarities with respect to the proportion of acidic, basic and non-charged residues. Using the definition of hydrophobic residues given above, gonococcal pilin has 49% hydrophobic residues.

#### *E. Immunological Cross-reactivity Between Pili Strains*

In the past (Bradley & Pitt, 1975), the polar pili associated with strains PAK and PAO of *Pseudomonas* were considered to be serologically unrelated. However, these conclusions were based upon agglutination tests and upon observation of antibodies bound to pili in the electron



microscope. Using the more sensitive enzyme-linked immunosorbant assay (ELISA), however, we found that anti-PAK pilus antisera recognized PAO pili and vice versa.

The principles of ELISA have been described by Voller *et al.* (1974) and are explained diagrammatically in figure III.6. The antigen, which can be a protein, peptide or carbohydrate, is bound to the wells of a microtiter plate by incubation at 4°C for 10-16h at pH 9.6 (Figure III.6A). Following appropriate washing steps, serial dilutions of antiserum are added to the wells and allowed to interact with bound antigen for approximately 2hr at room temperature. The antigen-antibody interaction is carried out in the presence of 1% BSA to prevent non-specific binding to the wells (figure III.6B). After further washing, the bound antibodies can be detected by several methods. For example, if rabbit antiserum were used, one can add goat antiserum against rabbit IgG (goat anti-rabbit IgG) which has been conjugated to the enzyme alkaline phosphatase (figure III.6C). The bound enzyme-conjugate is then detected by adding a colorimetric substrate and reading the absorbance in the wells after an appropriate time interval. It is advisable to include a reagent blank and an assay blank (an antigen which is unrelated to the one of interest) on each microtiter plate. One normally coats the antigen at a series of concentrations to determine the point at which binding to the wells saturates.





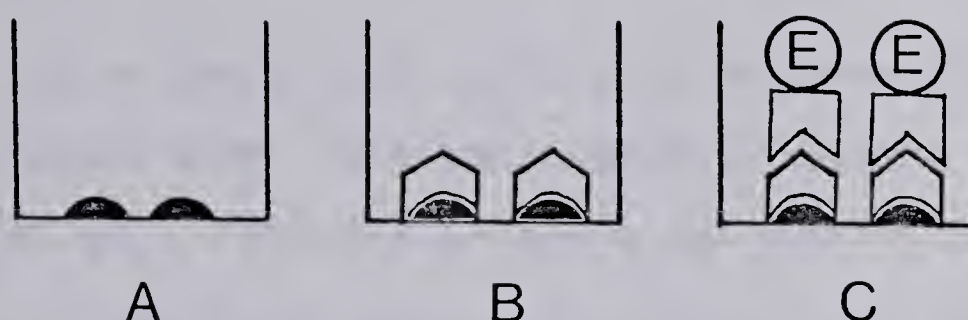


Figure III.6. Principles of Elisa.

- A. The wells of a microtiter plate are coated with antigen. Incubation is for 10-16h at 4°C in pH 9.6 coating buffer, followed by 3x 3 minute washes in phosphate buffered saline containing 0.05% v/v Tween 20.
- B. The antigen-coated wells are incubated with serial dilutions of antiserum for 2hr at room temperature, followed by 3 washes in PBS-Tween.
- C. The antigen-antibody coated wells are incubated with (for example) alkaline phosphatase-conjugated goat anti-rabbit IgG, followed by washing, followed by addition of a colorometric substrate.



Figure III.7 shows the results of an ELISA in which 5 types of pili were tested for their ability to react with anti-PAK and anti-PAO pilus antisera. It can be seen that PAK and PAO pili show a significant cross-reactivity in both directions. On the other hand, little or no reaction was observed between anti-*Pseudomonas*-pili antisera and pili isolated from *Neisseria gonorrhoeae*, *E. coli* H-10407 or *E. coli*/EDP208.

This cross-reactivity could also be demonstrated in an immunoblot experiment. The immunoblot procedure (described by Towbin *et al.*, 1979 and by Burnette, 1981) is similar, in principle, to the ELISA assay, but differs in that it incorporates a separation procedure which allows one to attribute antigenicity to a specific component in a multicomponent system. In this procedure, proteins or large peptides are subjected to SDS-polyacrylamide gel electrophoresis and then transferred electrophoretically to nitrocellulose paper. The nitrocellulose paper is then incubated with polyclonal or monoclonal antibodies for 2-12hr followed by a washing step. There are several methods available for detecting bound immunoglobulins on the nitrocellulose paper. These involve either an enzyme-conjugated reagent or a radioactively labelled reagent. In this case we have used  $^{125}\text{I}$ -labelled Protein A from *Staphylococcus aureus*. Protein A binds specifically to the Fc domain of rabbit IgG (and to a lesser extent to rabbit IgM) as well as to various IgG subclasses of the



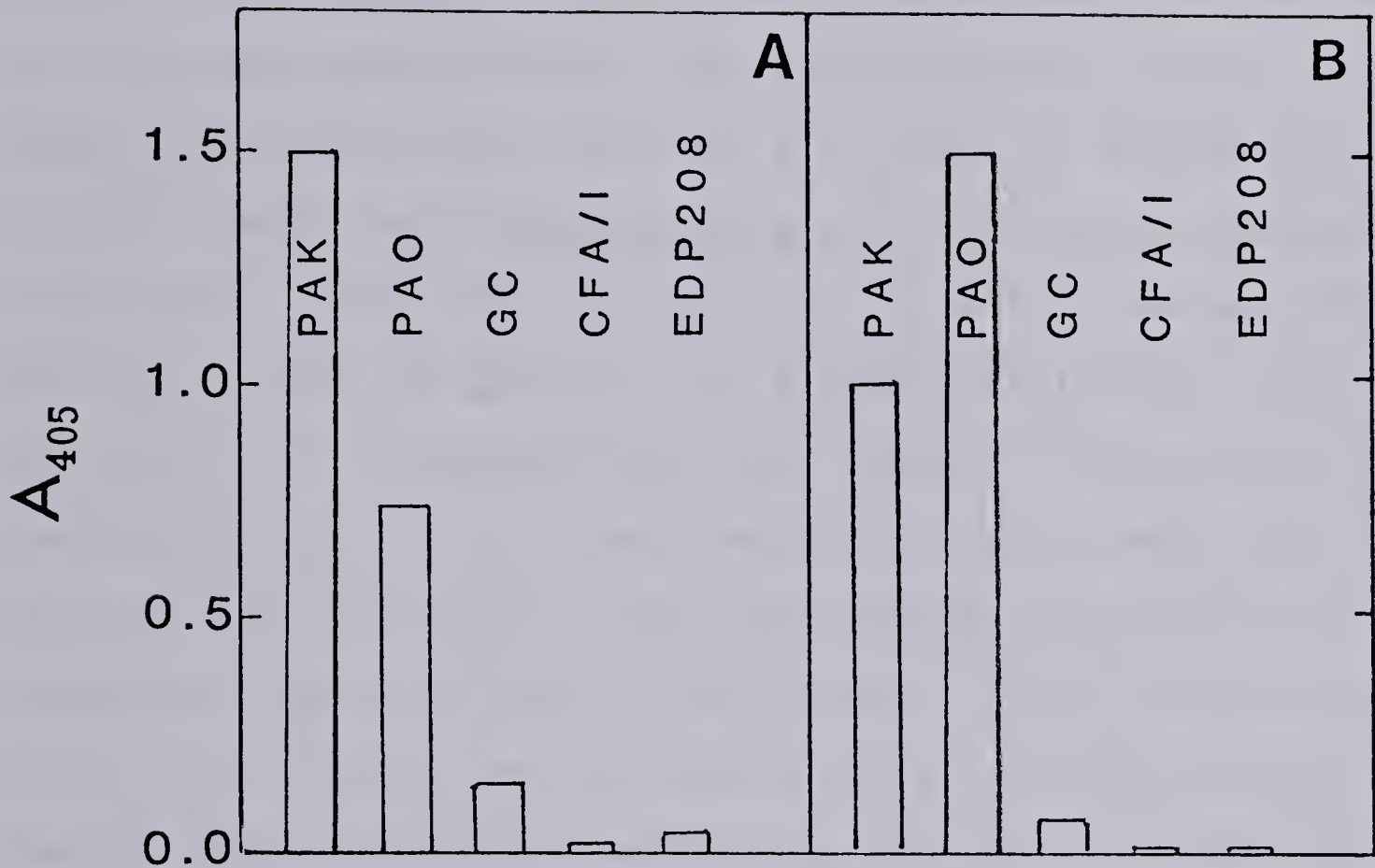


Figure III.7. ELISA assay showing cross-reactivity between pili isolated from *Pseudomonas aeruginosa* strains PAK and PAO.

A. Results obtained at a 1:500 dilution of anti-PAK pilus antiserum.

B. Results obtained at a 1:500 dilution of anti-PAO pilus antiserum. All pili were coated at a saturating concentration of 5  $\mu$ g/ml. The results with the two types of antiserum were normalized so that the reaction with the homologous antiserum gives an  $A_{405}$  of 1.50. PAK, PAO, GC, CFA/I and EDP208 refer to the pili isolated from these strains. GC is gonococcal pili.





immunoglobulins of a number of other animals (Forsgren & Sjoquist, 1966; Goding, 1978; Langone, 1979).

The results of the immunoblot for the five strains of pili versus anti-PAK pilus antisera are shown in figure III.8. Surprisingly, the anti-PAK pilus antisera recognized not only PAK and PAO pilin, but also gonococcal pilin. Again, no reaction was observed with CFA/I or EDP208 pili. A similar result was obtained using anti-PAO pilus antiserum (not shown). Since the only region of homology between PAK, PAO and GC pili is found at the N-terminus (residue 1-22) of the proteins, it appears that this region is responsible for the cross-reactivity in the 'immunoblot' experiment. We attribute the failure of anti-*Pseudomonas*-pili antisera to recognize gonococcal pili in the ELISA to the possibility that the N-terminus of gonococcal pilin is buried in the native state and becomes exposed in SDS-polyacrylamide gels.

### *F. Summary*

The results presented in this chapter show that PAK, PAO and gonococcal pili are very similar at the resolution of the electron microscope. The pilin subunits of PAK and PAO pili have similar molecular weights and are about 17% smaller than gonococcal pilin, according to SDS-polyacrylamide gel electrophoresis. N-terminal amino acid sequence analysis and tryptic peptide mapping indicates some sequence homology between PAK and PAO pilin. In fact, more recent



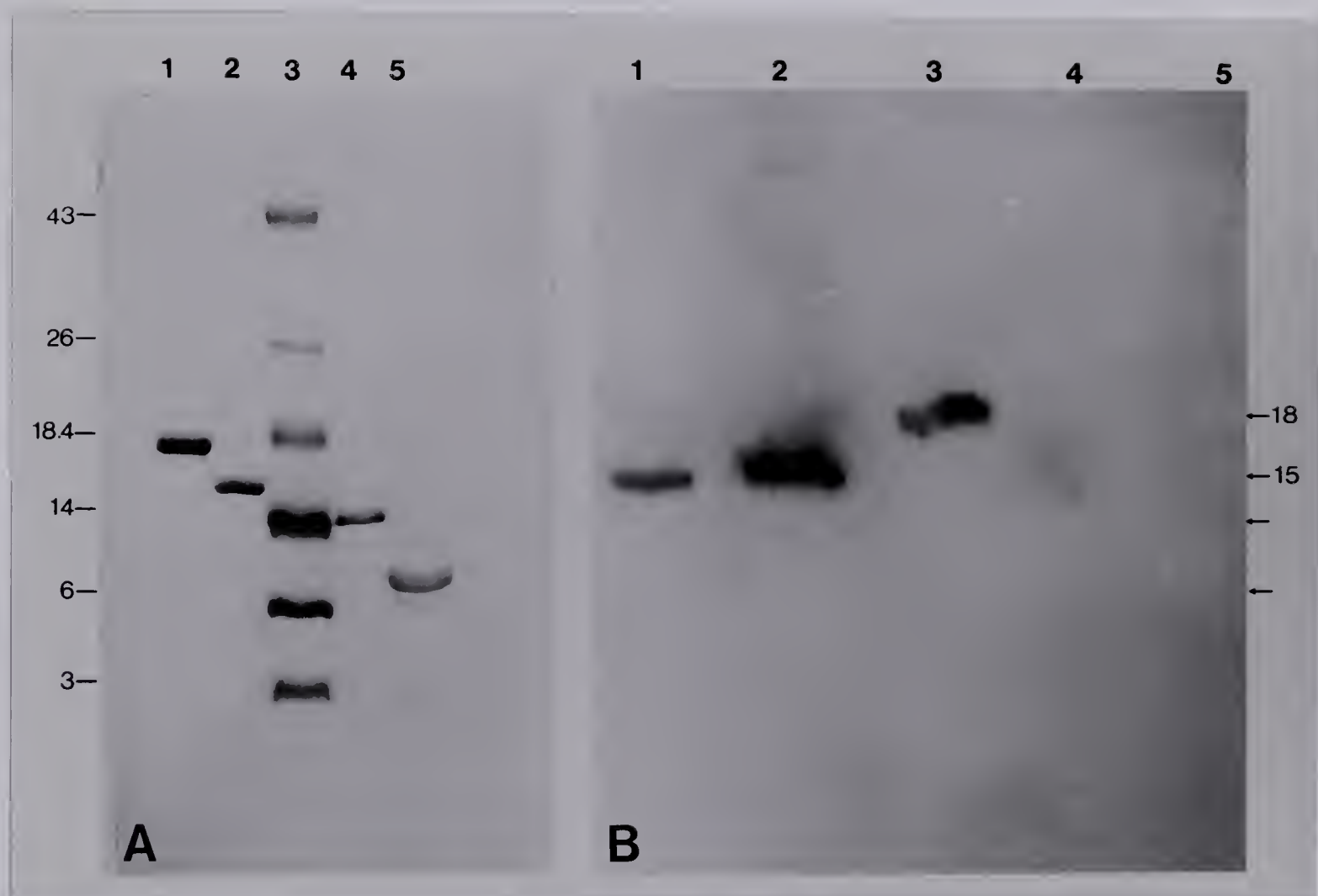


Figure III.8. Cross-reactivity between pilins demonstrated by the immunoblot technique using anti-PAK pilus anti-sera.

A. Coomassie-blue stained 20% polyacrylamide gel. Lanes 1 through 5 contain, respectively, gonococcal pilin (4ug); PAK pilin (4ug), standard proteins with molecular weights as indicated in thousands; CFA/I pilin (4ug) and EDP208 pilin (4ug).

B. Results obtained after electrophoresis of pilins on a 20% polyacrylamide gel, transfer to nitrocellulose and reaction with anti-PAK pilus antibodies and  $^{125}\text{I}$ -Protein A as described in the text. 1=PAO pilin, 1.5ug; 2=PAK pilin, .5ug; 3=GC pilin, 4 ug; 4=CFA/I pilin, 4 ug; 6=EDP208 pilin, 4 ug.



work (Sastry, Pearlstone, Smillie and Paranchych, unpublished) has shown that PAK and PAO pilin are highly homologous from residue 1 to 53, but differ in sequence at their C-termini. The overall amino acid compositions of PAK, PAO and gonococcal pilins are similar with respect to the proportion of hydrophobic amino acids, the relative number of prolines and the proportions of acidic and basic residues.

Immunological analysis of PAK, PAO and gonococcal pilin, suggests that the three proteins share a common antigenic determinant, most likely near the N-terminus of the proteins where their sequences are most homologous.





## CHAPTER IV

### Dissociation and Characterization of Pilin in Detergent

Previously, it has been possible to obtain monomers of *Pseudomonas* pilin only by resorting to strong denaturants such as SDS (Frost & Paranchych, 1977). In order to characterize the pilus structure it was of interest to obtain pilin subunits in a native conformation. This would make possible hydrodynamic studies, to determine the shape of the subunit, which would complement X-ray diffraction data (to be discussed in Chapter V). In addition, the availability of pilin subunits would allow studies on the *in vitro* assembly of the pilus, as has been done for other filamentous assemblies such as bacterial flagella (Abram & Koffler, 1964). Since pili are too flexible and too heterogeneous in length to form three-dimensional crystals, monomers of pilin would also be useful as starting material for crystallization trials. For this reason, a systematic search was made to find a condition or treatment that would cause dissociation of pili into subunits without denaturing the protein.

As will be seen below, a detergent, octyl-glucoside (n-octyl- $\beta$ -D-glucopyranoside), turned out to be the reagent of choice for this purpose. The pilin/octyl-glucoside complex was subsequently studied using a classical hydrodynamic approach in order to gain information about the



shape of the pilin subunit in detergent and to infer from this, information about pilin shape in the intact pilus. These studies were carried out on both PAK and PAO pilin in order to extend the structural comparison of the two related proteins.

Since these studies involve the interaction of a detergent with pilin, it is useful to first consider some generalizations that have been made on the properties of detergents and their interaction with proteins.

#### *A. Some Comments on the Interaction of Detergents with Proteins*

The term non-ionic detergent has been applied to neutral amphiphiles (possessing a polar head group and a non-polar tail) which are capable of forming water-soluble aggregates, micelles, in aqueous solution. In general, the non-ionic detergents are milder than the ionic detergents (such as SDS) and are less likely to cause denaturation of proteins. Some non-ionic detergents which are in common use for solubilizing membrane proteins are the polyoxyethylene detergents (these include the Triton X, Brij and Tween series of detergents) and the alkyl-glucosides (most commonly, octyl-glucoside). In addition, the bile salts (such as deoxycholate) are frequently used in the study of membrane proteins. The bile salts, while ionic in nature, are intermediate between the alkyl-ionic detergents (such as SDS) and the non-ionic detergents in their properties. They





are stronger 'solubilizers' than octyl-glucoside, for example, but are less likely to denature proteins than is SDS. The properties of these detergents and their use in solubilizing membrane proteins have been reviewed by Helenius and Simons (1975) and by Helenius *et al.*, (1979). It should be noted that the  $\alpha$ - and  $\beta$ -anomers of octyl-glucoside are quite different in their properties as solubilizing agents (Baron & Thompson, 1975). Recently, Rosevear *et al.* (1980) have introduced the use of a number of other alkyl-glycosides, such as laurylmaltoside, dodecyl-lactopyranoside and  $\beta$ -D-cellubiopyranoside.

At low concentrations, detergents exist in the monomeric form. Above a certain concentration, known as the critical micelle concentration (CMC), monomers and micelles exist in equilibrium. The CMC therefore represents the highest concentration of monomer attainable. The physical properties of micelles have been discussed in detail by Tanford (1973). In general, the detergent molecules in a micelle are arranged so that their polar head groups face outwards towards the aqueous phase and their non-polar groups form a hydrophobic core which has the properties of a liquid hydrocarbon. The micelles can be spherical, ellipsoidal or cylindrical. Tanford (1973) also includes bi-layer arrangements of detergent in the term micelle. The dimensions, number of detergent monomers per micelle, and the critical micelle concentration are characteristic of a particular detergent. The number of detergent molecules per





micelle tends to increase with increasing detergent concentration, but under fixed conditions detergent micelles are somewhat like proteins in having a defined molecular weight (Tanford & Reynolds, 1976). In addition, the critical micelle concentration is fairly sensitive to the presence of added salt and to trace impurities of other detergents. For example, Shinoda *et al.*, (1961) determined that the CMC of octyl-glucoside in water is 25mM but decreases to 17mM in 0.93M NaCl. Furthermore, both the concentration and the type of anion were found to effect the CMC of octyl-glucoside in this study.

Tanford and Reynolds (1976) describe two modes of interaction of detergents with proteins. In one case, there exist discrete binding sites which are capable of interaction with monomers of detergent in a saturable manner. This type of binding is observed in the interaction of deoxycholate or triton X100 with the high affinity detergent binding sites of bovine serum albumin (Robinson & Tanford, 1975).

Another type of binding, seen more often with membrane proteins is the cooperative binding of several detergent molecules at concentrations close to or above the CMC of the detergent. Tanford and Reynolds suggest that this type of binding site may be a preformed hydrophobic area which is capable of interacting with a detergent micelle or even of nucleating micelle formation. This type of cooperative



binding above the CMC of the detergent has been observed in the binding of deoxycholate or Triton X100 to cytochrome b5, for example (Robinson & Tanford, 1975). On the other hand, cooperative binding may also be observed below the CMC if the binding of detergent causes an unfolding of the protein, thereby exposing more detergent binding sites. This type of binding behaviour is observed in the interaction of SDS with a number of soluble proteins (Reynolds and Tanford, 1970).

Cooperative binding of detergent in the form of micelles without denaturation of the protein appears to be a general phenomenon exhibited by non-ionic detergents and bile salts interacting with lipophilic proteins. Helenius and Simons (1972) and Clarke (1975) have demonstrated that a number of hydrophilic proteins bind little or no deoxycholate or Triton X100 while lipophilic proteins bind large amounts (up to 70% of their weight) of these detergents.

It should be noted that, besides membrane proteins, lipophilic proteins can also include water soluble protein aggregates. For example, erythrocyte spectrin, a cytoplasmic protein found in association with the cell membrane (reviewed in Marchesi, 1979) exists as large aggregates in aqueous solution but can be dissociated into a mixture of monomers and dimers in deoxycholate (Schechter *et al.*, 1976). Similarly, dissociation of the filamentous phage f1 can be accomplished in deoxycholate resulting in the formation of coat protein dimer/detergent complexes. (Makino *et al.*,





1975). However, the coat protein is in a sense a membrane protein since it is inserted into the bacterial membrane prior to assembly of the virus (Smilowitz, 1972).

In many cases, proteins which bind non-ionic detergents (or bile salts) cooperatively appear to bind approximately 1 micelle of detergent (summarized in Tanford & Reynolds, 1976). These authors suggested that the micelle should be able to surround such proteins with very little distortion of the original micelle shape.

It is also interesting to note that a large number of membrane proteins are isolated as oligomers (usually dimers or trimers) in mild detergents. Some examples are the coat protein of fd phage ( $\alpha_2$  in deoxycholate, Makino *et al.*, 1975); band 3 glycoprotein ( $\alpha_2$  in Triton X-100; Yu and Steck, 1975); and cytochrome b ( $\alpha_2$  in deoxycholate; Visser *et al.*, 1975). In many cases, cross-linking studies have suggested that the same oligomeric state exists in the membrane (Klinenberg, 1981). It may be that it is more efficient for membrane proteins to exist as oligomers so that the same hydrophobic face can be presented on all sides of the oligomer rather than having a monomeric protein which must have its entire exterior membrane (or detergent) soluble.





## B. Dissociation of Pili

In order to find a treatment that would dissociate the pilus without disrupting pilin secondary structure, the size of pilin aggregate was monitored under varying conditions in the analytical ultracentrifuge. At the same time, the effect of a given treatment on protein conformation was followed by circular dichroism (CD).

Figure IV.1 shows representative CD spectra of PAK and PAO pili in the presence and absence of denaturants. It can be seen that the CD spectra of PAK and PAO pili are very similar in the native state (curve 1) and in the presence of denaturants (curves 2 and 3). From the spectrum of native pili in phosphate buffer (curve 1) the amount of secondary structure was calculated to be 42%  $\alpha$ -helix and 40%  $\beta$ -structure using the method of Chen *et al.*, (1972) as described in Materials and Methods (Chapter II). This suggests that *Pseudomonas* pilin belongs to the  $\alpha/\beta$  or  $\alpha+\beta$  class of proteins as defined by Levitt and Chothia (1976). In other words, pilin may consist of domains containing a mixture of  $\alpha$ - and  $\beta$ -structure or the two classes of secondary structure may be segregated in different regions of the protein.

The fact that pili are filamentous and tend to aggregate raises the question of whether light scattering could



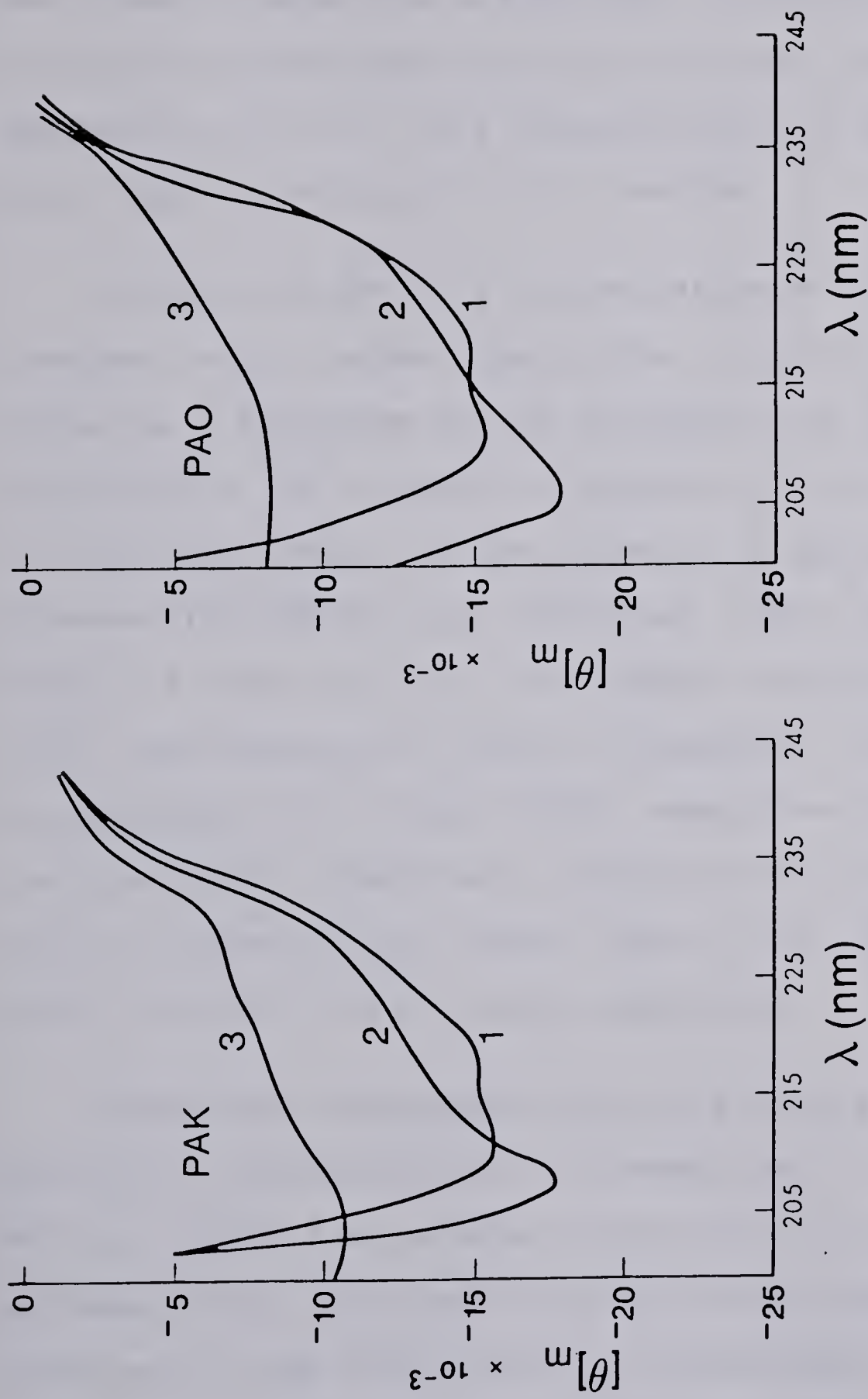


Figure IV.1. Circular dichroism spectra of PAK and PAO pilin as measured in 50 mM phosphate buffer, pH 7.2 at 20°C. Curve 1: buffer only or buffer + 30 mM octyl-glucoside. Curve 2: buffer + 1% SDS. Curve 3: buffer + 4 M Guanidine-HCl.  $[\theta]_m =$  molar ellipticity in  $\text{deg cm}^2 \text{decimol}^{-1}$ .



cause anomalies in the CD spectrum. This problem was avoided by centrifuging each sample prior to making spectral measurements in order to remove large aggregates as described in Materials and Methods. Furthermore, the fact that pilin solubilized in octyl-glucoside gives an identical spectrum to that of the filamentous form of pilin suggests that light scattering is not a problem.

Addition of SDS to a concentration of 1% (w/v), a treatment which causes dissociation of pili into monomers, causes an enhancement of the ellipticity at 209nm (curve 2), suggesting a 12% increase in apparent  $\alpha$ -helix. An increase in  $\alpha$ -helical content in the presence of SDS has also been observed for EDP208 pili (Armstrong, 1980), as well as for a number of other proteins, for example concanavalin A (Kay, 1970), apolipoprotein (Steele & Reynolds, 1979) and several oligopeptides (Wu & Yang, 1978). Guanidine hydrochloride, on the other hand, drastically denatures both types of pili while ultracentrifuge studies (Table IV-I) show that the pilin is still in quite large aggregates.

Some other treatments which were tested for their ability to dissociate pili are summarized in Table IV-I. Brinton (1965) demonstrated dissociation of Type I pili by extremes of pH. Treatment with both alkali and acid also resulted in some dissociation of *Pseudomonas* pili, but the sedimentation coefficient remained much larger than that in the presence of SDS suggesting that quite large aggregates





TABLE IV-I

*Effect of Various Agents on the Aggregation  
State and Secondary Structure of Pseudomonas Pili.*

Treatment <sup>1</sup>	% $\alpha$ -helix <sup>2</sup>	S <sub>20,w</sub> <sup>3</sup>
-	42	10-30S
1% SDS	47	1.6S
4M Guanidine HCl	21	11S
pH 1.8 (NaH <sub>2</sub> PO <sub>4</sub> )	22	6S
pH 12.5 (Na <sub>2</sub> HPO <sub>4</sub> )	22	5S
8M Urea	20	nd
1M NaCl	42	10-15S
10mM Cholate or Deoxycholate	40	10-15S
10mM Glycodeoxycholate	40	3S
10mM Taurodeoxycholate	40	3S
30mM Octyl-glucoside	42	2.2S

1. Pili concentration was 1 mg/ml in 50 mM phosphate buffer (pH 7.2) plus the reagent in question. Samples were dialyzed overnight prior to ultracentrifugation or circular dichroism measurements.

2. %  $\alpha$ -helix was determined as described in Materials and Methods. The CD spectra of native, SDS-treated, Guanidine-HCl and octyl-glucoside treated pili are shown in figure IV.1.

3. Sedimentation coefficients were determined and standardized as described in Materials and Methods.



remained. Neutralization of pilin after treatment at pH 12.5 resulted in regeneration of the original CD spectrum. Treatment with acid, on the other hand, led to problems with precipitation and was therefore less readily reversed.

The most useful agents for dissociating pili appear to be detergents. The structures of some of the detergents used in this study are shown in Figure IV.2. Both octyl-glucoside and two deoxycholate derivatives (sodium glycodeoxycholate and sodium taurodeoxycholate, but not deoxycholate itself) resulted in a slow sedimenting, apparently homogeneous species without any detectable change in CD spectra (c.f. figure IV.1, curve 1). It should be noted that at neutral pH, deoxycholate is uncharged, while taurodeoxycholate is an ionic species, hence the difference in effectiveness of these detergents. However, the deoxycholate derivatives possess a lower critical micelle concentration and caused problems in the sedimentation experiments due to their tendency to form gels. On the other hand, the high critical micelle concentration and small micelle size of octyl-glucoside eliminates the problem of gel formation and also allows the detergent to be removed easily (Baron & Thompson, 1975). For these reasons, the pilin/octyl-glucoside complex was selected for further characterization.

Figure IV.3 shows the dissociation of PAK pili with increasing detergent concentration as measured by viscometry. Similar results were also obtained for PAO pili.



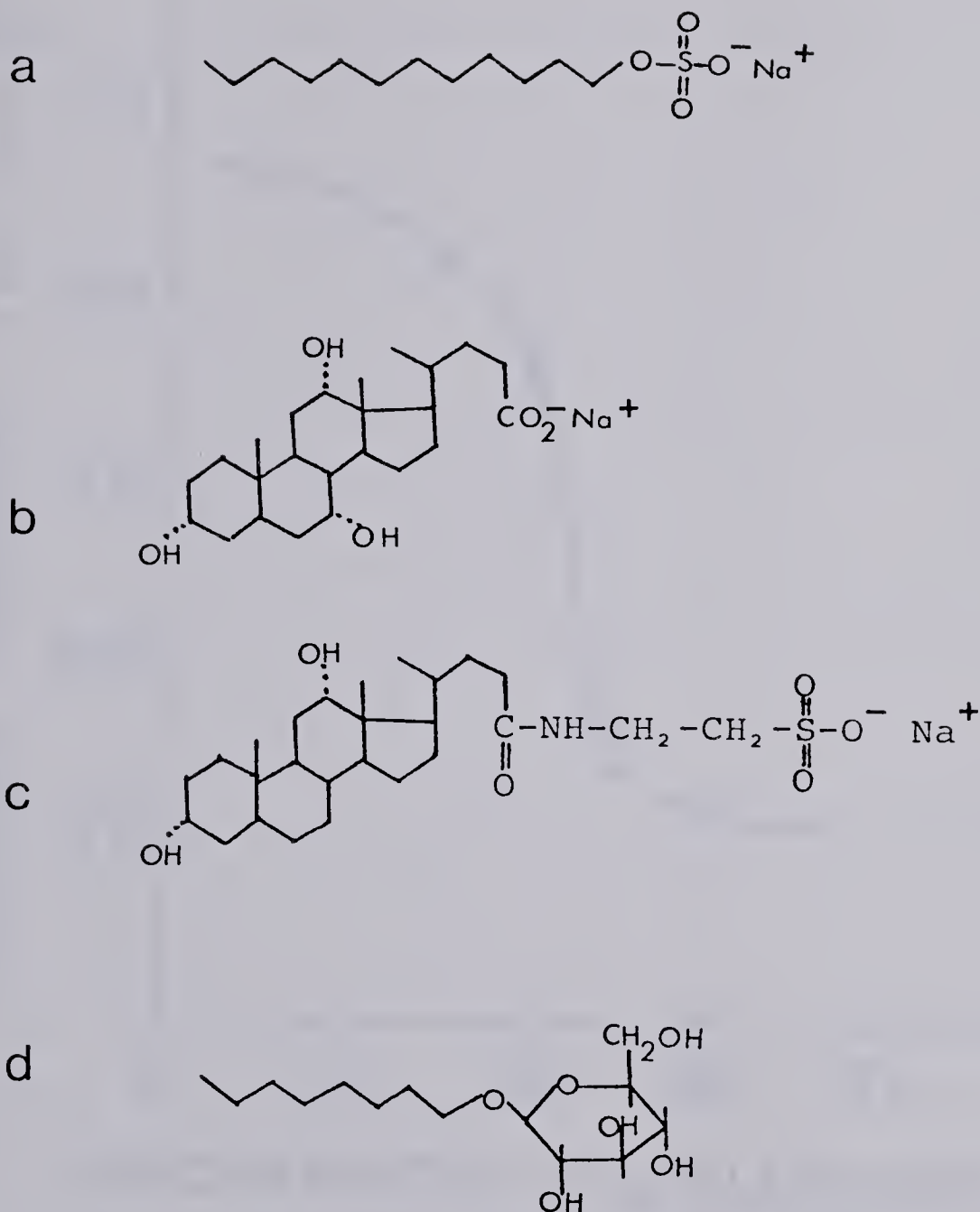


Figure IV.2 Structure of some common detergents:  
 a. sodium dodecyl sulfate; b. sodium cholate;  
 c. sodium taurodeoxycholate; d. octyl-glucoside  
 (n-octyl- $\beta$ -D-glucopyranoside).





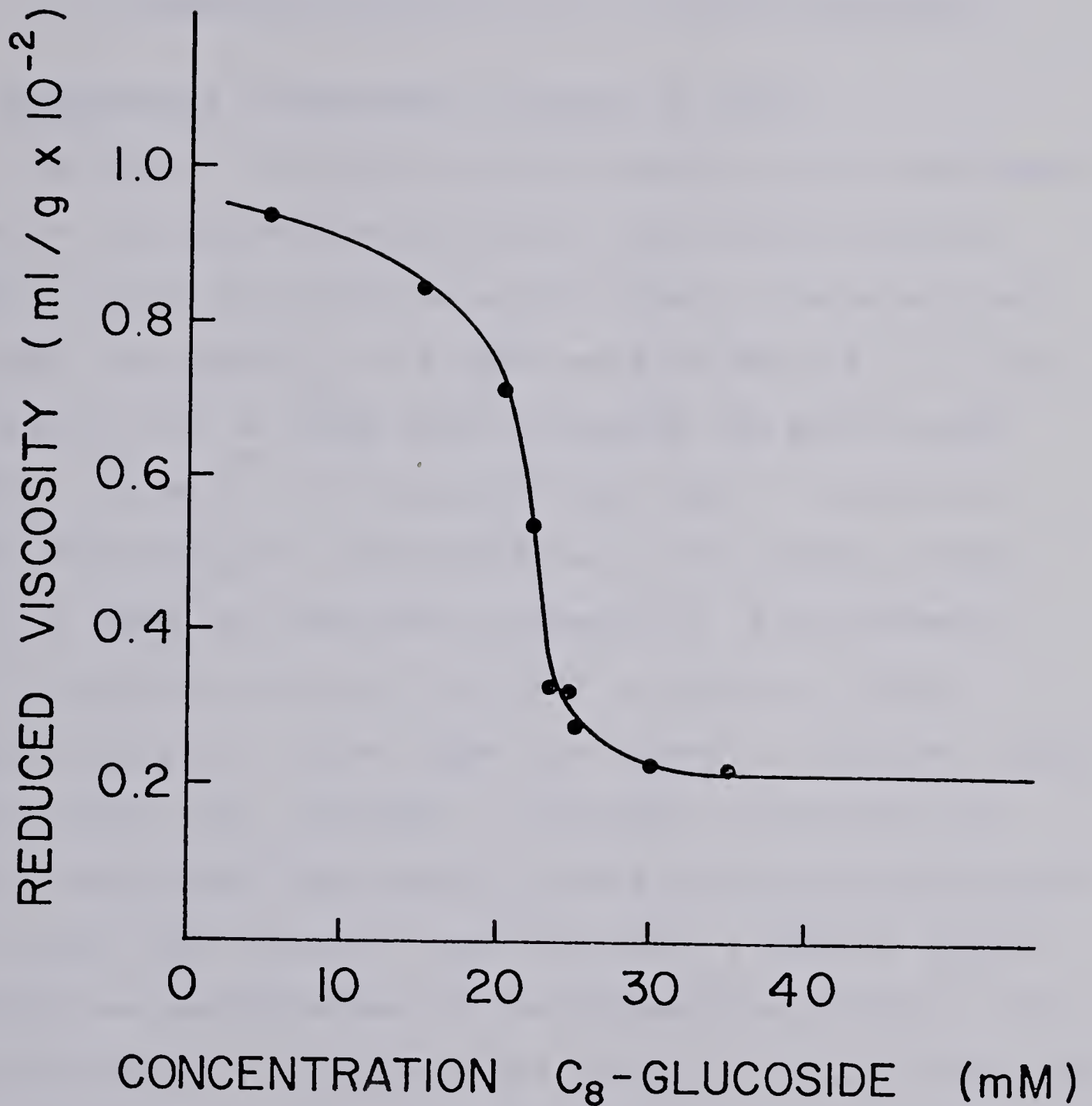


Figure IV.3. Dissociation of PAK pili in octyl-glucoside as measured by viscometry. A similar result was obtained for PAO pili. A protein concentration of 1 mg/ml was used for each determination. Samples were dialyzed against octyl-glucoside at the appropriate concentration overnight prior to determination of viscosity.



Beyond a concentration of 30 mM octyl-glucoside, no further dissociation was apparent. Subsequent studies were therefore carried out at 30 mM octyl-glucoside.

### *C. Characterization of Pilin in Octyl-glucoside*

#### **1. Measurement of detergent binding to pilin**

The amount of octyl-glucoside bound to pilin was determined at various concentrations by equilibrium dialysis using [ $^{14}\text{C}$ ]-octyl-glucoside as described in Materials and Methods. The binding curve obtained with PAK pilin is shown in figure IV.4. At 30mM octyl-glucoside PAK pilin binds  $12.5 \pm 1.4$  moles of octyl-glucoside per mole of protein or 0.24g OG/g PAK pilin. Determination of OG binding to PAO pilin at 30mM free detergent showed that  $12.9 \pm 2$  moles of octyl-glucoside are bound per mole of pilin or 0.25g detergent/g pilin. Above 30mM, the amount of detergent bound continued to rise. However, at detergent concentrations higher than 35mM, measurements became increasingly difficult due to the long dialysis times required. A similar type of binding has been observed in the interaction of Triton X100 with cytochrome b5 (Robinson and Tanford, 1975), whereby the amount of detergent bound continued to rise after the critical micelle concentration had been reached. The fact that the curve is fairly flat at low detergent concentrations suggests that below the critical micelle concentration, where the detergent is in the monomer form, little detergent binds to pilin. Rosevear *et al.* (1980) have



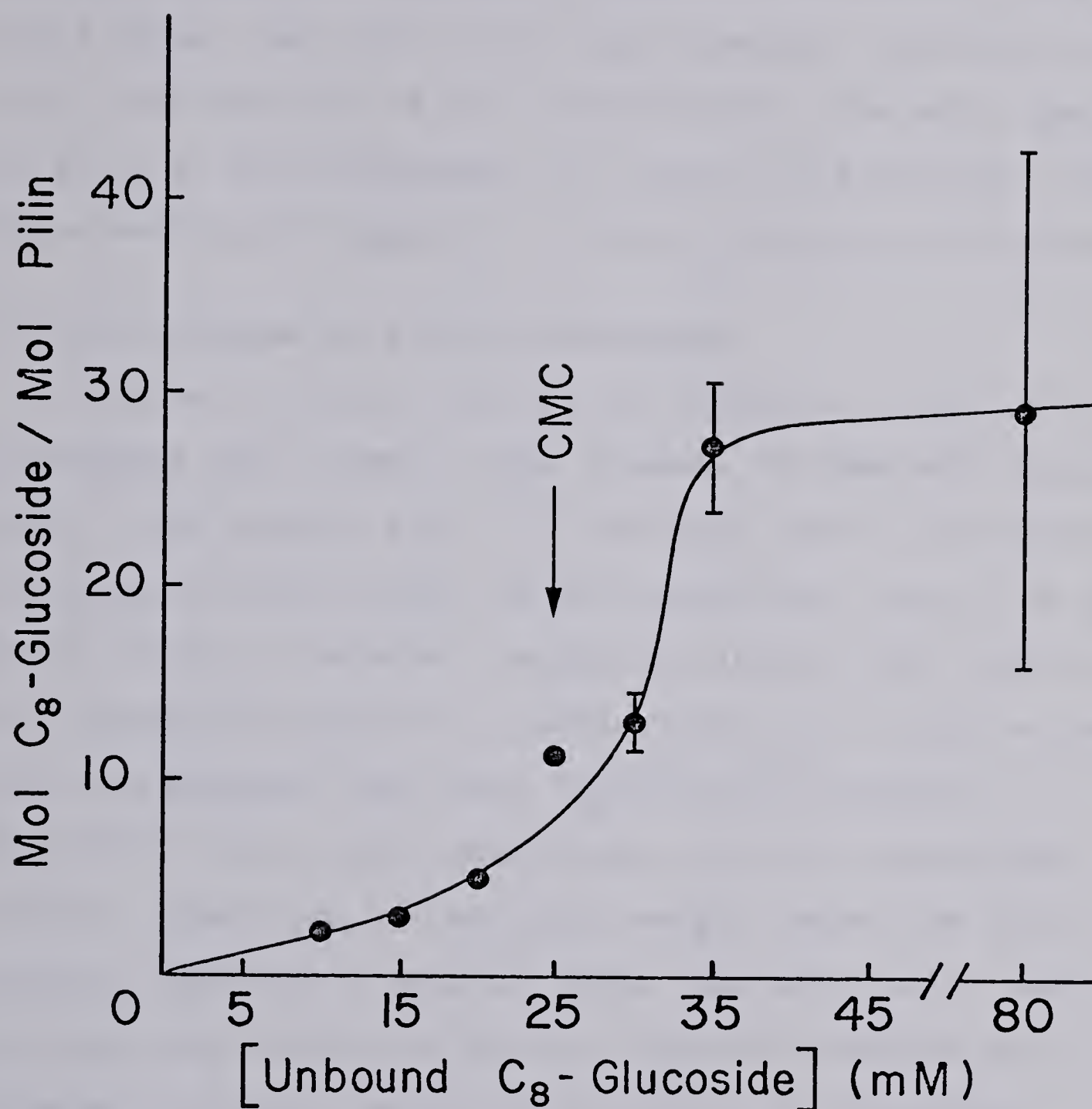


Figure IV.4. Binding of octyl-glucoside to PAK pilin as measured by equilibrium dialysis at 20°C. The measurements were carried out at a pilin concentration of 1mg/ml. The detergent concentration was monitored using [<sup>14</sup>C]- octyl-glucoside as described in Materials and Methods. CMC indicates the critical micelle concentration of octyl-glucoside at 25mM (Shinoda *et al.*, 1961).





reported that, at a concentration of 30mM, octyl-glucoside micelles have a molecular weight of 8000. This corresponds to approximately 27 detergent monomers per micelle. Thus it would appear that pilin binds approximately 1 micelle for every two subunits. As will be seen below, the major species of pilin in octyl-glucoside is a dimer and therefore, one detergent micelle appears to interact with one pilin dimer.

## 2. Gel exclusion of pilin in detergent

Figure IV.5 shows the elution properties of PAK pilin on a Sephadex G200 column in the presence of 30mM octyl-glucoside, 0.05M phosphate pH 7.0. The inset shows a calibration of the same column under similar conditions. As will be seen below, pilin in detergent is fairly globular and therefore the standards chosen were globular proteins. It can be seen that the Sephadex G200 has a fractionation range of 8000-89000 under these conditions, which is considerably shifted toward the low molecular weight range from what is normally observed in aqueous media. The major pilin peak, representing 87% of the material applied, migrates at an apparent molecular weight of 37,000 (or at an apparent Stokes' radius of 27Å) on Sephadex G200. If one subtracts the contribution due to detergent (based on the equilibrium dialysis result), one calculates that the major peak is a dimer consisting of 30,000 molecular weight due to protein plus 25 octyl-glucoside molecules, contributing 7300 to the apparent molecular weight. The small peak at the void volume (about 5% of the material) is due to larger aggregates of



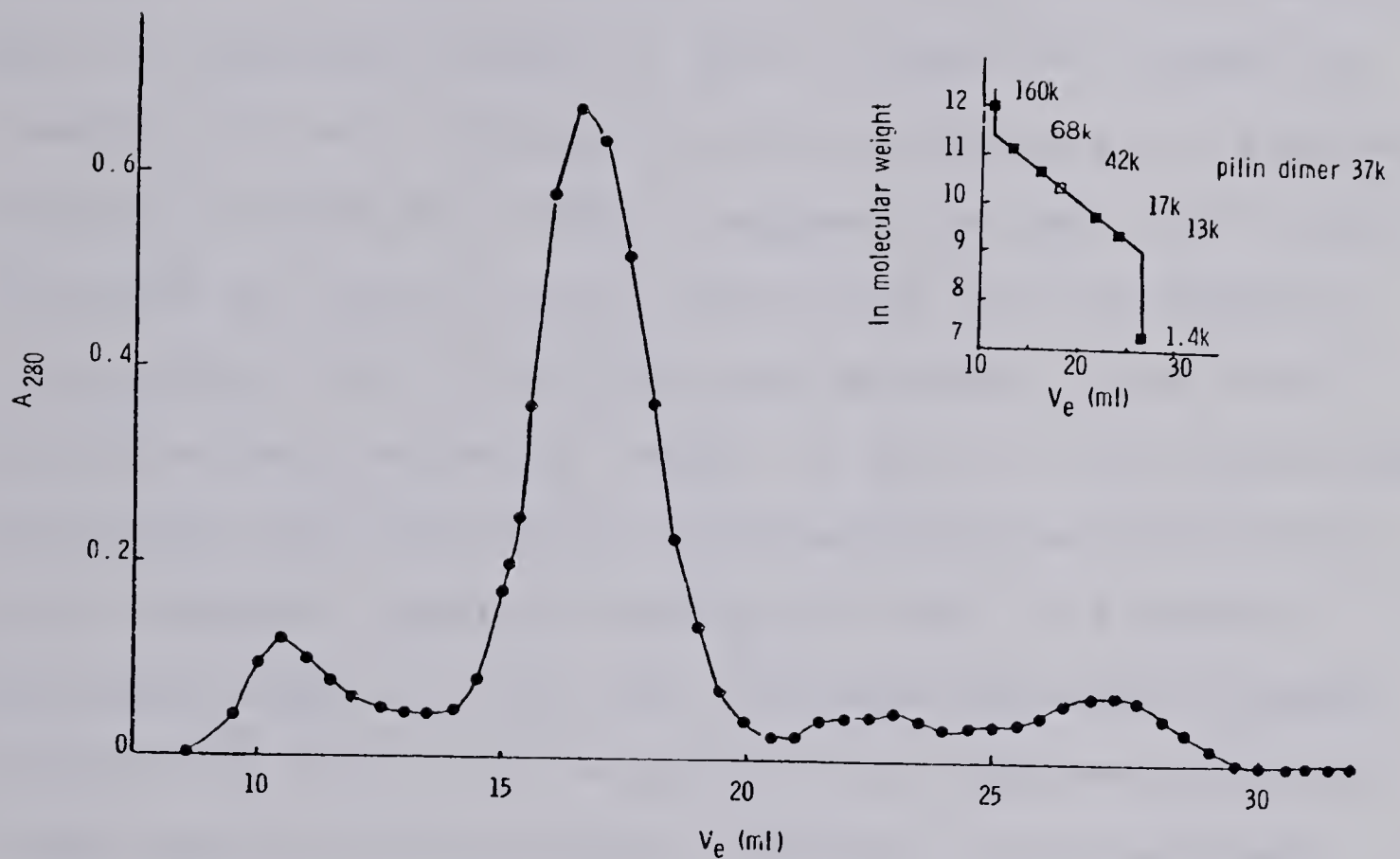


Figure IV.5 Gel exclusion chromatography of pilin on a 1x30cm Sephadex G200 column in the presence of 30mM octyl-glucoside, 0.05M  $\text{Na}_2\text{HPO}_4$ , pH 7.4. The inset shows a calibration run carried out under the same conditions. The elution positions of the standard proteins are filled squares, the open square represents the elution position of the major pilin peak.



pilin, while the small peak at  $V_e = 22\text{ml}$  may be the pilin monomer. The last peak on the elution profile, at  $V_e = 27\text{ml}$ , was ninhydrin negative.

An attempt was also made to use gel exclusion in the presence of [ $^{14}\text{C}$ ]-octyl-glucoside to obtain another measurement of detergent binding to pilin. Figure IV.6 shows the results obtained. Although the pilin migrates at an apparent molecular weight of 37,000, it appears to bind  $123 \pm 17$  octyl-glucoside per mole of pilin (calculated from two separate runs as described in Materials and Methods). Since octyl-glucoside has a molecular weight of 292, 123 octyl-glucoside molecules would contribute 36,000 molecular weight to the pilin detergent complex. This would result in a monomer/detergent complex of  $M = 51,000$  or a dimer/detergent complex of  $M = 66,000$ . Since pilin migrates at an apparent molecular weight smaller than ovalbumin ( $M = 43,000$ ), this detergent binding measurement is inconsistent with the migration position of the complex, with the equilibrium dialysis binding studies and, as will be seen below, with the molecular weight of the complex as determined by sedimentation equilibrium. Thus it appears, that the octyl-glucoside micelles are interacting with the Sephadex column in some way, so that the excess detergent loaded with the pilin fails to separate from the complex during the chromatography. This excess detergent does not appear to be tightly bound, however, since it does not effect the migration position of the pilin/detergent complex. Makino *et al.*, (1973) have also





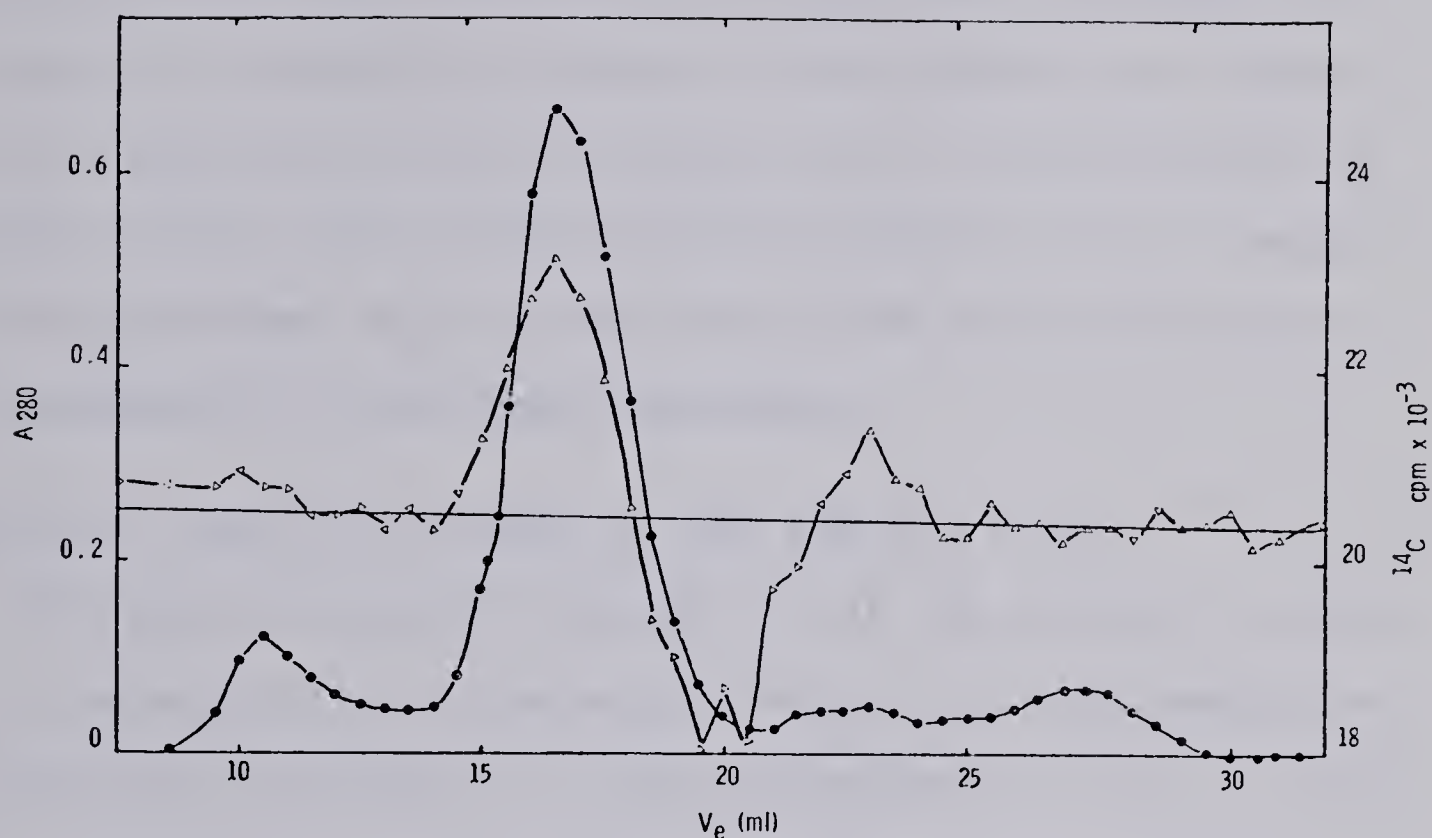


Figure IV.6. [ $^{14}C$ ]-octyl-glucoside binding to pilin monitored by gel-exclusion chromatography as described in Materials and Methods. (●),  $A_{280}$ ; pilin concentration is determined using a value of 1.3, for the extinction coefficient of a 1 mg/ml solution of pili in a 1cm cell. (Δ) [ $^{14}C$ ]-octyl-glucoside cpm associated with 100  $\mu$ l of each fraction. The specific activity of the detergent was determined using the base-line drawn through the [ $^{14}C$ ]-cpm profile. The column used is the same one as used in Figure IV.5 after equilibration with two column volumes of labelled octyl-glucoside.



noted problems in measuring detergent binding to various proteins. They found a number of spurious peaks and troughs that could not be explained by detergent/protein interactions. A similar problem is not usually encountered in measuring detergent binding to proteins whose detergent binding curves show saturation. In this case, monomers of detergent are capable of binding to the protein and therefore the experiment can be carried out at concentrations of detergent below the critical micelle concentration, thereby avoiding problems which arise due to the partitioning and the aggregation of detergent micelles.

### 3. Partial Specific Volumes of PAK and PAO Pilin

The partial specific volume,  $\bar{v}$ , of the protein is used in the determination of molecular weight from sedimentation equilibrium experiments, in the determination of  $S^{\circ}_{20,w}$  and in the calculation of the Stokes' radius of the protein based on sedimentation properties. In general, calculated values of  $\bar{v}$  are used for this purpose. Most commonly used is the method of Cohn and Edsall (1943), in which  $\bar{v}$  is calculated from the summation of the partial molal volumes of the free amino acids in solution based on the amino acid composition of the protein in question. Using this approach we obtain a value of 0.717 ml/g for PAK pilin (based upon its amino acid sequence) and a value of 0.732 ml/g for PAO pilin (based upon its amino acid composition).



An alternate method for calculating  $\bar{v}$  has been suggested by Chothia (1975). In this case the volumes for the amino acids used in the summation were determined by an accessible surface area calculation (Lee & Richards, 1971) on buried amino acid residues in 13 proteins whose crystal structures were available. The accessible surface area of an atom is defined as the area over which the center of a water molecule can be placed while maintaining van der Waals contact with the atom and without penetrating any other protein atom. Using the volumes tabulated in Chothia (1975) for the individual amino acids, one obtains a volume of  $19,234\text{\AA}^3$ , or a  $\bar{v}$  of 0.767 ml/g for PAK pilin. For PAO pilin, the value is again slightly higher at 0.773 ml/g.

Since the values calculated by the two approaches were so different, it was of interest to determine  $\bar{v}$  empirically. Assuming that partial specific volumes are additive, one can relate the  $\bar{v}$  of the free protein to that of the protein/detergent complex using the equation (Tanford *et al.*, 1974):

$$\bar{v}_C = \frac{\bar{v}_P + \delta_D \bar{v}_D}{1 + \delta_D} \quad \dots\dots (4.1)$$

where  $\bar{v}_C$ ,  $\bar{v}_P$  and  $\bar{v}_D$  are the partial specific volumes of protein/detergent complex, the protein and the detergent respectively and  $\delta_D$  is the amount of detergent bound in g/g protein.

The partial specific volume was determined by measuring the density of the detergent and of the protein/detergent





complex in an Anton Paar densitometer as described in Materials and Methods. The detergent density was measured above and below the CMC and the  $\bar{v}$  calculated from these measurements was found to be  $0.86 \pm 0.01$  ml/g below 25mM and  $0.85 \pm 0.01$  ml/g above 25mM. The  $\bar{v}$ 's of PAK and PAO pilin were both found to be independent of protein concentration and were indistinguishable within experimental error. The values obtained by densitometry were  $0.79 \pm 0.01$  ml/g in 80mM octyl-glucoside, where pilin binds  $0.58 \pm 0.2$  g of detergent per g of protein, according to equilibrium dialysis measurements (Figure IV.4). After subtracting the detergent contribution using equation 4.1, one obtains a value of 0.77 ml/g for pilin alone. One can also use equation 4.1 to determine  $\bar{v}_C$  for pilin in 30mM octyl-glucoside, resulting in a value of 0.78 ml/g. These values compare more favourably with the calculated  $\bar{v}$  obtained by the method of Chothia than they do with the values obtained using Cohn and Edsall's method. This is not surprising since Cohn and Edsall's method is based upon partial specific volumes of amino acids in solution while that of Chothia is obtained from volumes determined for amino acids buried in proteins.

#### 4. Sedimentation equilibrium

Sedimentation equilibrium analysis of the pilin/octyl-glucoside complex was carried out as described in Materials and Methods (Chapter II). Figure IV.7 shows the concentration dependence of the molecular weight of the PAK pilin/octyl-glucoside complex (a similar result was obtained



for PAO pilin). Extrapolation of the data to infinite dilution suggests a molecular weight of 18,400 for the PAK pilin-monomer/detergent complex. A value of 18,500 was obtained for PAO pilin (not shown). Since a 1% change in  $\bar{v}$  results in a 3% change in  $M$ , the uncertainty in this value is at least 3% or  $\pm 500$ . The molecular weight expected using  $M$  from the sequence and adding the detergent contribution based on equilibrium dialysis measurements is 18,650. From the results of the gel-exclusion experiment which suggested a dimer molecular weight of 37,000 in the presence of detergent one can deduce a monomer/octyl-glucoside molecular weight of 18,500. Therefore all 3 sets of data are in agreement within experimental error. From the shape of the molecular weight vs. concentration plot it appears that the system is aggregating as a function of concentration. This is in agreement with sedimentation velocity experiments described below. However, at a fixed concentration of protein and detergent it is possible to define the species present. The gel exclusion results showed that a 1-2mg/ml pilin solution in 30mM octyl-glucoside exists primarily as a dimer. The molecular weight ranges observed in the sedimentation equilibrium experiment at 1 mg/ml (not shown) also suggest that there is a large amount of dimer present under these conditions.



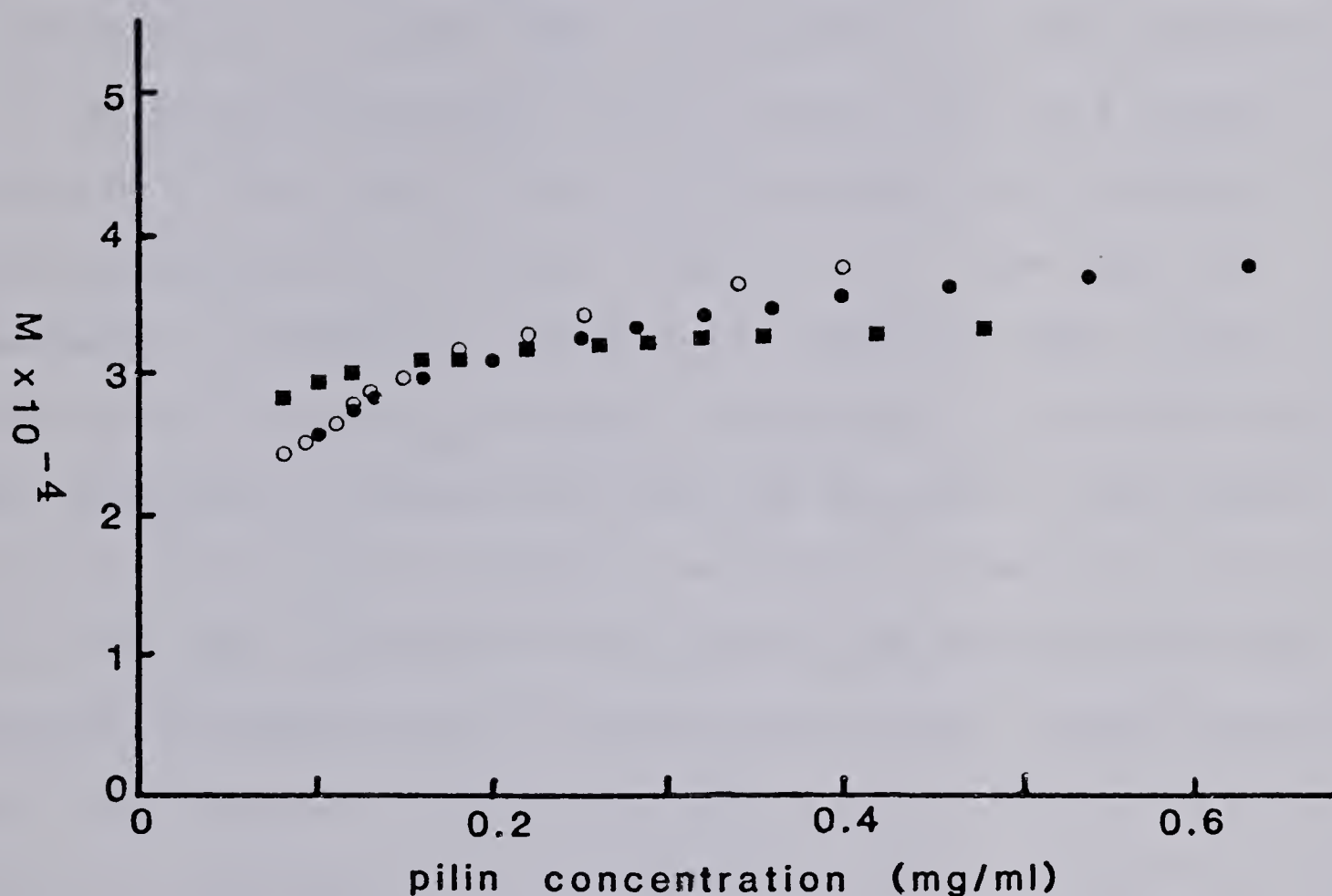


Figure IV.7. Effect of protein concentration on the molecular weight of the PAK pilin/octyl-glucoside complex, as measured by sedimentation equilibrium analysis. Loading concentrations were 0.6mg/ml (■), 0.5 mg/ml (●) and 0.4 mg/ml (○). All runs were carried out at 20°C, 17,000 rpm and used UV optics. Samples were dialyzed against 30mM octyl-glucoside for 48 hours prior to centrifugation.





## 5. Sedimentation velocity experiments

The sedimentation coefficient of the pilin/detergent complex as a function of protein concentration is shown in Figure IV.8. The system appears to be aggregating from zero concentration onwards. This heterogeneity is also observed in the Schlieren pattern (inset Figure IV.8) as a slight tailing of the peak on the solution side. Since sedimentation equilibrium studies (Figure IV.7) show that the monomer is present at low protein concentrations, extrapolation to infinite dilution gives the  $s^{\circ}_{20,w}$  of the monomer/detergent complex and hence can be used in the determination of  $R_s$  for the monomer. We obtain values of  $1.9_0 \pm 0.4S$  for PAK and  $1.9_2 \pm 0.2S$  for PAO pilin. The slope of the sedimentation coefficient vs concentration plot is also similar for the two pili, with a value of .44 for PAK and 0.47 for PAO. By calculating the average sedimentation coefficient of PAK and PAO pilin between 0.5 and 2.5 mg/ml, one can also obtain an estimate of the sedimentation coefficient of the pilin dimer of  $2.5 \pm 0.4 S$ .

## 6. Determination of the Stokes' Radius of Pilin

The parameters used in the determination of the Stokes' radii of the pilin dimer and the pilin monomer/detergent complexes are summarized in Table IV-II. The parameters shown are the average values obtained for PAK and PAO pilin, since the two proteins were indistinguishable within experimental error for most measurements. From the sedimentation coefficient, partial specific volume and



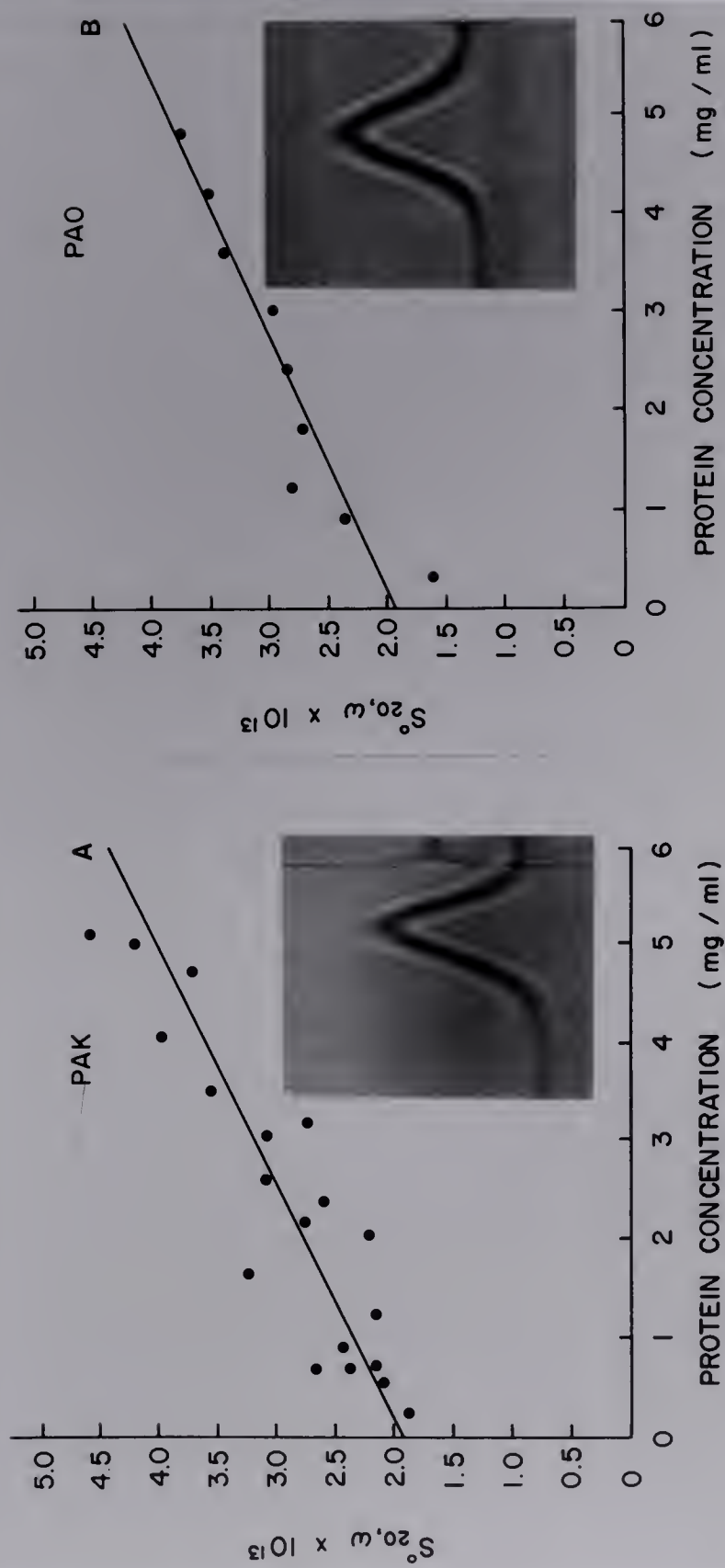


Figure IV.8. Determination of the sedimentation coefficient of a) PAK and b) PAO pilin. The sedimentation coefficient at infinite dilution was determined from the best fit line obtained by linear regression. All samples were dialyzed against of 30 mM octyl-glucoside prior to sedimentation. Sedimentation velocity runs were carried out at 20°C at 60,000 rpm.  
Inset: Typical Schlieren photograph of 1 mg/ml pilin in 30 mM octyl-glucoside used in determination of sedimentation coefficient.



TABLE IV-II

*Parameters used in the determination of the Stokes' radius of pilin monomers and dimers in detergent*

		monomers	dimers
M		15,000	30,000
$M_c$ <sup>1</sup>		18,500±500	37,000
$\bar{v}_c$ (ml/g) <sup>2</sup>	a.	-	0.79±0.01
	b.	-	0.78
$\bar{v}_p$ (ml/g) <sup>3</sup>		-	0.77
$\delta_D$ (g/g protein) <sup>4</sup>	a.	-	0.58±0.2
	b.	-	0.24±0.02
$s_{20,w,c}$ <sup>5</sup>		1.9±0.4	2.5±0.4
$R_{s,c}$ (Å) <sup>6</sup>		18.9±3	28.9±3
$R_{min,c}$ (Å) <sup>7</sup>		17.9	22.6
$(R_s/R_{min})_c$ (Å)		1.06±0.15	1.28±0.15

1. The subscript c indicates parameters determined for the pilin/detergent complex.  $M_c$  was determined from figure IV.7 for the monomer and from figure IV.5 for the dimer/detergent complex.
2. Measured by densitometry in 80mM octyl-glucoside, a., and calculated for 30mM octyl-glucoside from a,  $\delta_D$ , and equation 4.1, b.
3. Calculated from  $\bar{v}_c$  and  $\delta_D$  using equation 4.1.
4. Measured by equilibrium dialysis in a. 80mM and b. 30mM octyl-glucoside.
5. Determined from figure IV.8.
6. Calculated from equation 4.2.
7. Calculated from equation 4.3.





molecular weight of the protein detergent complex, one can calculate a Stokes' radius for the complex using the equation (Tanford *et al.*, 1974; Tanford, 1961):

$$R_{S,C} = \frac{M_C (1 - \bar{v}_C \rho)}{6 \pi \eta N S_{20,w}^0} \quad \dots\dots (4.2)$$

where the subscript c indicates parameters determined for the protein/detergent complex, N is Avagadro's number, and  $\eta$  is the viscosity in centipoise of water at 20°C. The ratio  $R_s/R_{min}$  is the measured Stokes' radius divided by the radius calculated for an unhydrated sphere of known volume, where,

$$R_{min,C} = \left( \frac{3 M_C \bar{v}_C}{4 \pi N} \right)^{1/3} \quad \dots\dots (4.3)$$

Therefore the ratio  $R_s/R_{min}$  reflects both hydration and asymmetry. The terminology  $R_s/R_{min}$  is equivalent to the ratio  $f/f_{min}$  and can be separated into its asymmetry and hydration components using the equation (Oncley, 1941):

$$f/f_o = f/f_{min} \left( \frac{1}{1 + w/\bar{v}\rho} \right)^{1/3} \quad \dots\dots (4.4)$$

where  $w$  is the hydration in g/g protein and  $f/f_o$  is the frictional ratio due to asymmetry alone. Since proteins in solution are always hydrated to some degree,  $f/f_{min}$  is always greater than 1.0. For globular proteins typical values are of the order of 1.10 to 1.30 while an asymmetric protein such as tropomyosin has a value of 3.22 (cf. Tanford, 1961). The value of  $R_s/R_{min}$  obtained for the pilin



dimers in octyl-glucoside (Table IV-II) is therefore indicative of a fairly globular hydrodynamic particle. Assuming that the hydration were negligible, an  $R_s/R_{min}$  of 1.28 suggests an axial ratio of about 6:1 for either a prolate or an oblate ellipsoid, as determined from Table IX of Schachman (1959). (An oblate ellipsoid is disk shaped, while a prolate ellipsoid is cigar shaped). Including a hydration term reduces this asymmetry. An upper limit of the hydration can be obtained by the summation of the degree of hydration of the individual amino acids as tabulated in Kuntz and Kauzmann (1974). This gives a value of 0.30g/g protein for completely unfolded pilin. Since pilin has about 80% secondary structure according to CD measurements, this estimate is clearly high. An additional complication, which will most likely add to the hydration term, is the hydration of the polar portion of the bound octyl-glucoside. If one substitutes the value of 0.3g of water/g pilin into equation 4.4, one obtains a value of 1.15 for the frictional ratio due to asymmetry alone. This is suggestive of an axial ratio of between 3 and 4:1 for a prolate or oblate ellipsoid model of revolution for the pilin dimer/detergent complex.

The value of  $R_s/R_{min}$  for the pilin monomer/detergent complex (Table IV-II) implies a more symmetric structure than that of the dimer/detergent complex. In fact, the value obtained (1.06) is somewhat low even for a globular protein. Again, this value is reduced further by including a hydration term. If one uses the value of 0.3g/g protein in





equation 4.3, one obtains a frictional ratio due to asymmetry of 0.95 for the pilin monomer/detergent complex, which is clearly impossible. The parameters used in the determination of the frictional ratio of the monomer/detergent complex were obtained by extrapolation of the sedimentation data to infinite dilution and by making the assumption that  $\bar{v}_C$  is the same for the pilin monomer and pilin dimer/detergent complexes. Since the detergent may not bind in the same way to the pilin monomers as it does to the pilin dimers, this approximation may explain the anomalously low value of  $R_s/R_{min}$  for the pilin monomer. Nevertheless, it seems reasonable to assume that the pilin monomer detergent complex is less asymmetric than the dimer/detergent complex. Therefore a conservative estimate of the asymmetry of the pilin monomer/detergent complex is that its axial ratio is less than 3:1. Since the far UV CD spectrum of native pili does not change in octyl-glucoside, one could also interpret this result as applicable to pilin in the intact pilus. However, one must be somewhat cautious in applying this result to pilin in the pilus, since the geometry of detergent binding most certainly affects the hydrodynamic properties of the complex to some degree.

One way to eliminate the need for an independent measurement of hydration is to determine the weight intrinsic viscosity for the protein and from this derive the viscosity increment (by multiplying by  $\bar{v}$ ) and using this value together with the sedimentation data to derive a new





term,  $\beta$ , defined by Scheraga & Mandelkern (1953) which varies as a function of axial ratio. The weight intrinsic viscosity is obtained by measuring viscosity as a function of protein concentration and extrapolating to infinite dilution. In practice, protein concentrations of over 3mg/ml must be used in order to get reasonably long flow times in the viscometer. For pilin, since there is a significant change in aggregation state between 0 and 3 mg/ml in octyl-glucoside, this rules out this type of experiment. Another type of experiment that would be feasible, however, is the technique of X-ray solution scattering as described by Luzzatti and Tardieu (1980). By varying the solvent density in X-ray solution scattering experiments, it is possible to eliminate the contribution of bound water or detergent to the measured radius of gyration. Similarly, one can carry out sedimentation equilibrium experiments in the presence of sufficient  $D_2O$ , such that the term,  $(1 - \bar{v} \rho)$  goes to zero, thereby eliminating the contribution of bound detergent to  $M$  (Reynolds & Tanford, 1976).

#### *D. Discussion and Conclusions*

In conclusion, we have found conditions for obtaining dimers and, at very low protein concentrations, monomers of pilin without affecting the overall protein conformation as monitored by circular dichroism. At 1mg/ml pilin in 30mM octyl-glucoside, 87% of the pilin subunits are in the dimer form. This is sufficiently homogeneous to allow further



studies on the properties of the pilin dimer (see Chapter VIII). At infinite dilution, on the other hand, the sedimentation properties reflect the pilin monomer and therefore can be used to obtain information on the shape of a single subunit.

The pilin dimer should also be a good starting point from which to attempt pilin crystallization from octyl-glucoside. The recent success of several laboratories in crystallizing membrane proteins from octyl-glucoside (Michel & Osterhelt, 1980; Garavito & Rosenbusch, 1980; Michel, 1983), suggests that this approach to solving the three-dimensional structure of pilin might be a fruitful one.

The fact that the octyl-glucoside can be readily removed from the pilin dimers is useful in that it allows studies on reassembly of pilin to be undertaken (Chapter IV). Furthermore, the fact that pilin in detergent does not undergo conformational changes detectable by CD suggests that pilin in the membrane may have a conformation very similar to that in assembled pili. The ease with which pili are taken apart with non-ionic detergents suggests that hydrophobic interactions may play an important role in holding the assembly together. Finally, these studies have shown that PAK and PAO pili are indistinguishable with respect to subunit shape and dimensions at the resolution of the hydrodynamic studies.





## CHAPTER V

### X-ray Diffraction Studies of Oriented Pili Fibers

Long flexible assemblies, such as bacterial pili, do not in general form 3-dimensional crystals suitable for analysis by X-ray crystallography. However, filamentous particles can often be induced to align along their long axes to form oriented bundles which can diffract X-rays. X-ray fiber diffraction deals with the study of such oriented assemblies. In most cases the assemblies are long filaments of identical subunits arranged in helices. The subunit can be a nucleotide in a helix of nucleic acid or it can be an amino acid (many of the poly- $\alpha$ -amino acids have been studied by fiber diffraction; Elliot, 1967). In other cases the repeating unit is a protein subunit. Some examples of protein assemblies which have been studied by fiber diffraction are tobacco mosaic virus (Holmes & Klug, 1963; Stubbs *et al.*, 1977), striated muscle (Huxley & Brown, 1967), bacterial flagella (Champness, 1971), filamentous bacteriophage (reviewed in Marvin & Wachtel, 1976) and bacterial pili (Type I pili, Brinton, 1965 and Mitsui *et al.*, 1973; F pili, Folkhard *et al.*, 1979a).

Because X-rays only report what is regular or repetitive in the crystal or fiber, X-ray fiber diffraction provides less information, in general, than does the study of a highly ordered 3-dimensional crystal, since the fibers are usually less well-ordered than crystals. The type of





information available from fiber diffraction is usually limited to information about the arrangement of subunits in the structure, although this is not always the case. Details such as the position of amino acid side chains in a protein are not usually attainable by X-ray fiber diffraction because the side chains do not occupy defined positions in the fiber but are disordered and cylindrically rotated from one filament to the next. However, there is a large amount of information in a diffraction pattern because at high angles where there is no lattice sampling, the diffraction pattern is related to the transform of a single repeating unit. In some cases this information can be utilized by constructing models and attempting to fit the diffraction data using a trial and error approach. This type of approach will be treated in more detail below.

The technique and theory of X-ray fiber diffraction has been thoroughly review in several books and articles (Holmes & Blow, 1966; Vainshtein, 1966; Kakudo & Kasai, 1972; Fraser & MacRae, 1973; Cantor & Schimmel, 1980; Marvin & Nave, 1982). For this reason, the theory of X-ray fiber diffraction will be treated only briefly below.



## A. Theory

### 1. Types of Orientation Observed in Fibers

Figure V.1 illustrates schematically the types of order observed in oriented fibers which are used for X-ray diffraction measurements. Figure V.1a represents a crystalline fiber. The fiber consists of a series of microcrystals each with a 3-dimensional ordered lattice. The microcrystals share a common axial direction (described by the angle  $\psi$  in this diagram) but are rotated with respect to each other (the angle  $\phi$  describes the rotational averaging). This type of averaging has been observed with some forms of DNA (Langridge *et al.*, 1960). The diffraction pattern from such a fiber is essentially the same as a rotation photograph of a single crystal (see Blundell & Johnson, 1976 for a discussion of rotation photographs).

Figure V.1b illustrates a semi-crystalline fiber. There is a regular spacing in the direction perpendicular to  $z$  but the particles are disordered and rotated about  $\phi$ . In semi-crystalline systems, the filaments often form a two-dimensional pseudo-lattice perpendicular to  $z$ . In other words, although many of the components may be imperfectly aligned and rotated with respect to one another, they fall on a rough lattice. This lattice gives rise to crystalline reflections on the diffraction patterns of such fibers at low angles (large periodicities) of diffraction. However, at high angles (higher resolution) the lattice does not sample the molecular transform and only the *continuous* molecular



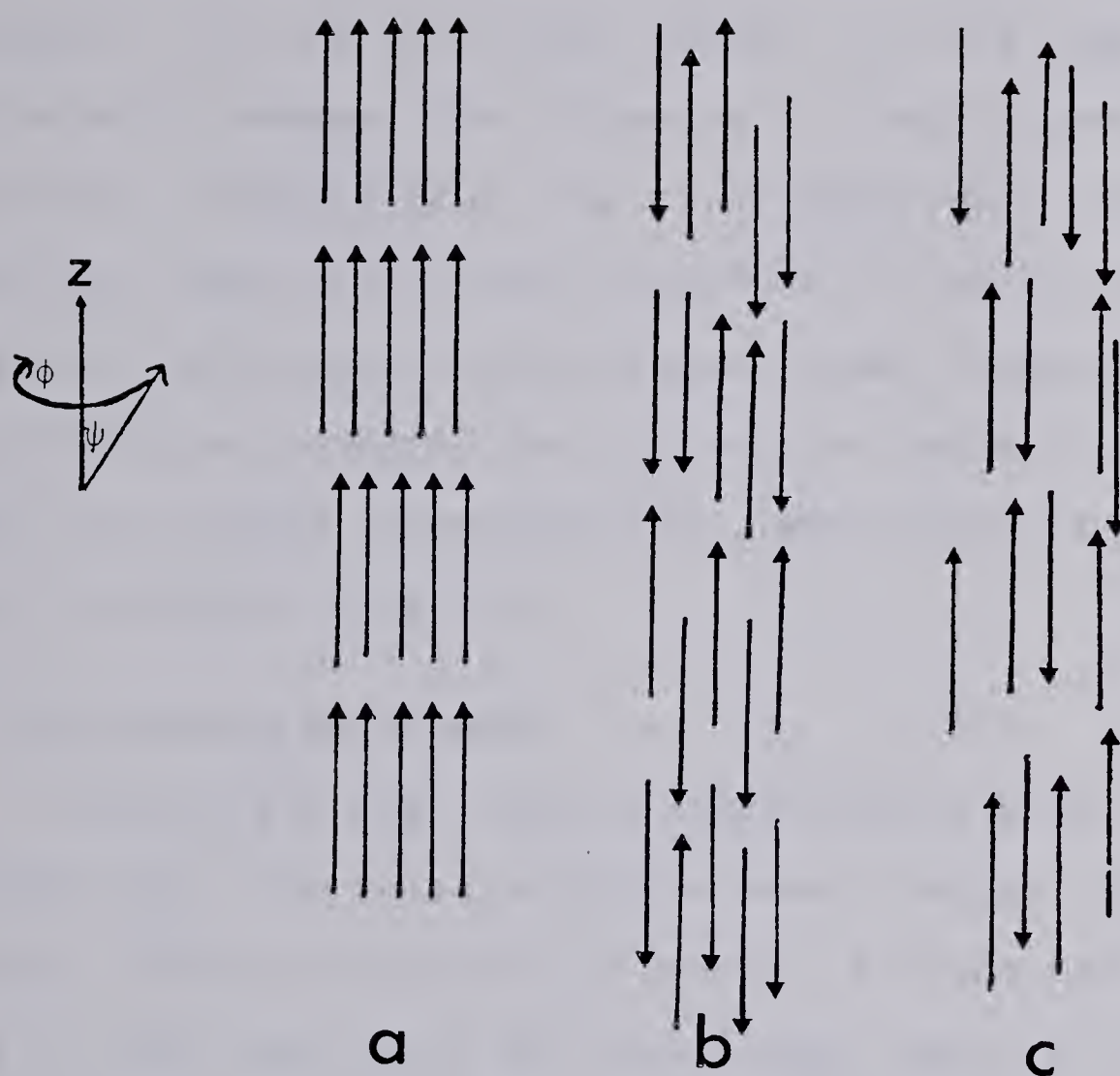


Figure V.1. Types of orientation found in fibers. a. crystalline b. semi-crystalline c. non-crystalline. (adapted from Cantor & Schimmel, 1980).





transform (that is, the transform of a single repeating unit) is in evidence.

The packing arrangements in a non-crystalline fiber (figure V.1c) are even less regular. In this case, the only correlation between the filaments is their common axial direction. This is true also of oriented gels. Such gels are obtained from concentrated solutions of rod-like molecules and show spontaneous birefringence under crossed polars in a polarizing microscope. The diffraction patterns of these gels are usually non-crystalline, and therefore show only the continuous transform.

## 2. Diffraction by a Helix

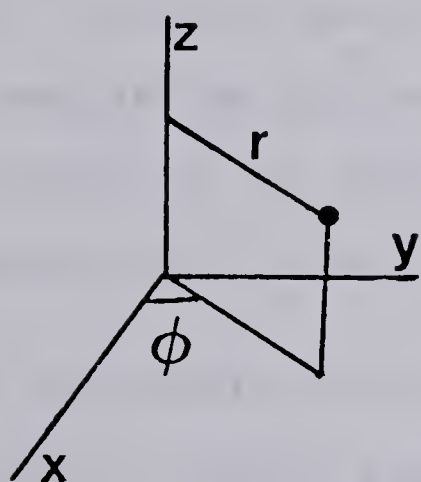
Helices are most readily described in polar-cylindrical coordinates. The relationship between the cylindrical-polar and the Cartesian coordinate system is illustrated in figure V.2 in both real space and reciprocal space. By convention, coordinates in real space take lower case letters, while coordinates in reciprocal space take capital letters. In an X-ray diffraction experiment, film space is roughly equivalent to reciprocal space, the diffraction pattern being equivalent to the square of the Fourier transform of the scattering object.

A helix is defined as a set of points which satisfies the equations:

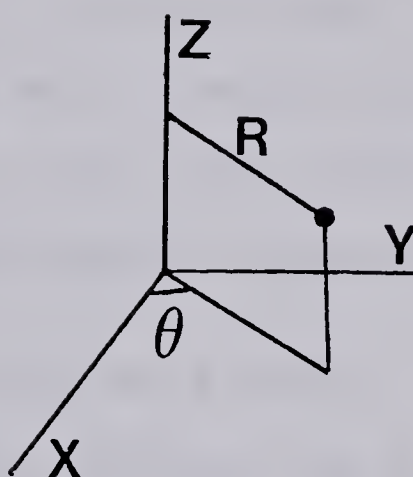


$$\begin{aligned}x &= r \cos \phi \\y &= r \sin \phi \\z &= z\end{aligned}$$

$$\begin{aligned}X &= R \cos \theta \\Y &= R \sin \theta \\Z &= Z\end{aligned}$$



a



b

Figure V.2. Relationship between the Cartesian and polar-cylindrical coordinate systems in a). real space and b). reciprocal space.



$$r=\text{constant}$$

$$z=P \phi /2 \pi$$

where  $P$  is the pitch of the helix and  $r, \phi, z$  are cylindrical-polar coordinates. Helical assemblies consisting of many subunits are called discontinuous helices. The subunits are related to each other by a unit rise,  $p$ , and a unit twist  $P/p$ , where  $p$  is the axial separation between subunits and  $P$  is the pitch of the helix. This is illustrated schematically in figure V.3A which shows a discontinuous helix with 5 subunits in 1 turn of pitch,  $P$ . In this case, the helix repeat,  $c$  (defined as the distance in  $z$  in which the structure repeats exactly) is equal to the pitch. This is not the case for helices which show non-integral symmetry.

In discussing diffraction by a helix, it is instructive to consider a simple example, such as the 5 unit/turn helix in figure V.3. Diffraction from helical assemblies falls on a series of lines called layer-lines, where the position of diffracted intensity obeys the helix selection rule:

$$l=nt+um$$

for a helix of  $u$  units in  $t$  turns.  $l, n$  and  $m$  are integers.  $l$  is the layer-line index,  $m$  is any integer from  $-\infty$  to  $+\infty$  (but in practice one is only concerned with small values of  $m$ ) and  $n$  is the order of the Bessel function contributing to a given layer-line.

Bessel functions are cylindrical wave functions which are used in describing the Fourier transform in polar







Figure V.3. A simple helix and its diffraction pattern.

A. A  $5u/t$  discontinuous helix of pitch  $P$  with an axial ratio between subunits,  $p$ .

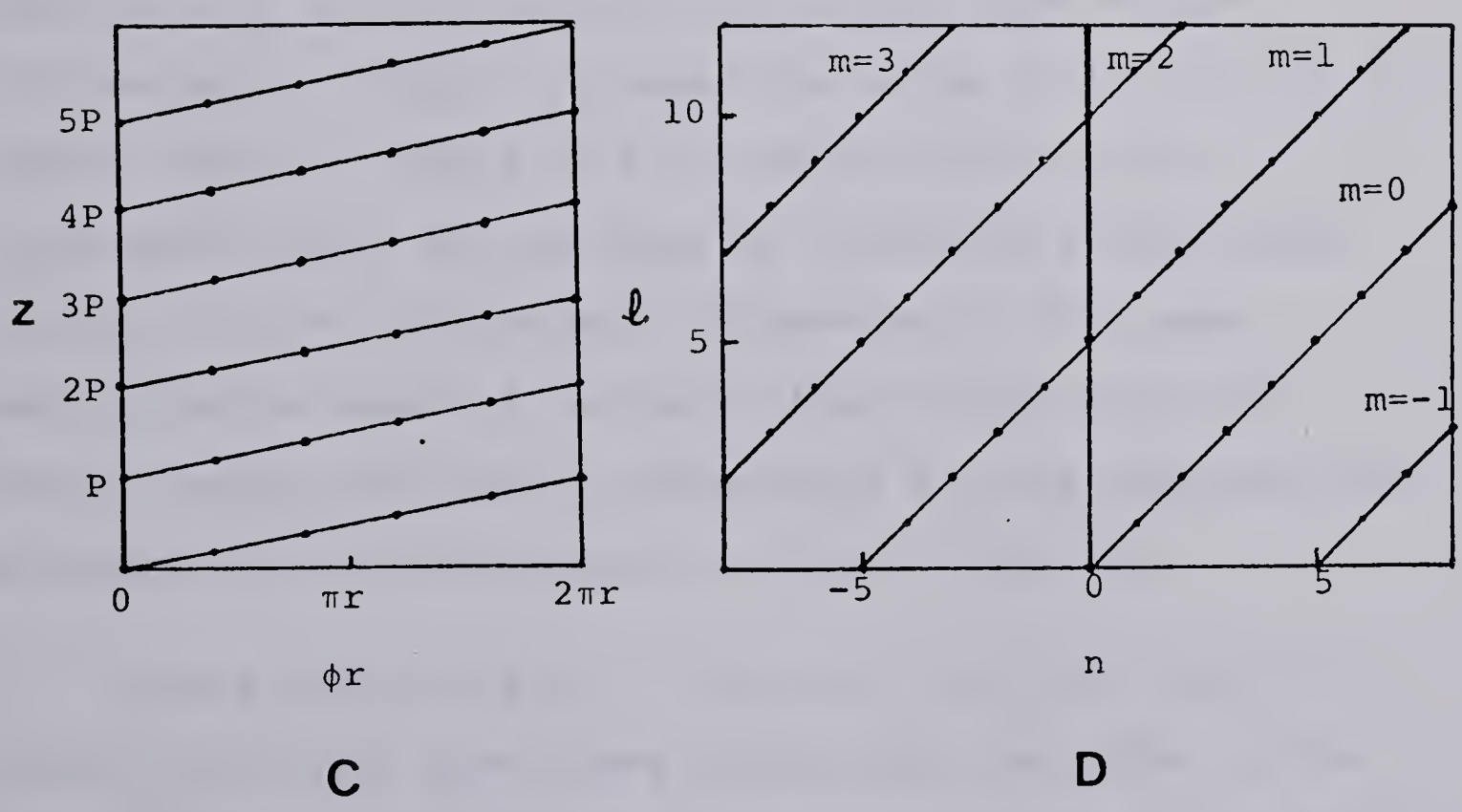
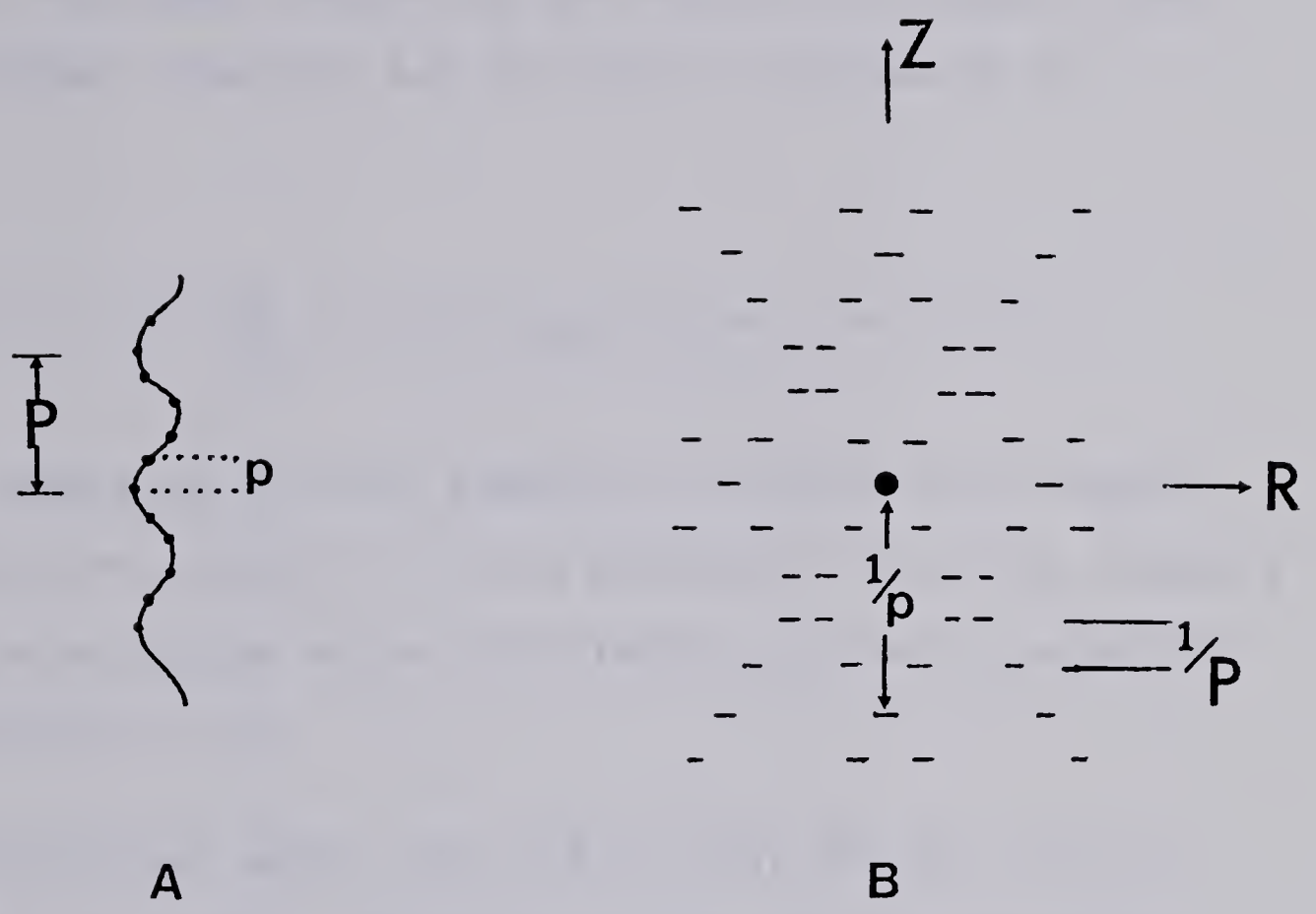
B. The diffraction pattern of the helix shown in A.

$Z$ , the fiber axis, is called the meridian of the diffraction pattern.

$R$  indicates the equatorial direction.  $1/p$  is determined from the distance between meridional reflections and  $1/P$  is given by the spacing between layer-lines. Only the  $m = 0, -1$  and  $+1$  sets of layer-lines are shown. These are centered at the origin,  $-1/p$  and  $1/p$ , respectively.

C. The radial projection (Surface Lattice representation) of the helix shown in A. One can imagine that the helix has been projected radially onto a cylinder and that the cylinder has been cut along its long axis and opened flat.

D. The  $n, l$  plot for the  $5u/t$  helix. This plot embodies the relation:  $l = um + nt$ , the helix selection rule. It is used to predict the Bessel function order,  $n$ , for each layer-line,  $l$ , on the diffraction pattern. Bessel functions with the same  $m$  value are connected by a straight line.





cylindrical coordinates. Bessel functions have the form  $J_n(2\pi rR)$ , where  $R$  is the reciprocal space radius and  $r$  is the real space radius of the scattering object. The *Fourier-Bessel* function has the form: (Cochran *et al.*, 1952),

$$F(R, \theta, l/c) = \sum_n J_n(2\pi Rr) \exp i[(\theta - \phi + \pi/2) + 2\pi lZ/c]$$

In the absence of helical symmetry,  $n$  can be any integer from  $-\infty$  to  $+\infty$ . However, in the presence of helical symmetry  $n$  takes on only the values dictated by the helix selection rule (equation V.1).

As mentioned above, the diffraction pattern is the square of the Fourier transform of the scattering object. Therefore it is the value of  $J_n^2(2\pi rR)$  that we are interested in. Figure V.4 shows the value of  $J_n^2(2\pi rR)$  for Bessel function orders of 0-7. One should note the progressive shift and decrease in intensity of the first maximum of the function with increasing  $n$ . This same modulation is observed in the diffraction patterns of helical structures and is responsible for the characteristic X-shaped diffraction patterns of these structures.

Figure V.3D shows an  $n, l$  plot for the  $5u/t$  helix in figure V.3A. This plot shows graphically the order of the Bessel functions predicted for each layer-line by the helix selection rule  $l = n + 5m$ , for the helix in figure V.3A. The





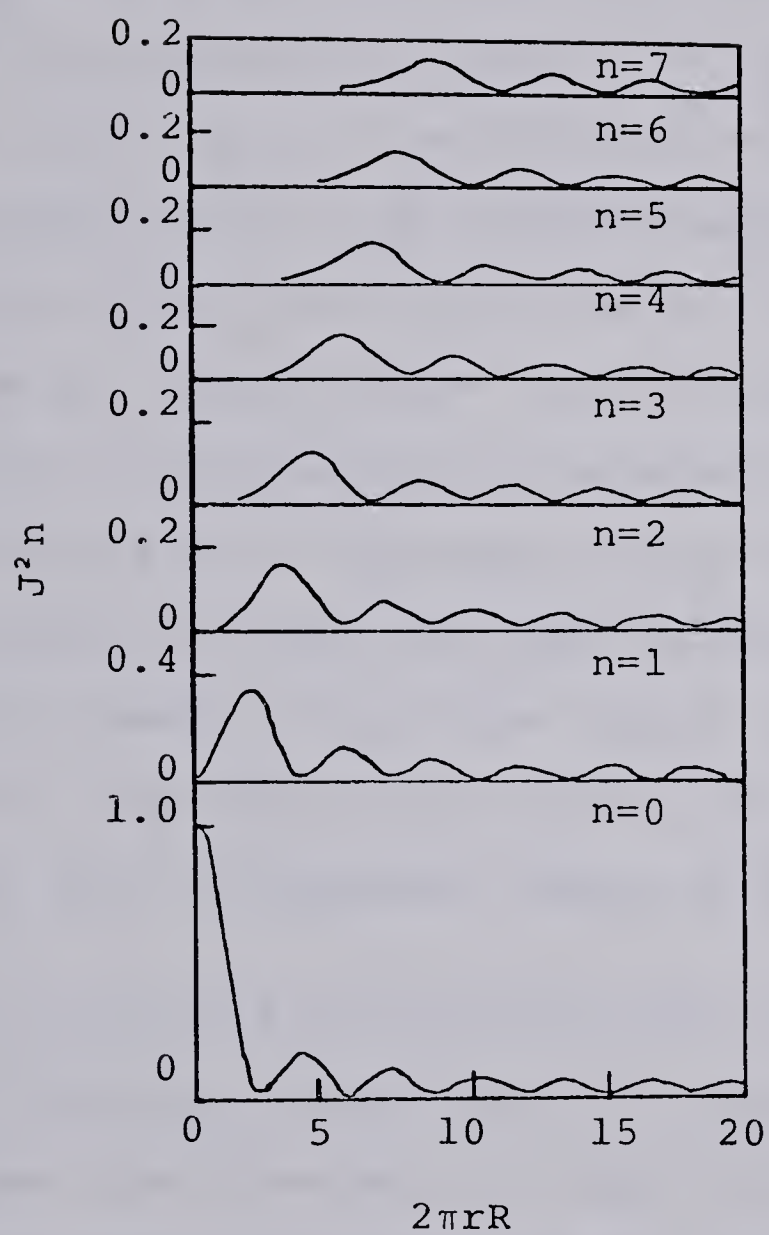


Figure V.4. Values of  $J^2_n(2\pi rR)$  for  $n=0-7$ .  $n$  is the Bessel function order;  $R$  is the reciprocal space radius and  $r$  is the real space radius of the scattering object. (adapted from Fraser & MacRae, 1973).



relation is plotted only for values of  $m$  close to zero because contributions from higher values of  $m$  are not usually observable on fiber diffraction patterns. Bessel functions with the same  $m$  value are connected by a straight line. This can be related to the diffraction pattern as follows. For  $m=0$ , a set of layer-lines with Bessel functions of order  $n=1$  are predicted. This set of layer-lines is centered at the origin of the diffraction pattern and the Bessel functions occur in an X-shaped pattern with its center on the origin. Similarly, the  $m=1$  set of layer-lines are centered at  $1/p$  and the  $m=-1$  set of layer-lines are centered at  $-1/p$ . For helices of integral symmetry, such as the one in figure V.3, equivalent layer-lines arising from different values of  $m$  have the same coordinate in  $Z$ . For non-integral symmetry, layer-line "splitting" is observed because  $|l|=1$  from the  $m=0$  and the  $m=1$  set of reflections, for example, fall on different values of  $Z$ .

Figure V.3B shows the expected positions of the diffracted intensity for the helix in figure V.3A. Only the contributions from three sets of layer-lines are shown. These are the  $m=0$ , the  $m=1$  and the  $m=-1$  layer-lines as discussed above. A few features are worth noting. The  $Z$  direction is referred to as the meridian of the diffraction pattern. It is colinear with the fiber axis. Spacings along this axis represent periodicities along the long axis of the filament. The smaller periodicity (between each layer-line) is inversely related to the helix pitch while the larger



repeat (between meridional reflections) is the reciprocal of the axial separation between subunits. One converts these spacings into real space distances using Bragg's law and a knowledge of the specimen to film distance.

The R axis is also called the equator of the diffraction pattern. In the absence of crystalline reflections, the continuous intensity distribution along this axis provides information about the electron density distribution of the molecule projected down its long axis onto a plane perpendicular to Z.

The *radial projection* of the helix in real space is illustrated in figure V.3C. This plot can be considered to be the reciprocal of the  $n, l$  plot in figure V.3D. The radial projection is obtained by projecting the helix onto the surface of a cylinder which is coaxial with the z axis. If one imagines that the cylinder is cut along a line parallel to the z-axis and opened flat then one arrives at the two-dimensional representation shown in figure V.3C. This is also called the surface lattice representation of the helix.

Figure V.3B shows the positions (but not the amplitudes) of the reflections expected for a  $5u/t$  helix. The intensity distribution on the layer-lines, however, will be modulated by the transform of the repeating unit. Furthermore, systematic absences of certain reflections can also occur in some cases. In practice fiber diffraction patterns do not show such discrete reflections, but show arcs of





intensity due to disorientation of the sample. This makes it difficult to identify which Bessel functions are contributing to a given layer-line. In particular, it is often a problem to distinguish between a truly meridional reflection ( $J_0$ ) and a near meridional reflection ( $J_1, J_2$  etc.). This distinction is important in determining the axial separation of the subunits and hence the number of units per turn of the helix. In addition, layer-lines are not always clearly resolved and this leads to difficulties in measuring the intensity distribution as a function of layer-line index.

### 3. The Use of Model Building in Solving the Phase Problem in Fiber Diffraction Analysis

Just as in X-ray crystallography, the amplitudes but not the phases of scattered waves are recorded in an X-ray fiber diffraction experiment. In solving the three-dimensional structure of a protein crystal, the phases are generally obtained using the technique of multiple isomorphous replacement (MIR). This approach is described in most textbooks which cover protein crystallography (for example, Blundell & Johnson, 1976; Cantor & Schimmel, 1980). MIR can occasionally be used in fiber diffraction, but only when the degree of orientation of the fibers is unusually high. In other cases, the unambiguous interpretation of the heavy atom position is not possible and the technique is next to useless. MIR has been used to solve the structure of oriented gels of tobacco mosaic virus (Holmes & Klug, 1963; Stubbs *et al.*, 1977) and more recently, the same approach



has become possible for the filamentous phage Pf1 by virtue of the fact that extremely well oriented fibers of native and derivitized phage could be obtained in a strong magnetic field (Nave *et al.*, 1981).

In most cases, however, sufficient orientation is not achieved to allow interpretation of heavy atom substituted diffraction patterns and in these cases a trial and error approach is used to solve the phase problem. This type of approach was introduced in the early 1950's for the determination of DNA structures from fiber diffraction data (Lipson & Cochran, 1954). The approach used is to construct stereochemically reasonable models which are based on a general consideration of the diffraction pattern together with any available chemical data. The Fourier transform of the molecule is then calculated and compared with the observed transform (the diffraction pattern). If several different starting models are conceivable, it is necessary to refine each of these separately so that each possibility can be evaluated. If a model is found that fits the data so well as to eliminate the possibility of a different model fitting the data equally well, then one would consider the phase problem solved. However, in practice, there will always be some controversy as to whether a model actually represents a unique solution. Furthermore if the diffraction data only goes out to 10Å resolution for example, the phases will be unreliable beyond this point and at higher resolution will be dependent on the detailed nature of the





starting model. In the case of proteins, where the large number of atoms lead to an enormous number of possible arrangements it is unlikely that this type of approach will lead to an atomic resolution structure. However, it can be useful in determining the structure of filamentous assemblies at low resolution (10-50 Å).

### *B. Analysis of the Diffraction Patterns of PAK and PAO Pili*

Oriented fibers of PAK and PAO pili were prepared as described in Materials and Methods. In general, the optimum conditions for preparing fibers were to use a 20mg/ml solution of pili in distilled water that had been allowed to stand for several days at 4°C to promote orientation. Only about one in ten fibers produced high quality diffraction patterns of PAK and PAO pili. As will be seen below, attempts to orient other types of pili were even less successful. It is thought that the tendency of pili to form "ropes" upon standing in concentrated solutions (see chapter VI, figure VI.3) may be important in obtaining good orientation.

The fiber diffraction patterns obtained for PAK and PAO pili are shown in figure V.5. It can be seen that they are very similar within the resolution attained. As is the case for helical assemblies in general, the intensity falls on a series of layer-lines which lie perpendicular to the meridian of the diffraction pattern (the meridian and the equator of the diffraction pattern were defined in figure





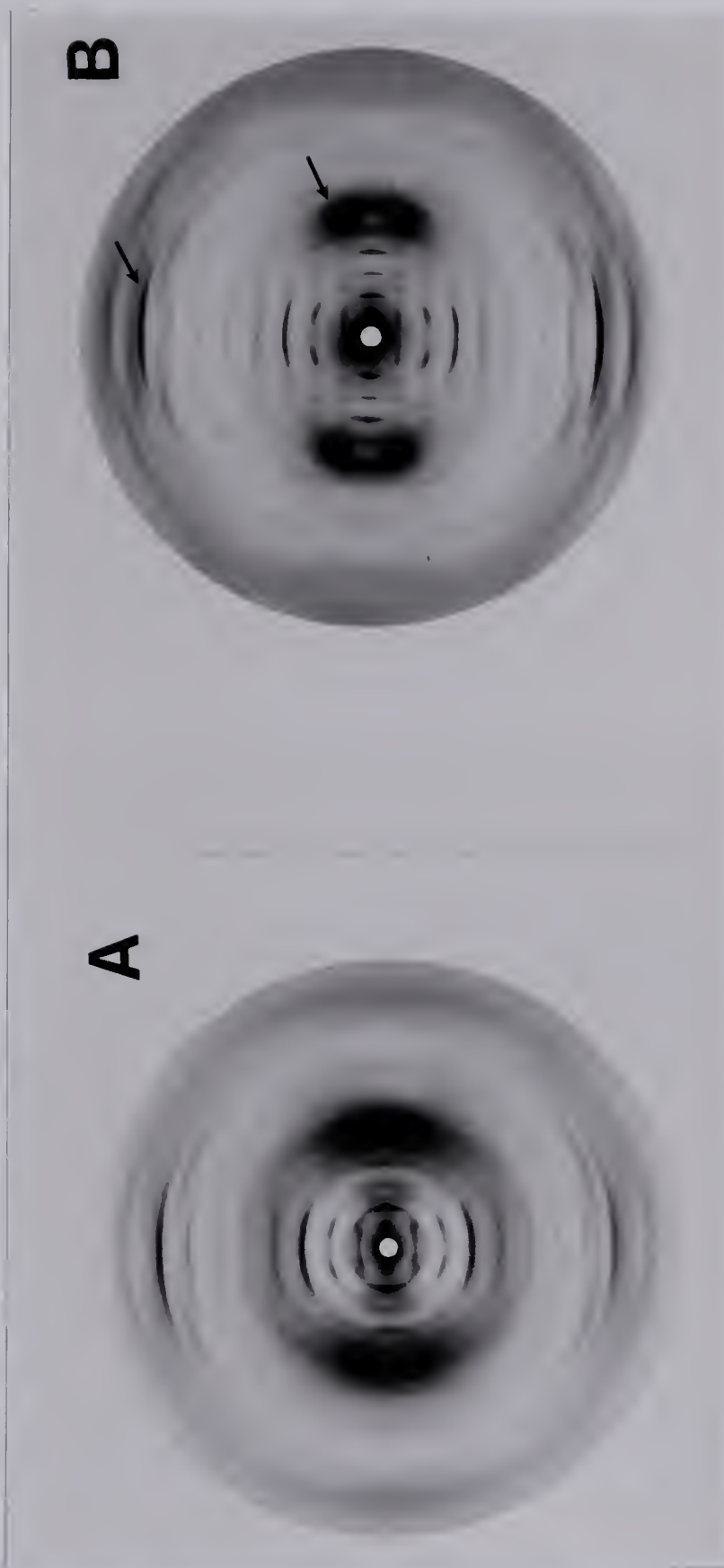


Figure V.5. X-ray fiber diffraction patterns of pili at 75% relative humidity and a specimen to film distance of 7.4cm. a)PAK pili b)PAO pili. The arrows indicate the "10Å-equatorial" and the "5Å-meridional" reflections.



V.3B). The sharp reflections observed at low  $R$  on the equator of the diffraction patterns are crystalline (Bragg) reflections and give information about the packing of pili in the fiber. A striking feature of the diffraction pattern is the strong equatorial reflection at  $1/10\text{\AA}$  on  $l=1$  and the strong meridional intensity at  $1/5\text{\AA}$  on  $l=8$  (henceforth called the  $10\text{\AA}$ -equatorial and the  $5\text{\AA}$ -meridional reflections). This intensity distribution is characteristic of  $\alpha$ -helical rods lying roughly in the direction of the fiber axis. The  $10\text{\AA}$  spacing corresponds to the side by side packing of  $10\text{\AA}$ -diameter  $\alpha$ -helices and the  $5\text{\AA}$  spacing to the pitch of an  $\alpha$ -helix. Each of these features will be discussed in turn below.

## 1. Analysis of equatorial data

### a. Crystalline reflections

The crystalline reflections on the diffraction patterns of PAK and PAO pili can be indexed on a hexagonal lattice as shown in Table V-I. Hexagonal packing is common for cylindrical structures and has been observed also for F pili (Folkhard *et al.*, 1979a) and Pf1 bacteriophage (Marvin, 1966). The greatest extent of crystallinity was found between 75% and 98% relative humidity (r.h.) where crystalline reflections extend to  $(h,k)$  values of  $(3,1)$  for PAK pili and  $(4,1)$  for PAO pili. The fibers lose crystallinity at low water content and usually only the  $(1,0)$  and the  $(1,1)$  reflections are observed in dry



TABLE V-I

*Indexing of Crystalline Reflections on a Hexagonal Lattice<sup>a</sup>*

$(h,k)^b$	$(h^2+hk+k^2)^{\frac{1}{2}}^c$	$R(A^{-1})^d$	ratio <sup>e</sup>
1,0	1	0.0213	-
1,1	1.73	0.0367	1.72
2,0	2	0.0433	2.03
2,1	2.65	0.0572	2.69
3,0	3	0.0461	3.01
2,2	3.45	0.0735	3.45

a. The data shown are for PAO fiber F67B, film 4524A. Similar results were obtained for PAK and for other PAO fibers.

b.  $(h,k)$  are the Miller indices of reflections arising from the hexagonal lattice.

c.  $(h^2+hk+k^2)^{\frac{1}{2}}$  expresses the expected ratio of  $R_{(h,k)} / R_{(1,0)}$  for a hexagonal lattice.

d.  $R$  is the reciprocal space coordinate of the observed crystalline reflection.

e. Ratio is the observed ratio  $R_{(h,k)} / R_{(1,0)}$ .





specimens.

The unit lattice dimension,  $a$ , is determined from  $R$  ( $\text{\AA}^{-1}$ ) for the (1,0) reflection. Figure V.6 shows the effect of water content on the unit lattice spacing,  $a$ , and on the axial periodicity in the fiber.  $a$  is a measure of the center to center distance between pili in the fiber. In dry fibers, where  $a$  is a minimum,  $a$  is equal to the pilus diameter (determined to be 51-52 $\text{\AA}$  from figure V.6). It can be seen that the lattice swells from 51-52 to 61-62 $\text{\AA}$  and that there is an axial expansion of 1-2% between dry and wet pili fibers.

Crystalline reflections are also observed on the first layer-line and sometimes on the second layer-line of pili diffraction patterns. These reflections follow the hexagonal lattice defined by the equatorial crystalline reflections implying that there is no larger unit cell in 3-dimensions.

#### b. The continuous equatorial transform

At higher water content, achieved by swelling fibers in a capillary, the hexagonal packing in the fibers is disrupted and the pili diffract as individual particles. From the analysis of the equatorial diffraction intensity of such specimens, one can obtain the *radial electron density distribution* of the particle. The radial electron density distribution is the cylindrically averaged electron density of the particle projected down its long axis onto a plane perpendicular to  $z$ . In other words, it is the cross-



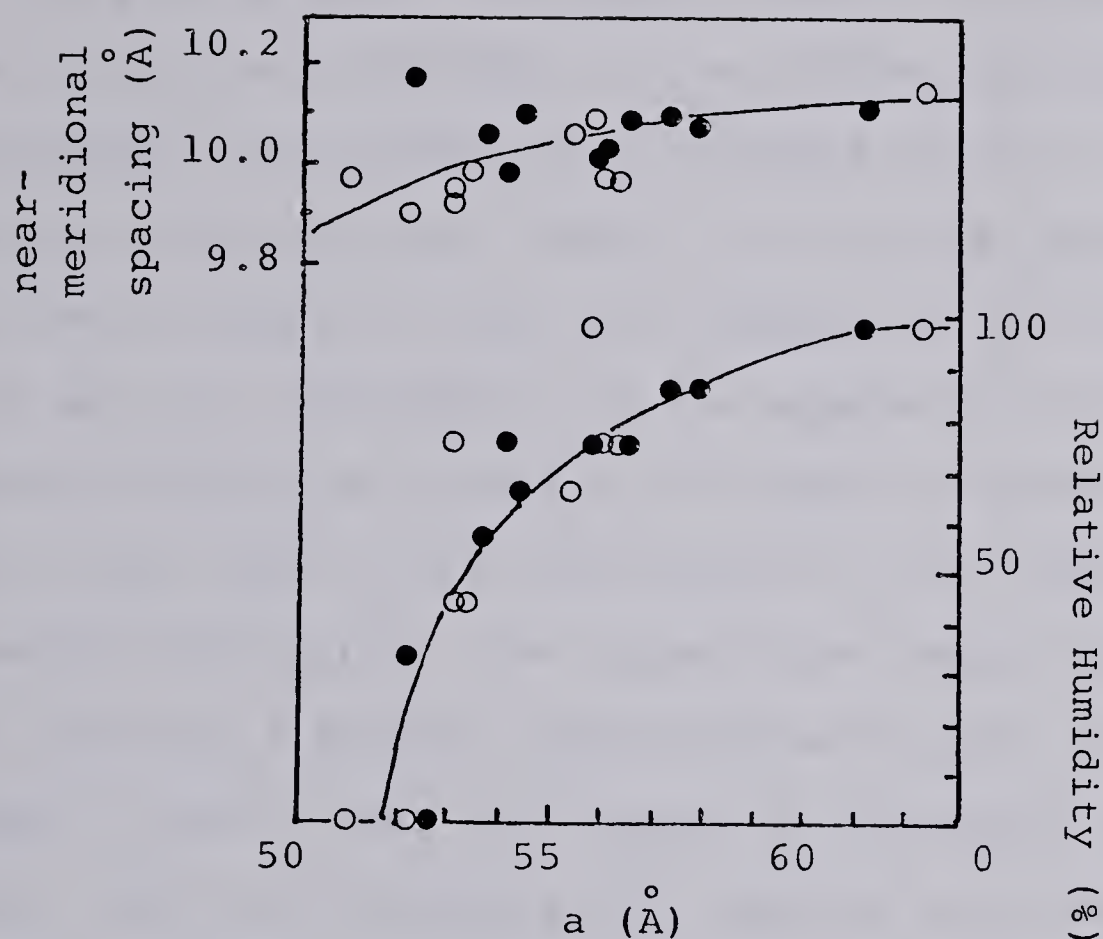


Figure V.6. Relationship between the center to center distance  $a$  (the unit lattice dimension), the spacing corresponding to the near meridional intensity on the fourth layer-line and the relative humidity for three PAK pili fibers (O) and six PAO pili fibers (●). The upper curve shows the meridional spacing versus  $a$ . The lower curve shows the expansion of the unit lattice with increasing humidity.



sectional electron density distribution in 1 dimension (the radial direction).

Figure V.7 shows the continuous diffraction amplitudes measured from the diffraction patterns of oriented wet gels of PAK and PAO pili. The Bessel function of order zero ( $J_0$ ) that starts at the origin of the diffraction pattern represents the cylindrically averaged Fourier transform of a single pilus particle. However, the helical symmetry (see section 2, below) of the pilus suggested that there would also be a  $J_1$  contributing to the equatorial intensity, albeit starting at higher  $R$ . In order to ensure that only the  $J_0$  was used in the calculation of the radial electron density distribution, the crystalline reflections from one PAO fiber at different humidities were used to define the shape of the  $J_0$  that they sample at different reciprocal space radii with changing unit lattice size (Wachtel *et al.*, 1974). The fiber chosen for these measurements showed crystalline reflections only on the equator. Because of the high intensity of the crystalline reflections, the possibility that the continuous  $J_1$  could be contributing to the crystalline diffraction intensity was judged negligible. It can be seen (figure V.7b) that the crystalline equatorial diffraction amplitudes of the PAO fiber follow the continuous equatorial amplitudes of the oriented gel implying that only the  $J_0$  is represented out to  $R = .08 \text{ \AA}^{-1}$





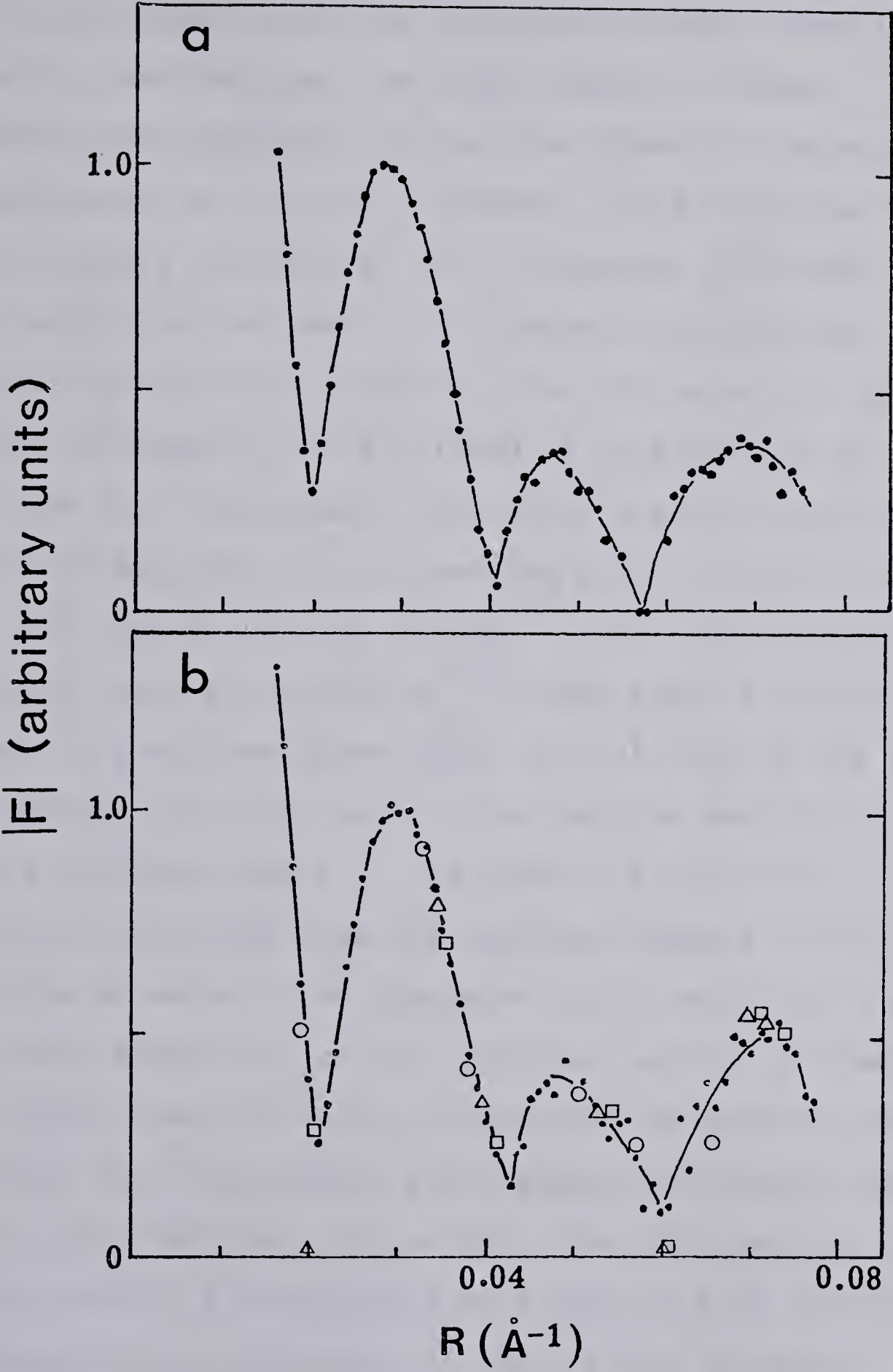


The following table shows the results of the experiment. The first column shows the number of trials, the second column shows the number of correct answers, and the third column shows the percentage of correct answers. The data shows that the percentage of correct answers increases as the number of trials increases, and that the percentage of correct answers is higher for the first trial than for the subsequent trials.

Number of trials	Number of correct answers	Percentage of correct answers
1	8	80%
2	6	60%
3	7	70%
4	5	50%
5	6	60%
6	4	40%
7	5	50%
8	3	30%
9	4	40%
10	5	50%

The results of the experiment show that the percentage of correct answers is highest for the first trial (80%) and lowest for the ninth trial (30%). The percentage of correct answers for the other trials is between 40% and 70%.

Figure V.7. Continuous equatorial diffraction amplitudes,  $|F|$ , from X-ray fiber diffraction patterns of wet gels (points and line).  $R$ =reciprocal space radius. a. a PAK pili wet gel b. PAO pili: the points on the line show the continuous transform of the wet gel, while the symbols show the crystalline reflection amplitudes of a PAO fiber at different humidities ( $\circ$ ) 98%; ( $\Delta$ )86%; ( $\square$ ) 75%. The crystalline reflections were put on the same scale as the continuous transform by scaling the (1,1) reflection (the reflection of highest amplitude) to the continuous transform.





The Fourier transform of the continuous equatorial diffraction amplitudes was calculated as described in Materials and Methods. The total number of phase combinations possible for the four nodes in the equatorial transform is 16 ( $\pm, \pm, \pm, \pm$ ). However, since the pilus is known to be roughly cylindrical with a diameter of 50-60Å, this information can be used to eliminate some solutions. In combination with the constraint that the electron density cannot be negative, this allowed us to eliminate all but one solution as unreasonable. The radial electron density distribution obtained for PAK and PAO pili is shown in figure V.8. The radial electron density,  $\rho(r)$ , was put on an absolute scale by setting  $2\pi \int \rho(r) dr$  equal to the total number of electrons above water in a 1Å slab of the pilus. The baseline was then set to the electron density of water (0.334 electrons per Å<sup>3</sup>). The number of electrons in a 1Å slab was calculated from the electron density of pilin relative to water (from the amino acid composition) and from the axial separation of the subunits (section B.2 below). The radial electron density distributions obtained for the two pili are very similar and apparent differences may be due to the inaccuracy of the data. The low electron density at the center is interpreted as a hole of 6-7Å radius, by analogy with the structure of the F pilus (Folkhard *et al.*, 1979a). However, with F pili, which has an inner diameter of 20Å, stain penetration into a central channel has been observed in electron micrographs of epoxy-embedded





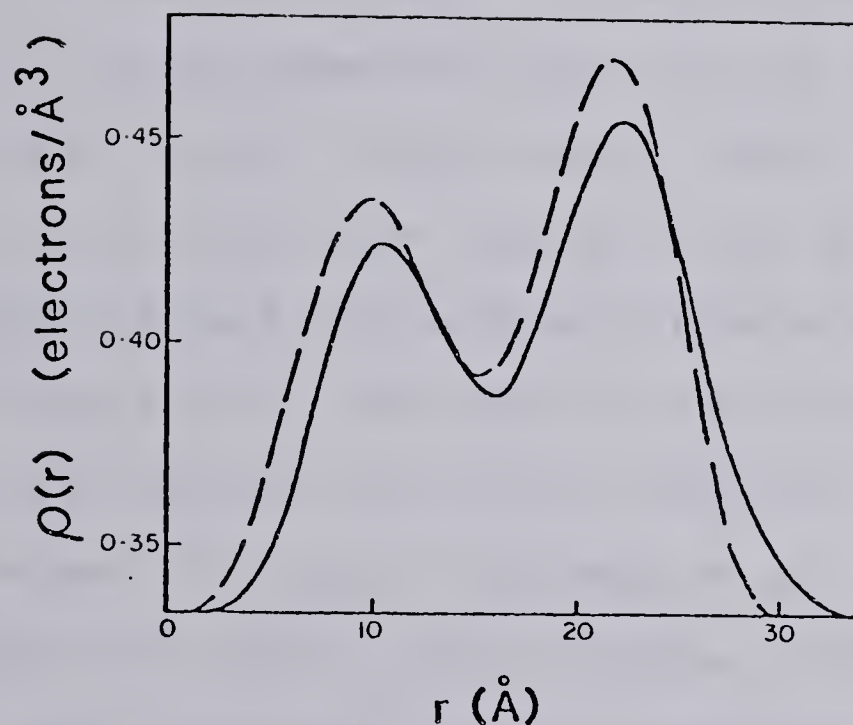


Figure V.8. Radial electron density distributions calculated from the continuous data of figure V.7. (—)PAK pili; (---) PAO pili. The signs of the amplitudes were chosen (+,-,+,-). Other sign combinations did not lead to a physically plausible solution. The radial electron density,  $\rho(r)$ , was put on an absolute scale as described in the text. The baseline is the radial electron density of water at 0.334 electrons /Å<sup>3</sup>.



pilus cross-sections. Since this data is not available for *Pseudomonas pili*, one cannot rule out the possibility that the low electron density at the center of the pilus is due to a concentration of low density side chains rather than an aqueous channel.

The minimum in electron density at 15-16Å radius could be interpreted in two ways. It could arise from the presence of a girdle of hydrophobic amino acids of low electron density. On the other hand, it could arise from a loose packing of the polypeptide chain at this radius. Taking the width at half height of the radial density distribution, the average outer radius of the pilus is 26Å. This corresponds to half the minimum distance between pili in dry fibers (figure V.6). The shape of the radial electron density distribution for PAK and PAO pili is very similar to that obtained for F pili (Folkhard *et al.*, 1979a). A similar dip in electron density at the center of the protein shell has also been observed for the filamentous phage Pf1 (Wachtel *et al.*, 1974).

## 2. Determination of the helix parameters for PAK and PAO pili

The diffraction patterns of PAK and PAO pili (figure V.5) show that the meridional and near meridional intensity is nearly equally spaced. This suggests that the pilin subunits are arranged so that there is a near integral number of units per turn. A  $J_1$  can be assigned to the near



meridional reflection on the first layer-line because the reciprocal space radius,  $R$ , is compatible only with the first maximum at  $2\pi Rr$  of a  $J_1$  term for an outer radius of  $26\text{\AA}$ . The corresponding spacings in the meridional direction lead to a helix pitch of  $41.1\text{\AA}$  for PAK pili and  $41.6\text{\AA}$  for PAO pili.

The number of units per turn in a helical structure is determined from the position of the layer-line on which the first meridional reflection falls (section A.2). Examination of figure V.5 shows that the near meridional reflections on  $l=1-3$  appear to be off-meridional. However, for the reflections at low  $R$  on  $l=4,5$  and greater it is difficult to determine whether or not they are truly meridional reflections, particularly because of the greater disorientation with increasing  $l$  (higher resolution).

The area occupied by the pilus in the unit lattice in dry fibers is given by  $\sqrt{3}a^2/2$ , where  $a$  is the minimum lattice dimension. If one defines a unit cell of  $1\text{\AA}$  thickness based on this lattice it would have a volume of  $2342\text{\AA}^3$  for dry PAO fibers. The volume occupied by the pilus in this unit cell can be obtained from the volume of the pilin subunit divided by the axial separation between subunits. This gives the volume of a  $1\text{\AA}$  thick slice of the pilus. The volume of a single pilin subunit is  $19,200\text{\AA}^3$  (calculated in Chapter IV). For a  $4u/t$  helix, the axial separation between subunits would be  $10.4\text{\AA}$  for PAO pili.





This results in a volume of  $1849 \text{ \AA}^3$  for the  $1\text{\AA}$  thick slice. Therefore, if the correct symmetry were  $4u/t$ , the pilus would occupy 79% of the unit cell in dry fibers. This is somewhat unlikely because in dry fibers one expects there to be very little water. For Pf1 phage for example, only 5% water is associated with the virions in dried fibers (Nave *et al.*, 1981). As described in Chapter III, the molecular weight of pilin was previously thought to be about 18,000. Therefore our initial interpretation of the fiber diffraction data (Folkhard *et al.*, 1981) was that there were 4 subunits per turn occupying 95% of the unit cell. The fact that the diffraction intensity fits this interpretation can be seen by examining the right-hand side of figure V.9. Furthermore, this model could not be ruled out on the basis of model building (see figure V.16B, below). Therefore, the only argument against the  $4u/t$  helical symmetry is based on unit cell occupancy being too low, given the smaller subunit molecular weight of 15,000.

For the  $5u/t$  case, the axial separation between subunits is  $8.3\text{\AA}$ , resulting in a unit volume of  $2313\text{\AA}^3$ . This occupies 99% of the unit lattice in dry fibers. For higher numbers of  $u/t$ , the subunit is too large to be contained within the unit cell. For example, if the symmetry were  $6u/t$ , the pilus would occupy 118% of the unit cell. Therefore, within experimental error, the  $5u/t$  case fits the unit cell dimensions best.



In fact, the exact symmetry must be slightly off this value since layer-line "splitting" can be observed on well oriented PAO diffraction patterns, especially on the second layer-line. This can be seen on the diffraction pattern shown in figure V.9. The arrows in this figure indicate meridional reflections at different  $Z$  values that fall on a single broadened layer-line. On the basis of this splitting, the symmetry is closer to 5.08 units per turn rather than 5.00 units per turn. The corresponding  $(n, "l")$  plot is shown for the 5.08 unit per turn helix in figure V.10. " $l$ " is defined as the non-integral layer-line index, where

$$"l" = ZP = n + mu/t$$

where the pitch  $P$  is used as a reference, rather than the helix repeat  $C$ . In qualitative discussions of the diffraction pattern, where the first, second layer-lines etc. are referred to, we mean the set of overlapping layer-lines with similar " $l$ " values that appear as one broadened layer-line on the diffraction pattern. A helical symmetry of  $4.92u/t$  rather than  $5.08u/t$  can be ruled out because the ratio between  $Z$  values on " $l$ "=5 and the  $J$ , on " $l$ "=1 is always greater than 5 on all diffraction patterns analyzed. On PAK diffraction patterns the second layer-line is broadened but splitting is not resolved.

In order to determine the exact symmetry more accurately, all measured spacings (summarized in figure V.11) on the diffraction patterns where  $n, m$  values could be assigned (9-11) per film, were used to calculate the pitch





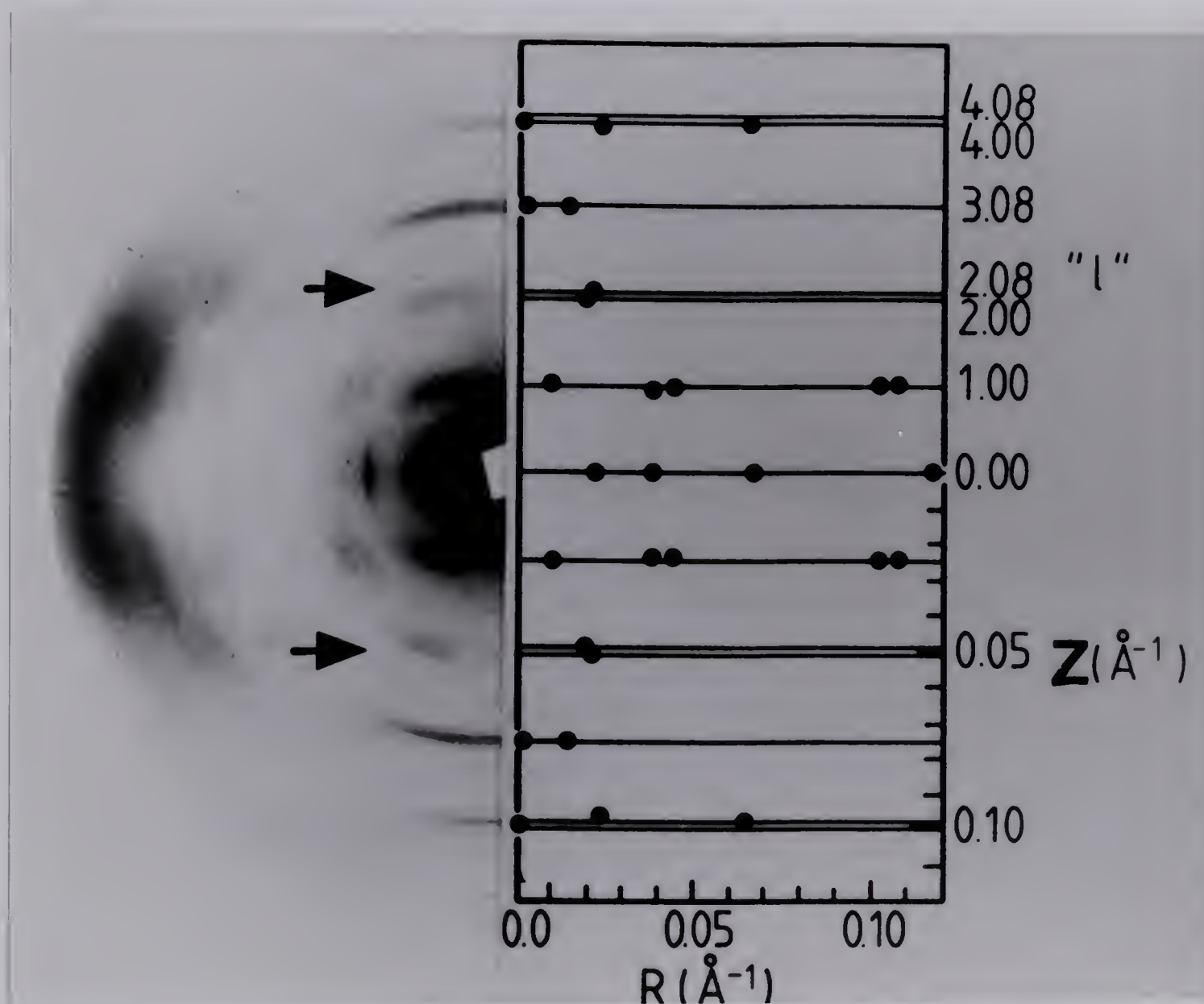


Figure V.9. X-ray fiber diffraction pattern of PAO pili obtained using a doubly focussing camera with a 10.4 cm specimen to film distance. The arrows mark the resolved splitting on the second layer-line. On the left is the diffraction pattern at 33% r.h.; at right is the reciprocal layer-line pattern for " $l$ "= $n-4m$ . However, one could also interpret this fiber diagram in terms of a  $5u/t$  helical symmetry.  $Z$  and  $R$  are the reciprocal space coordinates in the meridional and equatorial directions, respectively.





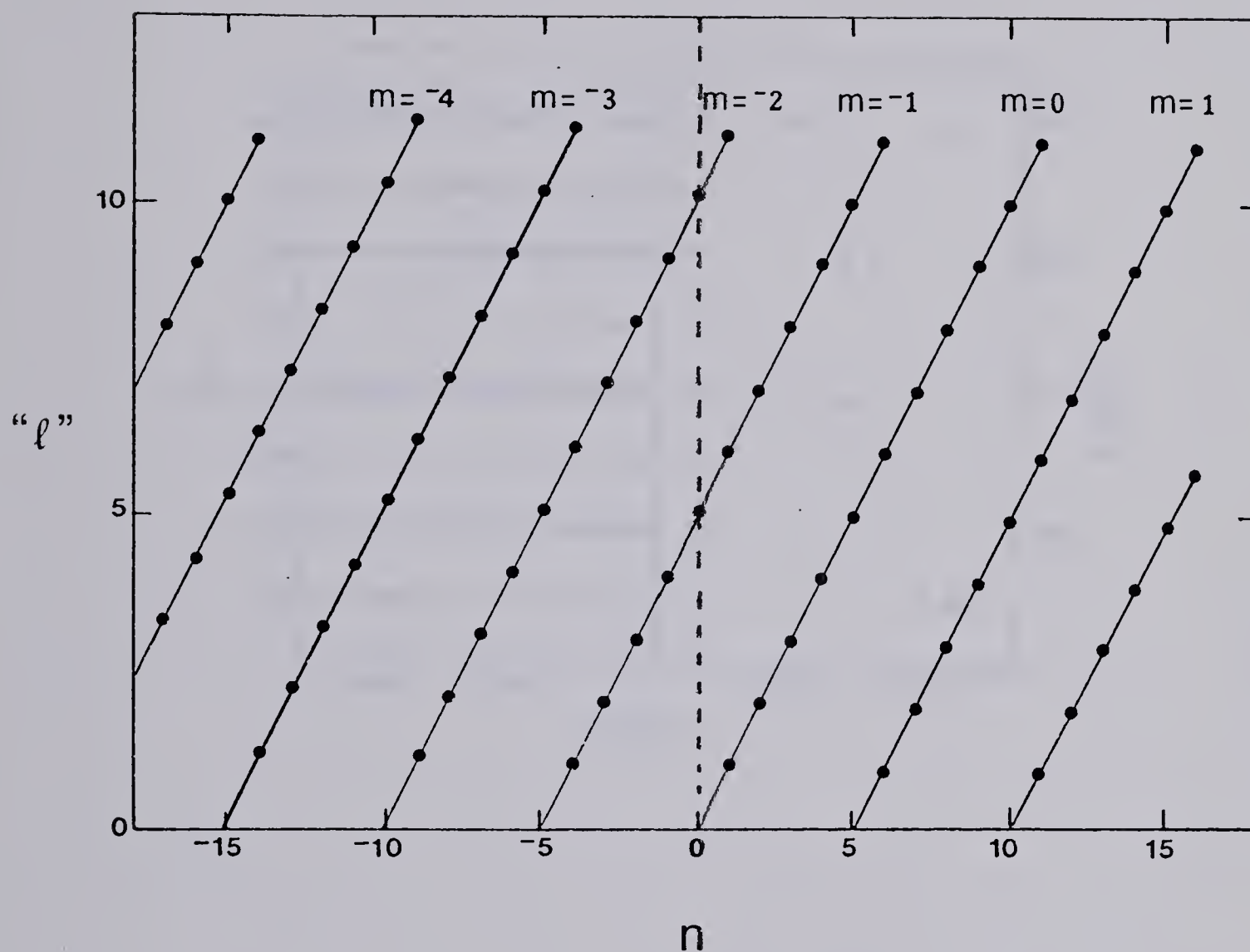


Figure V.10.  $(n, "l")$  plot for the helix selection rule  $"l" = n - 5.08m$ , where  $n$  is the Bessel function index,  $"l"$  is the non-integral layer-line index and  $m$  is an integer. The negative sign indicates a left-handed helix.



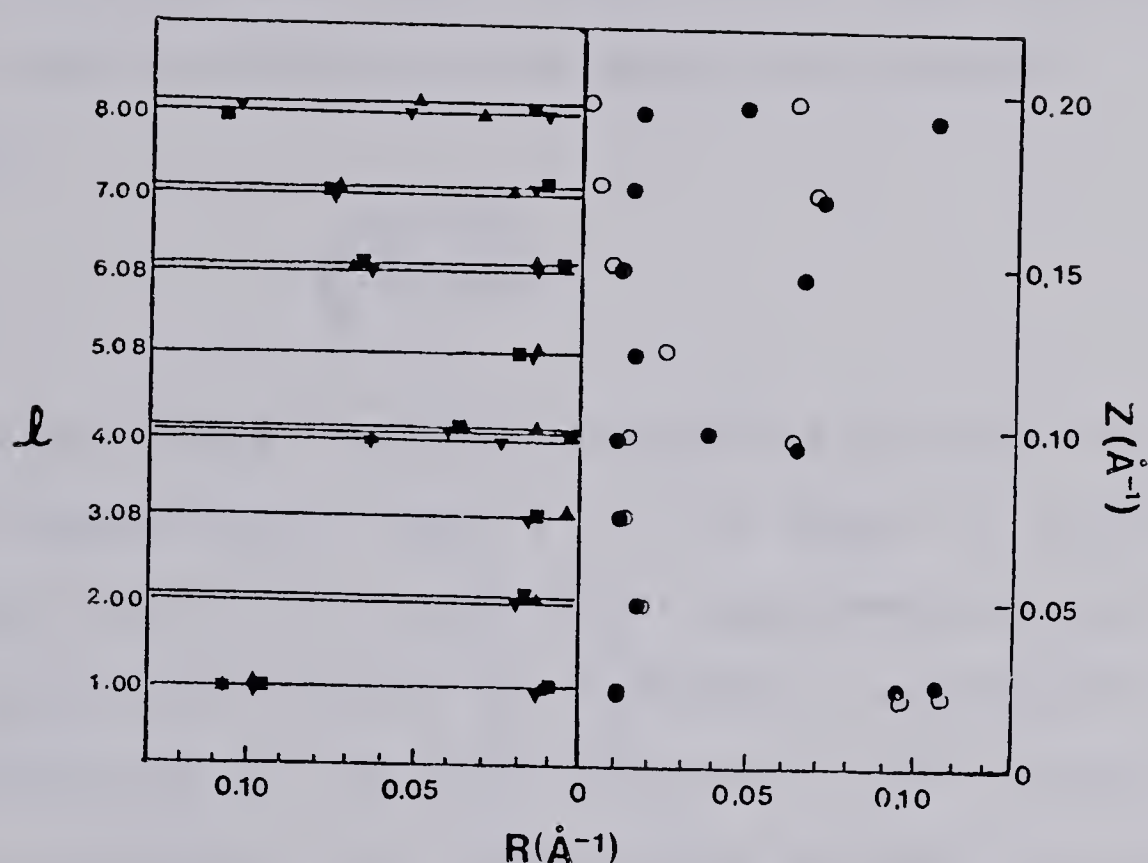


Figure V.11. Measurements of reciprocal space coordinates on diffraction patterns with comparable  $a$  spacings at 75% r.h.

The left side of the figure shows the variation of measurements within three PAO fibers. The right side shows a comparison of measurements for PAK pili (O ; average of 2 fibers) and PAO pili (● ; average of 3 fibers). The lattice spacing,  $a$ , was  $56.1, \pm 0.2$  for the PAK fibers and  $56.2 \pm 0.3$  for the PAO fibers.



of the helix using the equation:

$$P = 1/j \sum P_j = \sum \frac{n_j - m_j u/t}{Z_j}$$

The pitch,  $P$ , was calculated for a range of values between 5.00 and 5.15 units per turn (figure V.12) and the helical symmetry was determined as that where the standard deviation:

$$\sqrt{\frac{P - P_j}{j-1}}$$

has a minimum value. The helix parameters derived from this plot are summarized in Table V-II. The number of units per turn (5.06-5.08) is the same within experimental error for the two pili, but PAO pili has a slightly larger pitch. These values are for the pilin helices at 75% relative humidity. Although in dry fibers there is room for very little water, at 75% relative humidity, the lattice swells sufficiently that it could contain 13% (v/v) water or 0.19g H<sub>2</sub>O/g pilin. This value is calculated from  $\bar{v}$  and from the helix parameters at 75% r.h. (Table V-II) and is typical of fibrous proteins (Tanford, 1961).

Examination of the right-hand side of figure V.11 shows that the positions of diffracted intensity are very similar for the two strains of pili. Figure V.13 shows the surface lattice representation of the two pilin helices. It can be seen that the slightly larger pitch observed for PAO pili results in a slight displacement of the position of the PAK





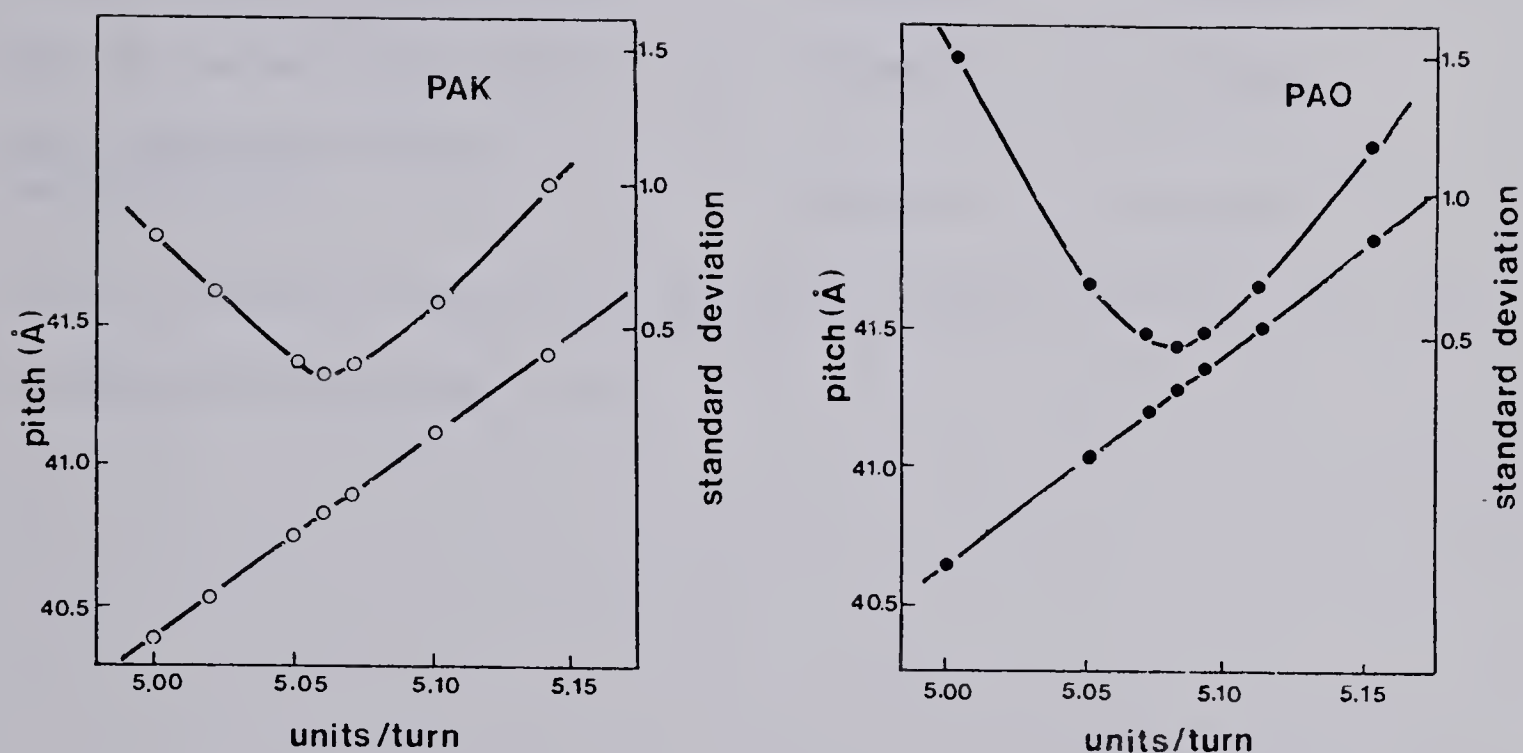


Figure V.12. Determination of the helix parameters for PAK and PAO pili at 75% relative humidity. The lower curve shows the relationship between the number of units per turn and the pitch of the helix. For each value of  $u/t$ , the pitch of the helix was calculated using reflections where  $n, m$  values could be assigned. The upper curve shows the standard deviation associated with each value of  $u/t$ .



TABLE V-II

*Helix Parameters of PAK and PAO Pili at 75% Relative Humidity\**

	PAK	PAO
Helical symmetry (units/turn)	$5.06 \pm 0.02$	$5.08 \pm 0.02$
Pitch of the basic helix ( $\text{\AA}$ )	$40.8 \pm 0.2$	$41.3 \pm 0.2$
Axial separation between subunits ( $\text{\AA}$ )	$8.0_6 \pm 0.1$	$8.1_3 \pm 0.1$

\* determined from figure V.12.



and PAO pilin subunits from one another with increasing  $z$ .

### 3. Comparison of PAK and PAO diffraction patterns with those of related structures

The overall intensity distribution on *Pseudomonas* pili diffraction patterns is strikingly similar to that observed on diffraction patterns of bacterial flagella (Champness, 1971; figure V.14). Examination of figure V.14 (which was kindly provided by Dr. J.N. Champness) shows the presence of strong equatorial intensity at  $1/10\text{\AA}$  and strong meridional intensity at  $1/5\text{\AA}$ . As mentioned earlier, this can be attributed to the side by side packing of  $10\text{\AA}$ -diameter  $\alpha$ -helical rods of pitch  $5\text{\AA}$  with their long axes oriented roughly parallel to the fiber axis. This suggests that the  $\alpha$ -helices in flagellin may be arranged in a similar manner to those in *Pseudomonas* pilin even though the radius, subunit molecular weight and axial periodicities are quite different for the two structures.

On the other hand, the diffraction patterns obtained from F pili (Folkhard, *et al.*, 1979a) are very different from those of PAK and PAO pili with respect to pilus dimension, helical symmetry and overall intensity distribution, implying a different subunit shape. In particular, there is no evidence of a common axial orientation for the  $\alpha$ -helices in F pilin even though the F pilus possesses about 70%  $\alpha$ -helix (Date *et al.*, 1977). Similarly, the diffraction patterns obtained for Type I pili (Brinton, 1965; Mitsui





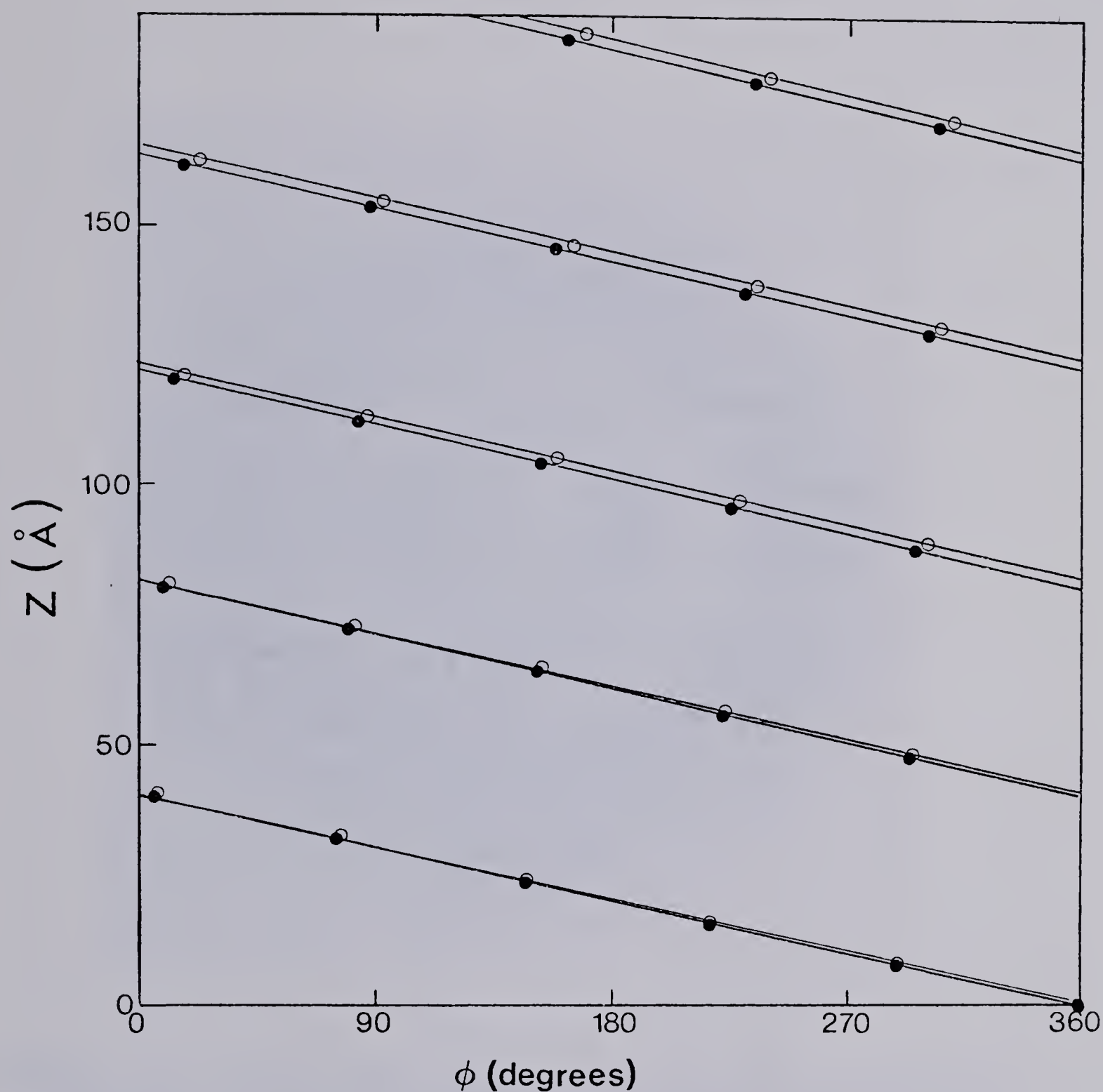


Figure V.13. The surface lattice representation of a left-handed PAK pilus of 5.06 units/turn of 40.8Å pitch (●) and of a left-handed PAO pilus (○) of 5.08 units/turn of 41.3Å pitch.  $z$  and  $\phi$  are the real space coordinates in the axial and angular directions. This representation has been explained in figure V.3 and in the text (section A.2).



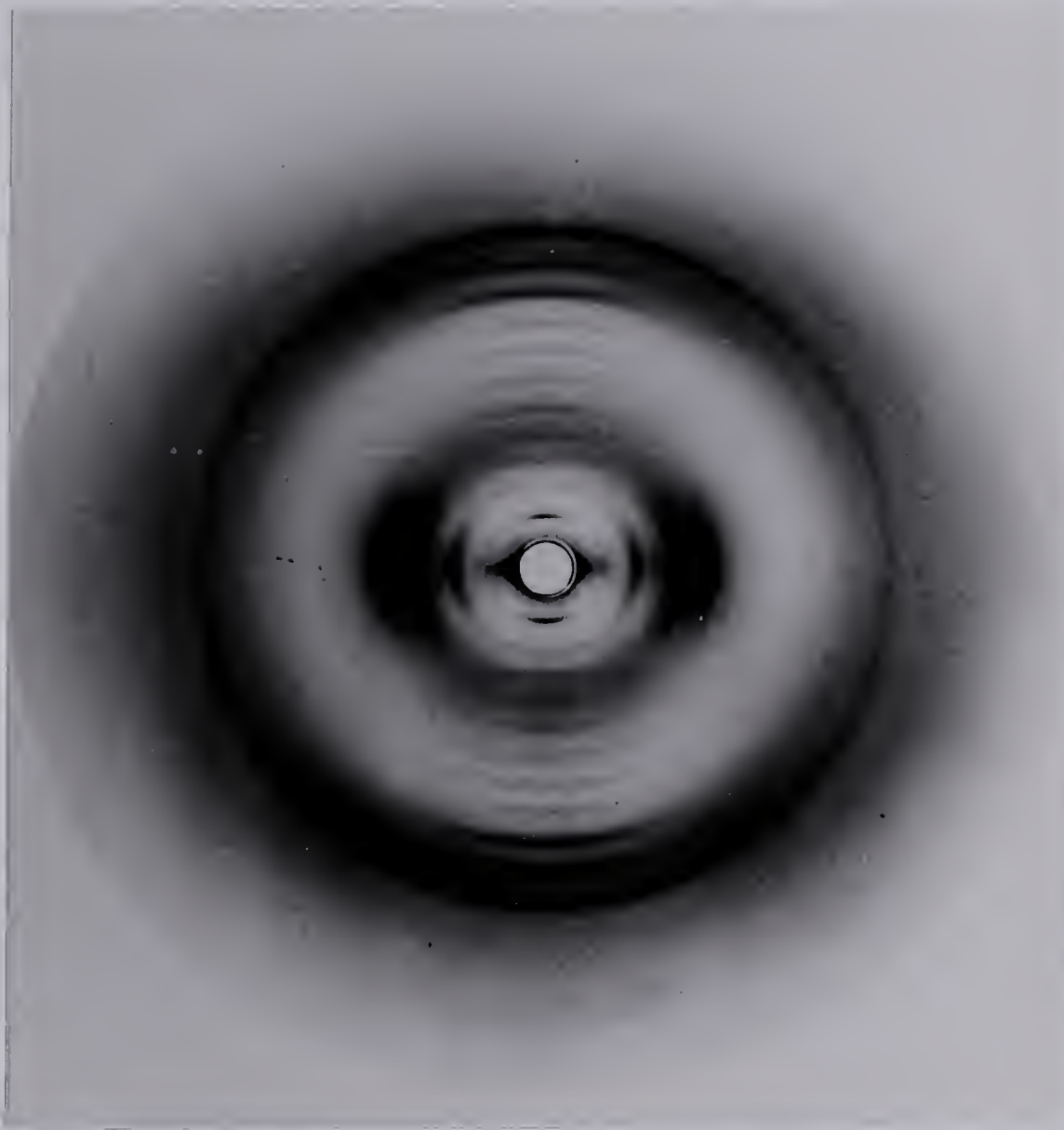


Figure V.14. X-ray fiber diffraction pattern of bacterial flagella. The diffraction pattern shown is plate I of Champness *et al.*, (1971) and was kindly provided by Dr. J.N. Champness. The diffraction pattern was recorded with a pinhole camera at a specimen to film distance of 4.86 cm and a relative humidity of 75%.



et al., 1973) are also quite different from those of *Pseudomonas* pili.

It was thought however, that the pili of *N. gonorrhoeae* (gonococcal pili) might have a similar structure to *Pseudomonas* pili because the two types of pili have the same diameter (Chapter III) and share a common N-terminal sequence (Frost & Paranchych, 1977; Chapter III). Oriented fibers were prepared from gonococcal pili and one of the diffraction patterns obtained is shown in figure V.15A. Figure V.15B shows the diffraction pattern obtained from a PAK pili fiber under similar conditions (75% r.h., 4.5cm specimen to film distance). Although numerous attempts were made at orienting gonococcal pili, figure V.15A shows the best diffraction pattern we could obtain. The only explanation we can offer for the difference in the quality of the diffraction patterns of the two types of pili is that PAK pili tend to align into more extensive "ropes" than do gonococcal pili (see chapter VI, figure VI.3). An additional factor may be the length of the purified pili. Sonication of PAK pili to reduce the length of the filaments results in less well-oriented specimens. Nevertheless, it can be seen even in poorly oriented specimens that the diffraction patterns of gonococcal pili also show the 10Å-equatorial and 5Å-meridional reflections observed in the diffraction patterns of *Pseudomonas* pili and of bacterial flagella. This might be taken to imply that the N-terminal region of the pili is important in defining the folding pathway of the





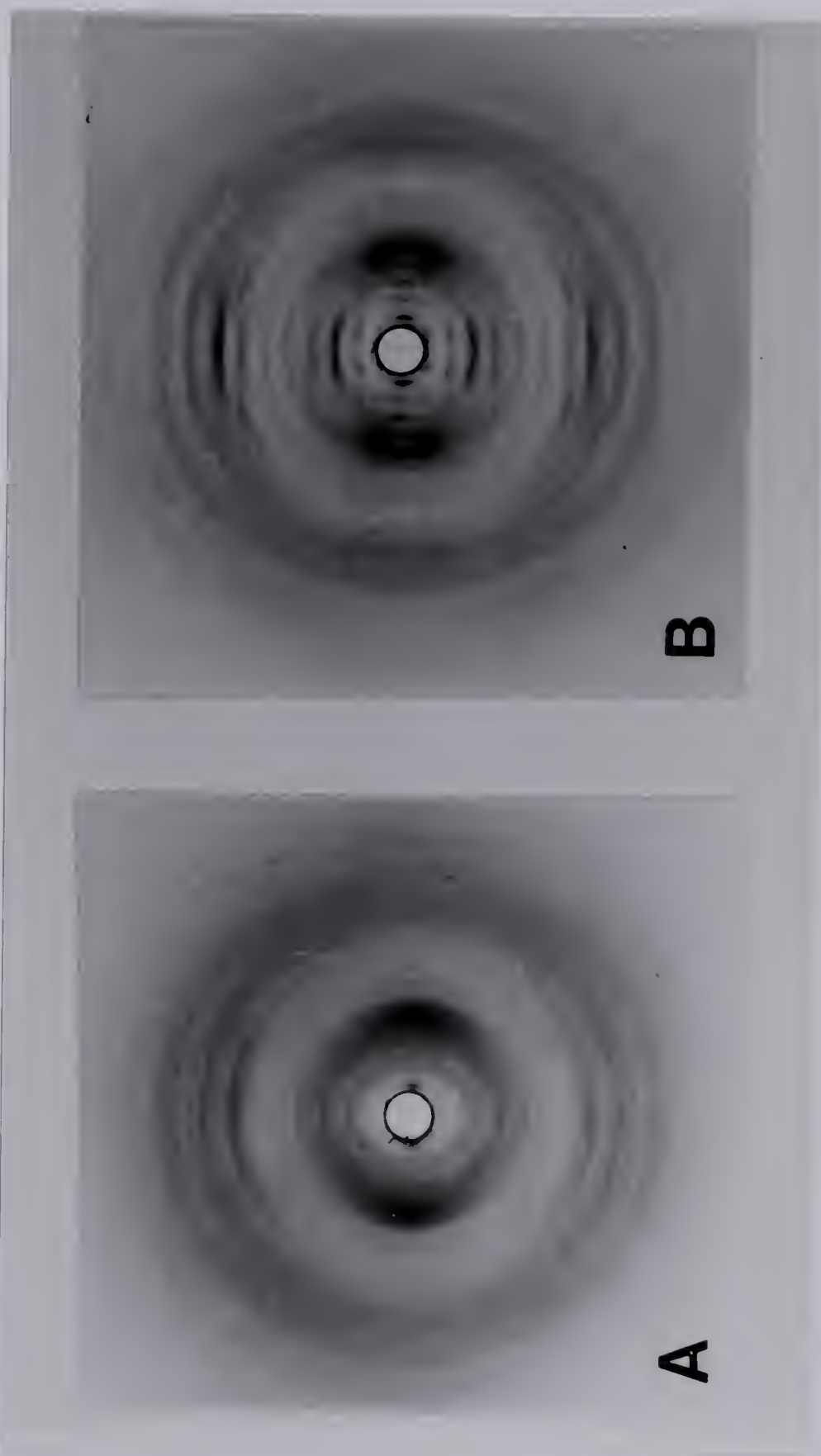


Figure V.15. X-ray fiber diffraction patterns of a) Gonococcal pili and b) PAK pili recorded at 75% r.h. with a pinhole camera at a specimen to film distance of 4.5cm.



pilin subunit, perhaps by forming a hydrophobic  $\alpha$ -helical surface against which other helices can pack. Since no sequence data is available for the bacterial flagellin subunit, we cannot speculate on why the  $\alpha$ -helix orientation is similar in these structures also.

The shape of the radial electron density distribution which indicates a central low-density channel and a girdle of low electron density between the inner and outer density maxima is common to F, PAK and PAO pili, as well as to the protein shell of the filamentous phage Pf1 (Wachtel *et al.*, 1974) and may indicate common structural features for helical assemblies of hydrophobic proteins.

#### 4. Orientation of the $\alpha$ -helices in pilin

As discussed above, the presence of strong 10Å-equatorial and 5Å-meridional reflections suggested that the  $\alpha$ -helices in pilin were oriented roughly parallel to the fiber axis. In order to determine more precisely the orientation of the  $\alpha$ -helices that contribute to this intensity distribution, a computer model-building approach was used in which  $\alpha$ -helical models were constructed such that their transforms simulated the intensity distribution of the strong 10Å region on  $|l|=1$ . For simplicity, the helical symmetry was approximated as integral for these calculations.

The models consisted of gently curved  $\alpha$ -helical rods of polyalanine. Curvature was introduced by specifying the



helix as 3 separate rods whose orientations could be varied independently. The parameters  $dz/d\phi$  (the slope in the  $z$  vs.  $\phi$  direction),  $dz/dr$  (the slope in the  $z$  vs.  $r$  direction) and the starting radius of the helix were varied. For each model, the transform of a  $5U/t$  assembly of  $\alpha$ -helical subunits was calculated and compared with the observed transform on  $l=1$ .

The best fit obtained using this approach is shown in figure V.16A. The starting radius for this model was  $26\text{\AA}$  and the polyalanine chain sloped inwards to a final radius of  $6\text{\AA}$ . The orientation of the model in the  $z$  vs  $\phi$  direction is shown in figure V.17B. Changing the starting radius or the slope by more than a few percent results in a much worse fit to the data on  $l=1$ . The fit shown in figure V.16 is for a left-handed helix. Crick (1953) has shown that optimum packing of right-handed  $\alpha$ -helices in  $\alpha$ -helical coiled-coils occurs when the helices follow a left-handed super-helix. The polyalanine helices in the left-handed model pack in this manner. However, the equivalent right-handed model, the mirror image of figure V.17 is also possible. In this case the right-handed  $\alpha$ -helices would follow a right-handed super-helix. Comparison of the transform for the best right-handed model (not shown) shows that the fit is not sufficiently different between the two forms to allow us to distinguish between the two possibilities. Figure V.16B shows the fit of the transform of the polyalanine model when it is packed in a  $4U/t$  helix. One can see that the fit is





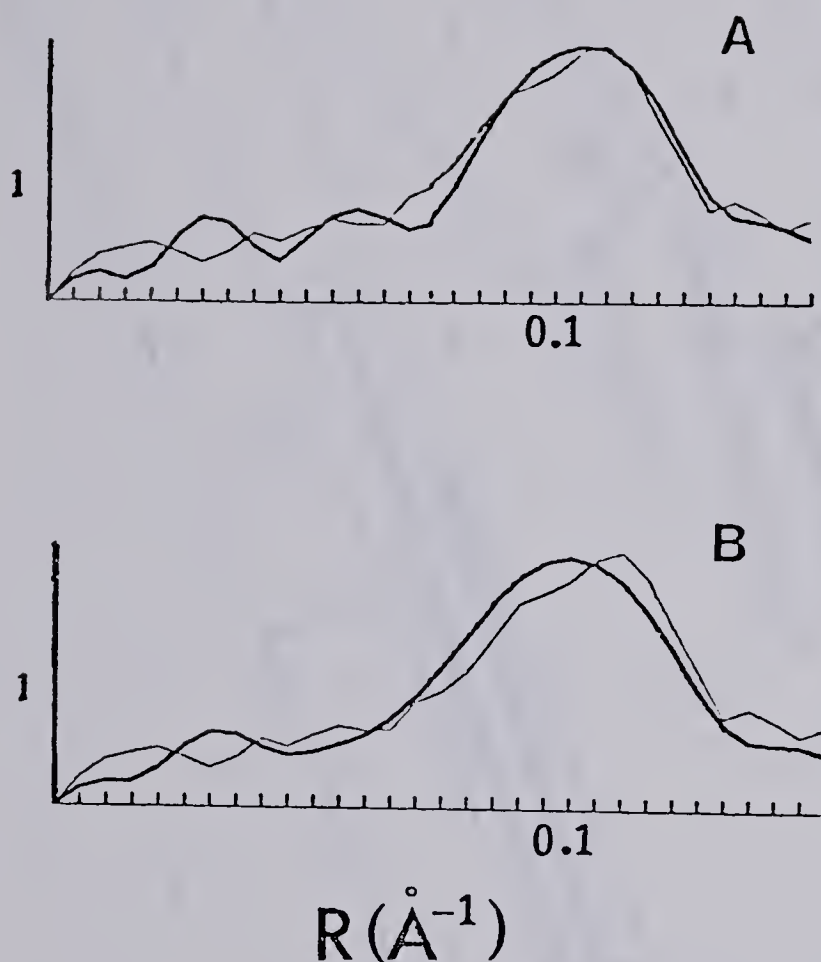


Figure V.16. Comparison of the calculated Fourier transform of an  $\alpha$ -helical model (thick line) with the observed PAO diffraction amplitudes (thin line) along the first layer-line at 86% relative humidity. A. A  $5U/t$  basic helix. B. A similar model with 4 pilin subunits per turn. The model consists of interdigitating  $\alpha$ -helical rods. The helical symmetry was approximated as integral for these calculations, since the overlapping layer-lines cannot be resolved except at low reciprocal space radii.



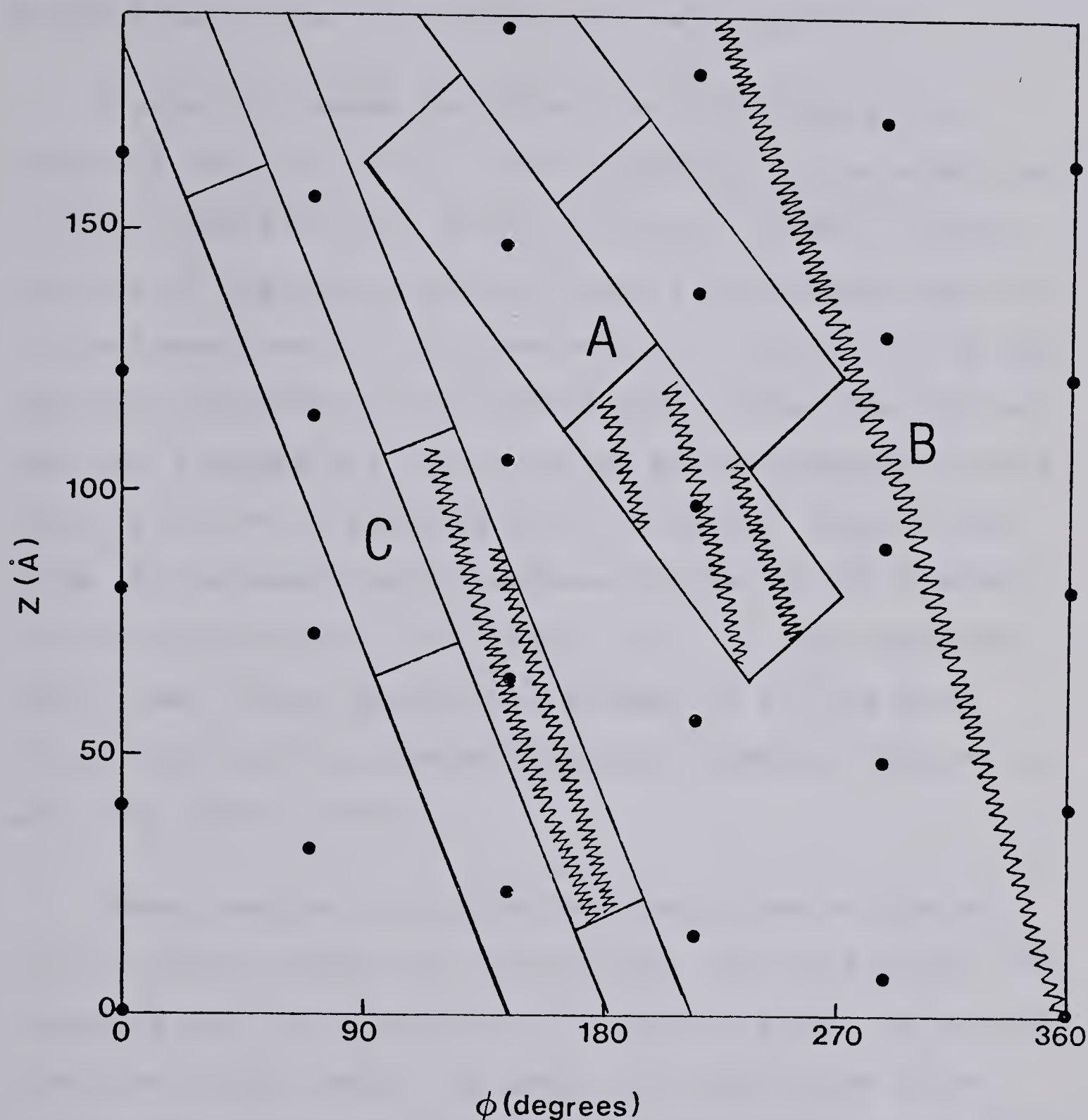


Figure V.17. Surface lattice representation of the  $5u/t$  pilin helix with 3 models of subunit shape superimposed. Model A has an axial ratio of 2.5:1 when approximated as a cylinder. Model B is the gently curved  $\alpha$ -helical rod that was used to define the  $\alpha$ -helix orientation that produces the best fit on the first layer-line (figure V.16). Model C has an axial ratio of 3.5:1. (●) represents the origin of each pilin subunit on the surface lattice. (~~~~~) represents the path followed by the  $\alpha$ -helix in each of the three models.



sufficiently similar that one cannot use this approach to decide between the two possible helical symmetries.

Figure V.17 shows two other  $\alpha$ -helical models that produce a good fit on  $l=1$ . The orientation of the  $\alpha$ -helices in these models is very similar to that in model B, which consists of one long  $\alpha$ -helix. Figure V.18 compares the fit of the transforms of the three models in figure V.17 to the observed transform on the first 8 layer-lines. One can see that all 3 models fit the  $J_0$  on  $l=0$  at low reciprocal space radii fairly well, implying that the overall shape of the pilus is the same in all 3 models. Similarly, all 3 models fit the intensity at  $1/10\text{\AA}$  fairly well. For the remaining layer-lines, there has been no attempt to fit the data, since this intensity almost certainly depends on the amino acid side chains present.

These results illustrate that regardless of the particular subunit shape and orientation, one can simulate the intensity due to the packing of  $\alpha$ -helices simply by placing  $\alpha$ -helices of any length  $10\text{\AA}$  apart in a particular orientation (that shown in figure V.17) with respect to the fiber axis.

### *C. A Model for Pseudomonas Pili Based on X-ray Diffraction and Hydrodynamic Studies*

The model depicted in figure V.17A can be approximated as a cylinder of radius  $10.5\text{\AA}$  and length  $52\text{\AA}$ . This has an





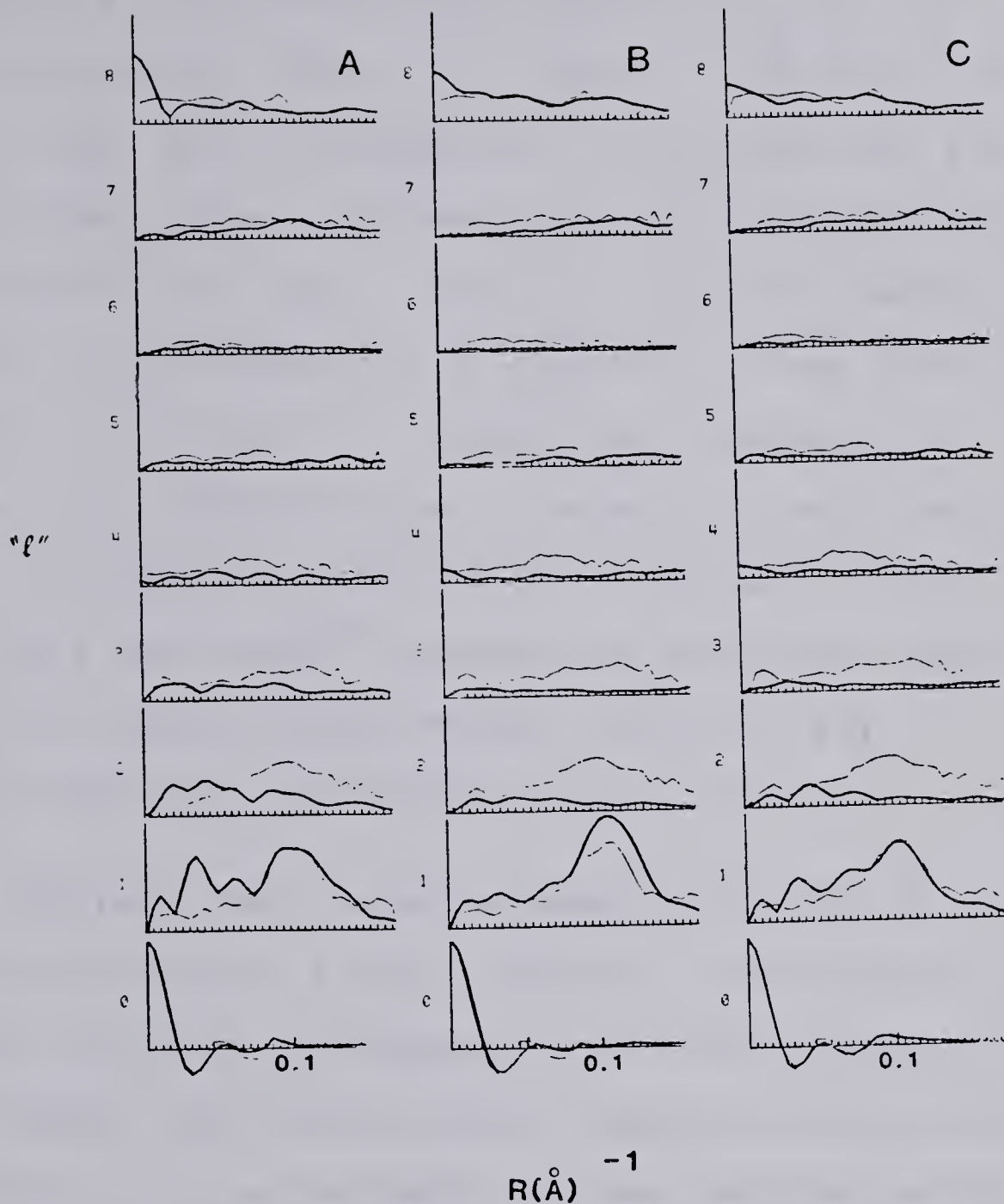


Figure V.18. Comparison of the observed and calculated diffraction amplitudes on  $l=1-8$  for the three models described in figure V.17. Thin lines represent the observed diffraction amplitudes of a PAO pili fiber; the thick lines represent the calculated transform of the polyalanine models. A, B and C correspond to model A, B and C in figure V.17. Scaling of the observed to calculated transforms was done using the reflection of maximum intensity on the observed transform, the  $J_0$  on  $l=0$ .



axial ratio of 2.5:1 which is consistent with axial ratio determined from hydrodynamic studies of pilin in octyl-glucoside (Chapter IV). Model V.17B and C, on the other hand, are too asymmetric to be consistent with the hydrodynamic data. Although there are several possible arrangements and exact shapes for the pilin subunit, it is evident from examination of figure V.17 that these are limited on the basis of geometrical considerations. That is, there are a limited number of ways to arrange the pilin subunit (of specified dimensions) on the  $5u/t$  surface lattice such that each subunit occupies an equivalent environment and fills space without being involved in any stereochemically unfavourable short contacts.

The fact that the major species of pilin in octyl-glucoside is a dimer (Chapter IV) raises the question of why a helical arrangement of identical subunits would form dimers upon dissociation. The most efficient way for the pilus to be assembled is to use the same packing arrangement repeatedly (Crick & Watson, 1956). Thus one would expect all subunits to occupy an equivalent environment and to be dissociated into monomers if 100% of a specific set of bonds were broken. However, if the basic building unit of pili were a dimer of two identical subunits related by a two-fold rotational axis of symmetry, then one could expect dissociation into dimers by disrupting one set of interactions while maintaining the interaction that relates the two halves of the pilin dimer. This possibility



is shown schematically in figure V.19.

Figure V.19 represents our current model for the structure of the *Pseudomonas* pilus based on the results of Chapters IV and this Chapter. It should be emphasized that this represents only one of many possible models as far as the exact subunit shape and orientation are concerned and is intended only as a working model from which to pursue structural hypotheses. Figure V.19A shows the dimensions of the pilus as viewed in the electron microscope and is included to emphasize the asymmetry of the structure. Figure V.19B shows the subunit of model A of figure V.17 arranged in dimers so that there are 10 such dimers in every two turns of the helix. Thus at low resolution, the structure has the same periodicities as would a model consisting of pilin monomers in a  $5u/t$  helix. Only one of the hypothetical two-fold axes is shown in the figure. The pilus is depicted as roughly cylindrical in shape with an outer diameter of  $52\text{\AA}$  and a central low density channel of  $6\text{\AA}$  radius. The pilin subunits are believed to be tightly packed with no deep grooves which would allow stain penetration or the trapping of large amounts of solvent in dry fibers. The stars on each subunit are included to emphasize that there are two different environments for the pilin subunit in the helix. The  $\alpha$ -helix orientation in this model is expected to be similar to that shown in figure V.17A, but the exact number and length of the  $\alpha$ -helical segments or their coordinates in three-dimensions are not known.







Figure V.19. A model for pilus structure based on X-ray fiber diffraction and hydrodynamic data.

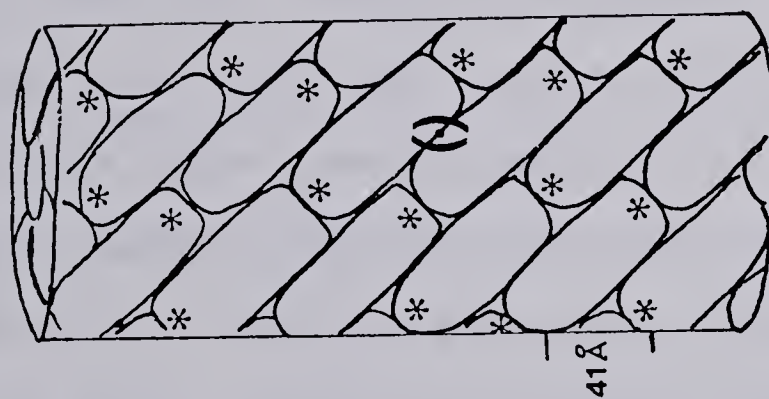
A. A scale drawing of the pilus based upon measurements from electron microscopy and X-ray diffraction.

B. A schematic representation of the pilus incorporating the helical symmetry and pitch derived from the X-ray diffraction data. The subunit shape and orientation is arbitrary, but is consistent with hydrodynamic data presented in Chapter IV. The subunits are arranged in dimers related by a two-fold rotational axis of symmetry (  $\odot$  ). Only one of the hypothetical 2-folds is indicated. The stars are included to show that there are two types of environment for the pilin subunit in this model.

C. The surface lattice representation of the model in B. Only 4 hypothetical subunits are shown.

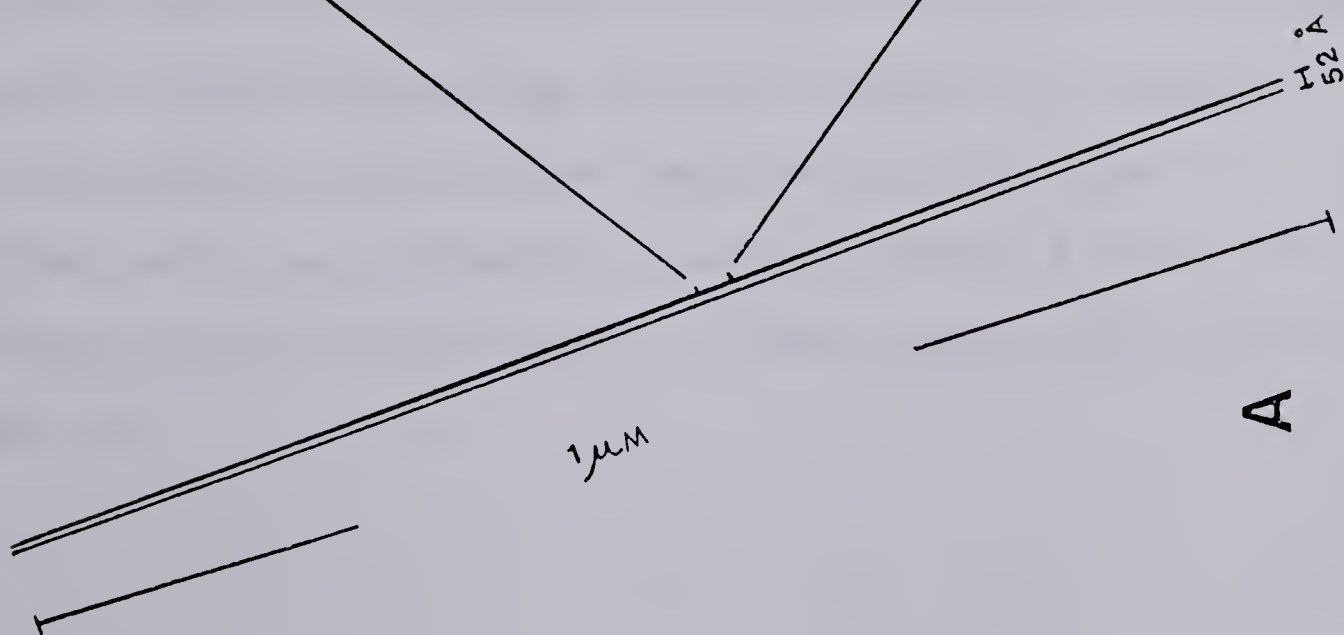
52 Å

12 Å

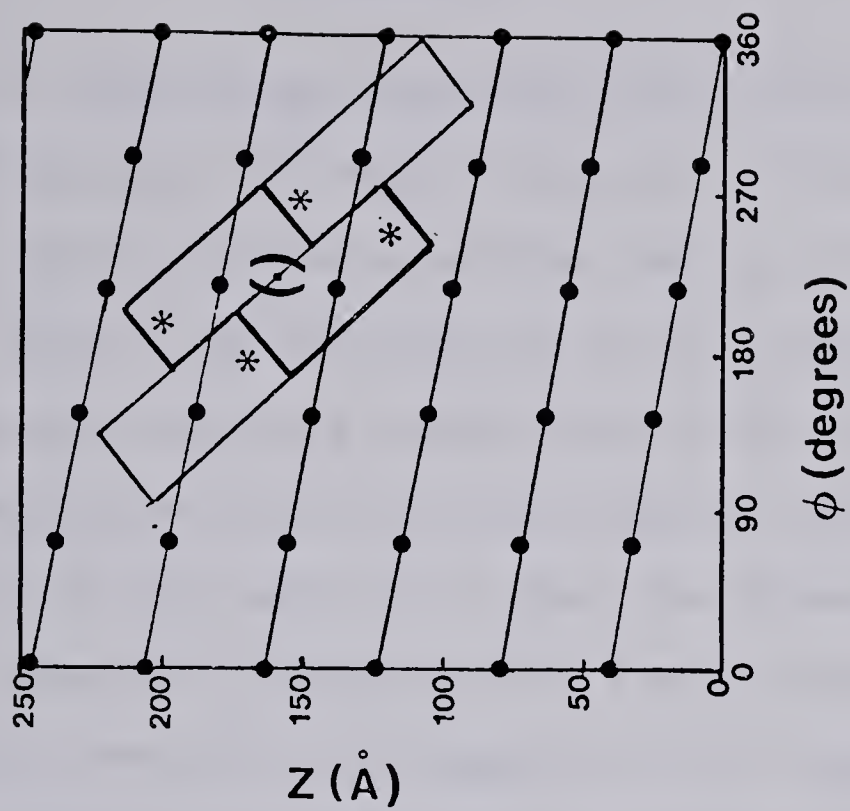


B

250 Å



A



C



### D. Summary

The pili of *Pseudomonas aeruginosa* strains PAK and PAO are hollow cylinders of 52Å outer diameter and 12Å inner diameter with a girdle of low electron density at the center of the protein shell. The two strains of pili have similar diffraction patterns out to a resolution of 7Å in the equatorial direction and 4Å in the meridional direction. Careful analysis of the layer-line spacings reveals slight differences in the helix parameters of the two pili at 75% relative humidity. The helical symmetry which best fits the data is 5.06-5.08  $u/t$  of 40.8Å pitch for PAK pili and 41.3Å pitch for PAO pili. In dry fibers, the pili are very densely packed leaving room for little or no water. At 75% r.h., the lattice expands to allow 0.19g water/g pilin. The  $\alpha$ -helices in the pilus are aligned roughly parallel to the long axis of the pili and are packed side by side with the result that a strong periodicity at 10Å is observed on the diffraction pattern. A more exact  $\alpha$ -helix orientation was determined using a computer model-building approach. No information is available about the orientation of  $\beta$ -structure in the pilus, although circular dichroism studies (Chapter IV) suggest that pili possess significant amounts of this type of secondary structure. Finally, a working model for pili is presented (figure V.19) based on these results and those of Chapter IV.





## CHAPTER VI

### Studies on the *In vitro* Assembly of Pili

Since pili could be dissociated into dimers by octyl-glucoside without any apparent damage to the subunit (Chapter IV), it was of interest to remove the octyl-glucoside in order to determine whether or not *in vitro* reassembly was possible. At the same time it was necessary to develop a biological assay for pili so that proper assembly could be monitored functionally as well as physically. As will be described below, the approach used was a competition plaque assay using the tailed bacteriophage PO4. These studies were carried out using strain PAK pili.

#### A. *In Vitro* Assembly of an Alternate Form of Pilin Filament

As was described in Chapter IV, the dissociation of pilin by octyl-glucoside can be followed by viscometry. Using the same technique, the assembly process was followed as octyl-glucoside was removed by dialysis as shown in figure VI.1. The amount of detergent remaining in the preparation after varying times of dialysis was determined by constructing a calibration curve of octyl-glucoside concentration vs. time of dialysis based on results obtained with [<sup>14</sup>C]-octyl-glucoside. Curve B of figure VI.1 shows the increase in viscosity of the pilin solution as octyl-glucoside was removed. It can be seen that there was very little change in viscosity until virtually all the octyl-glucoside



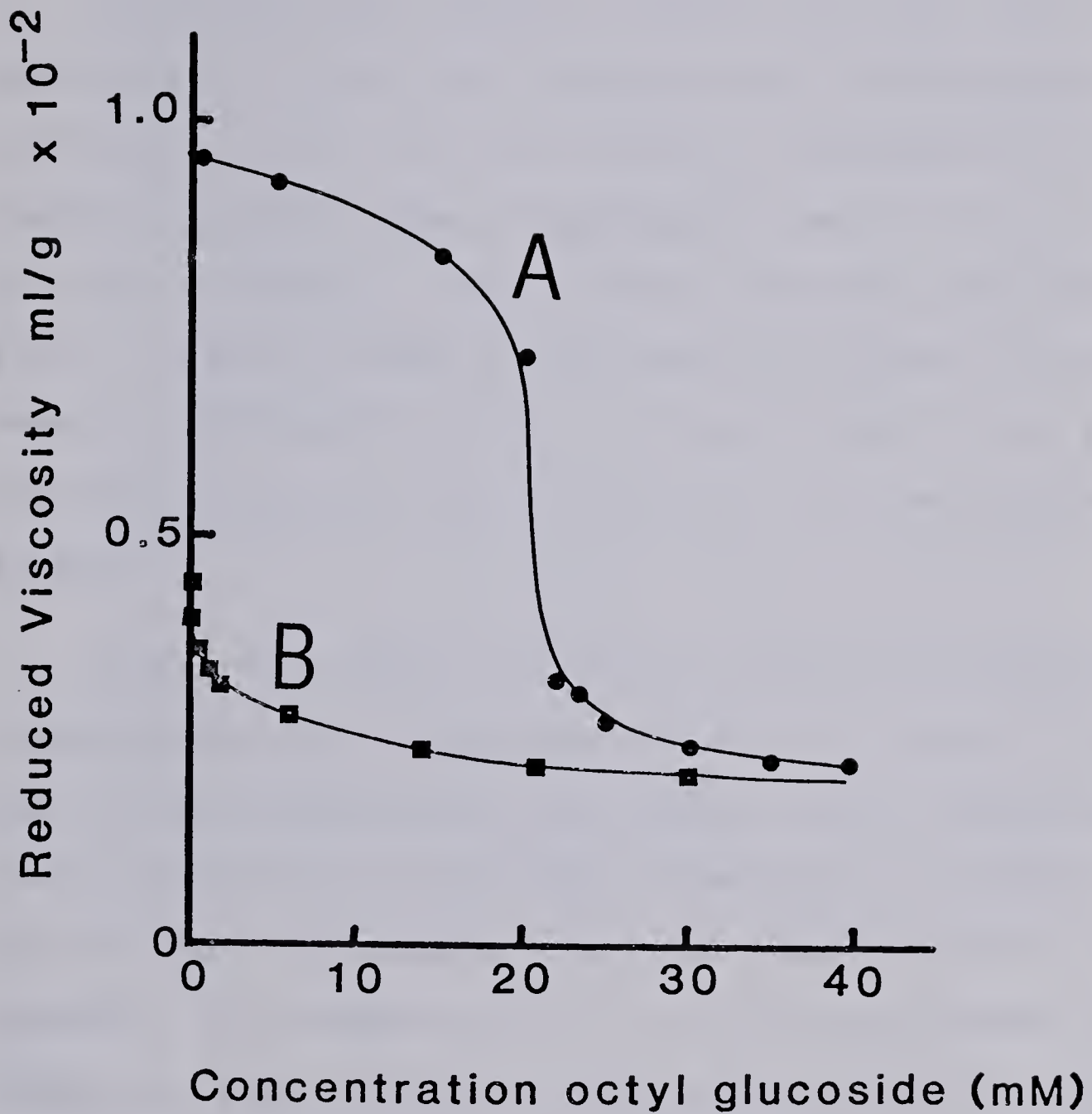


Figure VI.1. Dissociation and Reassociation of Pili as Measured by Viscometry. A: dissociation of PAK pili in the presence of increasing amounts of detergent. B: aggregation of pilin as detergent is removed by dialysis.



had been removed. Octyl-glucoside removal was complete within 24 hours and dialysis for up to 48 hours did not result in any further increase in the viscosity, which never returned to that of the original preparation.

Ultracentrifuge analysis (Chapter IV) has shown that 1 mg/ml pilin in 30mM octyl-glucoside has a sedimentation coefficient of 2.3S. With native pili, the measured s value ranges from 10-30S due to aggregation and to the heterogeneity in length of the filaments. With the reassembled pilin, a similar range of sedimentation values was observed. However, examination of the two preparations in the electron microscope suggested that the two structures were quite different.

Figure VI.2 shows a series of electron micrographs comparing the two structures. Native pili (figure VI.2A) are fairly rigid filaments of 52Å diameter and 2.5µm average length. The fact that no stain penetration is evident implies that the subunits are quite tightly packed in the assembly. The tendency of pili to form longitudinal aggregates, or "ropes" has been noted earlier (Chapter V) and the preparation of oriented fibers for diffraction is based on this property. The reassembled filaments, on the other hand, are considerably wider (figure VI.2B). Their diameter was measured using native pili as an internal standard (figure VI.2C) and found to be  $90 \pm 15 \text{Å}$ . The diameter obtained for native pili ( $52 \pm 4 \text{Å}$ ) was found to be in agreement with the





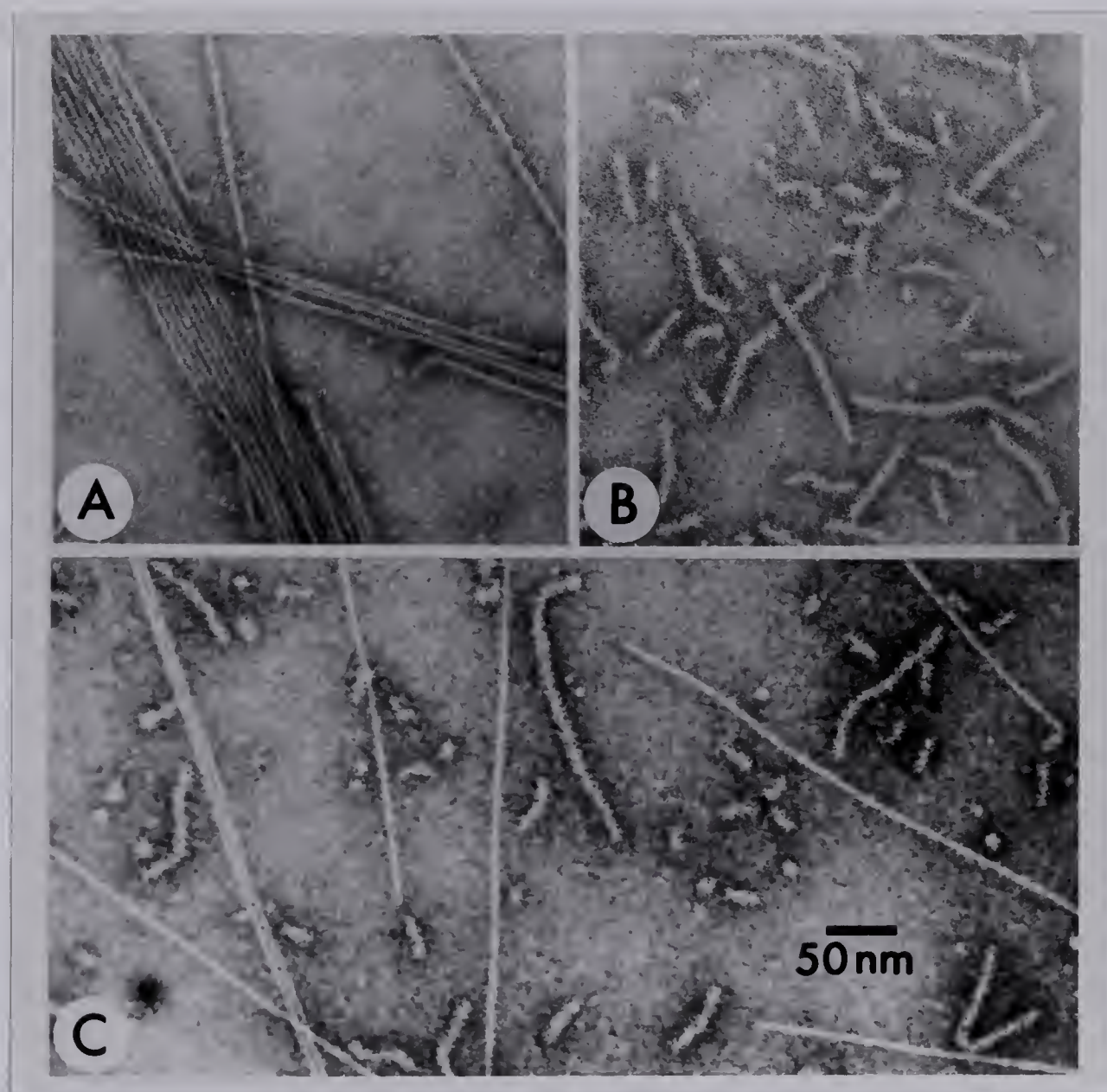


Figure VI.2. Electron microscopy of native and "reassembled" pili. A. Pure PAK pili, most of the pili in this picture are aligned in a "rope". B. 9 nm filaments observed after dialysis to remove detergent from pilin/octylglucoside. C. A mixture of the material in A and B. Native pili were used as an internal standard to determine the diameter of reassembled pili. The bar corresponds to 50 nm.



## X-ray diffraction results (Chapter V).

No aggregation of the reassembled filaments was apparent in the electron microscope, even though concentrations of protein as high as 1mg/ml were used. Fibers prepared from reassembled pili diffracted only poorly, showing circles at 5 and 10Å, attributed to disoriented  $\alpha$ -helix, and two weak crystalline reflections on the equator, which indicate a regular spacing between the filaments in the fiber. (data not shown). Failure to obtain well-oriented specimens of reassembled pilin is most likely due to their short length and their failure to form "ropes".

In Chapter III, the appearance of unusual structures at the ends of purified pili was noted. Some of these bear a remarkable similarity to the reassembled pilin filaments shown in figure VI.2B. Therefore it would appear that a certain amount of dissociation can occur at the ends of the pilus even though the preparations have never been exposed to detergent. This is even more apparent in figure VI.3 which shows an electron micrograph of PAK pili after 2 years at 4°C. It appears that over a long period of time considerably more dissociation and reassembly into the thicker filaments has taken place. The aggregation into ropes also tends to increase with time.





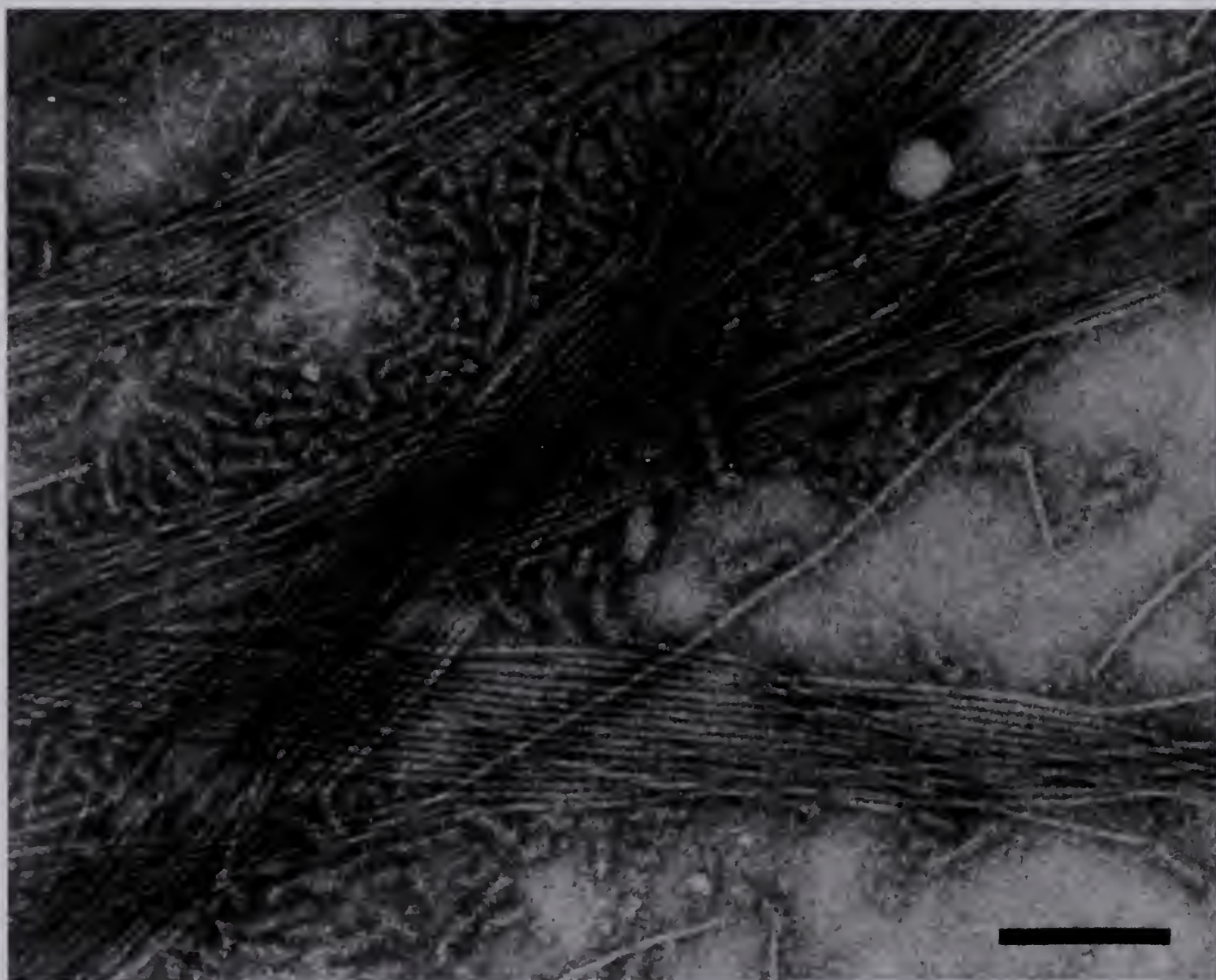


Figure VI.3. Electron micrograph of a solution of PAK pili after standing at 4°C for 2 years.





## *B. A Biological Assay for Pili*

The bacteriophage PO4 infects *Pseudomonas aeruginosa* by adsorbing to the lateral surfaces of the pili apparently by wrapping its tail fibers around the pilus (Bradley, 1974). If the attachment site for the phage were contributed by residues on more than one subunit it is likely that PO4 phage would fail to recognize monomers or wrongly assembled pilin aggregates. This reasoning allowed us to develop an assay for biologically active pili based upon the ability of purified pili to compete with pili on the bacterial cell for phage binding. The details of the assay are provided in Materials and Methods. Figure VI.4 (curve A) shows the effect of incubating PO4 phage with increasing amounts of native PAK pili prior to adding PAK cells and plating. About  $80 \pm 20\%$  was the maximum adsorption obtained. The failure to obtain 100% absorption most likely reflects the equilibrium between irreversibly adsorbed and reversibly adsorbed phage on the pili. That is, a small amount of phage may become detached from pili upon dilution into soft agar and reattach either to free pili or infect the *Pseudomonas aeruginosa* indicator strain added. Curves B and C show the effect of increasing amounts of pilin subunits in detergent (B) or reassembled pili (C). Although the reassembled pilin filaments appear to show a slight inhibitory effect on phage infection, the inhibition is much less than that observed with native pili. Thus it appears that the bacteriophage PO4 binds with a lowered affinity to the reassembled pilin



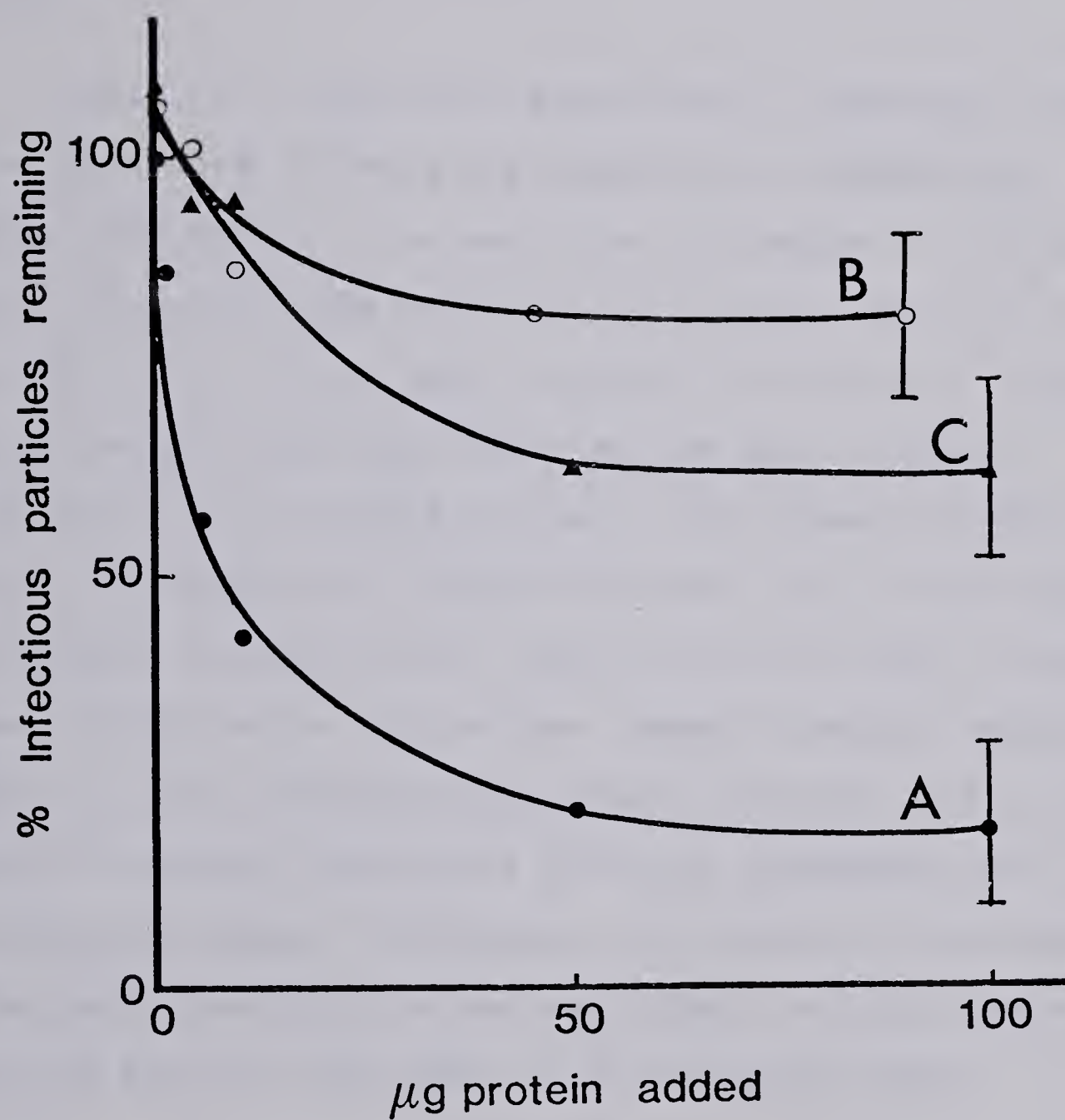


Figure VI.4. Reduction in the number of plaque-forming units upon incubation of various forms of pilin assembly with phage P04 prior to carrying out a standard plaque assay as described in Materials and Methods. A. native PAK pili. B. pilin/octyl-glucoside. C. reassembled pili.



filaments or pilin dimers as compared to native pili, implying that the quaternary arrangement of pilin subunits is important in the recognition of pili by bacteriophage. Therefore, this experiment provides further evidence that we have assembled an alternate structural form of polymeric pilin.

Table VI-I summarizes some control experiments which show that these effects are specific to *Pseudomonas aeruginosa* PAK pili. As mentioned in Chapter I, P04 adsorbs about four-fold less efficiently to strain PAO than it does to PAK cells. In our hands, PAO pili were unable to prevent infection of strain PAK cells by the bacteriophage. Similarly, pili encoded by the *E. coli* plasmid EDP208 were unable to compete for phage attachment. Pili which have been sonicated to reduce their length are still able to prevent phage infection as well as the longer filaments suggesting that it is the different quaternary structure and not the shorter average length that prevents reassembled pili from binding P04 phage. Furthermore, the amount of detergent added with the pilin is not sufficient to block phage infection as shown by the addition of detergent alone.

The above experiments were repeated for the filamentous phage Pf1 (Bradley, 1973a) which adsorbs to the tip of the pilus. It was found that addition of native pili resulted in an 88% inhibition of phage attachment to piliated PAK cells, while PAO pili gave 32% inhibition, PAK pilin/octyl-





TABLE VI-1

*Inhibition of Phage Attachment to Pseudomonas aeruginosa\**

Addition	%Inhibition
None	0
PAK pili (100 $\mu$ g)	80 $\pm$ 20
PAO pili (100 $\mu$ g)	-7 $\pm$ 14
EDP208 pili (100 $\mu$ g)	10 $\pm$ 15
Pilin/octyl-glucoside (100 $\mu$ g pilin)	18 $\pm$ 23
Sonicated PAK pili (100 $\mu$ g; sonicated for 2 min.)	72 $\pm$ 20
Reassembled pilin filaments (100 $\mu$ g)	37 $\pm$ 20
Octyl-glucoside control	0 $\pm$ 10

\* The assay is described in Materials and Methods and in the text.



glucoside, 10% inhibition and the reassembled filaments a 5% stimulation of the number of plaque forming units available for infection of the PAK cells. Therefore, it appears that Pf1 phage also require a native quaternary arrangement of pilin subunits for attachment.

### *C. Discussion*

Recently, Eshdat and collaborators (1981) have reported the dissociation and reassembly of *E. coli* Type I pili, using guanidine-hydrochloride to dissociate the pili into subunits. Although these workers have demonstrated by electron microscopy that removal of guanidine hydrochloride leads to the formation of a rod-like structure, they did not demonstrate that the rods have the characteristics of functional, properly assembled pili. In light of our results we suggest that more rigorous criteria be used in future to define pilus reassembly.

As discussed in Chapter I, 12 transfer genes are involved in the expression of the plasmid-encoded F pilus on the cell surface (Willems & Skurray, 1980). Similarly, the plasmid encoded *E. coli* adhesion pilus, K88ac requires 5 cistrons for expression on the cell surface (Dougan *et al.*, 1983). Recently, the chromosomally encoded pilus from *N. gonorrhoeae* has been cloned and expressed in minicells (Meyer *et al.*, 1982). The pilin subunits were found in the mini-cell membranes, but were not assembled and expressed on the cell surface, implying that other gene products or



functions are necessary for assembly.

The above results imply that assembly of *Pseudomonas* pili requires additional factors. It is also likely that assembly requires the presence of a lipid bilayer as appears to be the case for filamentous phage assembly (Smilowitz, 1972). Furthermore, there is evidence at least for F pili, that pilus outgrowth is an energy requiring process that is inhibited by energy poisons (O'Callaghan *et al.*, 1973; Novotony & Fives-Taylor, 1974).

The fact that we have obtained a population of aggregates of *Pseudomonas* pilin of uniform diameter suggests that there are at least two stable quaternary structures for this protein. Native pili are formed when pilin is assembled from the cell membrane (perhaps in the presence of other protein factors and an electrochemical gradient); an alternate quaternary structure, reassembled pilin filaments, is formed upon removal of detergent from octyl-glucoside solubilized pilin or from purified native pili upon prolonged standing at 4°C.





## CHAPTER VII

### Pilin in the membrane of *Pseudomonas aeruginosa*

To date, little is known about the assembly of *Pseudomonas aeruginosa* pili *in vivo*. However, by analogy with filamentous phage assembly (Smilowitz *et al.*, 1972), it appeared likely that pilin exists in a membrane bound state at some stage of its synthesis/assembly. For this reason, experiments were carried out to identify pools of pilin in the isolated inner and outer membranes of *Pseudomonas aeruginosa* using the technique of immunoblotting (Towbin *et al.*, 1979; described in Chapter III). These studies were carried out on wild-type *Pseudomonas aeruginosa* PAK and on the multipiliated strain PAK/2Pfs in order to determine whether the multipiliated strains had an altered pool size.

Once it had been tentatively established that pilin was a membrane protein, it was of interest to reconstitute the protein into synthetic phospholipid vesicles with a view to studying the pilin structure in the membrane.

#### *A. Identification of Pilin Pools in the Isolated Inner and Outer membranes of Pseudomonas aeruginosa*

##### **1. Separation of Inner and Outer Membranes.**

Membranes from *Pseudomonas aeruginosa* strains PAK and PAK/2Pfs were isolated by the method of Hancock and Nikaido, (1978). Details of the membrane separation are provided in Materials and Methods but are repeated in part here. It



should be noted that it is important to carry out all steps (after the pressure cell treatment) at 0°C. This seems to be important in preventing fusion of the two membranes. Briefly, isolated cells were suspended in 20% sucrose containing RNase and DNase and then passed 2-3 times through a pressure cell. Subsequently, the cells were treated with lysozyme and the protease inhibitor PMSF and then centrifuged to remove unbroken cells. The supernatant was then applied to a two-step sucrose gradient and the crude membrane fraction was collected on a 70% sucrose cushion. The crude membranes were then further fractionated on a four-step sucrose gradient yielding four membrane fractions: OM1, OM2, M and IM in the nomenclature of Hancock and Nikaido. IM (inner membrane) is deep red in colour due to the presence of cytochromes; OM1 (outer membrane) is a translucent white; while the impure fractions OM2 and M are orange. The purity of the membrane fractions was assessed using the enzyme succinate dehydrogenase (SDH) as an inner membrane marker and the lipopolysaccharide sugar, 2-keto-3-deoxy-octonic acid (KDO) as an outer membrane marker. The results are summarized for the wild-type and multipiliated strains in Table VII-I. It can be seen that OM1 is highly purified outer membrane and IM is highly purified inner membrane in agreement with the findings of Hancock and Nikaido (1978).



TABLE VII-I

*Characterization of Isolated Membrane Fractions*

Fraction	Protein <sup>1</sup>		KDO <sup>2</sup>		SDH <sup>3</sup>	
	PAK	PAK/2Pfs	PAK	PAK/2Pfs	PAK	PAK/2Pfs
OM1	24	24	141	217	7	6
OM2	5	9	90	63	8	17
M	5	6	42	55	57	83
IM	12	8	30	9	223	255

1. Total protein from 4/ late log phase expressed in mg.
2. nmol KDO/mg membrane protein, KDO=2-keto-3-deoxy-octonic acid.
3. succinate dehydrogenase activity expressed as  $\mu$ mol DCPIP reduced/minute/mg membrane protein.





## 2. Immunoblotting

The identification of pilin in the membranes of *Pseudomonas aeruginosa* was carried out as follows:

The proteins from the isolated membrane fractions were subjected to SDS-polyacrylamide gel electrophoresis and then transferred electrophoretically to nitrocellulose paper as described in Materials and Methods. The pilin was visualized by reacting the nitrocellulose paper first with anti-pilus antibodies and subsequently with  $^{125}\text{I}$ -labelled Protein A from *Staphylococcus aureus*. The nitrocellulose paper was then subjected to autoradiography for visualization of the bound label.

Figure VII.1 (A and B) shows the Coomassie blue staining patterns obtained from each membrane fraction of the two strains. It is difficult to assess from Coomassie blue staining alone whether or not there is a band migrating at the same position as the pilin standard, due to the large number of proteins present. Figure VII.1 (C and D) show that within 4 hours of transfer the removal of lower molecular weight proteins from the gel is virtually quantitative; transfer of the higher molecular weight bands is somewhat less efficient.

Figure VII.2 shows the autoradiograms obtained after treatment of the nitrocellulose transfers with pilus-specific antibodies and  $^{125}\text{I}$ -Protein A as described in Materials and Methods. The autoradiograms shown in



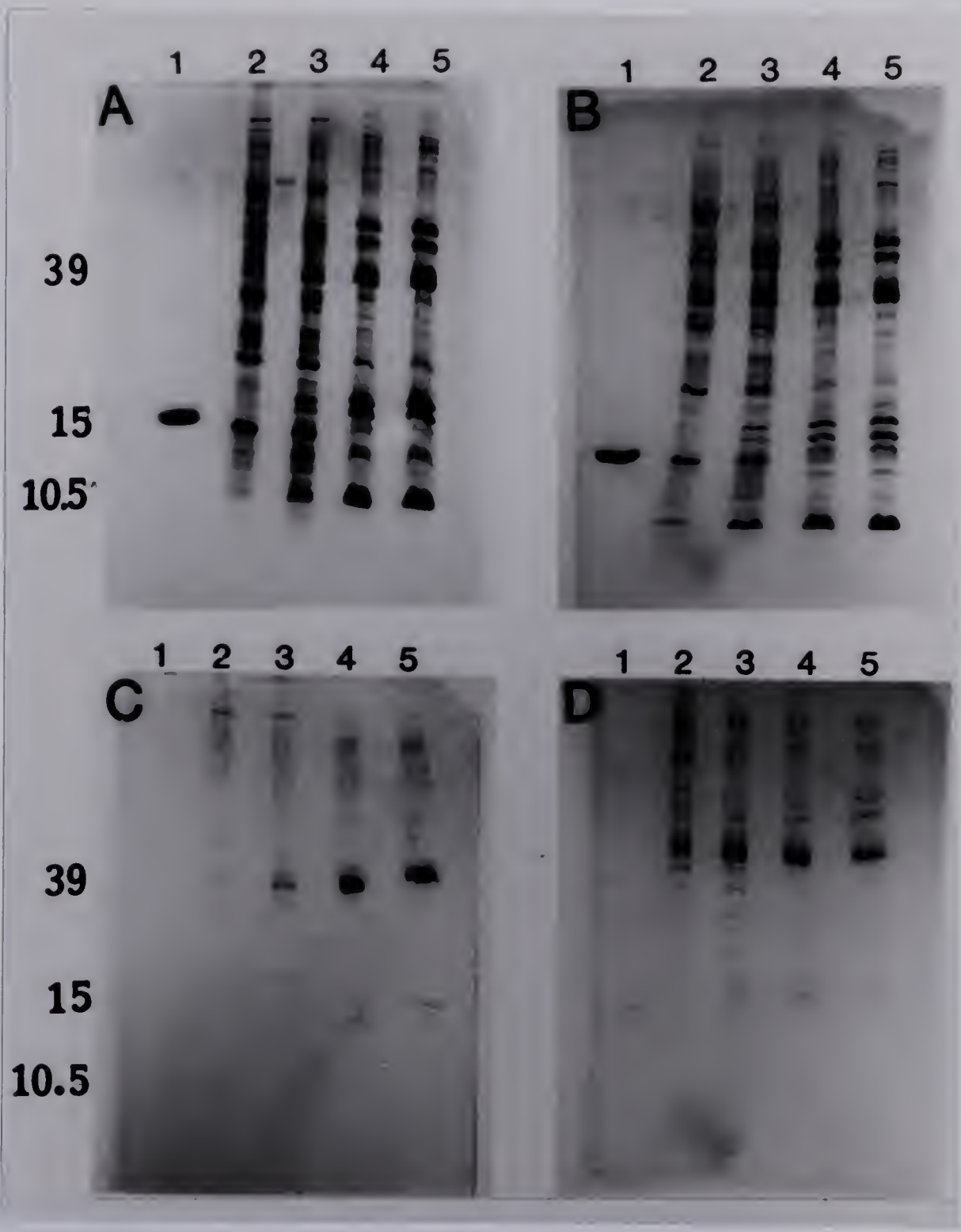


Figure VII.1. SDS-polyacrylamide gel electrophoresis and transfer to nitrocellulose of *Pseudomonas* membranes. A and B: Coomassie blue-stained 15% polyacrylamide SDS-gels of *Pseudomonas* membrane fractions. A: PAK. B: PAK/2Pfs.

Lane 1 in each case contains 10 ug of pure PAK pilin, lanes 2 through 5 are respectively IM, M, OM2 and OM1; 90 ug of membrane protein were applied per lane.

The molecular weight markers are the major porin of *Pseudomonas* outer membrane at M=39,000 (Hancock & Carey, 1979), pilin at M=15,000 and the lipoprotein of *Pseudomonas* outer membrane, reported at 9-12,000 by Hancock & Carey (1979), shown here as 10,500.

C and D are the Coomassie blue staining patterns obtained after the proteins have been transferred to nitrocellulose paper for 4 hr. Samples in each lane are identical to those in A and B.







1 2 3 4 5

A

1

2

3

4

5

B

Figure VII.2. Autoradiograms of nitrocellulose transfers. The proteins on the gels in figure VII.1 were transferred to nitrocellulose paper and treated with pilus-specific antibodies and  $^{125}$ I-Protein A as described in Materials and Methods. Lanes 1 through 5 are as described in Figure VII.1.



Figure 7.2 correspond to the gels shown in Figure 7.1. In lane 1, the more intense band is the pilin monomer at  $M = 15,000$ . A small amount of pilin dimer ( $M = 30,000$ ) is visible using the  $^{125}\text{I}$  detection method although the dimer was not apparent in the Coomassie blue stained gels.

A protein that reacts with pilus-specific antibodies and migrates at the same position as purified pilin is present in all four membrane fractions from each strain. We therefore concluded that this represents pilin in the membrane of *Pseudomonas aeruginosa*. With both PAK and PAK/2Pfs there appears to be a slight gradient in pool size, with a larger amount associated with the inner membrane. Comparison of the intensity of the pilin standard (lane 1) with the band in lane 2, suggests that the inner membrane of PAK possesses 3-6 ug of pilin/100 ug of membrane protein. In the case of 2Pfs, the pool size is, if anything, slightly smaller. Thus, increased piliation does not necessitate a larger pool size, and perhaps depletes the pool slightly.

### 3. Evidence that extracellular pili do not contaminate the membrane preparations

Examination of the cells by electron microscopy at various stages of membrane isolation showed that a large amount of pili is lost during centrifugation and washing steps. The remainder is completely sheared from the cell into small fragments after being run two times through the pressure cell. This is evident upon examination of Figure



VII.3 which shows electron micrographs of the membrane fractions OM (VII.3A) and IM (VII.3B). One can see that no whole pili remained attached to the membranes in either fraction. It is also of interest to note the difference in morphology between the inner and the outer membrane vesicles.

In order to demonstrate that mature pili which have been sheared from the cell surface do not contaminate the membrane preparations, [ $^{35}\text{S}$ ]-labelled-whole pili were added during an early stage of membrane isolation and their fate followed throughout the separation procedure.

Table VII-II shows the fate of [ $^{35}\text{S}$ ]-pili that were added to 250 ml cultures of PAK and PAK/2Pfs after they had been centrifuged and resuspended in 50 ml of Tris buffer. Of the  $2 \times 10^6$  cpm added, more than 98% remained in the supernatant of the PAK cells, while 85% remained in the supernatant of the multipiliated strain. In the case of PAK cells, very few pili were left on the cell surface at this stage. However, with the multipiliated strain several pili remain per cell and these may be responsible for trapping the labelled pili, resulting in higher counts associated with the cell pellet than in the wild-type strain. Fractionation of the first sucrose gradient showed a large radioactive peak near the top of the gradient (free pili) while the crude membranes, obtained from the bottom 2 ml of the gradient had very few counts associated with them.





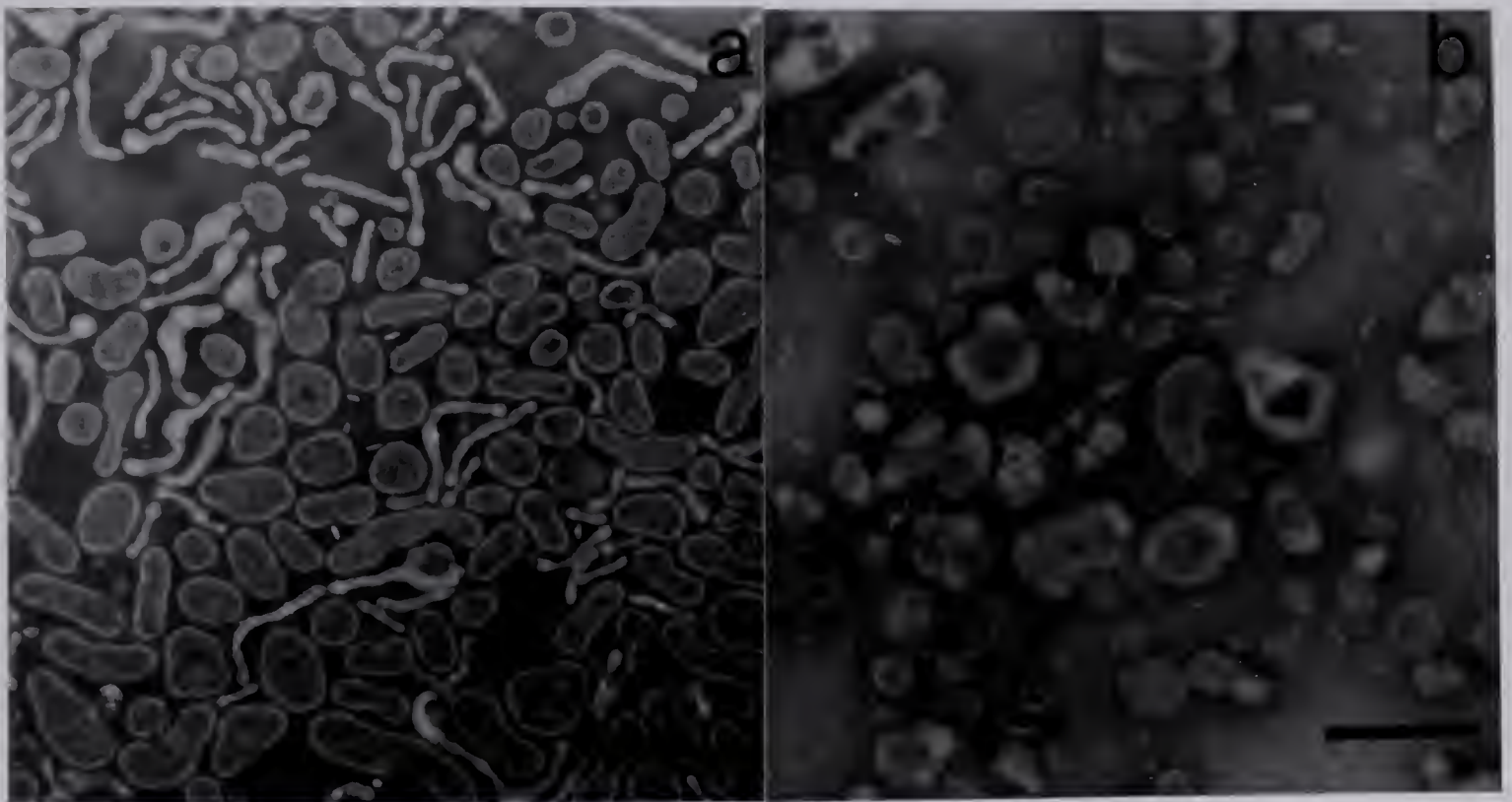


Figure VII.3. Electron micrographs of isolated membrane fractions of *Pseudomonas*, negatively stained with sodium phosphotungstenate. a. Outer membrane fraction OM1. b. Inner membrane fraction IM. The bar indicates 100 nm.



TABLE VII-II  
*Fate of Added [<sup>35</sup>S]-Pili During Membrane Isolation*

Step*	Data for strain:					
	PAK			PAK/2Pfs		
	Total cpm <sup>a</sup>	<sup>35</sup> S-pili <sup>b</sup> (μg)	% recovery	Total cpm <sup>a</sup>	<sup>35</sup> S-pili <sup>b</sup>	% recovery
1.	2.37x10 <sup>6</sup>	172	-	2.35x10 <sup>6</sup>	171	-
2.	2.37x10 <sup>6</sup>	172	100	2.00x10 <sup>6</sup>	146	85.1
3.	3.87x10 <sup>4</sup>	3	1.6	1.77x10 <sup>5</sup>	13	7.5
4.	1.0x10 <sup>3</sup>	0.07	0.4	1.5x10 <sup>3</sup>	0.1	-
5.	3.40x10 <sup>4</sup>	2.5	1.43	1.71x10 <sup>5</sup>	12.4	7.3
6.	0	<0.01	<0.005	0	<0.01	0.00

\*The steps monitored were as follows:

1. Cells in 50.0ml of Tris after first centrifugation
2. Cell supernatant after 2nd centrifugation
3. Cell pellet in 20% sucrose
4. Crude membranes from lower 2ml of 1st sucrose gradient
5. Peak at the top of 1st sucrose gradient
6. Final membrane preparation

a. 100 μl of each sample was counted in duplicate at each stage of the membrane isolation, and multiplied by the the total volume at that stage to obtain Total cpm.

b. The specific activity of the [<sup>35</sup>S]-pili was 1.375x10<sup>7</sup> cpm/mg.



Upon separation of the 4 membrane fractions on a second sucrose gradient, followed by a washing step to remove sucrose, negligible amounts of radioactivity were found associated with each fraction. This was taken as evidence that the pilin observed in the membranes of *Pseudomonas aeruginosa* PAK and PAK/2Pfs represent a pool of pilin subunits and not contamination from mature extracellular pili.

#### 4. Discussion

Moore *et al.*, (1981) have reported the existence of an F pilin pool in the membranes of *E. coli* harbouring an F plasmid. In contrast to our results with *Pseudomonas* pili, they found pilin only in the inner membrane fractions. This group determined the amount of F pilin in the membrane to represent 4-5% of the total membrane protein which is comparable to our findings with the *Pseudomonas* pilin. However, this is somewhat surprising since one normally finds only 0-2 F pili per cell (Frost, 1978) while PAK and PAK/2Pfs are much more heavily piliated. Another difference between the two studies is that Moore *et al.* based their identification of pilin in the membrane upon comigration with purified F pilin and upon the fact that this protein is absent in F-minus strains. The present study, on the other hand, uses a specific detection method (using anti-pilus antisera) and thereby eliminates the danger of artifacts arising from proteins of similar molecular weights comigrating on gels.





Recently, the pilin gene of K88ac pilin has been cloned and expressed in minicell-producing strains of *E. coli* (Dougan, *et al.*, 1983). Fractionation of the minicell membranes showed that K88ac pilin is found in both the inner and outer membrane fractions of *E. coli*, in agreement with our findings for *Pseudomonas*. In addition, these authors determined the location of the gene products of several other cistrons which are essential for expression of pili on the cell surface. In particular, a 70,000-dalton polypeptide, the product of the *adhA* (for adhesion cistron A) was found to be associated primarily with the outer membrane, while the products of the *adhB* and *adhC* cistrons were found in the periplasm. This implies that the outer membrane may be the site of assembly of pili.

Both our results and those of Dougan *et al.*, suggest that one of the first steps in pilus assembly is accumulation of pilin in the cytoplasmic membrane as has been observed in filamentous phage assembly (Smilowitz *et al.*, 1972). However, in the case of filamentous phage assembly, no phage coat protein was found in the periplasm or the outer membrane, but the phage appeared rapidly in the growth medium.

Bayer (1975) has observed pili emerging from points of adhesion between the inner and outer membranes of bacteria, which have become known as "Bayer's junctions". It has been suggested that these junctions are important in the



translocation of outer membrane and exported proteins to their final destinations (Dirienzo *et al.*, 1978). Whether pili are assembled at the cytoplasmic membrane and extruded through these junctions, as originally suggested by Bayer, or assembled at the outer membrane cannot be determined at this time. The fate of the Bayer's junctions in our membrane preparations is not clear, although they are most likely found in the impure fractions OM2 and M.

In the Immunoblot experiments described in this chapter, at no time was a larger precursor of pilin observed that could be attributed to a cleavable signal sequence for pilin (Blobel & Dobberstein, 1975; Wickner, 1979; von Heijne & Blomberg, 1979). It may be, however, that processing of such a pilin precursor occurs too rapidly to allow detection in our system. It would therefore be useful to treat *Pseudomonas* cells with phenethylalcohol in order to inhibit processing (Halegoua & Inouye, 1979). On the other hand, the existence of a 29-residue hydrophobic stretch at the N-terminal of *Pseudomonas* pilin (Paranchych *et al.*, 1978) may obviate the need for a cleavable signal sequence. Dougan and coworkers on the other hand, did observe the accumulation of a precursor to the 23,500-dalton K88ac pilin upon treatment of minicells with ethanol, but examination of the mature sequence of K88ac pilin (Klemm, 1981) does not show any long uninterrupted stretch of hydrophobic residues analogous to residue 1-29 of PAK pilin that could substitute for a cleavable signal sequence.





## *B. Reconstitution of Pilin into Synthetic Phospholipid Vesicles*

Since the above experiments suggested that pilin is a membrane protein, it was of interest to attempt to reconstitute pilin into a synthetic bilayer so as to allow studies on the mode of pilin insertion into the membrane in a simplified system. Since pilin could be dissociated into dimers by octyl-glucoside but not by the traditional reconstitution detergents, cholate and deoxycholate, the reconstitution method chosen involved removal of octyl-glucoside from pilin/octyl-glucoside/phospholipid mixtures. Octyl-glucoside has been used successfully, for example, in the reconstitution of Semliki forest virus membrane (Helenius *et al.*, 1977), cytochrome oxidase (Racker *et al.*, 1979) , glycophorin A (Mimms *et al.*, 1981) and rhodopsin (provided that cholate is also included, Borochoy-Neori & Montan, 1983). The method used was essentially the detergent-dialysis method of Kagawa & Racker (1971, reviewed by Racker, 1979).

### **1. Reconstitution**

The details of the reconstitution procedure are given in Materials and Methods and are briefly summarized below. Pilin was dissolved to 1 mg/ml in 1% octyl-glucoside and centrifuged to remove any large aggregates. A mixture of 80% dimyristylphosphatidylcholine (DMPC), 10% dipalmitoyl-phosphatidic acid (DPPA) and 10% cardiolipin were dissolved





in 1.5% octyl-glucoside in Tris/EDTA buffer. The incorporation of 20% acidic phospholipids has been used in the past to prevent aggregation of the vesicles (Hagen *et al.*, 1978). The lipids were sonicated in the detergent until clear (about 10 minutes) and the pilin in octyl-glucoside was immediately added. After gentle mixing at 37°C for 15 minutes, the mixture was dialyzed against 4 changes of Tris/EDTA/methanol buffer for a total of 24 hours at 4°C. The phospholipid vesicles were then concentrated by centrifugation and the pellet material was applied to a 1x70cm Sepharose 4B column.

Figure VII.4 shows the elution profile obtained on Sepharose 4B. The four areas A through D were pooled separately and concentrated by centrifugation. All four pools were found to contain both phospholipid and protein to varying degrees. Most of the protein was found in peak B, the major peak. The phospholipid to protein ratio of peak B was found to be 8.3:1 by weight or 220 phospholipid molecules for every protein molecule. An electron micrograph of the vesicles from peak B is shown in figure VII.5. The vesicles appear to be unilamellar and range in size from about 500-1000Å. One cannot actually see pilin in the vesicles, however this is not surprising due to the low protein content and to the fact that the pilin subunits are only about 20x50Å in size (Chapter IV & V).



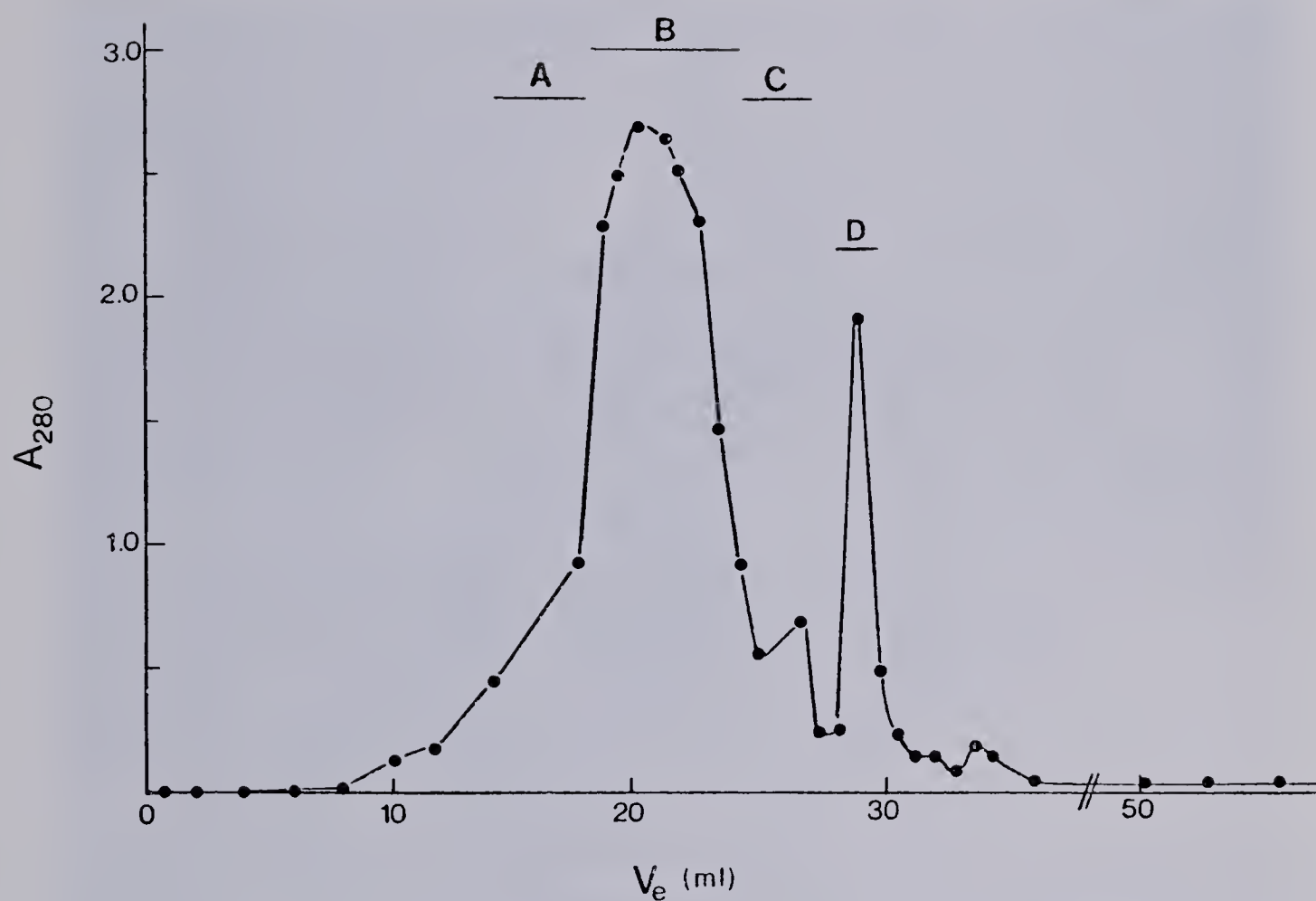


Figure VII.4. Chromatography of pilin/vesicles on Sepharose 4B. A through D indicate the pooled regions described in the text.



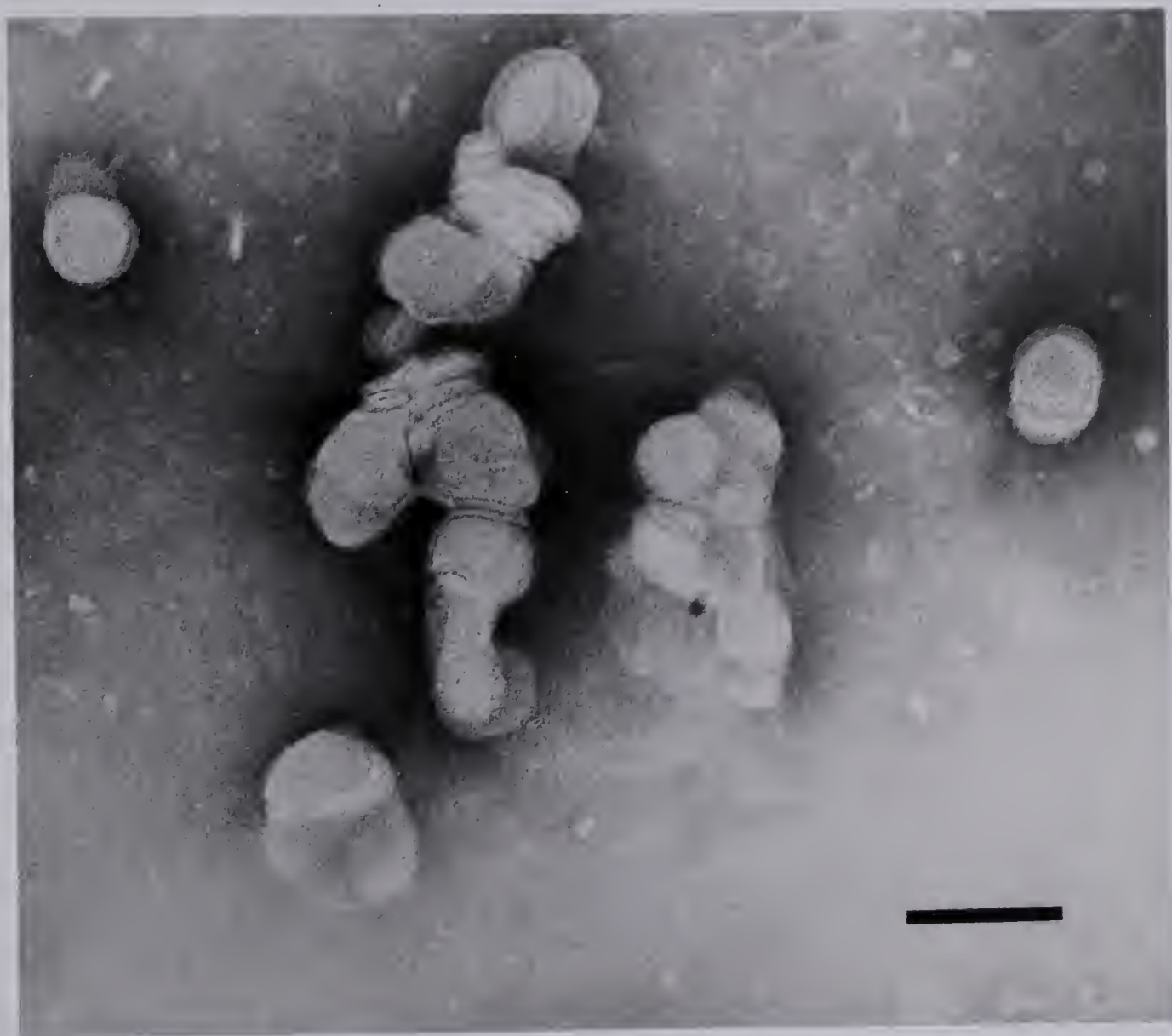


Figure VII.5. Electron microscopy of pilin vesicles obtained from fraction B of the column described in figure VII.4. The bar indicates 100 nm.





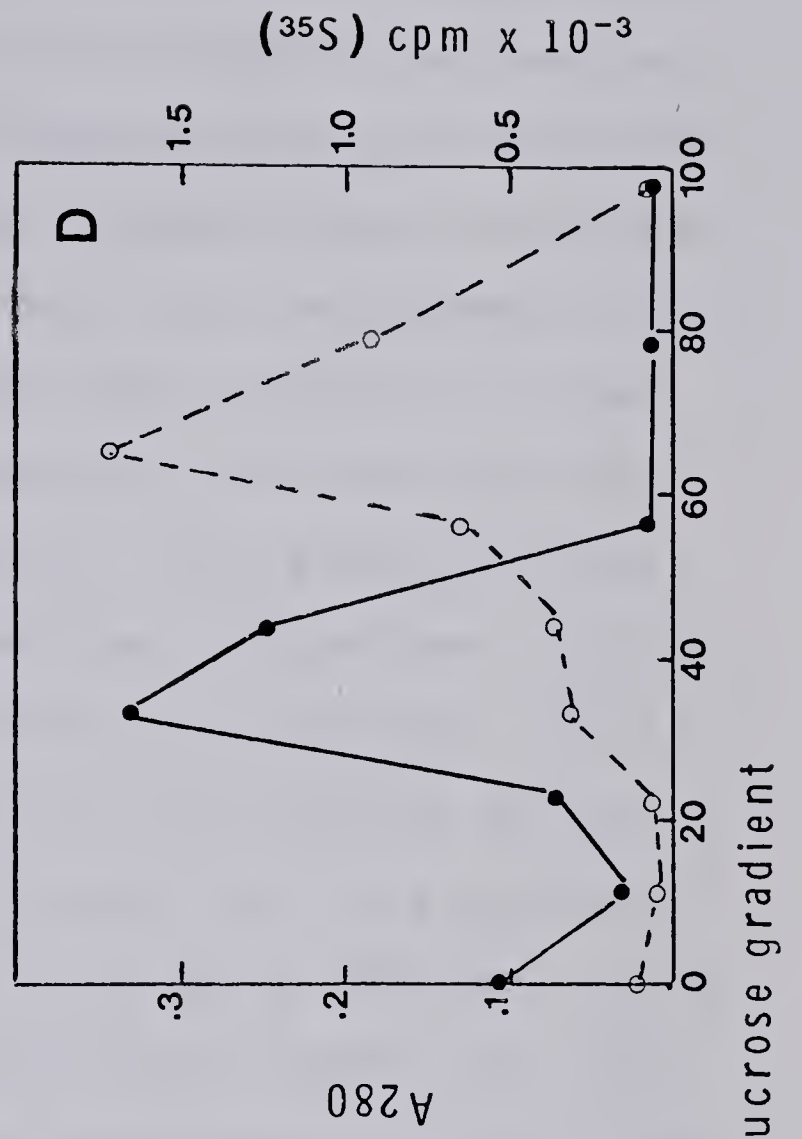
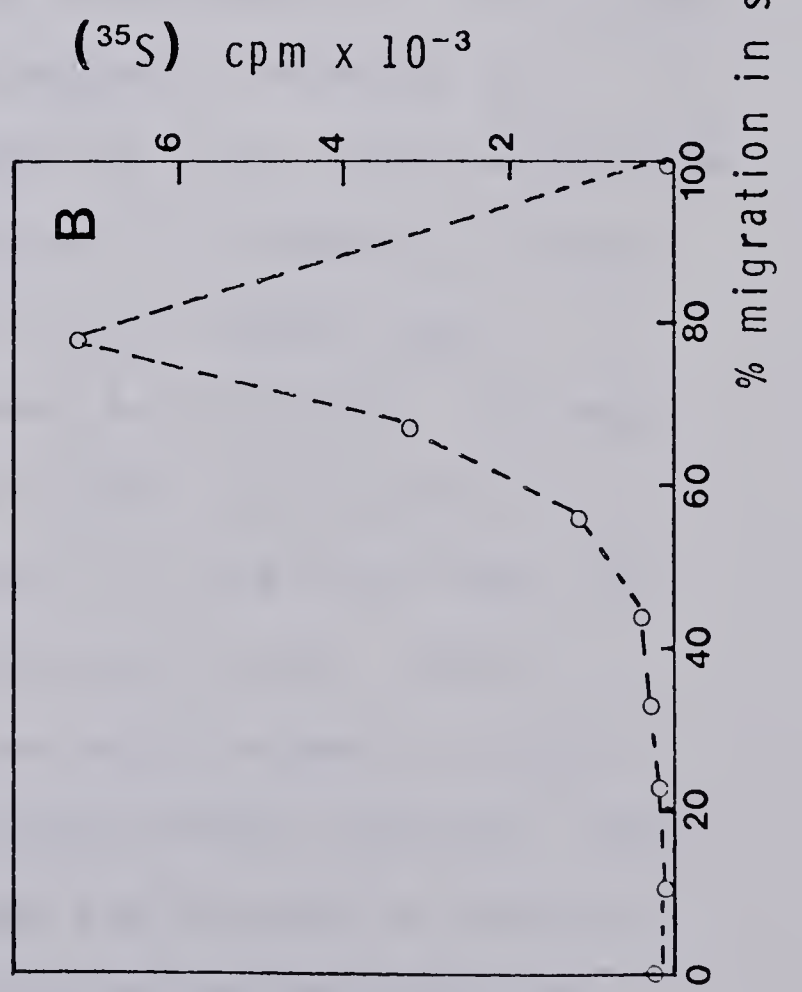
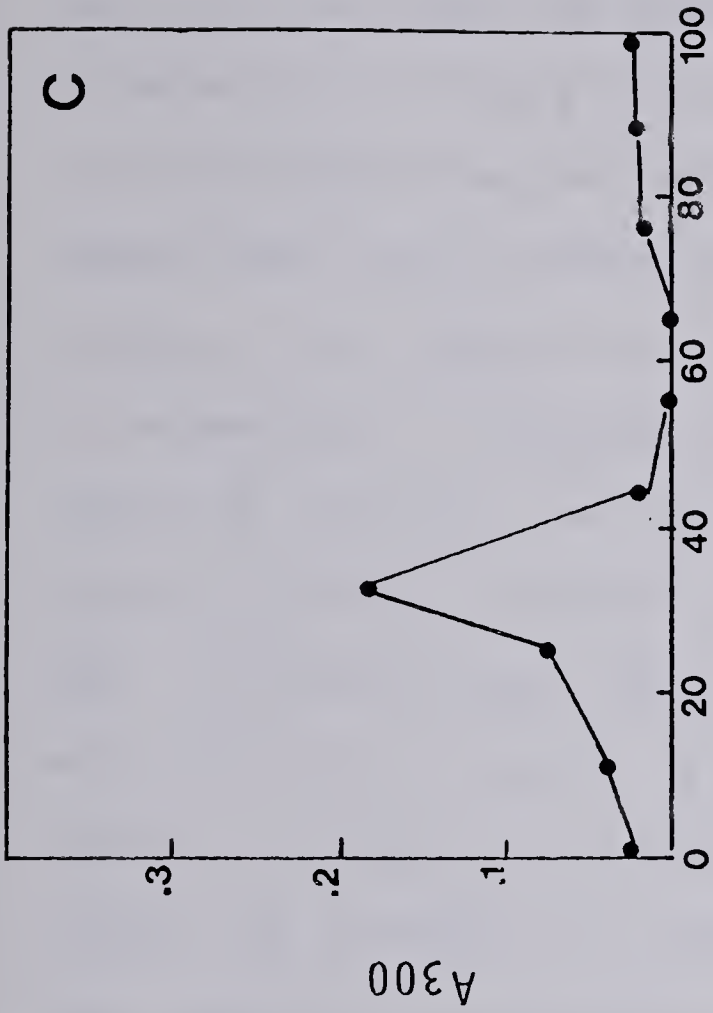
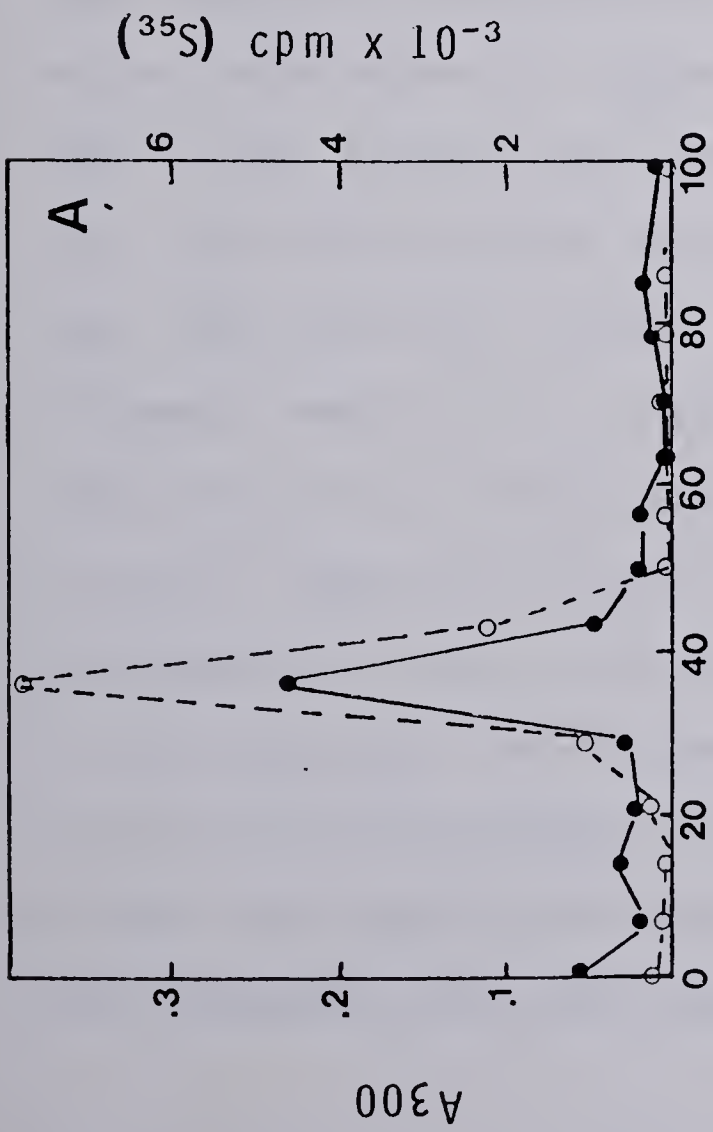
## 2. Evidence that pilin is tightly associated with the phospholipid vesicles.

In order to demonstrate that the pilin was tightly associated with the vesicles and not just sticking to them, attempts were made to dissociate pilin from the vesicles by incubation of the vesicles in high salt or at high pH prior to sedimentation on sucrose gradients. The results of these experiments are shown in figure VII.6A for the high salt case (0.5M NaCl). Similar results were obtained in low salt at pH 10.5, under conditions where pilin is negatively charged and should be repelled by the negatively charged vesicles. Figure VII.6A shows the sedimentation profile of vesicles that were prepared with [ $^{35}\text{S}$ ]-pilin. It can be seen that the pilin (followed as [ $^{35}\text{S}$ ]-cpm) and the phospholipids (followed by monitoring the  $A_{280}$ ) co-sediment under these conditions. Panel B shows the sedimentation profile of native [ $^{35}\text{S}$ ]-labelled pili. It can be seen that the whole pili sediment much faster than the pilin vesicles. Phospholipid vesicles without pilin sediment only slightly less rapidly than the pilin vesicles (Figure VII.6C), probably because the pilin content (about 10% by weight) is not sufficient to change the density significantly. Figure VII.6D shows the results obtained when labelled-whole pili are incubated with a preparation of unlabelled pilin/vesicles. Although a slight shoulder implies some sticking of whole pili to the vesicles, more than 80% of the whole pili separate from the vesicles during the





Figure VII.6. Sedimentation of pilin/vesicles in a 0-64% sucrose gradient. A. 0.25ml [ $^{35}$ S]-pilin/vesicles in 0.5M NaCl were applied to a 4.5ml sucrose gradient. B. Sedimentation of [ $^{35}$ S]-whole pili under the same conditions as in A. C. vesicles containing no pilin. D. cold pilin/vesicles + [ $^{35}$ S]-whole pili. (-----)=[ $^{35}$ S]-pilin; (——)Absorbance due to phospholipids.







centrifugation. These results show that the "reconstituted" pilin is tightly associated with the phospholipid vesicles. There are at least two possible explanations for this tight association. a) The pilin may be trapped inside the vesicles or b) the pilin may be incorporated into the bilayer. If the latter were true, then one would expect a portion of the protein to be exposed on the outside of the vesicles and to be accessible to protease digestion. This possibility was tested by treating the pilin/vesicles with pronase. It was found that after 12 hours incubation with pronase, 40% of the [ $^{35}$ S]-counts were associated with the vesicle pellet, while 60% of the counts were released into the supernatant. However, analysis of the pellet material by SDS-PAGE did not reveal the presence of a membrane-bound fragment that had been protected from digestion by the presence of the bilayer as has been shown for bacteriorhodopsin (Huang *et al.*, 1980). This implies that the peptides that remain associated with the vesicles have been cleaved to fragments of less than 4000 molecular weight (in the gel system used, fragments smaller than 4000 cannot be detected). This may imply that only a small portion of the pilin subunit is actually inserted into the bilayer, as has been shown for glycophorin A (for review see Marchesi *et al.*, 1976). A likely candidate for the membrane bound segment of pilin would be the hydrophobic N-terminal stretch (residue 1-29). On the other hand, pilin may span the bilayer in several short segments which are separated by pronase-sensitive



loops, as has been shown for bacteriorhodopsin (Huang *et al.*, 1980). Both these cases could lead to small fragments upon pronase digestion of pilin in a bilayer. Further analysis of the vesicle-associated products of pronase digestion will be necessary to distinguish between these two possibilities.

### 3. Circular dichroism of pilin/vesicles

Figure VII.7 shows the circular dichroism spectrum of pilin incorporated into phospholipid vesicles as compared to the CD spectrum of native pili. It can be seen that pilin in the presence of phospholipids has a very similar CD spectrum to that of native pili. Although we do not know whether pilin in the reconstituted system spans the bilayer, these results do show that pilin in association with phospholipids has a similar structure to native pili or pilin in detergent (Chapter IV). On the other hand, Wu *et al.* (1982) have shown that some proteins adopt a more helical structure upon addition of phospholipids. Similarly, the secondary structure of fd coat protein reconstituted into a phospholipid bilayer, has been shown to vary depending on the history of the preparation (Nozaki *et al.*, 1978). This does not appear to be the case with PAK pilin.

### 4. Summary

In summary, we have developed a method for reconstituting pilin into synthetic phospholipid vesicles. The word reconstitution is used rather loosely, however,



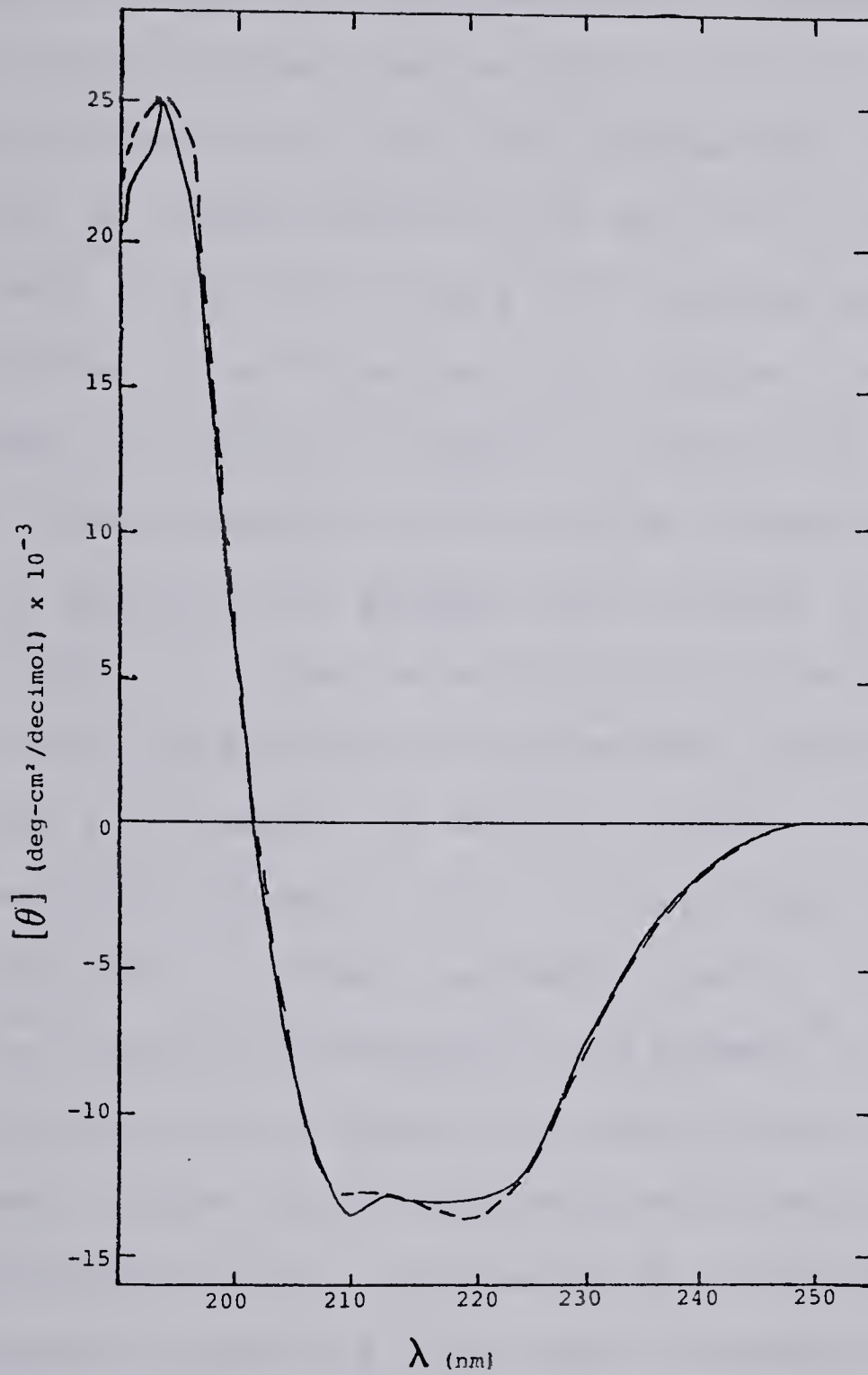


Figure VII.7. Circular dichroism spectrum of pilin reconstituted into phospholipid vesicles, (-----), compared with the circular dichroism spectrum of native PAK pili (——). A sample of vesicles without pilin was used as a blank for the reconstituted pilin.





since we do not know the mode of integration of pilin into *Pseudomonas* membranes, and therefore cannot tell whether or not we have achieved this same mode of integration in the reconstituted system. The reconstituted pilin was shown to be tightly associated with the phospholipid vesicles as it could not be dissociated in high salt or at pH 10.5. On the other hand, only 40% of the pilin remained associated with the vesicles after digestion with pronase, implying that a large part of the pilin subunit is exposed to the external medium. These results do not provide evidence that pilin is actually spanning the phospholipid bilayer in the reconstituted system. In order to establish this fact more detailed analysis of the products of proteolytic digestion are required. For example, it would be useful to solubilize the membrane bound fragments after pronase digestion of the pilin/vesicles in organic solvents, purify them by high pressure liquid chromatography and attempt to identify which part(s) of the pilin subunit is associated with the vesicles. Another useful approach would be to attempt to modify residues which are exposed on the surface of the vesicles using chemical means and to compare the labelling patterns obtained with those obtained on pilin in the absence of phospholipids. In conclusion, although these results are somewhat preliminary, they are included here to show that the reconstitution of pilin into phospholipid vesicles from octyl-glucoside shows some promise and merits further study.



## CHAPTER VIII

### Spectral properties of three quaternary arrangements of *Pseudomonas aeruginosa* PAK pilin

In Chapter IV, the dissociation of pili into dimers by octyl-glucoside was demonstrated. Subsequently, it was demonstrated (Chapter VI) that removal of octyl-glucoside from this preparation resulted in the formation of flexible filaments of almost twice the diameter of native pili. These were called reassembled pilin filaments. These three species, native pili, pilin dimers in octyl-glucoside and reassembled pilin filaments, represent three different quaternary arrangements of *Pseudomonas* pilin. A comparison of the interactions at the regions of intersubunit contact in the three forms of pilin assembly should contribute to our understanding of the mechanism of assembly and disassembly (retraction) of *Pseudomonas* pili.

One approach to determining the regions of intersubunit contact in a protein assembly is to establish the degree of accessibility of various amino acids in the intact and dissociated complex. The aromatic amino acids are particularly attractive candidates for this type of approach for two reasons. Firstly, most proteins have a limited number of aromatic amino acids thereby making the task of identifying specific residues simpler. Secondly, tyrosine, tryptophan and phenylalanine have unique spectral properties. They are the only amino acid residues in proteins which absorb





significantly in the near ultraviolet (250-350nm; for review see Wetlaufer, 1962) and they are the primary contributors to the intrinsic fluorescence of proteins (discussed in Cantor & Schimmel, 1980). As will be seen below, the limited number of aromatic residues in pilin suggested some simple experiments using difference spectroscopy and fluorescence measurements to examine the environments of tyrosine and tryptophan in the three forms of pilin. Since the complete sequence was available for strain PAK pilin, these studies were carried out using this strain.

The sequence of PAK pilin is shown in figure VIII.1 (updated from Sastry *et al.*, 1983). It can be seen that there are two tyrosines at position 24 and 27 and two tryptophans at position 54 and 127. The tyrosines are found in an extremely hydrophobic N-terminal stretch of 29 residues containing only one charged group, glutamic acid 5. Since octyl-glucoside breaks hydrophobic interactions, we hypothesized that octyl-glucoside binds in this region to disrupt subunit/subunit interactions. In fact it will be shown below that dissociation of pilin into dimers by octyl-glucoside results in exposure of tyrosine 24 and 27 and in partial exposure of at least one tryptophan residue. In addition, the region around tyrosine 24 and 27 appears to be utilized in the assembly of the reassembled pilin filaments.





5 10 15  
 N-Me-Phe-Thr-Leu-Ile-Glu-Leu-Met-Ile-Val-Val-Ala-Ile-Ile-Gly-Ile-  
 20 25 30  
 Leu-Ala-Ala-Ile-Ala-Ile-Pro-Gln-Tyr-Gln-Asn-Tyr-Val-Ala-Arg-  
 35 40 45  
 Ser-Glu-Gly-Ala-Ser-Ala-Leu-Ala-Ser-Val-Asn-Pro-Leu-Lys-Thr-  
 50 55 60  
 Thr-Val-Glu-Glu-Ala-Leu-Ser-Arg-Gly-Trp-Ser-Val-Lys-Ser-Gly-  
 65 70 75  
 Thr-Gly-Thr-Glu-Asp-Ala-Thr-Lys-Lys-Glu-Val-Pro-Leu-Gly-Val-  
 80 85 90  
 Ala-Ala-Asp-Ala-Asn-Lys-Leu-Gly-Thr-Ile-Ala-Leu-Lys-Pro-Asp-  
 95 100 105  
 Pro-Ala-Asp-Gly-Thr-Ala-Asp-Ile-Thr-Leu-Thr-Phe-Thr-Met-Gly-  
 110 115 120  
 Gly-Ala-Gly-Pro-Lys-Asn-Lys-Gly-Lys-Ile-Ile-Thr-Leu-Thr-Arg-  
 125 130 135  
 Thr-Ala-Ala-Asp-Gly-Leu-Trp-Lys-Cys-Thr-Ser-Asp-Gln-Asp-Glu-  
 140  
 Gln-Phe-Ile-Pro-Lys-Gly-Cys-Ser-Lys-COOH

Figure VIII.1. Primary structure of *Pseudomonas aeruginosa* PAK pilin (updated from Sastry *et al.*, 1983). The aromatic residues are underlined.



### A. Circular Dichroism

The far UV circular dichroism of the three forms of pilin assembly is shown in figure VIII.2. As has been demonstrated earlier (Chapter IV), the far UV CD of native pili and pilin/octyl-glucoside are indistinguishable. The far UV CD of reassembled pilin filaments, however, shows a slight enhancement of the ellipticity at 222nm. Previously (Chapter IV), the CD spectrum had been obtained only down to 200 nm for pilin. This data is extended to 190nm, allowing the application of a program for calculating secondary structure (Provencher & Glöckner, 1981) which uses the data in 1nm intervals from 190 to 240nm. The advantage of this program is that it includes the entire spectrum, while the more traditional approach (Chen *et al.*, 1972) uses the ellipticity values at 3 wavelengths only. Provencher and Glöckner emphasize the importance of including the region of the spectrum below 200nm, since it is the maximum at around 190-200nm that differs most between  $\alpha$ -helix and  $\beta$ -structure. Nevertheless, calculation of the amount of secondary structure for native pili and pilin/octyl-glucoside using this approach yielded values of 40%  $\alpha$ -helix and 38%  $\beta$ -structure in agreement with the previous calculations (Chapter IV). We calculate a 1% increase in apparent  $\alpha$ -helix and a 3% increase in  $\beta$ -structure for the reassembled pilin filaments. These results show that no gross changes in backbone conformation occur during the interconversion of the three forms of pili, so that changes in tyrosine and tryptophan



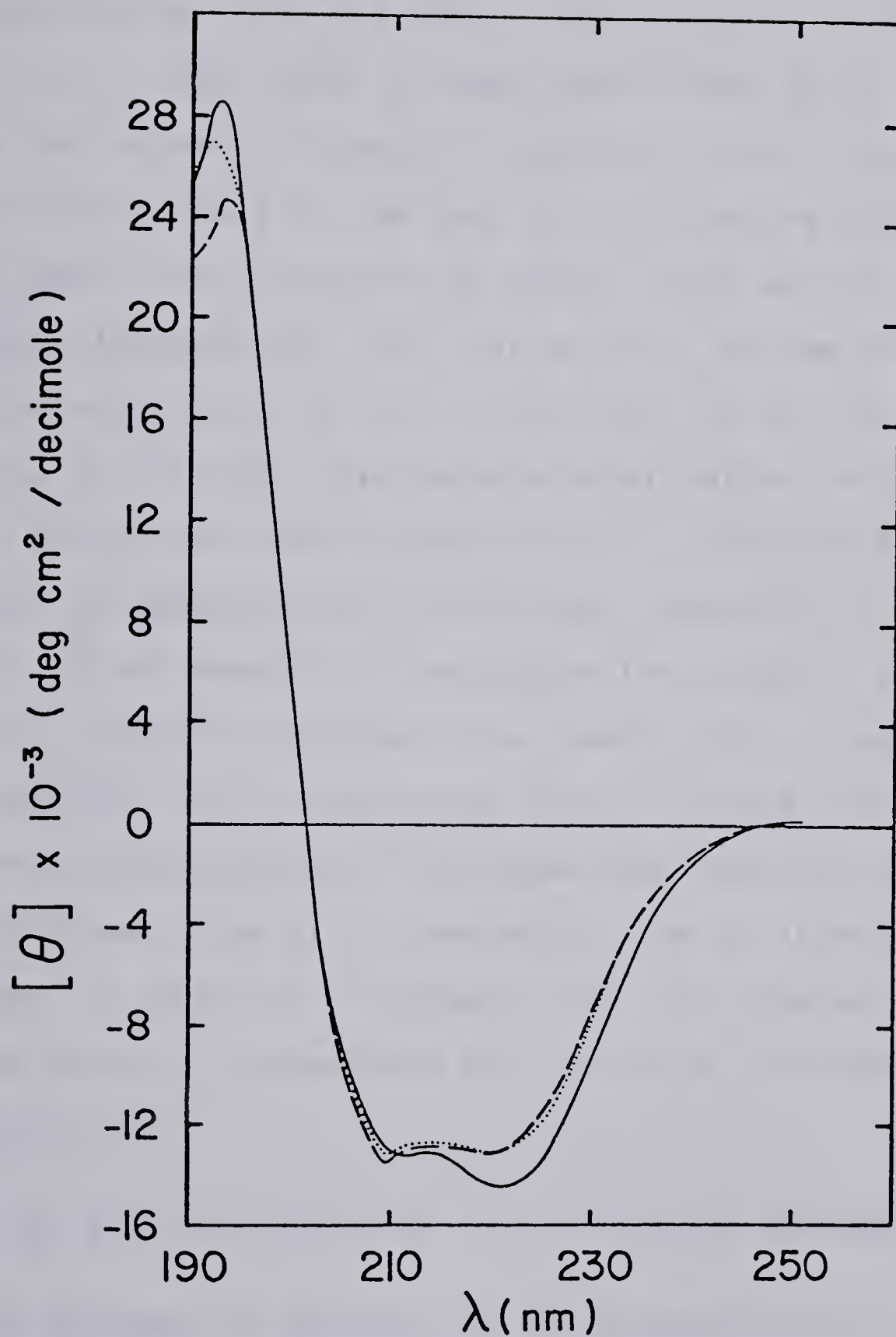


Figure VIII.2 Far UV circular dichroism of the three forms of pilin. (----)Native pili, (.....)pilin dimers in octyl-glucoside, (—) reassembled pilin filaments. Spectra were obtained as described in Materials and Methods. All samples were in 0.05M  $\text{Na}_2\text{PO}_4$  buffer pH 7.0.





accessibility can be attributed largely to dissociation rather than denaturation.

The near-UV CD of the three forms of pilin is shown in figure VIII.3. The noise in these spectra was quite high due to the low content of aromatic residues in pilin. However, one striking feature of the near UV CD of native pili at neutral pH is the intense CD at 297nm, which we attribute to tryptophan (Strickland, 1972). At pH 12.5, on the other hand, the ellipticity at 297 is the same for all three forms of pilin. At this pH, considerable denaturation has occurred (figure VIII.4) and some dissociation is indicated by a reduction in sedimentation coefficient (Chapter IV). At this point it is not possible to determine the cause of the unusually intense tryptophan CD at neutral pH in native pili. However, one can speculate that it arises from an interaction with another ring system that does not take place in dissociated pilin, perhaps across an intersubunit interface. In addition it appears that this interaction cannot take place in reassembled pili as it is not apparent in the near UV CD.

### *B. Alkaline pH Titration of Tyrosine Residues*

One approach to determining the accessibility of tyrosines in proteins is to examine the titration behaviour of the phenolic hydroxyl group (Donovan, 1964). The pK of this group may be altered if the hydrogen is involved in hydrogen bonding or if the tyrosine is buried in the protein



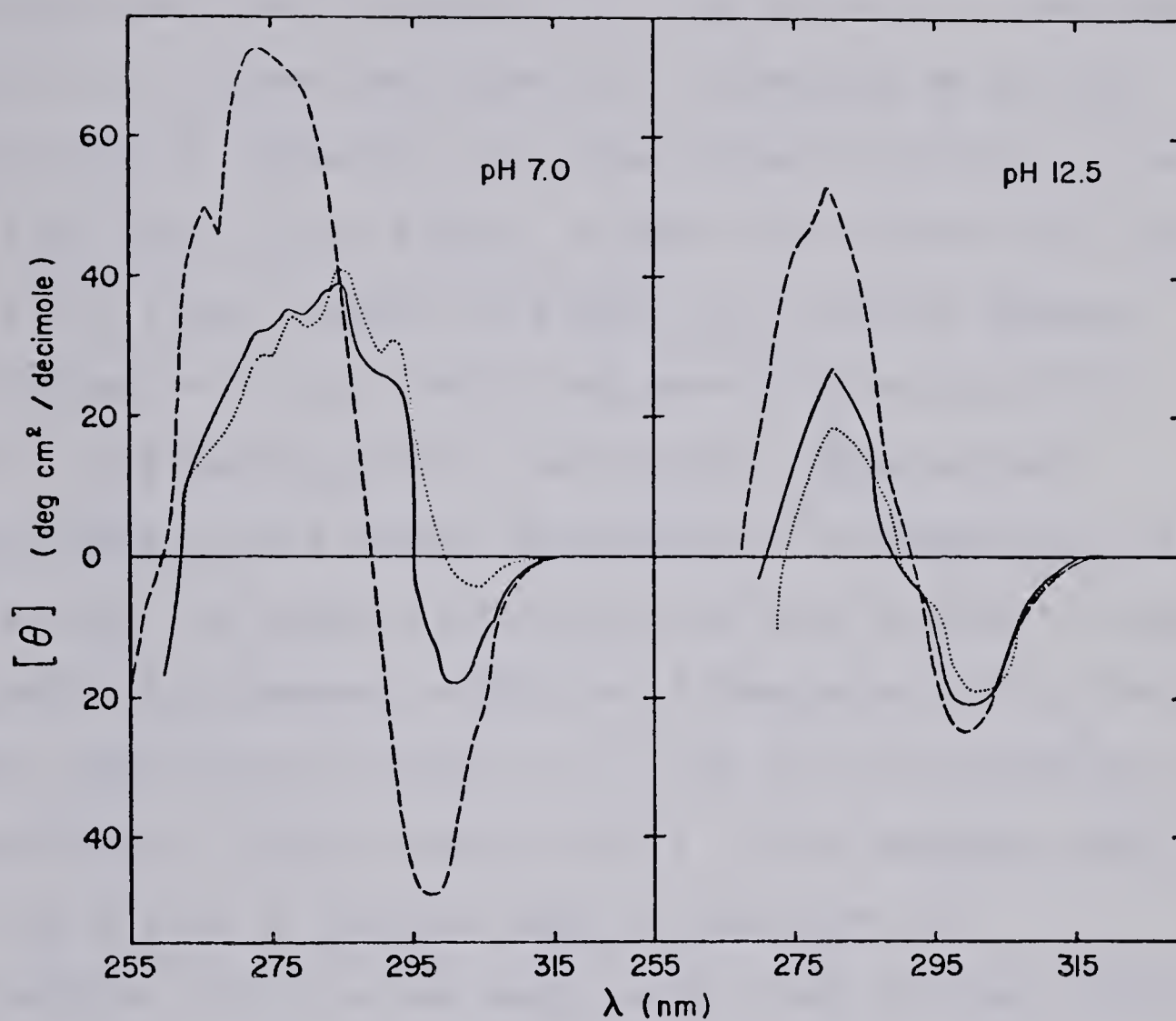


Figure VIII.3. Near UV circular dichroism of the 3 forms of pilin aggregate. (-----) Native pili, (——) pilin/octyl-glucoside, (.....) reassembled pilin filaments.



and thus shielded from hydroxyl ions (Herskovits, 1968). In the latter case one expects titration to occur only after some denaturation has occurred. It is therefore necessary to determine the alkali stability of the protein in question. Figure VIII.4 shows the effect of increasing pH on the ellipticity at 222nm for the three forms of pilin. It can be seen that very little effect is seen until about pH 11 and that all 3 forms respond to alkali in a similar manner. Neutralization of pili which has been treated at pH 13 results in regeneration of the original CD spectrum, suggesting that the alkali denaturation is reversible up to this point. The protein appears to be very stable to alkali treatment. Furthermore, addition of Guanidine.HCl to 5M or thermal denaturation result in a loss of only 20-50% of the ellipticity at 222nm (figure VIII.5). This suggests that there is a core of protein that is resistant to denaturation. This is not surprising since pili are extracellular proteins and therefore must be resistant to a varied environment. The only suggestion that native pili are more stable than the other two forms is offered by the thermal denaturation profile which shows a smaller effect for native pili than for the other two forms. Therefore it would seem that the unusual stability of pilin to a variety of conditions is largely due to the stability of the pilin dimer.

Figure VIII.6 shows the absorption spectrum of native PAK pili at pH 7 and 13.3. At the higher pH one notices the





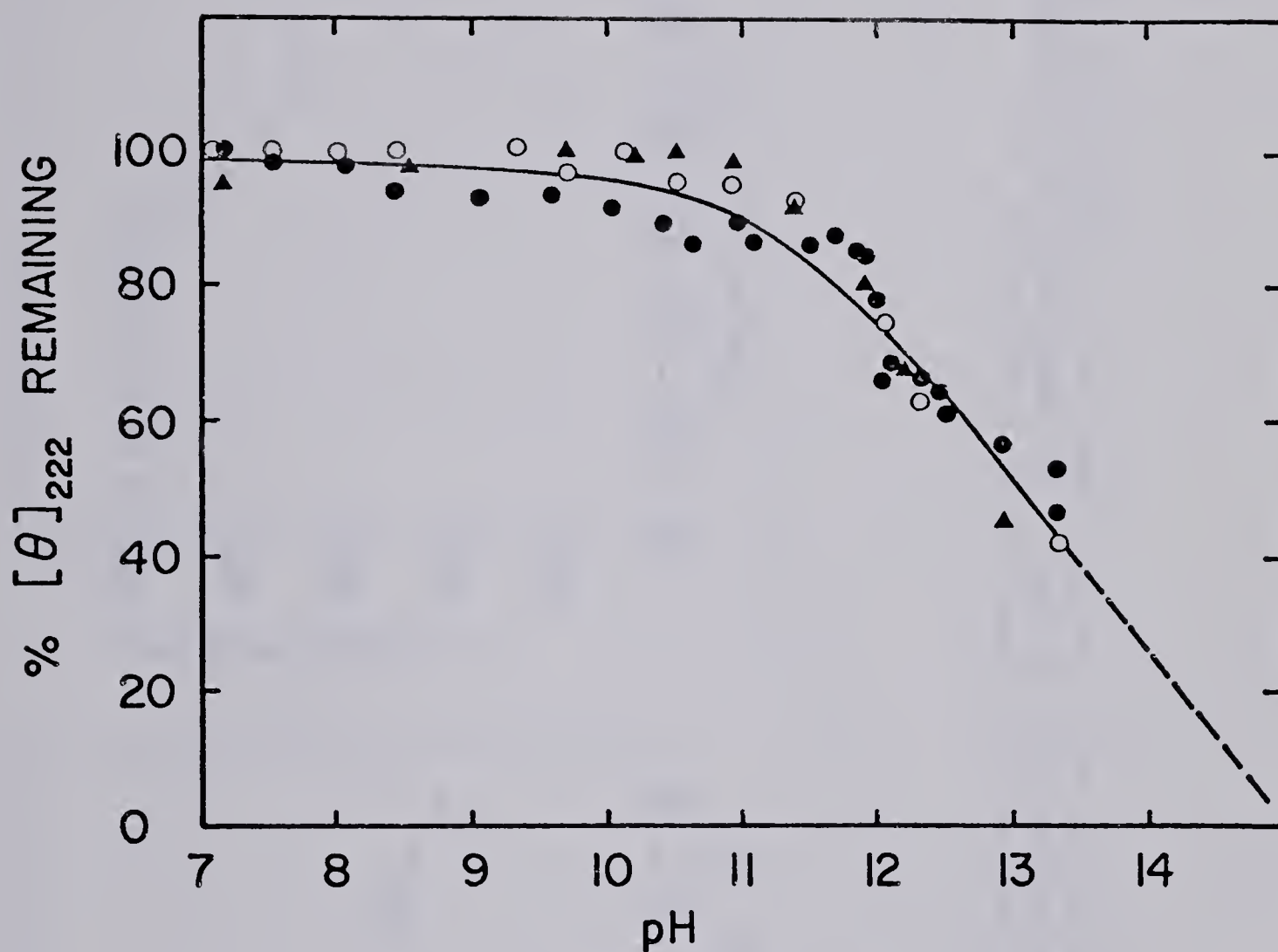


Figure VIII.4. Effect of alkali on  $[\theta]_{222}$  of three forms of pilin aggregate. ● Native pili; ○ pilin dimers in octyl-glucoside; ▲ reassembled pilin filaments. Samples were buffered using sodium phosphate or sodium bicarbonate.



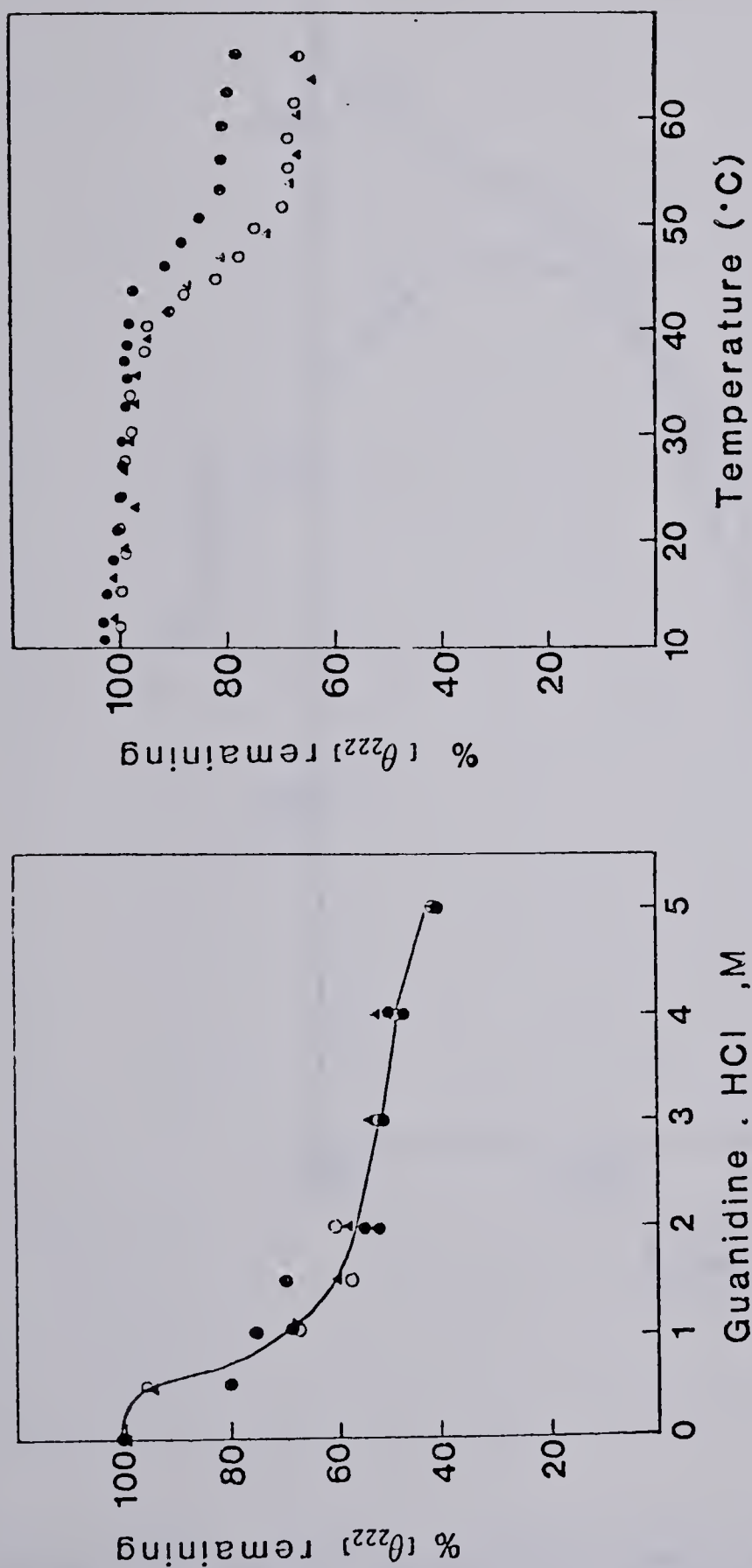


Figure VIII.5. Denaturation of three forms of pilin by guanidine-hydrochloride and by heat, as monitored by circular dichroism. The symbols used are the same as in figure VIII.4.



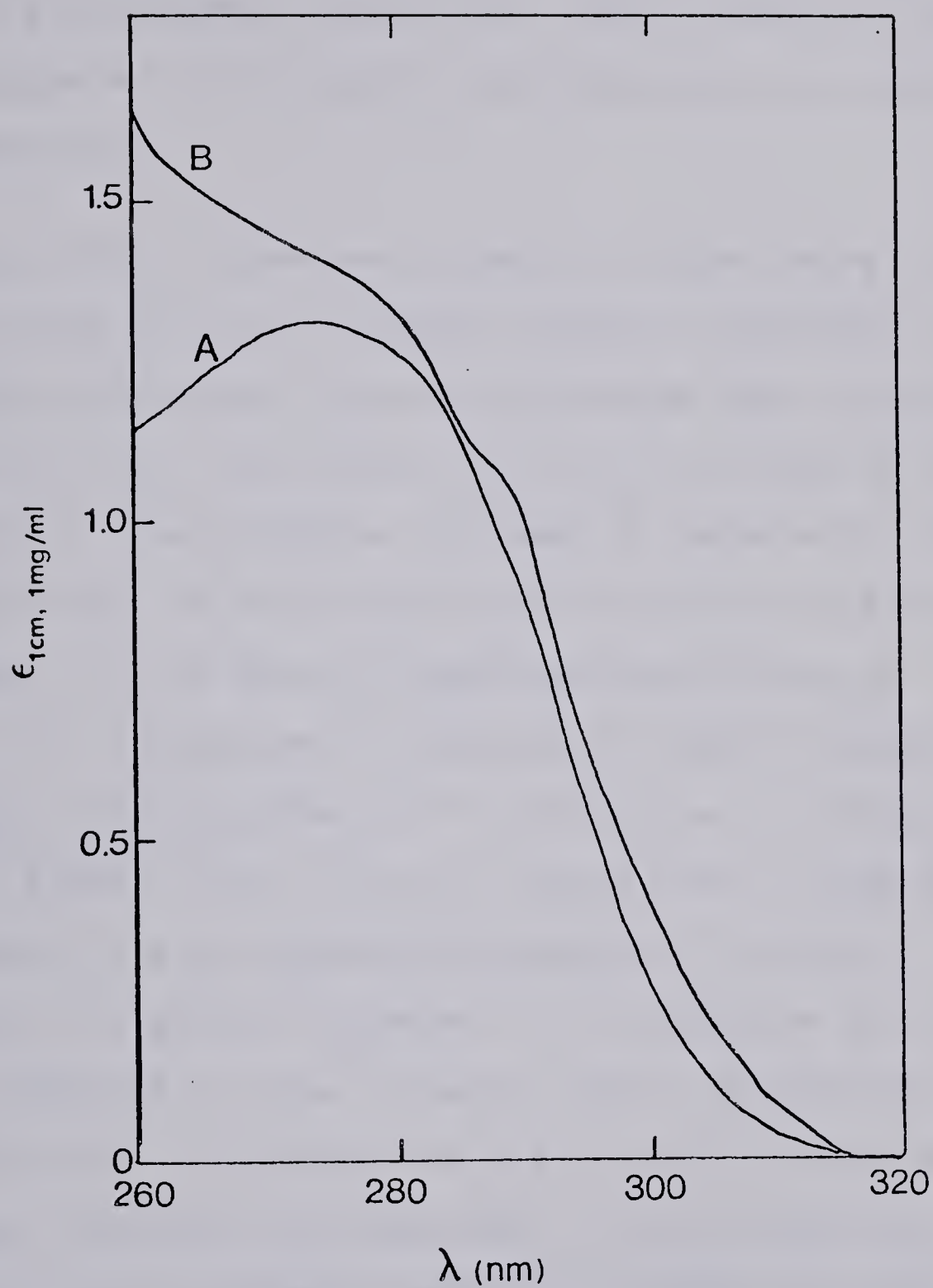


Figure VIII.6. UV absorption spectrum of native pili at A. pH 7.0 and B. pH 13.3 in phosphate buffer.





appearance of a shoulder at 290nm. With free tyrosine ionization of the hydroxyl usually results in the appearance of a peak at 293-295nm (Herskovits, 1968). Therefore the maximum appears to be slightly blue shifted in the case of *Pseudomonas pili*.

Figure VIII.7 shows the titration of the three forms of pilin followed by monitoring the change in absorbance at 290nm. The pilin dimers in octyl-glucoside show a titration with a pK of 9.9,. This value is within the range of values published for free tyrosine (reviewed in Herskovits, 1968), suggesting that the tyrosines are on the surface of the pilin dimer. If one uses the published extinction coefficient for ionization of tyrosine of  $2300\text{M}^{-1}$  (Herskovits, 1968), one calculates that 1.97 tyrosines are titrating in the pilin dimers. This titration occurs over a range of 2 pH units, which is not unreasonably broad for a single transition in a protein. However, it is possible that there are two components to the titration due to differences between the pK's of tyrosine 24 and 27, but if these differences exist they are not resolvable in this experiment. Thus it appears that tyrosine 24 and 27 are indistinguishable with respect to titration behaviour in the case of the pilin dimers in octyl-glucoside.

In the case of reassembled pilin filaments and native pili, the titration was not completed by pH 13. The change in molar extinction coefficient for the transition suggests



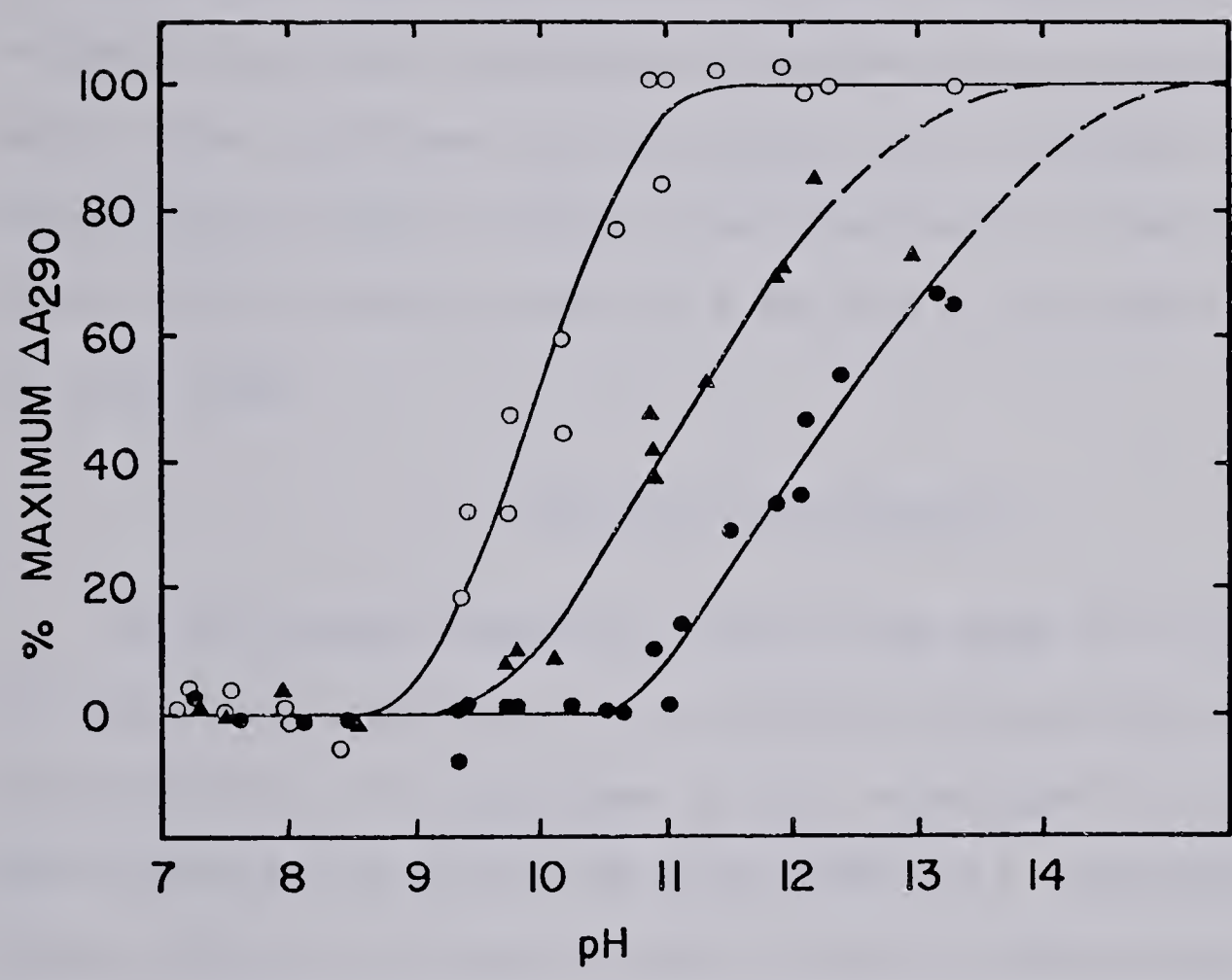


Figure VIII.7. Alkaline pH titration of pili. ● Native pili; ○ pilin dimers in octyl-glucoside; ▲ re-assembled pilin filaments (see Materials and Methods for details).



that 1.3 tyrosines have been titrated by pH 13.3 in native pili, while 1.4 tyrosines have been titrated in reassembled pili. By extrapolation to the full change of  $4600\text{M}^{-1}$  for the ionization of two tyrosines, one obtains a pK of 11.0 for the tyrosines in the reassembled pilin filaments and a pK of 11.9 for the tyrosines in native pili. Therefore it is evident that some denaturation/dissociation must occur before the tyrosines are accessible for titration in the filamentous forms of pilin. The broadness of the transition, which occurs over a range of 3 pH units, is also indicative of this fact.

### *C. Solvent Perturbation*

An alternate approach that can be used to look at tyrosine accessibility and to obtain information on the accessibility of tryptophan is the technique of solvent perturbation (as described by Herskovits & Laskowski, 1962a). This technique is based upon the observation that the absorption spectra of tyrosine and tryptophan residues on the surface of proteins are sensitive to changes in solvent composition, while tyrosines and tryptophans which are buried in proteins are insensitive to these changes, provided that the perturbant does not damage the protein in any way. Figure VIII.8 shows the perturbation spectrum of the three forms of pilin with 20% DMSO compared with the effect of DMSO on a 1:1 molar ratio of N-acetyl-tryptophan and N-acetyl-tyrosine ethyl esters in octyl-glucoside. DMSO does





not change the morphology of pili or reassembled pilin filaments as determined by electron microscopy (not shown). It was not possible however, to obtain CD data below 230nm with DMSO present. Nevertheless, DMSO is commonly used in this type of experiment because it causes a reasonably large perturbation without damaging protein structure (Herskovits & Laskowski 1962a&b). Curve C in figure VIII.8 shows the difference spectrum obtained for the pilin dimers in octyl-glucoside. The difference spectrum is blue shifted with respect to the model compound spectrum, as was the case in the alkaline difference spectrum. If one solves two equations in two unknowns (as described in Herskovits, 1968) for the contribution of tyrosine and tryptophan to each of the two maxima, using the extinction coefficients obtained for the model compounds in octyl-glucoside and DMSO one can calculate that 1.4 tyrosines and 0.9 tryptophans are fully exposed as compared to the model compounds. This could also be interpreted as two tyrosines 70% exposed and two tryptophans 45% exposed.

Curve A and B show the effect of DMSO on native pili and reassembled pilin filaments, respectively. It appears that the major effect here is a scattering effect. Pili being rather asymmetric tend to scatter light. In addition they have a tendency to aggregate along their long axis (see Chapter III & VI). If DMSO decreased or increased the aggregation of the particles, then the difference spectrum on exposing pili to DMSO would indicate this scattering. If



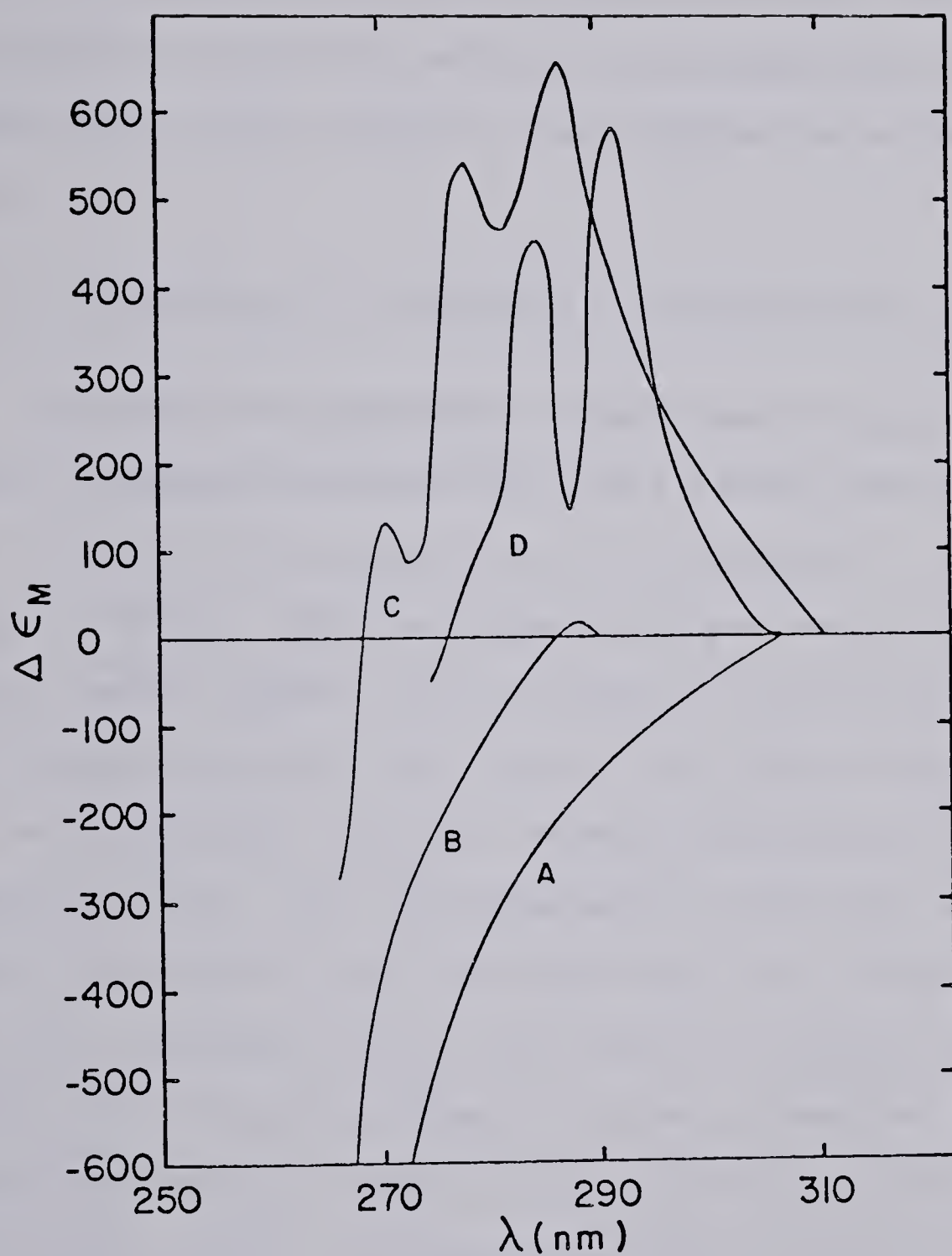


Figure VIII.8. Solvent perturbation of pili with 20% DMSO A. Native pili, B. Reassembled pilin filaments, C. Pilin dimers in octyl-glucoside, D. 1:1 molar ratio of N-acetyl-tryptophan and N-acetyl-tyrosine ethyl esters in octyl-glucoside.



tyrosines or tryptophans in pili or reassembled pilin filaments are perturbed by DMSO, the effect appears to be much smaller than in the pilin dimers as it is not visible above the scattering. It should be mentioned that it was not possible to judge from electron microscopy whether or not there was a large change in the aggregation state of the pili.

#### *D. Quenching of Tryptophan Fluorescence by Acrylamide*

An additional approach we have used to gain information about tryptophan accessibility is to study the quenching of the intrinsic fluorescence due to tryptophan as described by Lehrer (1971a). This technique involves the use of low molecular weight agents which decrease fluorescence intensity by physical contact with the excited indole ring. Therefore buried tryptophan residues, being inaccessible to the quenching agent, are not expected to experience any effect. Lehrer originally used the iodide ion as a quenching agent. However, problems due to electrostatic interactions of iodide with charged groups on proteins sometimes lead to anomalous results (Lehrer, 1971b). For this reason, Eftink and Ghiron (1976) introduced the use of acrylamide as a quenching agent. Since the sequence of PAK pilin shows that both tryptophans are in close proximity to lysine residues, acrylamide was chosen as the quenching agent for these studies. The excitation wavelength used was 295nm so that only tryptophan fluoresces. The emission maxima obtained





were as follows: L-tryptophan, 347nm; L-tryptophan in octyl-glucoside, 343 nm; native pili, 336nm, pilin in octyl-glucoside, 333nm. Thus octyl-glucoside causes a slight blue shift in the emission maximum of both pili and free tryptophan. The shift in fluorescence maximum for pili compared to free tryptophan is suggestive of a more hydrophobic environment. Upon dissociation of pilin by octyl-glucoside, the fluorescence maximum shifts by 3nm. However, the same shift was observed when octyl-glucoside was added to free tryptophan, suggesting that no additional effect besides the direct detergent effect is taking place.

The effect of acrylamide on tryptophan fluorescence of free tryptophan, native pili, pilin/octyl-glucoside and tryptophan in octyl-glucoside is shown in figure VIII.9. Plotted is the term  $F_0/F$ , where  $F_0$  and  $F$  are, respectively, the relative fluorescence intensities in the absence and presence of quencher after correction for dilution with acrylamide. The upward curvature observed for the acrylamide quenching of the fluorescence of free tryptophan has been attributed to a static quenching component (Eftink & Ghiron, 1976). This upward curvature is also observed for single tryptophan-containing proteins, while the plots are usually linear or show downward curvature for multi-component quenching. Comparison of the curves for native pili and pilin/octyl-glucoside suggest that at least one of the tryptophans in pili becomes more accessible to acrylamide upon dissociation into dimers. However, comparison with the



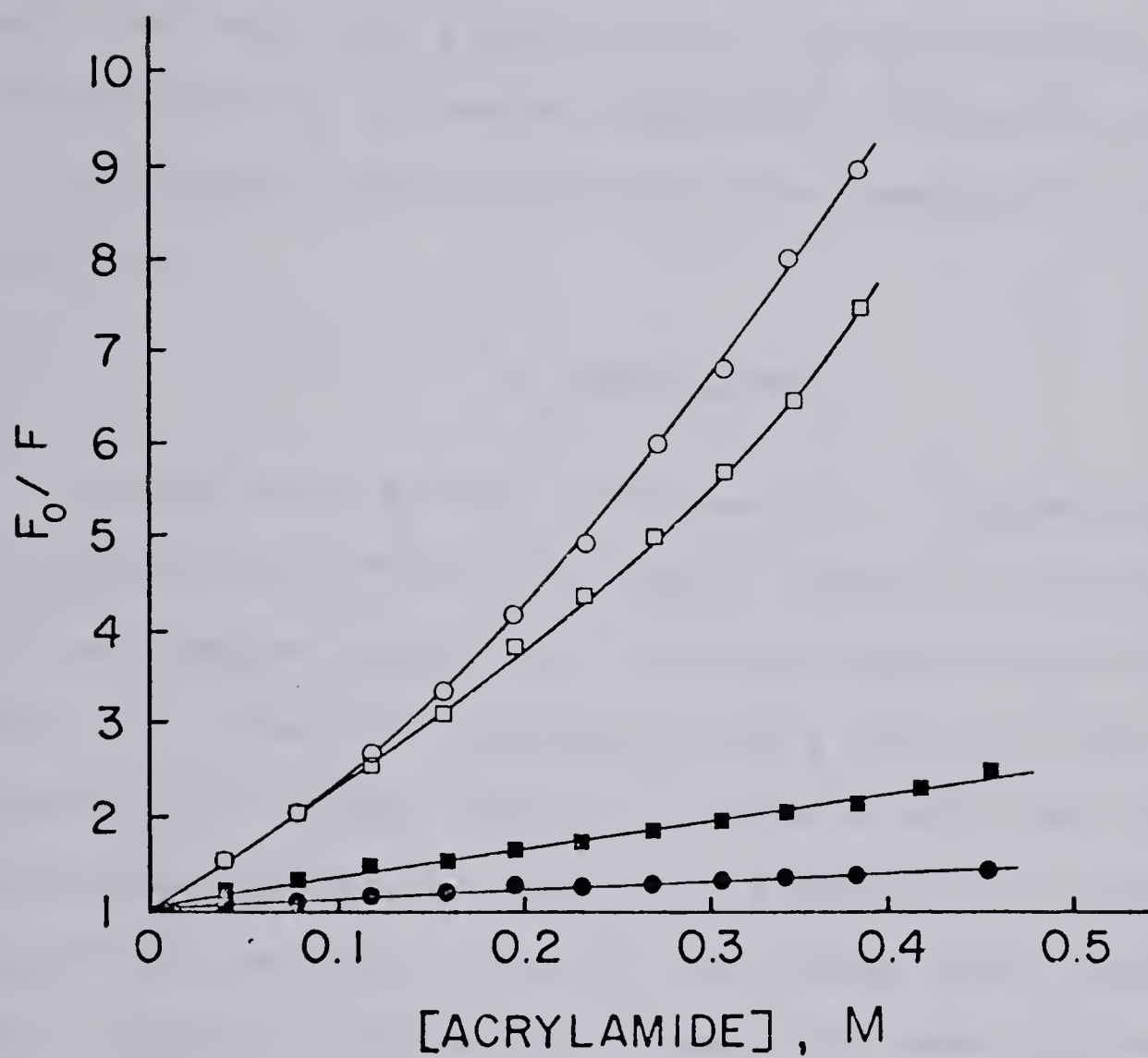


Figure VIII.9. Acrylamide quenching of tryptophan fluorescence in pili. ○ L-tryptophan; ● native pili; □ L-tryptophan in octyl-glucoside; ■ pilin dimers in octyl-glucoside.



effect of acrylamide on free tryptophan suggests that the effect is less than that expected if a tryptophan were fully exposed to the medium. Since the quenching effect is quite small for both native pili and for the pilin dimers in octyl-glucoside, it was not possible to deduce by curve fitting whether there were one or two components to the quenching.

### *E. Conclusions*

On the basis of the above results, it appears that tyrosine 24 and 27 are at a subunit/subunit interface in pili and become exposed to the medium upon dissociation of pilin into dimers by octyl-glucoside. The fact that the two tyrosines are close together in sequence and that they are indistinguishable with respect to alkaline pH titration simplifies the data, since one can assume that tyrosine 24 and 27 occupy a similar environment and hence can be treated as one residue. The unusually high  $pK$  of the tyrosines in native pili is attributed to their being buried at the subunit interface. An additional factor may be that the tyrosines are stacked either with each other (this is possible if they are at position  $n$  and  $n+3$  of an  $\alpha$ -helix) or that they interact with another aromatic ring across the subunit interface. It is possible that the region around residue 24-27 interacts with an alternate region of pilin in making dimer/dimer contact. This possibility is shown schematically in figure VIII.10A which shows the surface lattice representation of the pilus model that was presented





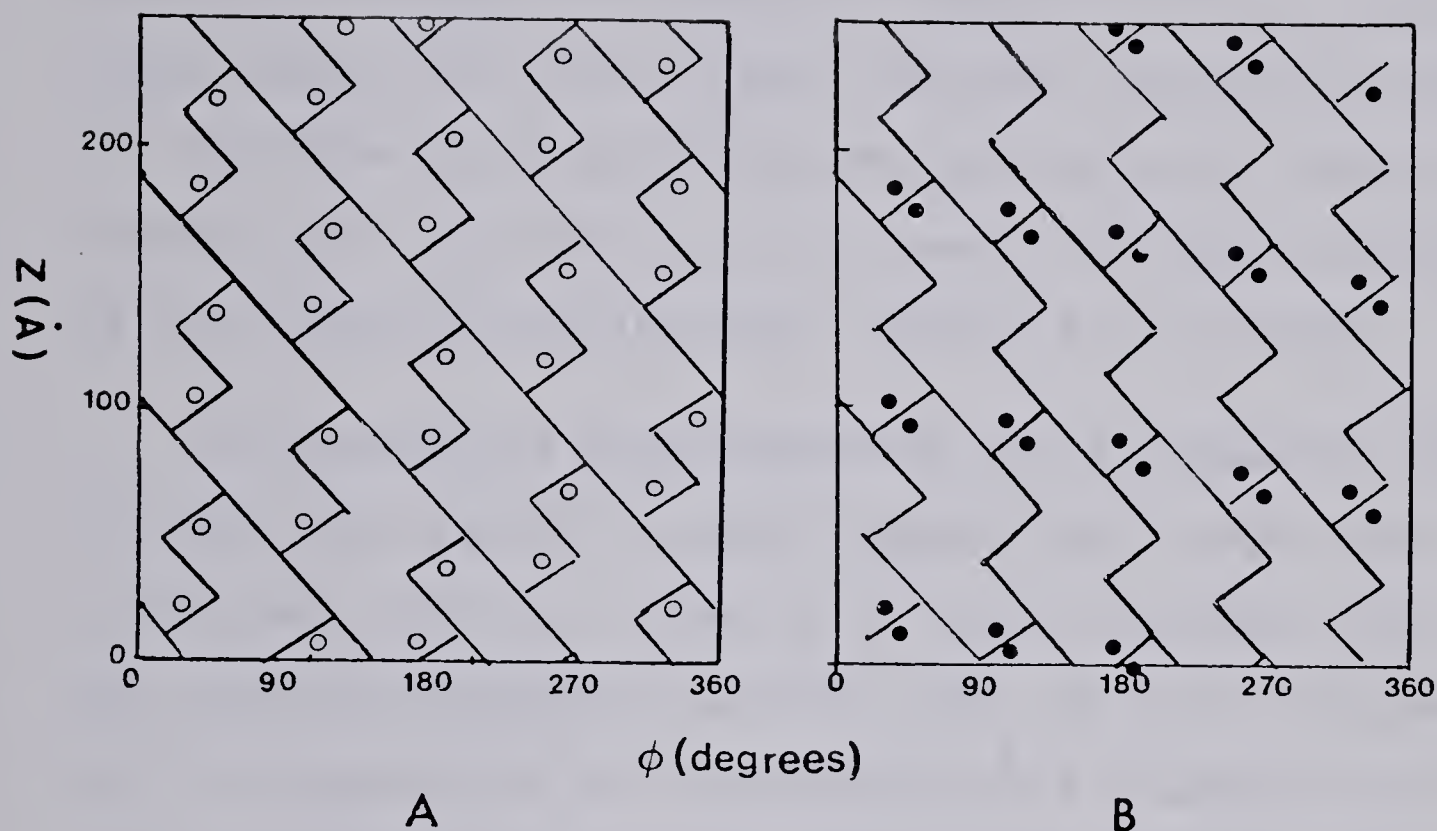


Figure VIII.10. Schematic representation of two possible packing arrangements of pilin dimers in which all the tyrosines (each pair is represented by a single circle) are exposed upon dissociation in octyl-glucoside. The solid lines represent interactions between dimers that are broken in octyl-glucoside. The surface lattice representation has been described in Chapter V. A. A head to tail packing arrangement, B. A head to head packing arrangement with respect to tyrosines. The sub-unit arrangement is the same as that shown in figure V.19.



in chapter V (figure V.19). On the other hand, the region containing the two tyrosines might interact with the same region on another pilin subunit forming a head to head packing arrangement as shown in figure VIII.10B. In both these figures all solid lines represent interactions that are disrupted in octyl-glucoside, leaving pilin dimers and exposing all tyrosines. In both cases, the symmetry dictated by the X-ray diffraction data (Chapter V) is obeyed.

In the case of the reassembled pilin filaments, the alkaline pH titration results suggest that roughly the same interface around tyr 24 and 27 is used in assembly but that the packing arrangement is less tight. This is in agreement with the appearance of reassembled pilin filaments in the electron microscope (Chapter VI). It should be noted, however, that in an assembly such as pili, one would expect a large portion of each subunit to be interacting with other pilin subunits, so that the hydrophobic region around tyrosine 24 and 27 is not sufficient to account for pilus assembly.

Our results are less conclusive for tryptophan residues. It appears that both tryptophans are buried in native pili and that dissociation into dimers results in increased exposure of at least one tryptophan. With reassembled pilin filaments it appears that at least one tryptophan occupies a different environment than its counterpart in native pili or pilin dimers.



## CHAPTER IX

### Mapping of the Antigenic Determinants of PAK Pilin

Two broad classes of antigenic determinants have been identified in proteins. These are sequential antigenic determinants and conformational antigenic determinants (Sela *et al.*, 1967; Sela, 1969). Sequential antigenic determinants (5 of which have been identified on the surface of sperm whale myoglobin; Atassi, 1975) are found in contiguous stretches of the polypeptide chain, so that it is possible to obtain proteolytic fragments of the protein that are capable of reacting with antibodies. In conformational antigenic determinants, on the other hand, the amino acids contributing to the antibody combining site do not occur in a linear sequence but are found in spacial proximity due to the folding of the polypeptide chain. In order to delineate this type of antigenic site, it is necessary to use techniques such as specific chemical modification or to study homologous series of proteins in order to identify antigenically important residues. Using these approaches, three such sites were identified on hen egg white lysozyme (Atassi and Lee, 1978).

In Chapter III, the antigenicity of PAK pili and its cross-reactivity with PAO pili and with gonococcal pili was demonstrated. In order to delineate, in part, the antigenic regions of pilin, proteolytic fragments of the protein were prepared and tested for their ability to react with





anti-pilus antibodies in the ELISA and 'immunoblot' procedures (described in Materials and Methods and in Chapter III). This approach was made possible by the elucidation of the amino acid sequence of PAK pilin and by the developement of procedures for preparing homogeneous proteolytic fragments of pilin which arose from this work (Sastry *et al.*, 1983).

Since antigenic determinants are generally located on the surface of proteins (Atassi, 1975; Atassi & Lee, 1978; Van Regenmortel, 1982), this approach should prove useful in identifying surface exposed regions of the polypeptide chain. Furthermore, these studies are potentially useful in identifying antigenic peptides which could be tested for their ability to generate antibodies which bind to whole pili to block the attachment process.

#### *A. Immuno-electrophoresis of Pili*

In order to determine whether one or several antigenic sites were responsible for the antigenicity of pilin, purified PAK pili were subjected to counter-immuno-electrophoresis and rocket-immuno-electrophoresis as described in Materials and Methods. The principles of immuno-electrophoresis have been reviewed by Oudin (1980). In counter-immuno-electrophoresis (electroendoosmosis) two wells are cut at opposite ends of an agarose gel and the antiserum is placed in the well nearest the anode, while the antigen is placed in the well nearest the cathode. The experiment is



carried out at a pH close to pH 8.3, where the immunoglobulins are neutral or carry a slight positive charge. The technique is only useful for antigens which are negatively charged at pH 8.3. During electrophoresis, the antigens migrate toward the anode while the antibodies migrate toward the cathode, primarily due to the phenomenon of electroendosmosis. Electroendosmosis is the flow of the bulk liquid of the gel in a direction opposite to that of the electric current. The technique operates under the same principles as double-immunodiffusion in agar (Ouchterlony, 1948) except that the appearance of precipitation zones occurs over a shorter period of time. In rocket immunoelectrophoresis, the antigen is also placed toward the cathode but the antiserum is present throughout a second gel, placed closest to the anode. In both these techniques, precipitation occurs due to the multivalency of immunoglobulins and, in the case of pili, due to the multivalency of the protein polymer. Initially, soluble antibody-antigen complexes form as the two species migrate towards each other in the gel. These then become cross-linked to form a lattice which gradually expands into a visible precipitate. The stoichiometry of the antibody to antigen is usually varied in order to maximize the precipitation reaction.

It can be seen in figure IX.1 that a least 3 PAK pilin-anti-pilus antibody precipitin lines are evident using both methods. The occurrence of multiple precipitin lines can be attributed to several causes (reviewed in Oudin, 1980).



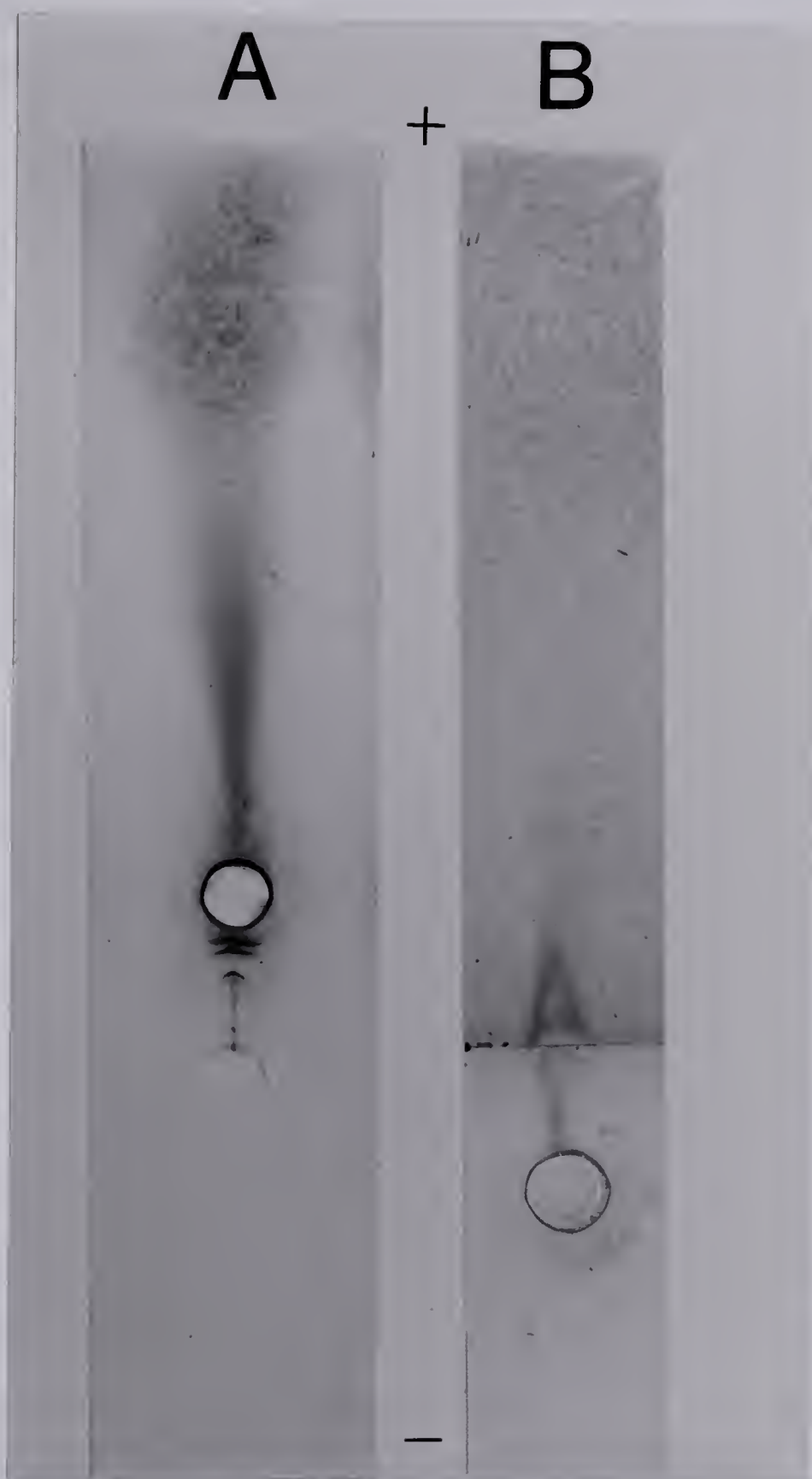


Figure IX.1. Immunoelectrophoresis of PAK pili:  
A. Counter-immunoelectrophoresis carried out for 16h at 3V/cm. B. Rocket immunoelectrophoresis carried out for 20h at 3V/cm. The upper gel contained 5% v/v anti-PAK pilus antisera.





The presence of several antigenic species of the protein, the presence of more than one class of immunoglobulin against the antigen (ie. IgG, IgM etc.) and the presence of multiple antigenic determinants within a single antigenic protein, each could give rise to multiple precipitation zones. This occurs because each antibody-antigen interaction has a specific dissociation constant ( $K_d$ ) associated with it. Therefore, the concentration of antigen and antibody required to form a precipitation zone and therefore the position in the gel of the precipitation zone are dependent on this  $K_d$ .

Since pilin has been shown to be immunologically homogeneous by the technique of immunoblotting (Chapter III), the multiple precipitin lines observed in figure 1 are most likely due to the presence of 3 kinds of antibodies against pili in the rabbit anti-pilus antiserum. As mentioned above, these could be due to the presence of immunoglobulins of more than one class reacting with a single type of antigenic site, or due to the presence of antibodies against multiple antigenic sites in the protein. In light of the results presented below, we favour the latter explanation. Since these techniques are fairly limited in resolution, this represents the minimum number of antigenic sites that one expects to find in pilin.



*B. Preparation of Proteolytic Fragments of PAK pilin.*

The sequence of PAK pilin was shown in figure VIII.1. It can be seen that there are three arginine residues at positions 30, 53 and 120, which conveniently divide the protein into 4 regions. Therefore arginine-specific cleavage was used to generate the four fragments TCI (residue 1-30), TCII (residue 31-53), TCIII (residue 54-120) and TCIV (residue 121-144). Arginine-specific cleavage was accomplished by modification of the 12 lysines in pilin with citraconic anhydride (Gibbons & Perham, 1970) followed by trypsin digestion as described in Materials and Methods.

TCI which encompasses the extremely hydrophobic N-terminus of pilin, was found largely in the insoluble pellet, obtained after centrifugation of the tryptic digest. This material could be solublized in the detergent octyl-glucoside and further purified on Sephadex G75 in the presence of octyl-glucoside (figure IX.2A). The fact that residue 1-30 is soluble in octyl-glucoside is not surprising since octyl-glucoside has been shown to bind to pilin, with the result that tyrosines 24 and 27 become exposed (Chapter IV and VIII). The major peak obtained on G75 elutes at an apparent molecular weight of 33,000 and consists of aggregated TCI plus bound detergent. After removal of detergent, the preparation consisted of pure TCI (see Materials and Methods).



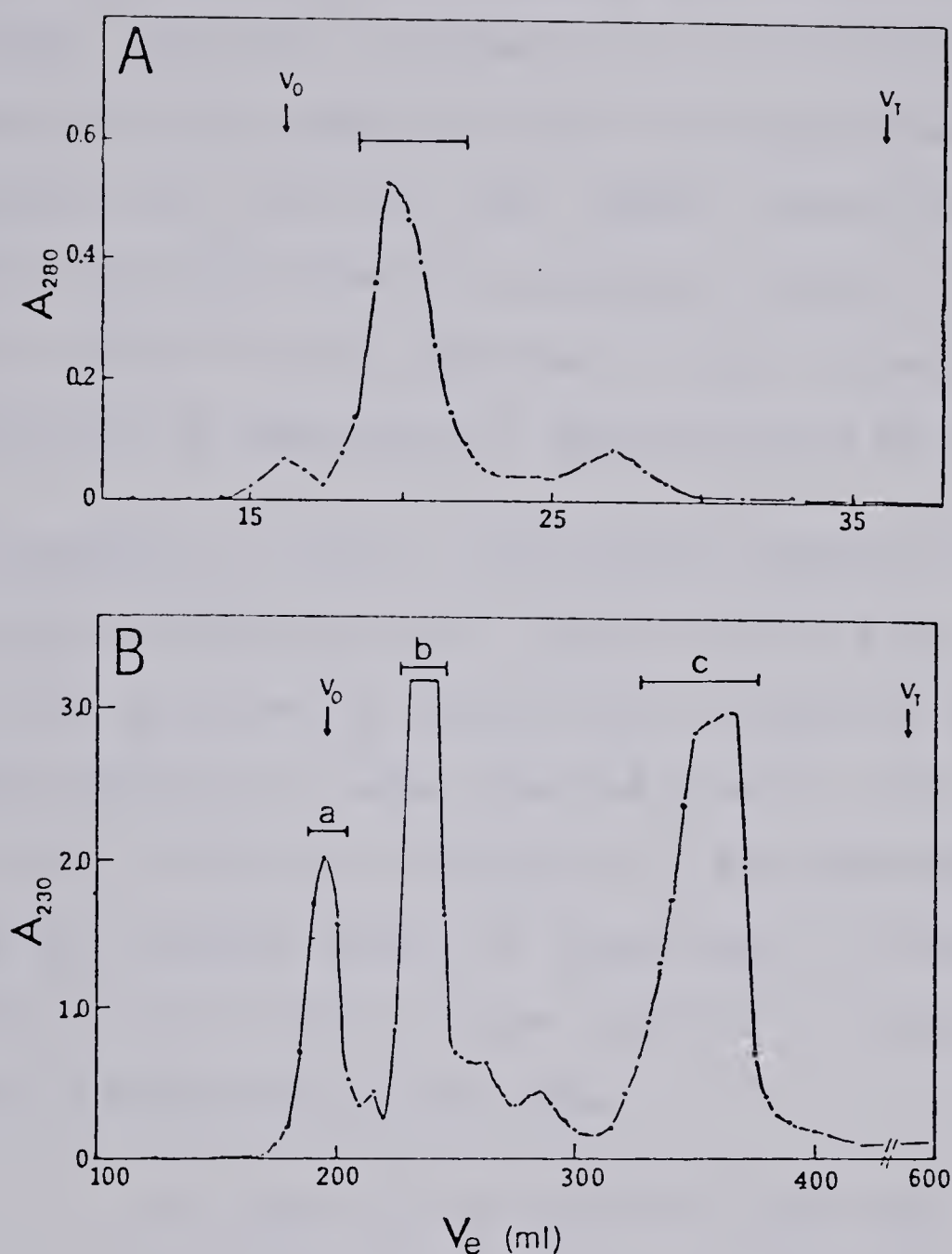


Figure IX.2. Chromatography of trypsin-treated citraconylated pili.

A. Purification of TCI from the TC-insoluble pellet on a G75 column (1x40cm) equilibrated with 30mM octyl-glucoside.

B. Separation of TC-soluble peptides on Sephadex G50 (2.5x120cm) in 0.1M  $\text{NH}_4\text{HCO}_3$ , pH 8.1. The bars indicate the pooled regions. a is TCI; b is TCIII; c is a mixture of TCII and TCIV.





The trypsin-soluble citraconylated material was initially fractionated on a Sephadex G50 column as shown in figure IX.2B. Some TCI is present in the TC-soluble material and elutes as an aggregate at the void volume (peak a). Peak b was found to be pure TCIII ( $M_r = 6800$ ), while peak c consisted of an approximately equimolar mixture of TCII and TCIV. TCII and TCIV were separated by high voltage paper electrophoresis as described in Materials and Methods.

Subfragments of TCIII, obtained by digestion of the decitraconylated peptide with trypsin, as well as a subfragment of TCIV, prepared by chymotryptic digestion of carboxymethylated whole pili, were obtained from Dr. P.A. Sastry. The positions in the pilin sequence of the peptides which were used for further study are summarized in figure IX.3 c and d. The purity of each of the peptides was assessed as described in Materials and Methods.

### *C. Antigenicity of PAK Pilin Peptides*

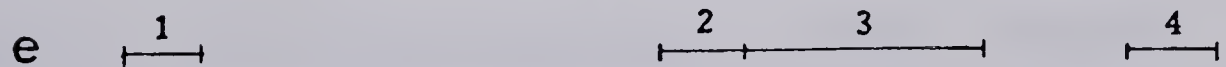
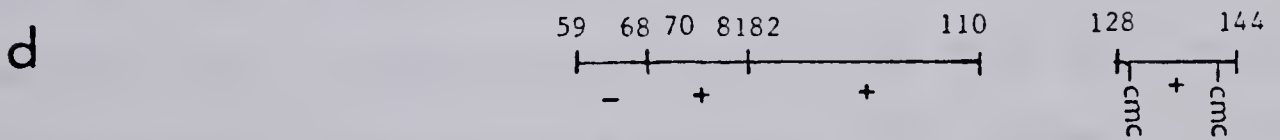
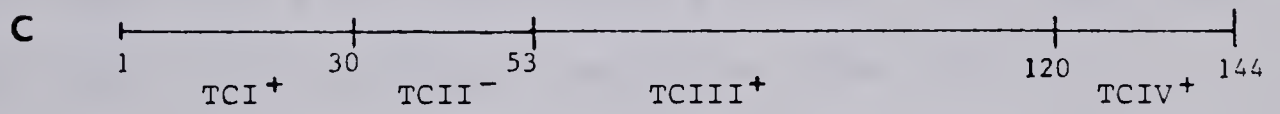
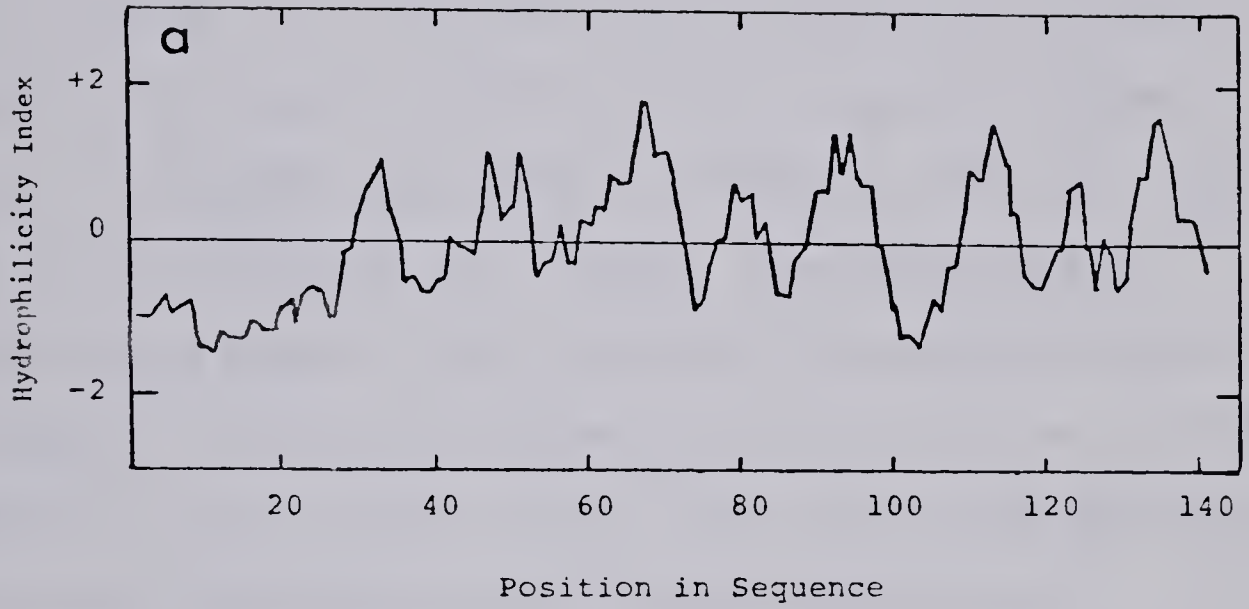
The proteolytic fragments of PAK pilin, described above, were tested for their ability to react with rabbit anti-pilus antiserum in an ELISA and in an 'immunoblot' experiment. Both TCI (which exists as an aggregate in aqueous media) and TCIII are sufficiently large to be used directly in these assays. The remaining peptides were chemically cross-linked through their primary amino groups to bovine serum albumin (BSA) using the N-hydroxy-succinimide ester of 4-azido benzoic acid (as described by Worobec



The first part of the paper is devoted to a general  
 introduction of the subject. It is then divided into  
 three main sections. The first section is devoted to  
 the study of the properties of the function  $f(x)$ . The  
 second section is devoted to the study of the  
 properties of the function  $g(x)$ . The third section  
 is devoted to the study of the properties of the  
 function  $h(x)$ . The paper concludes with a  
 summary of the results obtained.

Figure IX.3. Schematic representation of the locations of antigenic peptides in *Pseudomonas aeruginosa* PAK pilin.

- a. The hydrophilicity index calculated for pilin by the method of Hopp and Woods(1981), reproduced from Sastry *et al.* (1983).
- b. Schematic representation of the sequence of pilin. The buried tyrosines (24 and 27) and tryptophans (55 and 127) are indicated. The disulfide linkage between residue 129 and 142 is also shown.
- c. Map of the TC peptides of PAK pilin. (+) indicates a positive reaction with anti-PAK-pilus antisera, (-) indicates a negative reaction.
- d. Map of the smaller fragments of pilin that have been tested for antigenicity. CMC indicates that the disulfide linkages have been reduced and modified to form carboxymethyl-cysteine.
- e. Proposed antigenic determinants in pilin based on studies with peptide fragments, cross-reactivity studies and chemical modification. 1=residue 1-9; 2 and 3 are the same as the peptides in figure IX.3d, 4=residue 130-141.







*et al.*, 1983 and in Materials and Methods). The resulting molar ratios of peptide to BSA were  $2 \pm 1:1$  for all 6 peptides.

The results of the ELISA assay for PAK pili and its proteolytic fragments versus anti-PAK-pilus antiserum are shown in figure IX.4. The wells of the microtiter plates are saturated with respect to PAK pili at a coating concentration of 4-5  $\mu\text{g/ml}$  (not shown), therefore PAK pili was used at a concentration of 5  $\mu\text{g/ml}$ . The peptides and BSA-peptide conjugates were coated at a concentration of 1-1.5  $\text{nmol/ml}$ . Increasing these concentrations two-fold did not result in an increase in  $A_{405}$  for any of the peptides. BSA controls (not shown) gave no detectable  $A_{405}$ .

It can be seen that 3 of the 4 TC peptides show a positive reaction with anti-pilus antisera. The reaction with TCII-BSA was considered negative. The small  $A_{405}$  obtained with this peptide (5% of the reading for native pili) may be due to slight contamination of TCII with TCIV since the two peptides are very similar with respect to size and charge. Of the TCIII subfragments tested, residue (59-68) was negative, while residue (70-81) and residue (82-111) were positive.

As indicated in figure IX.3b, the two cysteines in pilin form an intra-chain disulfide bridge between residue 129 and 142 (Sastry, Pearlstone, Smillie & Paranchych, manuscript in preparation). The chymotryptic fragment



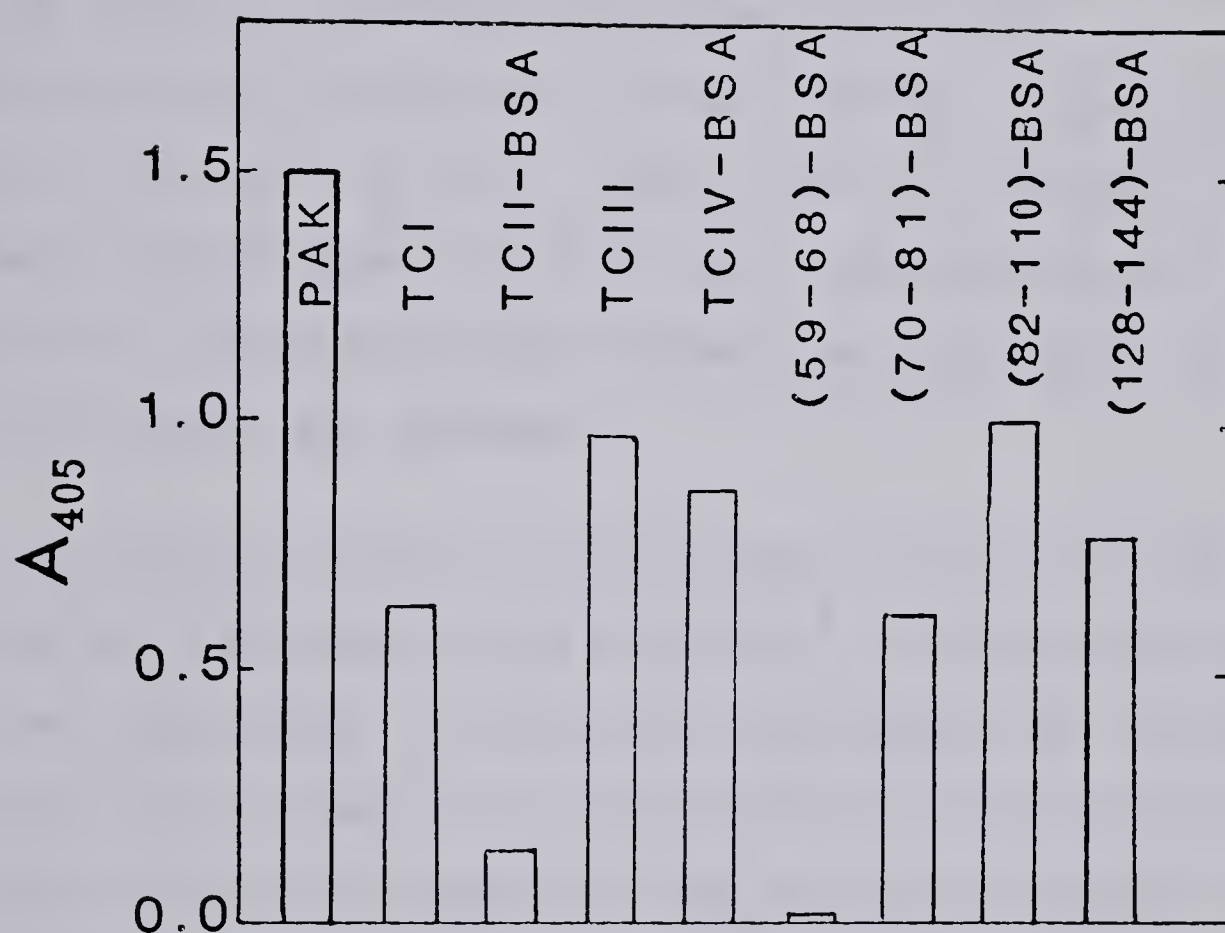


Figure IX.4. Elisa assay of PAK pilin and its peptide fragments with anti-PAK-pilus antisera. The results are shown for a 1:500 dilution of antisera. The location of the peptides in the sequence is diagrammed in figure 4. PAK indicates native PAK pili. Details are provided in the text.



(128-144) was derived from carboxymethylated pilin, and therefore the disulfide linkage has been reduced and the cysteines modified in this peptide. Since residue (128-144)-BSA gives a comparable reaction to TCIV-BSA in the ELISA assay, it appears that neither the disulfide linkage, nor the cysteine residues are important in the antigen-antibody interaction. This finding is contrary to those of Schoolnik *et al.*, (1982) with pili isolated from *Neisseria gonorrhoeae*. In this case, the antigenicity of a C-terminal cyanogen bromide fragment was lost when the disulfide linkage was reduced.

We obtained similar results when the peptides and the peptide-BSA conjugates were subjected to SDS-polyacrylamide gel electrophoresis, followed by electrophoretic transfer to nitrocellulose, reaction with anti-pilus antibodies and detection with  $^{125}\text{I}$ -Protein A. The results are shown for the TC-peptides of PAK pilin in figure IX.5. It can be seen that PAK pilin, TCI, TCIII and TCIV-BSA, but not TCII-BSA react with anti-pilus antisera in this assay.

We have therefore identified 4 antigenic regions in the PAK pilin subunit. These are residues 1-30, 70-81, 82-111 and 128-144, as summarized in figure IX.3. Figure IX.3a shows the hydrophilicity index calculated for pilin by the method of Hopp & Woods (1981). The hydrophilicity index is obtained by assigning a hydrophilicity value of between +3 and -3.4 to each amino acid in the sequence and then







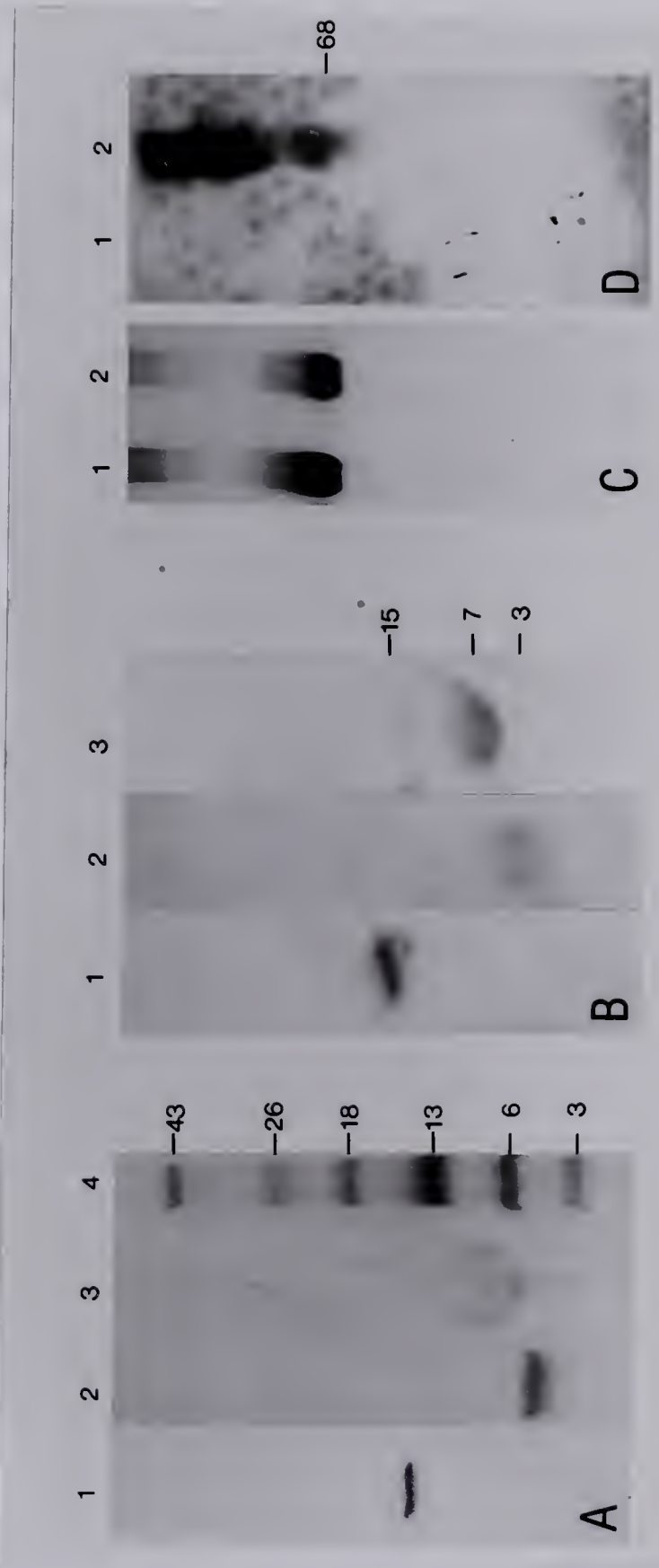
Figure IX.5. Polyacrylamide gel electrophoresis and transfer to nitrocellulose, followed by immunological detection of PAK pilin and its TC-peptides as described Materials and Methods.

*a.* 20% polyacrylamide gel stained with Coomassie blue. 1=PAK pilin; 2=TCI; 3=TCIII; 4=protein standards, with molecular weights as indicated in thousands.

*b.* Peptides from a duplicate gel to that in *a* were transferred to nitrocellulose and reacted with anti-pilus antiserum and  $^{125}\text{I}$ -Protein A. The lanes are the same as in *a*.

*c.* 10% polyacrylamide gel stained with Coomassie blue. 1=TCII-BSA; 2=TCIV-BSA.

*d.* Duplicate of the gel shown in *c*, after transfer of the peptide-BSA conjugates to nitrocellulose and immunological detection.





repetetively averaging these values in 6-amino acid segments along the polypeptide chain. Based on a study of 12 proteins for which extensive immunochemical data was available, Hopp and Woods have suggested that antigenic determinants on proteins are invariably found at, or immediately adjacent to, points of highest local hydrophilicity. Of the four antigenic peptides identified for PAK pilin, however, only two encompass peaks of hydrophilicity (residue 82-111 and residue 128-144). Residue 70-81, on the other hand, falls between two such peaks and TCI is found in the most hydrophobic region of the molecule.

As mentioned above, modification of the two cysteines in the C-terminal antigenic peptide does not appear to effect its antigenicity. Therefore we propose that the C-terminal antigenic site is contained within the region (130-141) as indicated in figure IX.3e, antigenic site 4. We further propose that the N-terminal antigenic determinant (located in TCI) is at the N-terminal end of TCI and includes N-methylphenylalanine, based upon the following rationale. Firstly, residue 24 and 27 have been shown to be buried in native pili (Chapter VIII). Since antigenic determinants are generally found on the surface of proteins, one would not expect to find an antigenic site at the C-terminal end of TCI. Secondly, the amino acid N-methylphenylalanine is a good candidate for an antigenic determinant due to its rare occurrence. Finally, (as was demonstrated in Chapter III) antibodies raised against PAK





pili cross-react with both PAO pili and with gonococcal pili. Since the region of highest sequence homology between these strains is found at residue 1-9, where the sequences are identical, this region is the most likely candidate for the common antigenic determinant. Also consistent with the data is the fact that tryptophan 55 and 127, which are buried in native pili (Chapter VIII), do not fall into any of the antigenic regions proposed above.

Of the four PAK-TC peptides, only TCI reacts with anti-PAO pilus antisera (figure IX.6). However, the cross-reactivity observed with TCI does not appear to account for the total cross-reactivity observed between intact PAK and PAO pili in the ELISA. This could be attributed to several possible causes. It is likely that TCI in the intact pilus exists in a fairly limited number of conformations. In solution, however, TCI may be more flexible and therefore the proportion of TCI that is in a suitable conformation for binding with antibodies may be diminished. It is also possible that proteolytic cleavage of the polypeptide has interrupted a second common sequential antigenic determinant. A third possibility is that an antigenic determinant that is present in intact pili, and consists of residues contributed by more than one subunit, might have been lost upon disruption of the pilus quaternary structure. This type of antigenic determinant (called a neotope) has been observed with tobacco mosaic virus (van Regenmortel, 1982). A further possibility is that a



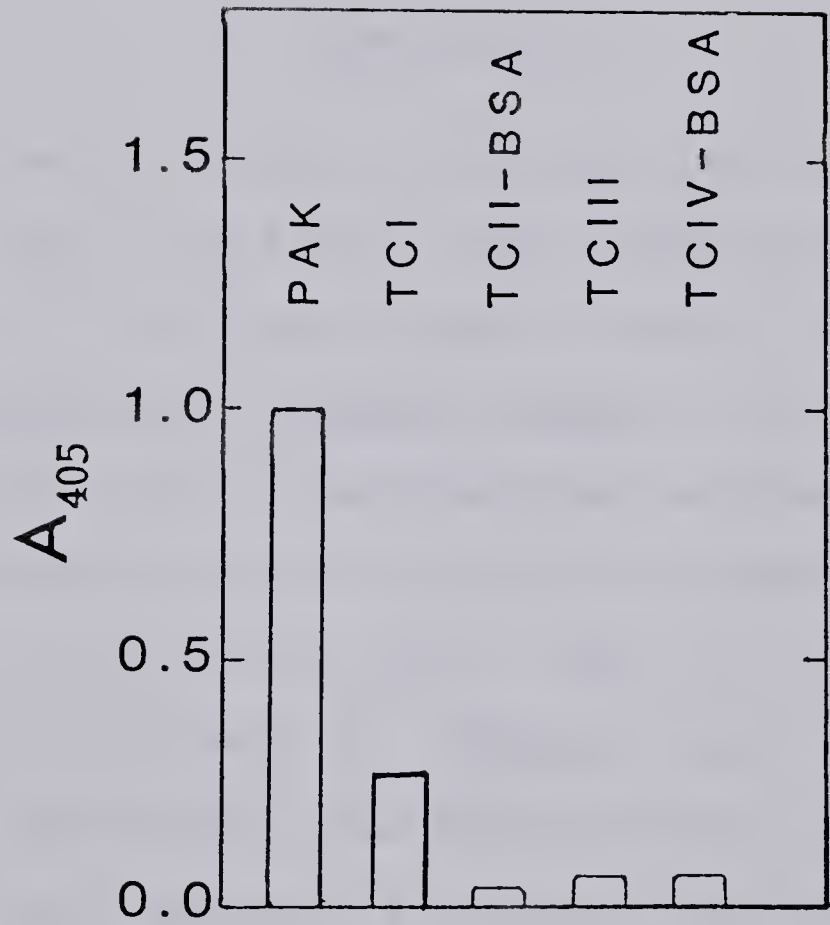


Figure IX.6. ELISA assay showing the reaction of PAK pili and its TC-peptides with anti-PAO pilus antisera. The results shown are for a 1 in 500 dilution of antisera and were normalized relative to an  $A_{405}$  of 1.5 for PAO pili with its homologous antisera (not shown).



conformational antigenic determinant, which is dependent on the native tertiary structure of pilin, has been lost upon proteolytic digestion of pili. The latter possibility is less likely since carboxymethylated pili, which retains only 50% of the secondary structure of native pili, according to circular dichroism studies, is equally reactive in the ELISA as native pili (data not shown).

### *Conclusions*

In conclusion, we have identified four proteolytic fragments of PAK pilin which contain sequential antigenic determinants. Of the four antigenic regions, the three C-terminal proteolytic fragments appear to be specific to strain PAK pilin, while the N-terminal antigenic peptide, TCI, contains an antigenic site which is common to PAK, PAO and possibly to gonococcal pilin. This is in keeping with the findings of Sastry *et al.* (Sastry, Pearlstone, Smillie & Paranchych, unpublished) that the N-terminal one-third of PAK and PAO pilin represent a constant sequence, while the C-termini are variable. Similarly, Schoolnik *et al.* (1982a) have shown that the C-terminus of gonococcal pilin shows antigenic variability, while the N-termini of these proteins are conserved (discussed in Chapter I). On the other hand, comparative sequencing of antigenically distinct K88 pilins (Gastra *et al.*, 1979) has shown that most changes occur at the center of the protein primary sequence. Yet another motif is observed with the distribution of antigenic sites





in EDP208 pilin (Worobec *et al.*, 1983). The major antigenic site in this protein is found at the N-terminus, while the C-terminus probably contains one or more weaker antigenic sites.

These findings are consistent with the observation that diffraction patterns of PAK and gonococcal pili indicate some structural similarity between the two proteins (Chapter V), while the diffraction pattern of EDP208 pili does not indicate any such structural homology (Folkhard *et al.*, 1979b).

Although the four peptides shown in figure IX.3 c and d are antigenic, it has not been established that they are immunogenic. In order to establish this fact, it will be necessary to raise antibodies against the BSA-conjugated peptides. Work is currently under way in the laboratory of Dr. R.S. Hodges to chemically synthesize analogues of the four antigenic sites proposed in figure IX.3e, in order to further delineate the antigenic sites and to prepare sufficient material for raising antibodies against the peptides.

Similarly, one must be cautious in interpreting these results as indicating that the antigenic peptides are on the surface in native pili, because of the danger of dissociation or breakdown of pili in the immunized animals. In order to establish this fact, it will be necessary to demonstrate that antibodies raised against the fragments



bind to native pili.

Extension of this approach to delineating the antigenic determinants of PAO pili would also be useful as a structural probe. It is likely, that the antigenic determinants in the proteins occur at similar positions in the sequence, since all the available data suggests that the two polypeptides have similar structures at the level of circular dichroism and X-ray fiber diffraction studies. It would also be worthwhile to extend these studies to include overlapping peptides of PAK pilin, in case any antigenic sites have been disrupted by the proteolytic digestion. Similarly, it would be useful to raise antibodies against the pilin dimers in octyl-glucoside and to test them for their ability to react with the peptide fragments. The reciprocal experiment should also be carried out, whereby antibodies raised against the peptide fragments are tested for their ability to react with the three quaternary arrangements of pili. Using this type of approach, it has been determined that tobacco mosaic virus had 3 sequential antigenic determinants which are always on the surface of the virion, an antigenic determinant that is only detected if the whole virus is injected and a fourth sequential antigenic determinant that is only detected using antibodies raised against the viral coat protein subunit (reviewed by van Regenmortel, 1982). This type of procedure, applied to pili, should be useful in mapping out surface exposed regions of pilin in each of the 3 quaternary arrangements, described in Chapter VIII.





## CHAPTER X

### Perspectives

The title of this work is the structure and assembly of *Pseudomonas pili*. Although some progress has been made in both these areas, a large number of questions remain unanswered. The following discussion offers some suggestions for future research in this field.

#### *A. Pilus Structure*

One of the most promising areas of pilin structural analysis is the mapping of the antigenic determinants using the approaches initiated in Chapter IX. As suggested in Chapter IX, it would be useful to raise antibodies against pilin dimers and against reassembled pilin filaments in addition to those obtained against native pili. Each of the antisera could then be tested for their ability to react with various pilin peptide fragments. Similarly, antisera raised against each of the antigenic peptides should be tested for their ability to react with each of the quaternary arrangements of pilin. Using these approaches, it should be possible to identify regions of the polypeptide chain which are on the surface of the pilin dimers, for example, but are buried in native pili. These approaches should complement the spectral studies of Chapter VIII.

It would also be of interest to determine whether tryptophan 55, 127 or both become partially exposed upon





dissociation of pili into dimers. One possible approach would be to attempt to selectively modify one of the tryptophans in the pilin dimer, using conditions under which an exposed residue would become modified while a buried one would not. The reagent 2-hydroxy-5-nitrobenzyl-bromide (HNBB; Horton & Koshland, 1965) would be useful in this regard. At a pH of less than 7.5, this reagent reacts only with tryptophan and sulfhydryl groups, and the reaction with the sulfhydryl groups occurs more than 5-fold more slowly than the reaction with tryptophan. Furthermore, the modified tryptophans can be quantitated by measuring the absorbance at 410nm at a pH of 10. The presence of modified sulfhydryls does not interfere with this determination. The following experiment is suggested. One could modify pilin with HNBB, remove the excess reagent, further modify the protein with citraconic anhydride and then carry out trypsin digestion to produce the TC peptides as described in Chapter IX. It would then be a relatively simple task to separate TCIII (containing tryptophan 55) from TCIV (containing tryptophan 127) and to determine the absorbance at 410nm on the purified peptides in order to identify which peptides contain a modified tryptophan.

Using the above approaches to map out the location of different regions of the polypeptide chain with respect to the protein surface, it may then be possible to continue with the model-building approach of Chapter V to fit the diffraction data. To do this, one would construct models of



the pilin subunit which fit all the available data and include the sequence information, apply a symmetry operation to build the pilin helix and then calculate the transform of the resulting model for comparison with the observed transform. However, because of the vast number of possible arrangements for a 144-residue polypeptide chain, it is unlikely that this approach will lead to a unique solution for pilin structure. However, it may be useful in eliminating certain models and in testing the feasibility of structural hypotheses.

In order to obtain the high resolution structure of pili, however, it will probably be necessary to obtain crystals of the pilin subunit. The 3-dimensional structure of a single subunit could then be used as the building block for the model building calculations described above, and the rigid subunit could be manipulated in the pilin helix until the structure obtained fit the fiber diffraction data. In this way the structure of the entire assembly could be solved. The most likely candidate for crystallization is the pilin dimer in octyl-glucoside. Although preliminary crystallization trials have primarily resulted in gel formation rather than crystallization, this was probably due to the salting out of the detergent micelles (Michel, 1983). Therefore, further crystallization trials using some of the 'tricks' described by Michel (1983) might be useful.





### *B. Pilus Assembly*

It has become apparent (Chapter I and VI) that pilus assembly is more complicated than the self-assembly processes that takes place with many other filamentous arrangements of proteins. Therefore, the *in vitro* assembly experiments of Chapter VI, are probably not worth pursuing. A more fruitful approach would be to carry out a genetic analysis of the PAO pilus operon analogous to the elegant studies of Dougan *et al.* (1983, discussed in Chapter I). Although PAO pilin is chromosomally encoded, it is likely, by analogy with the K88 system, that the genes required for pilus expression are clustered in a small region of the *Pseudomonas* chromosome (ie. a 6-7 kilodalton fragment). Therefore, it should be possible to isolate restriction endonuclease fragments of 10-20 kilodaltons which carry all the genes necessary for pilus expression. Such fragments could be cloned and expressed in *E. coli* and the resulting recombinant colonies could be screened for pilus expression using an immunological detection method with anti-pilus antiserum (a colony 'immunoblot'). This type of approach has been used by Meyer *et al.* (1982) to identify the structural gene for gonococcal pilin.

Another line of research that would contribute to our understanding of pilus assembly, would be to pursue the reconstitution experiments described in Chapter VII. As was discussed in Chapter VII, the identification of the regions





of the polypeptide which are protected by the bilayer from proteolytic digestion or from chemical modification would be one such approach. One obvious hypothesis is that the hydrophobic N-terminus of *Pseudomonas* pilin is inserted into the bilayer during protein synthesis and that this same region is used in the polymerization of pilin in the membrane.

Perhaps, the pilin subunits initially form a 2-dimensional array in the bilayer which can be induced to rearrange into a helix by a simple sliding of the subunits past one another in a repetitive manner, perhaps induced by a nucleation protein. Such rearrangements are not unprecedented in protein assemblies and have been observed, albeit on a smaller scale, in the disk to lock-washer rearrangement of tobacco mosaic virus (Champness *et al.*, 1976) and in the opening and closing of the connexons in gap junctions (Unwin & Zampighi, 1980).

In conclusion, the continued study of the structure and assembly of *Pseudomonas* pili is of interest for several reasons. Besides the clinical interest in *Pseudomonas* pili as a potential vaccine and the interest in the role of pili in pathogenesis, the study of pili also offers the opportunity of addressing some of the more basic questions of molecular biochemistry. For example, a thorough understanding of the structure of pili should provide valuable insights into the role of hydrophobic bonding in maintaining protein structure. The elucidation of the antigenic structure of pilin is also an interesting problem in its own



right. In particular, the fact that pili appears to possess one very hydrophobic antigenic determinant and one fairly hydrophilic one offers the opportunity of studying two quite diverse antibody combining sites. Finally, the complete elucidation of the mechanism of pilus assembly, which will require a knowledge of pilin structure in the membrane and in the mature pilus, as well as an understanding of the role of other protein factors and electrochemical gradients in the assembly process, should provide valuable insights into the coordination of a complex biological system.



## BIBLIOGRAPHY

- Abram, D. & Koffler, H. (1964) *J. Mol. Biol.* 9: 168-185.
- Achtman, M., Willets, N. & Clark, A.J. (1971) *J. Bacteriol.* 106: 529-538.
- Achtman, M. & Skurray, R. (1977) in "Microbial Interactions." Reissig, J.L. ed. Chapman and Hall, London, pp234-279. *J. Bacteriol.* 98: 1598-1601.
- Ames, B.N. (1966) *Meth. Enzymol.* 8: 115-118.
- Anderson, T.F. (1949) in "The Nature of the Bacterial Surface," Miles, A.N. & Purie, N.W., eds., Oxford University Press, p92.
- Armstrong, G.D. (1980). *PhD Thesis*, University of Alberta, Edmonton, Canada.
- Armstrong, G.D., Frost, L.S., Sastry, P.A. & Paranchych, W. (1980) *J. Bacteriol.* 141: 333-341.
- Armstrong, G.D., Frost, L.S., Vogel, H.J. & Paranchych, W. (1981) *J. Bacteriol.* 145: 1167-1176.
- Arnott, S. (1980) in "Fiber Diffraction Methods", French, A.D. & Gardner, K.H., eds., American Chemical Society, Washington. pp1-30.
- Atassi, M.Z. (1975) *Immunochemistry* 12: 422-438.
- Atassi, M.Z. & Lee, C.-S. (1978) *Biochem. J.* 171: 429-434.
- Baron, C. & Thompson, T.E. (1975) *Biochim. Biophys. Acta* 383:276-285.
- Bayer, M.E. (1975) in "Membrane Biogenesis" A.T. Zagloff, ed., Plenum Publ. Corp. New York. pp393-427.
- Beachey, E.H., ed., (1980) "Bacterial Adherence." Chapman & Hall, London & New York, 464p.
- Bernards, A., van der Ploeg, L.H.T., Frasch, A.C.C., Borst, P., Boothroyd, J.C., Coleman, S. & Cross, G.A.M. (1981) *Cell* 27: 497-505.
- Blobel, G. & Dobberstein, B. (1975) *J. Cell Biol.* 67: 835-851.
- Blumenstock, E. & Jann, K. (1982) *Infect. Immun.* 35:





264-269.

- Blundell, T.L. & Johnson, L.N. (1976) "*Protein Crystallography*" Academic Press, New York, 565p.
- Borochoy-Neori, H. & Montan, M. (1983) *Biochemistry* 22: 197-205.
- Bradley, D.E. (1972a) *Biochem. Biophys. Res. Comm.* 47: 1080-1087.
- Bradley, D.E. (1972b) *Genetic Research* 19: 39-51.
- Bradley, D.E. (1972c) *J. Gen. Microbiol.* 72: 303-319.
- Bradley, D.E. (1973a) *Can. J. Microbiol.* 19:623-631.
- Bradley, D.E. (1973b) *Virology* 51: 489-492.
- Bradley, D.E. (1973c) *J. Virol.* 12: 1139-1148.
- Bradley, D.E. (1974) *Virology* 58: 149-163.
- Bradley, D.E. (1977) in "*Microbiology-1977*" Schlessinger, D., ed., American Society for Microbiology, Washington, D.C., pp127-133.
- Bradley, D.E. (1978) in "*Pili*", Bradley, D.E., Raizen, E., Fives-Taylor, P. & Ou, J. eds., International Conferences on Pili, Washington, D.C. pp319-338.
- Bradley, D.E. (1980a) *Can. J. Microbiol.* 26: 146-154.
- Bradley, D.E. (1980b) *Can. J. Microbiol.* 26:155-160.
- Bradley, D.E. & Pitt, T.L. (1974) *J. Gen. Virol.* 24: 1-15.
- Bradley, D.E. & Pitt, T.L. (1975) *J. Hyg. Cambridge* 74: 419-431.
- Branton, D., Cohen, C.M., & Tyler, J. (1981) *Cell* 24: 24-32.
- Brauer, A.W., Margolies, M.N. & Haber, E. (1975) *Biochemistry* 14: 3029-3035.
- Brinton, C.C. (1965) *Trans. N.Y. Acad. Sci.* 27: 1003-1054.
- Brinton, C.C. Jr. (1971) *CRC Crit. Rev. Microbiol.* 1: 105-160.
- Buchanan, T.M. (1975) *J. Exp. Med.* 141: 1470-1475.
- Buchanan, T.M., Pearce, W.A. & Chen, K.C.S. (1978) in



"Immunobiology of Neisseria gonorrhoeae," Brooks, G.F., Gotschlich, E.C., Holmes, K.K., Sawyer, W.D. & Young, F.E., eds., American Society for Microbiology, Washington, D.C.

Burnette, W.N. (1981) *Anal. Biochem.* 112: 195-203.

Cantor, R.C. & Schimmel, P.R. (1980) "*Biophysical Chemistry*" Volume II. W.H. Freeman, San Fransisco.

Champness, J.N. (1971) *J. Mol. Biol.* 56: 295-310.

Champness, J.N., Bloomer, A.C., Bricogne, G., Butler, P.J.G. & Klug, A. (1976) *Nature* 251: 20-24.

Chen, Y-H., Yang, J.T., & Martinez, H.M. (1972) *Biochemistry* 11: 4120-4125.

Chervenka, C.H. (1970) "*A Manual of Methods for the Ultracentrifuge*," Spinco division of Beckman Instruments Inc., Palo Alto California.

Chong, P.C.S. & Hodges, R.S. (1981) *J. Biol. Chem.* 256: 5064-5074.

Chothia, C. (1975) *Nature* 254: 304-308.

Clarke, S. (1975) *J. Biol. Chem.* 250: 5459-5469.

Cochran, W., Crick, F.H.C. & Vand, V. (1952) *Acta Cryst.* 5: 581-586.

Cohn, E.J. & Edsall, J.T. (1943) "*Proteins, Amino Acids & Peptides*", Hafner Publ. Co., New York.

Coggins, J.R. & Benoiton, N.L. (1970). *J. Chromat.* 52: 251-256.

Crawford, E.M. & Gesteland, R.F. *Virology*. 22: 165-167.

Crick, F.H.C. (1953) *Acta Cryst.* 6: 689-691.

Crick, F.H.C. & Watson, J.D. (1956) *Nature* 177: 473-475.

Date, T., Inuzuka, M. & Tomoeda, M. (1977) *Biochemistry* 16: 5579-5585.

Dirienzo, J.M., Nakamura, K., Inouye, M. (1978) *Ann. Rev. Biochem.* 47: 481-532.

Donovan, J.W. (1964) *Biochemistry* 3: 67-74.

Dougan, G., Dowd, G. & Kehoe, M. (1983) *J. Bacteriol.* 153:



364-370.

- Duguid, J.P., Smith, I.W., Dempster, G. & Edmunds, P.N. (1955) *J. Pathol. Bacteriol.* 70: 335-348.
- Edman, P. & Begg, G. (1967) *Eur. J. Biochem.* 1: 80-91.
- Eftink, M.R. & Ghiron, C.A. (1976) *Biochemistry* 15: 672-680.
- Elliot, A. (1967) in "*Poly- $\alpha$ -amino acids*", G.D. Fasman, ed., Marcel-Dekker, New York.
- Eshdat, Y., Silverblatt, F.J. & Sharon, N. (1981) *J. Bacteriol.* 148: 308-314.
- Evans, D.G., Silver, R.P., Evans, D.J. Jr., Chase, D.G. & Gorbach, S.L. (1975) *Infect. Immun.* 12:656-667.
- Evans, D.G., Evans, D.J. Jr., Tjoa, W. & Dupont, H.L. (1978) *Infect. Immun.* 19: 727-736.
- Fairbanks, G., Stick, T.L. & Wallach, D.F.J. (1971) *Biochemistry* 10: 2606-2617.
- Falkow, S. & Baron, L.S. (1962) *J. Bacteriol.* 98: 1598-1601.
- Faris, A., Lindall, M., & Wadström, T. (1980) *FEMS Microbiol. Letters* 7: 265-269.
- Folkhard, W., Leonard, K.R., Malsey, S., Marvin, D.A., Dubochet, J., Engel, A., Achtman, M. & Helmuth, R. (1979a) *J. Mol. Biol.* 130: 145-160.
- Folkhard, W., Leonard, K.R., Dubochet, J., Marvin, D.A. & Paranchych, W. (1979b) *Abstracts XIth Internat. Congress Biochem.* 03-3-5116.
- Folkhard, W., Marvin, D.A., Watts, T.H. & Paranchych, W. (1981) *J. Mol. Biol.* 149: 79-93.
- Forsgren, A. & Sjoquist, J. (1966) *J. Immunol.* 97: 822-827.
- Franklin, R.E. & Gosling, R.G. (1953) *Acta Cryst.* 6: 678-675.
- Franks, A. (1958) *Bull. J. Appl. Phys.* 9: 349-352.
- Fraser, R.D.B. & MacRae, T.P. (1973) "*Conformation in Fibrous Proteins*", Acad. Press., New York.
- Frøholm, L.O. & Sletten, K. (1977) *FEBS Letters* 73: 29-32.
- Frost, L.S. (1978) *PhD. Thesis*, University of Alberta,





Edmonton, Canada.

- Frost, L.S. & Paranchych, W. (1977) *J. Bacteriol.* 131: 259-269.
- Frost, L.S., Carpenter, M. & Paranchych, W. (1978) *Nature* 271: 87-89.
- Frost, L.S., Armstrong, G.D., Finlay, B., Edwards B.F.P. & Paranchych, W. (1983) *J. Bacteriol.* 153: 950-954.
- Gaastra, W., Klemm, P., Walker, J.M. & de Graaf, F.K. (1979) *FEMS Microbiol. Letters* 6: 15-18.
- Gaastra, W., Mooi, F.R., Stuitje, A.R. & de Graaf, F.K. (1981) *FEMS Microbiol. Letters* 12: 41-46.
- Gaastra, W. & de Graaf, F.K. (1982) *Microbiol. Rev.* 46: 129-161.
- Garavito, R.M. & Rosenbusch, J.P. (1980) *J. Cell Biol.* 86: 327-329.
- Gibbons, I. & Perham, R.N. (1970) *Biochem. J.* 116: 843-849.
- Gibbons, I., Jones, G.W. & Sellwood, R. (1975) *J. Gen. Microbiol.* 86: 228-240.
- Goding, J.W. (1978) *J. Immunolog. Meth.* 20: 241-253.
- Gubish, E.R., Chen, K.C.S. & Buchanan, T.M. (1982) *Infect. Immun.* 37: 189-194.
- Hagen, D.S., Weiner, J.H. & Sykes, B. (1978) *Biochemistry* 17: 3860-3866.
- Halegoua, S. & Inouye, M. (1979) *J. Mol. Biol.* 130: 39-61.
- Hancock, R.E.W. & Nikaido, H. (1978) *J. Bacteriol.* 136: 381-390.
- Hancock, R.E.W. & Carey, A.M. (1979) *J. Bacteriol.* 140: 902-910.
- Hartley, B.S. (1970) *Biochem. J.* 119: 805-822.
- Heathcoat, J.G. & Haworth, C. (1969) *J. Chromatog.* 43: 84-92.
- Helenius, A. & Simons, K. (1972) *J. Biol. Chem.* 247: 3656-3661.
- Helenius, A. & Simons, K. (1975) *Biochim. Biophys. Acta* 415:



29-79.

- Helenius, A., Fries, E., Garoff, H. & Simons, K. (1976) *Biochim. Biophys. Acta* 436: 319-334.
- Helenius, A., Fries, E. & Kartenbeck, J. (1977) *J. Cell Biol.* 75: 886-880.
- Helenius, A., McCaslin, D.R., Fries, E. & Tanford, C. (1979) *Meth. Enzymol.* 56: 734-749.
- Henrichsen, J. (1975) *Acta. Pathol. Microbiol. Scand. Sect. B.* 83: 171-178.
- Hermodsen, M.A., Chen, K.C.S. & Buchanan, T.M. (1978) *Biochemistry* 17: 442-445.
- Herskovits, T.T. & Laskowski, M. (1962a) *J. Biol. Chem.* 237: 2481-2492.
- Herskovits, T.T. & Laskowski, M. (1962b) *J. Biol. Chem.* 237: 3418-3422.
- Herskovits, T.T. (1968) *Meth. Enzymol.* IX: 748-775.
- Holloway, B.W. (1975) in "*Genetics and Biochemistry of Pseudomonas*." R.H. Clarke and M.H. Richmond eds. John Wiley and sons, London. pp133-161.
- Holmes, K.C. & Blow, D.M. (1966) "*The Use of X-ray Diffraction in the Study of Protein and Nucleic Acid Structures*" Interscience, New York.
- Holmes, K.C. & Klug, A. (1963) *Acta Cryst.* 16A: 79.
- Hopp, T.P. & Woods, K.R. (1981) *Proc. Natl. Acad. Sci. USA* 78: 3834-3828.
- Horton, H.R. & Koshland, D.E. Jr. (1965) *J. Amer. Chem. Soc.* 87: 1126-1132.
- Houwink, A.L. (1949) in "*The Nature of the Bacterial Surface*", Miles, A.A. & Purie, N.W. (eds). Oxford University Press, p92.
- Huang, K. -S., Bayley, H. & Khorana, H.G. (1980) *Proc. Natl. Acad. Sci. USA* 77: 323-327.
- Huxley, H.E. & Brown, W. (1967) *J. Mol. Biol.* 30, 383-434.
- Jones, G.W. & Rutter, J.M. (1972) *Infect. Immun.* 6: 919-927.
- Kagawa, Y. & Racker, E. (1971) *J. Biol. Chem.* 246:



5477-5487.

- Kakudo, M. & Kasai, N. (1972) *"X-ray Diffraction by Polymers"* Elsevier, Amsterdam, N.Y., London.
- Kasahara, M. & Auraku, Y. (1974) *J. Biochem.* 76: 959-966.
- Kay, C.M. (1970) *FEBS Letters* 9: 78-80.
- Kehoe, M., Sellwood, R., Shipley, P. & Dougan, G. (1981) *Nature* 291: 122-126.
- Klemm, P. (1979) *FEBS Letters* 108: 107-110.
- Klemm, P. (1981) *Eur. J. Immunol.* 117: 617-627.
- Klemm, P. (1982) *Eur. J. Biochem.* 124: 339-344.
- Klinengberg, M. (1981) *Nature* 290: 449-453.
- Klug, A., Crick, F.H.C. & Wyckoff, H.W. (1958) *Acta Cryst.* 11: 199-213.
- Kratky, O., Leopold, H. & Stabinger, H. (1973) *Meth. Enzymol.* 27: 98-110.
- Kuntz, I.D. Jr. & Kauzmann, W. (1974) *Adv. Protein Chem.* 28: 239-345.
- Lambden, P.R., Robertson, J.N. & Watt, P.J. (1980) *J. Bacteriol.* 141: 393-396.
- Langone, J.J. (1980) *Meth. Enzymol.* 70: 356-375.
- Langridge, R., Wilson, H.R., Hooper, C.W., Wilkins, M.H.F. & Hamilton, L.D. (1960) *J. Mol. Biol.* 2: 19-37.
- Lapointe, J. & Marvin, D.A. (1973) *Mol. Cryst. and Liquid Cryst.* 19: 269-278.
- Lautrop, A. (1961) *Int. Bull. Bacteriol. Nomencl.* 11: 107-108.
- Lawn, A.M. (1967) *Nature* 214: 1151-1152.
- Lee, B. & Richards, F.M. (1971) *J. Mol. Biol.* 55: 379-400.
- Lehrer, S.S. (1971a) *Biochemistry* 10: 3254-3263.
- Lehrer, S.S. (1971b) *Biophys. J.* 11: 72a.
- Lenette, E.H., Spaulding, E.H. & Trauant, J.P. (eds) (1974) *"Manual of Clinical Microbiol."* 2nd edit. American





Society for Microbiology, Washington, D.C.

- Levitt, M. & Chothia, C. (1976) *Nature* 261: 552-557.
- Lipson, H. & Cochran, W. (1954) *"The Determination of Crystal Structures"* Macmillan, London.
- Liu, T-Y & Chang, Y.H. (1971) *J. Biol. Chem.* 246: 2842-2848.
- Lowry, G.H., Rosebrough, W.J., Farr, A.L. & Randall, J.T. (1951) *J. Biol. Chem.* 193: 265-270.
- Lugtenberg, B., Meyers, J, Peters, N., van der Hoek, P. & van Alphen, L. (1975). *FEBS Letters* 58: 254-258.
- Luzzati, V. & Tardieu, A. (1980) *Ann. Rev. Biophys. and Bioengineering* 9: 1-29.
- Makino, S., Reynolds, J.A. & Tanford, C. (1973) *J. Biol. Chem.* 248: 4926-4932.
- Makino, S., Woolford, J.L. Jr., Tanford, C. & Webster, R.E. (1975) *J. Biol. Chem.* 250: 4327-4332.
- Makowski, L. (1978) *J. Appl. Cryst.* 11: 273-283.
- Marchesi, V.T. (1979) *J. Membr. Biol.* 51: 101-131.
- Marchesi, V.T., Furthmayr, H. & Tomita, M. (1976) *Ann. Rev. Biochem.* 45: 667-698.
- Marvin, D.A. (1966) *J. Mol. Biol.* 15: 8-17.
- Marvin, D.A. & Hohn, B. (1969) *Bacteriol. Rev.* 33:172-209.
- Marvin, D.A., Wiseman, R.L. & Wachtel, E.J. (1974) *J. Mol. Biol.* 82: 121-138.
- Marvin, D.A. & Wachtel, E.J. (1975) *Nature* 253: 19-23.
- Marvin, D.A. & Wachtel, E.J. (1976) *Phil. Trans. Royal Soc. Lond.B.* 276: 81-98.
- Marvin, D.A. & Nave, C. (1982) in *"Structural Molecular Biology"*, D.B. Davies, W. Saenger & S.S. Danyluk, (eds.). Plenum Publ. Corp. pp3-44.
- McMichael, J.C. & Ou, J.T. (1979) *J. Bacteriol.* 138: 969-975.
- Meyer, T.F., Mlawer, N. & So, M. (1982) *Cell* 30: 45-52.
- Michel, H. (1983) *Trends in Bioch. Sci.* 8: 56-59.



- Michel, H. & Osterhelt, D. (1980) *Proc. Natl. Acad. Sci. USA* 77: 1283-1285.
- Mimms, L.T., Zampighi, G., Nozaki, Y., Tanford, C. & Reynolds, J.A. (1981) *Biochemistry* 20: 833-840.
- Minkley, E.G. Jr., Polen, S., Brinton, C.C. Jr. & Ippen-Ihler, K. (1976) *J. Mol. Biol.* 108: 11-121.
- Mitsui, Y., Dyer, F-P. & Langridge, R. (1973) *J. Mol. Biol.* 79: 57-64.
- Mooi, F.R. & de Graaf, F.K. (1979) *FEMS Microbiol. Letters* 5: 17-20.
- Mooi, F.R., de Graaf, F.K. & van Embden, J.D.A. (1979) *Nucleic Acids Res.* 6: 849-865.
- Mooi, F.R., Wouters, C., Wijffjes, A. & de Graaf, F.K. (1982) *J. Bacteriol.* 150: 512-521.
- Moore, D., Sowa, B.A. & Ippen-Ihler, K. (1981) *J. Bacteriol.* 146: 251-259.
- Moore, S. (1963) *J. Biol. Chem.* 238: 235-237.
- Nagy, B., Moore, H.W., Isaacson, R.E., To, C. -C. and Brinton, C.C. (1978) *Infect. Immun.* 21: 269-274.
- Nave, C., Brown, R.S., Fowler, A.G., Ladner, J.E., Marvin, D.A., Provencher, S.W., Tsugita, A., Armstrong, J. & Perham, R.N. (1981) *J. Mol. Biol.* 149: 675-707.
- Needleman, S.B. (ed) (1975) "*Protein Sequence Determination*," Molecular Biology, Biochemistry and Biophysics 8. Springer-Verlag. Heidelberg.
- Neidhardt, F.G., Block, P.L. & Smith, D.F. (1974) *J. Bacteriol.* 119: 736-747.
- Novick, R.P., Clowes, R.C., Cohen, S.N., Curtiss, R., Datta, N. & Falkow, S. (1976) *Bacteriol. Rev.* 40: 168-189.
- Novotony, C. & Fives-Taylor, P. (1974) *J. Bacteriol.* 117: 1306-1311.
- Nozaki, Y., Reynolds, J.A. & Tanford, C. (1978) *Biochemistry* 17: 1239-1246.
- O'Callaghan, R.J., Bundy, L., Bradley, R. & Paranchych, W. (1973) *J. Bacteriol.* 115: 76-81.
- Ofek, I. & Beachey, E.F. (1978) *Infect. Immun.* 22: 247-254.





- Oikawa, K., Kay, C.M. & McCubbin, W.D. (1968) *Biochim. Biophys. Acta* 168: 164-167.
- Oncley, J.L. (1941) *Ann. N.Y. Acad. Sci.* 41: 121-150.
- Osborn, M.J., Gander, J.E., Parisi, E. & Carson, J. (1972) *J. Biol. Chem.* 247: 3967-3976.
- Ottow, J.C.G. (1975) *Ann. Rev. Micro.* 29: 79-108.
- Ouchterlony, Ö. (1948) *Acta. Pathol. Microbiol.* 25: 186-191.
- Oudin, J. (1980) *Meth. Enzymol.* 70: 166-198.
- Paranchych, W. & Graham, A.F. (1962) *J. Cell. Comp. Physiol.* 60: 199-203.
- Paranchych, W., Frost, L.S. & Carpenter, M. (1978) *J. Bacteriol.* 134: 1179-1180.
- Provencher, S.W. (1979) *Makromol. Chem.* 180: 201-209.
- Provencher, S.W. & Glöckner, J. (1981) *Biochemistry* 20: 33-37.
- Racker, E. (1979) *Meth. Enzymol.* 55: 699-711.
- Racker, E., Violand, B., O'Neal, S., Alfonzo, M. & Telford, J. (1979) *Arch. Biochem. Biophys.* 198: 470-477.
- Reynolds, J.A. & Tanford, C. (1970) *Proc. Natl. Acad. Sci. USA* 66: 1002-1007.
- Reynolds, J.A. & Tanford, C. (1976) *Proc. Natl. Acad. Sci. USA* 73: 4467-4470.
- Robertson, J.P., Vincent, P. & Ward, M.E. (1977) *J. Gen. Microbiol.* 102: 169-177.
- Robinson, N.C. & Tanford, C. (1975) *Biochemistry* 14: 369-378.
- Rosevear, P. Van-Aken, T., Baxter, J. & Ferguson-Miller, S. (1980) *Biochemistry* 19: 4108-4115.
- Sack, R.B. (1975) *Ann. Rev. Micro.* 29: 333-353.
- Salit, I.E. & Gotschlich, E.C. (1977) *J. Exp. Med.* 146: 1182-1194.
- Sastry, P.A., Pearlstone, J.R., Smillie, L.B. & Paranchych, W. (1983) *FEBS Letters* 151: 253-256.





- Schachman, H.K. (1959) "*Ultracentrifugation in Biochemistry*," Acad. Press, New York.
- Schechter, N.M., Sharp, S., Reynolds, J.A. & Tanford, C. (1976) *Biochemistry* 15: 1897-1904.
- Scheraga, H.A. & Mandelkern, L. (1953) *J. Amer. Chem. Soc.* 75: 179-184.
- Schoolnik, G.K., Tai, J.Y. & Gotschlich, E.C. (1982a) in "*Microbiology-1982*" Schlessinger, D., ed., American Society for Microbiology, Washington, D.C. pp312-316.
- Schoolnik, G., Tai, J.Y. and Gotschlich, E.C. (1982b) *Progress in Allergy* 33: 314-331.
- Sela, M., Schechter, B., Schechter, I. & Borek, F. (1967) *Cold Spring Harb. Symp. Quant. Biol.* 32: 537-545.
- Sela, M. (1969) *Science* 166: 1365-1373.
- Shinoda, K., Yamaguchi, T. & Hori, R. (1961) *Bull. Chem. Soc. Japan* 34: 237-241.
- Shipley, P., Dougan, G. & Falkow, S. (1981) *J. Bacteriol.* 145: 920-925.
- Silverman, M. & Simon, M.I. (1977) *Ann. Rev. Micro.* 31: 397-419.
- Smilowitz, H., Carson, J. & Robbins, P.W. (1972) *J. Supra. Struc.* 1: 8-13.
- Spencer, H.M. (1926) *Internat. Crit. Tab.* I: 67-68.
- Steele, J.C. Jr. & Reynolds, J.A. (1979) *J. Biol. Chem.* 254: 1633-1638.
- Stirm, S., Ørskov, F., Ørskov, I. & Birch-Anderson, A. (1967) *J. Bacteriol.* 93: 740-748.
- Strickland, E.H. (1972) *CRC Crit. Rev. Biochem.* 2: 113-175.
- Stubbs, G., Warren, S. & Holmes, K. (1977) *Nature* 267: 216-221.
- Svedberg, T. & Pederson, K.O. (1940) "*The Ultracentrifuge*," Oxford University Press, London.
- Swaney, L.P., Liu, Y.-P., Ippen-Ihler, K. & Brinton, C.C. Jr. (1977) *J. Bacteriol.* 130: 506-511.
- Swanson, J., Kraus, S.J. & Gotschlich, E.C. (1971) *J. Exp.*



- Med.* 134: 886-906.
- Swanson, J. (1973) *J. Exp. Med.* 137: 571-589.
- Swanson, J. (1977) *J. Exp. Med.* 137: 571-589.
- Takeya, K. & Amako, K. (1966) *Virology* 28: 163-165.
- Tanford, C. (1961) "*Physical Chemistry of Macromolecules*", Wiley, New York.
- Tanford, C. (1973) "*The Hydrophobic Effect*" John Wiley & Sons, New York.
- Tanford, C., Nozaki, Y., Reynolds, J.A. & Makino, S. (1974) *Biochemistry* 13: 2369-2375.
- Tanford, C. & Reynolds, J.A. (1976) *Biochim. Biophys. Acta* 454: 133-170.
- Towbin, H., Staehelin, T. & Gordon, J. (1979) *Proc. Natl. Acad. Sci. USA* 76: 4350-4354.
- Tsang, L.-W.-L. & Marusyk, R.G. (1980). *Can. J. Microb.* 26: 1224-1231.
- Unwin, P.N.T. & Zampighi, G. (1980) *Nature* 283: 545-549.
- Vainshtein, B.K. (1966) "*Diffraction of X-rays by Chain Molecules*," Elsevier, Amsterdam.
- Van Regenmortel, M.H.V. (1982) "*Serology and Immunochemistry of Plant Viruses*" A.P. New York, 302p.
- Visser, L., Robinson, N.C. & Tanford, C. (1975) *Biochemistry* 14: 1194-1199.
- Voller, A., Bidwell, D.E., Hultdt, G. & Engvall, E. (1974) *Bull. Wld. Hlth. Org.* 51: 209-221.
- Von Heijne, G. & Blomberg, C. (1979) *Eur. J. Biochem.* 97: 175-181.
- Wachtel, E.J., Wiseman, R.L., Pigram, W.J., Marvin, D.A. & Manuelidis, L. (1974) *J. Mol. Biol.* 88: 601-618.
- Weber, K. & Osborn, M. (1969) *J. Biol. Chem.* 244: 4406-4412.
- Weiss, R.L. (1971) *J. Gen. Microbiol.* 67: 135-143.
- Wetlaufer, D.B. (1962) *Adv. Protein Chem.* 17: 303-390.
- Wickner, W. (1979) *Ann. Rev. Bioch.* 48: 23-45.



- Willets, N. & Skurray, R. (1980) *Ann. Rev. Genetics* 14: 41-76.
- Williams, R.O., Young, J.R. & Majewa, P.A. (1979) *Nature* 282: 847-849.
- Wood, R.E. (1976) *Hosp. Prac.* 10(10): 91-99.
- Woods, D.E., Strauss, D.C., Johanson, W.G., Berry, V.K. & Bass, J.A. (1980a) *Infect. Immun.* 29: 1146-1151.
- Woods, D.E., Bass, J.A., Johanson, W.G. & Strauss, D.C. (1980b) *Infect. Immun.* 30: 694-699.
- Worobec, E.A., Taneja, A.K., Hodges, R.S. & Paranchych, W. (1983) *J. Bacteriol.* 153: 955-961.
- Wu, C-S. & Yang, J.T. (1978) *Biochem. Biophys. Res. Comm.* 82: 85-91.
- Wu, C-S., Hachimori, A. & Yang, J.T. (1982) *Biochemistry* 21: 4556-4562.
- Young, V.M., ed., (1977) "*Pseudomonas aeruginosa*: Ecological Aspects and Patient Colonization" Raven Press, New York.
- Yu, J. & Steck, T.L. (1975) *J. Biol. Chem.* 250: 9176-9184.





## APPENDIX

### Publications arising from this thesis

- Paranchych, W., Sastry, P.A., Frost, L.S., Carpenter, M., Armstrong, G.D. & Watts, T.H. (1979). "Biochemical studies on pili isolated from *Pseudomonas aeruginosa* PAO." *Can. J. Microb.* 25: 1175-1181.
- Folkhard, W., Marvin, D.A., Watts, T.H. & Paranchych, W. (1981) "Structure of polar pili from *Pseudomonas aeruginosa* strains K and O." *J. Mol. Biol.* 149: 79-93.
- Watts, T.H., Scraba, D.G. & Paranchych, W. (1982) "Formation of 9nm filaments from pilin monomers obtained by octyl-glucoside dissociation of *Pseudomonas aeruginosa* pili." *J. Bacteriol.* 151: 1508-1514.
- Watts, T.H., Kay, C.M. & Paranchych, W. (1982) "Dissociation and Characterization of pilin isolated from *Pseudomonas aeruginosa* strains PAK and PAO." *Can. J. Biochem.* 60: 867-872.
- Watts, T.H., Worobec, E.A. & Paranchych, W. (1982). "Identification of pilin pools in the membrane of *Pseudomonas aeruginosa*." *J. Bacteriol.* 152: 687-691.
- Watts, T.H., Kay, C.M. & Paranchych, W. (1983) "Spectral properties of three quaternary arrangements of *Pseudomonas* pilin." *Biochemistry* in press.
- Watts, T.H., Sastry, P.A., Hodges, R.S. & Paranchych, W. (1983) "Mapping of the antigenic determinants of *Pseudomonas aeruginosa* PAK polar pili." *Infect. Immun.* manuscript submitted.





**B30397**